Strategies for surviving down-regulation : effects on tumour cell growth potential and chemosensitivity profile

Thesis

STRATEGIES FOR SURVIVIN DOWN-REGULATION: EFFECTS ON TUMOUR CELL GROWTH POTENTIAL AND CHEMOSENSITIVITY PROFILE

Marzia Pennati

Degree in Biological Sciences

Thesis submitted to the Open University for the degree of

Doctor of Philosophy

Discipline of Life Sciences

August 2007

Fondazione IRCCS Istituto Nazionale dei Tumori

Milan-Italy

DATE OF SUBMISSION: 27 AUGUST 2007
DATE OF AWARD: 24 MARCH 2008

ABSTRACT

Survivin is a bifunctional protein that acts as a suppressor of apoptosis and plays a central role in cell division. The protein is strongly expressed in the most common human neoplasms, has prognostic relevance for some of them, and appears to be involved in tumour cell resistance to anticancer agents and ionizing radiation. On the basis of these findings, survivin has been proposed as an attractive target for new anticancer interventions.

We generated a hammerhead ribozyme (Rz) targeting the CUA_{110} triplet in the survivin mRNA and transfected them into the JR8 human melanoma cell line. Cells endogenously expressing Rz were characterized by a lower survivin protein level than parental cells, and showed an increased caspase-9-dependent apoptotic response to treatment with the cytotoxic agents cisplatin and topotecan as well as with γ-irradiation. Moreover, an increased anti-tumour activity of oral topotecan was observed in Rz-expressing cells grown as xenograft tumours in athymic nude mice. In addition, we constructed a Moloney-based retroviral vector expressing Rz, encoded as a chimeric RNA within adenoviral VA1 RNA. Polyclonal cell populations, obtained by infection with the retroviral vector, of two androgen-independent human prostate cancer cell lines (DU145 and PC-3) were characterized by a significant reduction of survivin expression; the cells became polyploid and underwent caspase-9-dependent apoptosis. Survivin inhibition also enhanced their susceptibility to cisplatin-induced apoptosis and prevented tumour formation when cells were xenografted into athymic nude mice.

Again we used RNAi to specifically repress survivin in DU145 and PC-3 cell lines. RNAi-mediated survivin knock-down was able to significantly reduce cell proliferation and to enhance the rate of caspase-9-dependent

apoptosis. Moreover, sequential treatment with survivin-specific siRNA followed by the Hsp90 inhibitor 17-allylamino-17-demethoxy-geldanamycin produced supra-additive anti-proliferative effects in both cell lines.

Finally, we investigated the effects of the novel cdk inhibitor NU6140, in term of ability to potentiate the response to paclitaxel in HeLa cells, in relation to its interference with survivin. Sequential administration of cdk inhibitors resulted in escape from the mitotic block imposed by paclitaxel and significantly increased the apoptotic rate, with inhibition of survivin expression/phosphorylation as the potential mechanism.

Overall, such results suggest that strategies aimed at interfering with survivin expression/activity can be adopted to improve the chemo/radio-sensitivity profile of treatment-refractory human malignancies.

ACKNOWLEDGEMENTS

The present work was performed at the "Struttura complessa Ricerca Traslazionale" - Department of Experimenatl Oncology & Laboratories of the Fondazione IRCCS Istituto Nazionale dei Tumori of Milan.

I am most grateful to my supervisor Dr Nadia Zaffaroni who has been a constant source of guidance and support and who gave much of her time and interest to this project. I would like also to thank the Director of the UO#10, Dr Maria Grazia Daidone, who gave me the possibility to frequent the laboratories to develop this project.

I would like to thank Professor Gordon Peters, who acted as my English supervisor, for his advice, support and kindness.

In addition, I wish to express my gratitude to all the co-authors for their excellent contributions. A special thank to Dr Marco Folini, Dr Gennaro Colella, Dr Maria Curto, Dr Mara Binda, Dr Francesco Paduano and Dr Raffaella Villa, for their advice and support in performing cellular and molecular biology experiments, and miss Gabriella Abolafio for her technical assistance in flow cytometry analyses.

I also thank Prof Dario Altieri who kindly supplied the survivin cDNA and antibody for the detection of survivin Thr^{34}; Dr Lorenzo Citti for the analysis and production of the ribozymes; Prof Mauro Giacca and Dr Monica Zoppè for the production of the retroviral construct vector; Prof David R Newell who kindly hosted me at the laboratory of the Northern Institute for Cancer Research, Newcastle upon Tyne (UK), in order to perform the experiments with the NU6140.

Finally, I thank my parents Maria Rosa and Giovanni, the whole family and all friends, but most of all I am grateful to my husband Marco for his patience, invaluable encouragement and support.

This thesis is dedicated to my son Tommaso

TABLE OF CONTENTS

LIST OF
FIGURES & TABLES

Chapter 1

INTRODUCTION

1. APOPTOSIS

Apoptosis and necrosis represent two distinct types of cell death, which have been defined morphologically and biochemically [Kiechle & Zang, 2002].

Apoptosis, or programmed cell death, first described by Kerr, Wyllie and Currie [1972], plays important roles in the elimination of unnecessary, damaged or infected cells in multicellular organisms [Cory *et al*, 2002; Opferman & Korsmeyer, 2003]. Deregulation of apoptosis results in pathological conditions ranging from cancer [Vaux *et al*, 1988; Strasser *et al*, 2000; Opferman & Korsmeyer, 2003; Danial & Korsmeyer, 2004] to autoimmune diseases [Strasser *et al*, 2000; Franz *et al*, 2006].

Apoptosis is an active process characterized by morphological changes including condensation and fragmentation of the nucleus, shrinkage of the cytoplasm, and the formation of apoptotic bodies that contain fragments of the nucleus encircled by cytoplasm and cell membrane [Kerr & Kumar, 1998]. Apoptotic cells are rapidly eliminated by phagocytic cells including macrophages [Fadok *et al*, 1998]. Because their plasma membrane remains intact, apoptotic cells do not trigger an inflammatory response [Levine & Koh, 1999]. In contrast, necrosis is a passive form of cell death associated with inflammation, resulting from a non-specific injury such as blunt trauma, exposure to a toxin, or the loss of blood supply [Cohen, 1993; Kerr & Kumar, 1998; Proskuryakov *et al*, 2003; Edinger & Thompson, 2004]. Necrosis is characterized by cellular and organelle swelling, rupture of the plasma membrane and release of cytoplasmic contents, in addition to other events,

triggering a pronounced inflammatory response [Levine & Koh, 1999; Proskuryakov *et al*, 2003].

Apoptosis can be divided intro three stages [Kroemer *et al*, 1997]. In the first stage, the cell receives an apoptotic signal. A variety of stimuli both internal and external to the cell can activate apoptotic pathways. These include ligation of a cell surface receptor, removal of essential growth factor, exposure to various chemical agents [Au *et al*, 1997; Edinger & Thompson, 2004; Fumarola & Guidotti, 2004]. In addition, the exposure of a cell to UV, ionising radiation, or heat can also induce apoptosis [Sarin *et al*, 1996; Rehemtulla *et al*, 1997; Basu & Kolesnick, 1998; Garcia-Bermejo *et al*, 1998; Zundel & Giacca *et al*, 1998; Edinger & Thompson, 2004; Oancea *et al*, 2004; Boehm, 2006]. The cell integrates the various signals and may or may not execute the apoptosis. This process involves several signal transduction pathways such as the activation (or inactivation) or serine/threonine and tyrosine kinases and phosphatases. The final decision to undergo apoptosis depends upon several factors including the relative levels of both apoptotic and survival factors, as well as the metabolic state of the cell. In the final stage of the apoptosis, a degradative pathway is activated [Kroemer *et al*, 1997].

1.1. Features of Apoptosis

The biochemical and morphological changes induced by apoptosis influence different aspects of the cell from the plasma membrane to the nucleus (Table I).

Table I. Features of apoptosis.

Structure	Alteration
Plasma membrane	Exposure of phosphatidylserine Membrane blebbing Loss of integrity Loss of potassium gradient
Cytoplasm	Loss of cytoplasmic volume Degradation of cytoskeletal proteins
Mitochondria	Rupture of outer membrane Swelling of matrix Release of apoptotic proteins Loss of transmembrane gradient
Nucleus	Nuclear fragmentation Chromatin condensation DNA fragmentation

The plasma membrane is composed of a variety of phospholipids including both aminophospholipids (phosphatidylserine and phosphatidylethanolamine) and choline phospholipids (phosphatidylcholine, sphingomyelin) [Schlegel *et al*, 1996]. In the normal cellular state, the cell maintains an asymmetry between the phospholipid content of the inner and outer leaflet of the plasma membrane by actively translocating phosphatidylserine from the outer to the inner leaflet. In apoptosis, this asymmetry is lost as phosphatidylserine equilibrates between the inner and outer leaflets [Hampton *et al*, 1996; Bratton *et al*, 1997]. Another prominent apoptotic change concerning the structure of the plasma membrane is the formation of blebs, the small membrane-enclosed pieces of cytoplasm and condensed nuclear material [Cohen, 1993].

Cytoplasmic changes during apoptosis include the loss of cytoplasmic volume and degradation of cytoskeletal proteins [Cohen, 1993]. Cytoplasmic shrinkage results primarily from two processes: *i)* the formation of blebs results in a loss of volume, and *ii)* the loss of a potassium gradient that is normally maintained by the plasma membrane results in osmotic shrinkage of the cytoplasm [Dallaporta *et al*, 1999]. The degradation of cytoskeletal proteins is a consequence of the actions of caspases both directly cleaving proteins and activating other degradative enzymes [Krammer, 1999].

The mitochondrion consists of both an inner and outer phospholipid membrane. The inner membrane defines the central matrix space with mitochondrial DNA and where protein synthesis and respiration occurs [Scheffler, 2001]. Mitochondria normally maintain a voltage ($\Delta\psi_m$) and pH gradient across the inner membrane that is used by the F_1/F_0-ATPase in the formation of ATP [Scheffler, 2001]. During apoptosis this gradient is often lost, and is associated with the osmotic swelling of the matrix, the break of the outer mitochondrial membrane, and the release of pro-apoptotic proteins from the inter-membrane space [Kroemer *et al*, 2007].

In its normal state, the nucleus is a spherical structure with a relatively diffuse staining pattern. This staining pattern reflects different chromatin states with darker regions indicating inactive stretches of DNA bundled together with histones [Ferri & Kroemer, 2001]. Specific alterations are observed as a result of apoptosis and include the condensation of the nucleus [Thompson *et al*, 1999]. The nucleus fragments into several sections released from the cell as part of apoptotic bodies [Zamzami & Kroemer, 1999]. A reduction in the total DNA content of the cell is thus a sign of an

apoptotic cell death. On a biochemical level, these nuclear changes are associated with the activation of several different endonucleases. The action of the DNA degradative enzymes results in the formation of small fragments of DNA, often in multiples of 180 base-pairs reflecting basic nucleosome structure [Darzynkiewicz *et al*, 1997; Zamzami & Kroemer, 1999].

1.2. Apoptotic Death Pathways

Two major pathways of apoptosis have been identified in mammalian cells (Figure 1). An extrinsic pathway is triggered by the binding of ligands [Yuan, 1997] to cell-surface trimeric membrane death receptors and leads to caspase-8 activation. An intrinsic pathway involves mitochondria, which respond to pro-apoptotic signals by releasing cytochrome *c*, which in turn binds and activates the apoptotic protease activating factor-1 (Apaf-1), causing assembly of a multi-protein caspase-activating complex (apoptosome) and leading to activation of caspase-9 and initiation of a protease cascade [Cryns & Yuan, 1999]. Both pathways can be activated by genotoxic and metabolic stress, and result in the activation of effector caspases-3, -6 and -7 which cleave a variety of distinct substrates, resulting in nuclear fragmentation and cellular disassembly.

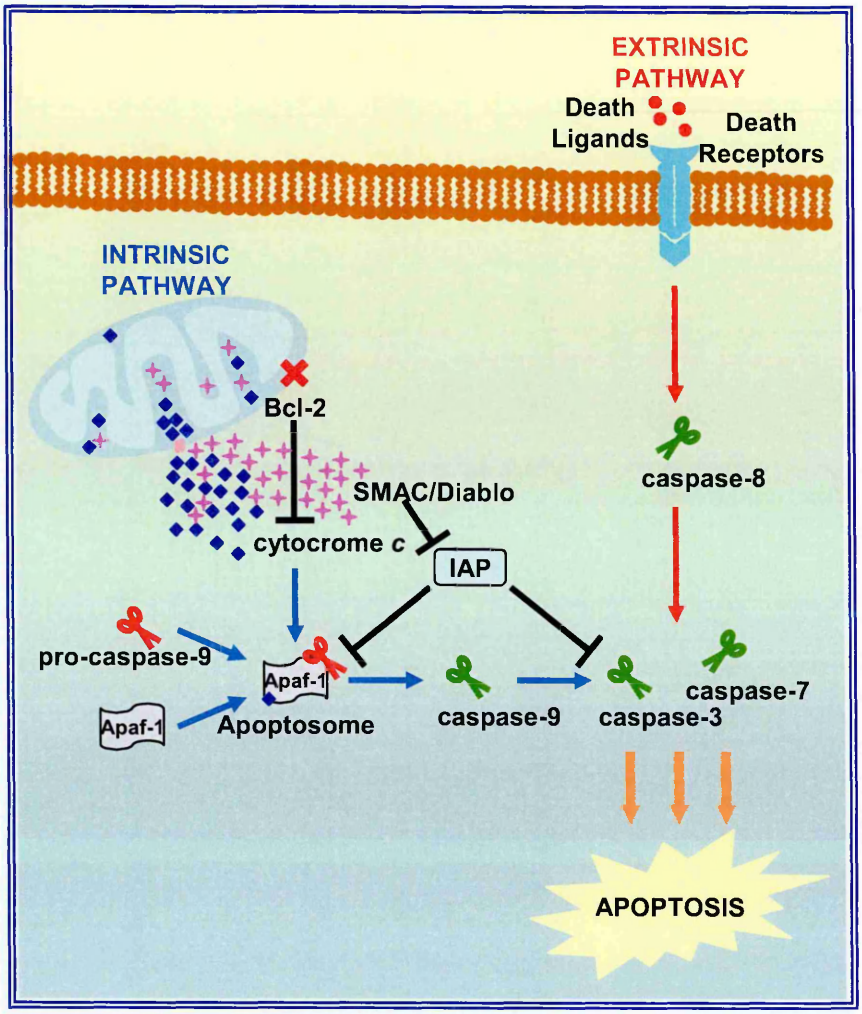

Figure 1. Schematic representation of the two major apoptotic pathways in human cells: the "extrinsic" (the death receptor-mediated) and "intrinsic" (mitochondrial) programmed cell death.

Apoptosis can be initiated by the death-receptor pathway that acts through caspase-8 or mitochondrial pathway that acts through caspase-9. Both apoptotic pathways converge to activate the effector caspases. Cell death is also regulated by the Bcl-2 and IAP protein families. Bcl-2 proteins are thought to regulate the mitochondria permeability transition by inhibiting (Bcl-2 and Bcl-x_L) or promoting (Bax and Bid) cytochrome *c* release. IAP proteins prevent processing of initiator caspase-9 from the apoptosome and inhibit the activity of the effector caspases. Proteins that are released by mitochondria during the permeability transition (i.e. cytochrome *c* and SMAC/Diablo) facilitate caspase activation by forming the apoptosome or relieving the caspase-inhibitory function of IAP proteins.

1.2.1. Death Receptor-Mediated Apoptotic Events

The extrinsic pathway is a primary mediator of cellular immunity, but can also be activated in response to drug therapy. The death receptor-mediated apoptotic events are initiated by binding of death receptors such as fibroblast-associated (Fas), tumour necrosis factor receptor (TNF-R), and TNF-related apoptosis-inducing ligand receptor (TRAIL-R) to their ligands [Trauth *et al*, 1989] (Figure 2).

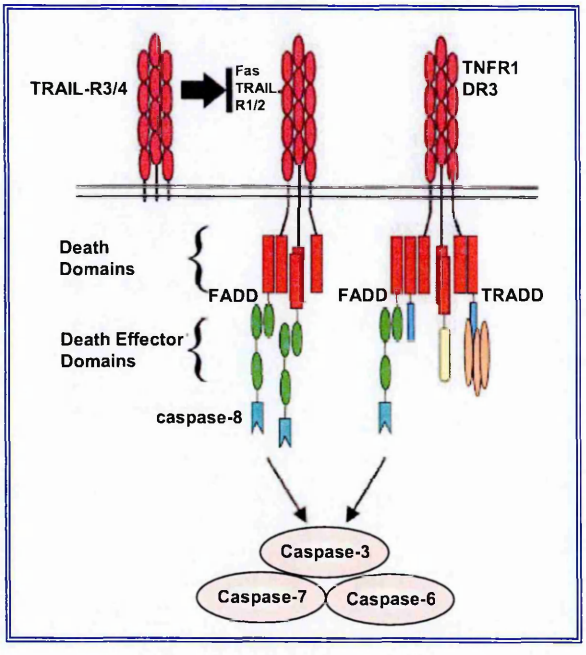

Figure 2. Signalling pathways triggered by death receptors.
After binding of FASL or APO2L/TRAIL, the death receptors Fas assemble the DISC complex: through the adaptor protein FADD, they recruit and activate the apoptosis-initiating proteases caspase-8. The physical proximity of the recruited enzymes in the ligand-induced signalling complex leads to their autoactivation by proteolysis, thereby triggering intracellular signalling cascades that induce specific cellular responses. After binding of TNF, TNF-R1 first recruits TRADD as a platform adaptor, and, in turn, assembles a complex which involves FADD and caspase-8 and triggers apoptosis in a manner similar to the other death receptors. Death receptor DR3 assembles signalling complexes that are similar to those of TNF-R1. Death domains are indicated in red; death-effector domains in green; caspase domains are shown in blue. [Adapted from Gupta *et al,* 2005]

This binding initiates ligation of the receptors and transmission of the apoptotic signals through motifs called death domains (DDs), death effector domains (DED), and caspase recruitment domains (CARD). The DDs are found in cytoplasmic proteins including Fas-associated protein with death domain (FADD), TNF receptor-associated protein with death domain (TRADD), and receptor-interacting protein (RIP) and in transmembrane proteins, including Fas, TNF-R1, TRAIL-R1/DR4, and TRAIL-R2/DR5. The DED are found in the adaptor molecules and in pro-caspases-8 and -10 and play an important role in death receptor-induced apoptosis where the interactions between death effector domains of the adaptor molecules and of pro-caspases-8 or -10 enable formation of the death-inducing signalling complex (DISC) [Lee *et al*, 2000]. The binding of the DISC (including the DED, the DED-containing adaptor molecules and the DED-containing cysteine protease caspase-8) to pro-caspase-8 initiates the caspase cascade [Weber & Vincenz, 2001]. These events can be regulated by Flip (FADD-like interleukin-1-converting enzyme-inhibitory protein), which prevents caspase activation [Peter, 2004].

1.2.2. Mitochondria-Mediated Apoptotic Events

In death receptor-mediated apoptosis, the apoptotic pathway is activated by the interaction of a relatively small number of structurally-related ligands with a relatively small number of structurally-related cell surface receptors. In contrast, mitochondrial apoptosis can be induced by a variety of agents

including chemotherapeutic drugs, reactive oxygen species, kinase and phosphatase inhibitors, UV and ionizing irradiation, and environmental stresses including growth factor withdrawal, heat, and osmolarity changes [Shimizu *et al*, 1996; Kroemer *et al*, 1997; Lilly *et al*, 1999; Galluzzi *et al*, 2006; Kroemer *et al*, 2007].

Cellular response to DNA-damage is a very complex process, involving a multitude of proteins that sense the damage, transduce signals into cells and execute cellular responses. This network of events includes a protein kinase cascade that connects the detection of DNA damage to the activation of transcription factors, which in turn regulate the expression of genes implicated in specific cellular pathways, including DNA repair mechanisms, cell-cycle checkpoints, cellular senescence and apoptosis [Zhou & Elledge, 2000; Sancar *et al*, 2004]. In response to the different types of DNA damage, the cell cycle checkpoints are activated to delay or arrest cell cycle progression, presumably in order to allow time to repair damaged DNA [Nyberg *et al*, 2002]. The blockage of DNA replication leads to collapse of replication forks and DNA double-strand breaks (DSBs) formation, which are thought to be crucial downstream apoptosis triggering lesions [Roos & Kaina, 2006]. DSBs are recognised by proteins that exert both kinase and repair activity. The most-important 'sensors' are ATM (ataxia telangiectasia mutated) and ATR (ataxia telangiectasia and Rad3 related) proteins, members of the phosphatidylinositol-3-kinase-related family [Durocher & Jackson, 2001; Ismail *et al*, 2005]. Whereas ATM is activated by ionizing radiation-induced DSBs, ATR is activated in response to UV light and presumably all chemical agents that give rise to stalled DNA replication forks

[Dart *et al*, 2004]. Upon activation, ATM phosphorylates various downstream substrates such as p53, Nbs1, MDC1, 53BP1, Rad9, Chk1 and Chk2, H2AX and BRCA1 [Lavin *et al*, 2005; Roos & Kaina, 2006]. ATM, and presumably also ATR, exerts three crucial functions: regulation and stimulation of DSB repair, signaling cell-cycle checkpoints and signaling apoptosis via p53 [Lavin *et al*, 2005]. Once phosphorylated, p53 becomes stabilised and blocks proliferation by up-regulation of $p21^{waf1}$, which triggers G_1/S arrest. It has been suggested that at low levels of DSBs only a minor fraction of p53 is activated, driving the transcription of the *p21* gene and causing cell-cycle arrest. By contrast, with high levels of DSBs, p53 becomes metabolically stable and transcriptionally activated, and accumulates above a particular threshold, inducing the transcriptional activation of pro-apoptotic genes such as Bax (Bcl-2-associated X protein), PUMA (p53 up-regulated modulator of apoptosis) and FAS receptor [Roos & Kaina, 2006]. p53 activation results from post-translational modifications (i.e., phosphorylations, acetylations or covalent attachments of small ubiquitin-like proteins), whereas p53 instability is due to its ubiquitination and proteosomal degradation. Both these processes are transiently suppressed after DNA damage [Bernstein *et al*, 2002].

Most human tumours lose the expression of a functional p53. However, it has been demonstrated that crucial DNA damage can activate a p53-independent apoptosis via backup systems [Roos & Kaina, 2006]. There are several strategies that cells seem to employ to trigger p53-independent DNA damage-induced apoptosis. The first one involves the p53 homologs p63 and p73 [Roos & Kaina, 2006]. It has been proposed that, upon DNA damage,

ATM and ATR activate Chk1 and Chk2, which in turn activate E2F1. This in turn stimulates transcription of the *p73* gene, giving rise to an increased level of p73 protein [Urist *et al*, 2004]. Whereas p53 requires p63 and p73 for triggering apoptosis, p73 has a pro-apoptotic activity even in the absence of p53 [Flores *et al*, 2002; Roos & Kaina, 2006]. p73-induced apoptosis was shown to be mediated by transcriptional up-regulation of PUMA, NOXA and Bax [Melino *et al*, 2004; Flinterman *et al*, 2005]. Another factor implicated in p53-independent apoptosis is NF-kB (nuclear factor-kB), which is generally anti-apoptotic as it transcribes anti-apoptotic genes. However, under some circumstances (i.e., topoisomerase inhibitor treatment [Piret *et al*, 1999], NF-kB exhibits pro-damage-signaled apoptosis, by inducing the transcription of a growing number of genes related to apoptosis, including Fas ligand [Schmitt *et al*, 2007].

Another trigger of apoptosis upon DNA damage is the inhibition of RNA synthesis, which leads to a decline in the level of critical gene products such as MKP1 (mitogen-activated protein kinase phosphatase). This causes sustained activation of JNK (Jun kinase) and AP-1, which stimulates death-receptor activation [Roos & Kaina, 2006].

The mitochondria-mediated apoptotic pathway is mediated by the mitochondrial release of cytochrome *c* [Kiechle & Zang, 2002; Reed, 2000; Zimmerman *et al*, 2002; Kroemer *et al*, 2007] (Figure 3). Bcl-2 homologous protein (including Bax) may oligomerize and form pores in the outer mitochondrial membrane, resulting in either a decrease in the inner mitochondrial transmembrane potential [Green, 2000] or opening of the voltage-dependent anion channel [Shimizu *et al*, 2001] releasing cytochrome

c from the space between the inner and outer mitochondrial membranes [Goldstein *et al*, 2000].

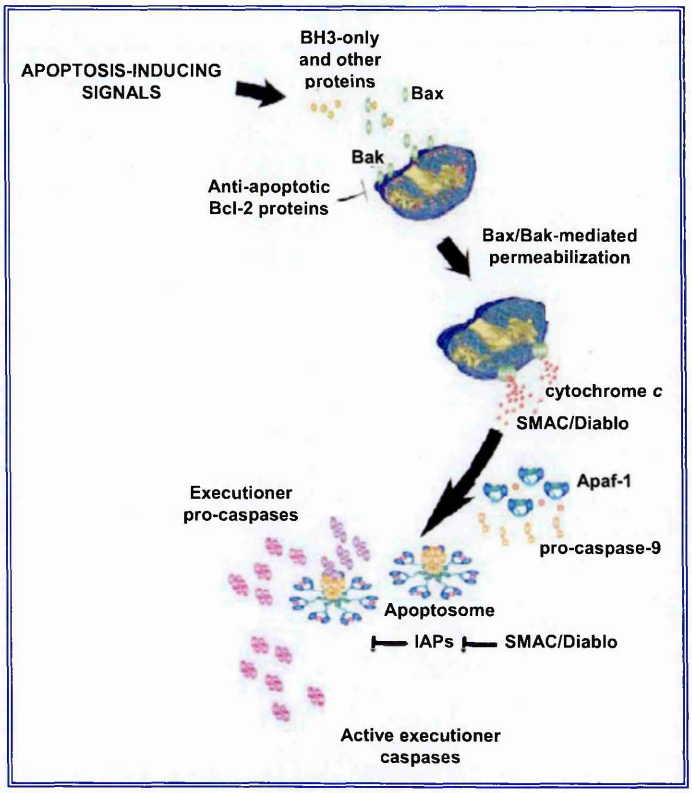

Figure 3. Mitochondrial apoptotic pathway.
Mitochondrial outer membrane permeabilization occurs when the pro-apoptotic Bcl-2 family proteins (Bax and/or Bak) are activated by BH3-only proteins in response to apoptosis-inducing signals. This results in the release of proteins of the mitochondrial intermembrane space, including cytochrome *c* and SMAC/Diablo. Cytochrome *c* activates Apaf-1, which oligomerizes to form the apoptosome, that in turn recruits and activates caspase-9. The activated caspase-9 cleaves and activates executioner caspases. IAPs block caspase-9 function and are themselves regulated by SMAC/Diablo.

Cytosolic cytochrome *c* induces the formation of the multi-subunit apoptosome composed of Apaf-1, pro-caspase-9 and either ATP or dATP [Hengartner, 2000; Cecconi & Gouss, 2001; Auchon *et al*, 2002; Zimmerman *et al*, 2002] (Figure 3). Activated caspase-9 recruits and activates caspases-3

and/or -6 and -7. Anti-apoptotic members of the Bcl-2 family, such as Bcl-2 and Bcl-x_L, control cytochrome *c* and SMAC/Diablo release [Thomadaki & Scorilas, 2006], whereas activation of caspase-9 and downstream caspases is controlled by the family of inhibitor of apoptosis proteins (IAPs) [Vaux & Silke, 2003] (Figure 3).

1.2.3. Caspases

The final pathway that leads to execution of the death signal in both intrinsic and extrinsic pathways of apoptosis is the activation of a series of proteases termed caspases [Thornberry & Lazebnik, 1998; Shi, 2002]. The name is derived from the specificity of these cysteine proteases to cleave their substrates after an aspartic acid [Thornberry & Lazebnik, 1998]. To date, more than 14 caspases have been identified [Kumar, 2007]. Of these, caspases-2, -8, -9, and -10 are thought to be initiator caspases, while caspases-3, -6 and -7 are considered to be death effectors. Other caspases including caspase-1, -4, -5, -11, -13 and -14 have been implicated in the inflammatory response [Scott & Saleh, 2007]. Caspase-12, which localizes to the endoplasmic reticulum, may play a role in the endoplasmic reticulum stress response [Nakagawa *et al*, 2000]. Generally, the cleavage of caspase specific substrates results in the biochemical destruction of the cell and phenotypic changes associated with the apoptotic program.

In cells, caspases exist as inactive zymogens that require processing to become biologically active. It is generally accepted that this occurs by either auto-proteolysis or by the proteolytic actions of other caspases. The

zymogenic form of the caspase, the pro-caspase, contains an amino terminal pro-domain, a large subunit (~20 kDa) containing the active cysteine residue, a small subunit (~10 kDa) and a variable length linker region which separates the large and small subunits [Nunez & Del Peso, 1998] (Figure 4).

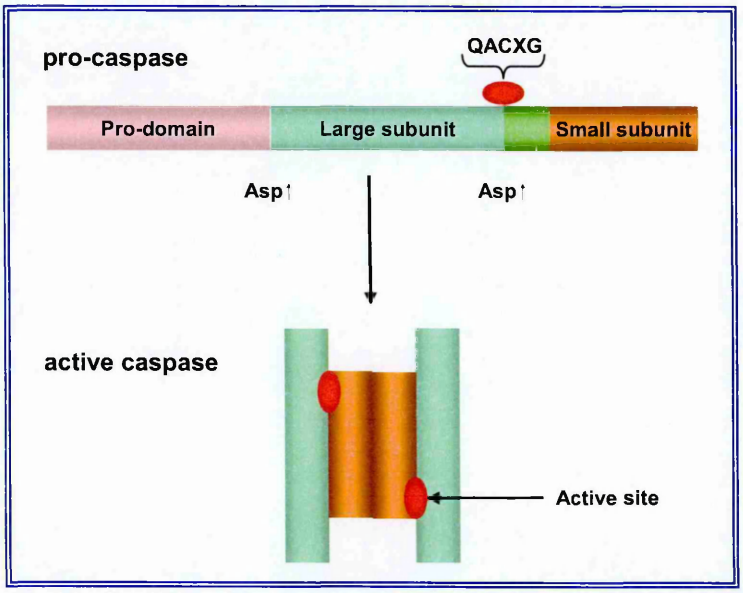

Figure 4. Schematic representation of caspase structure.
Caspases are cysteine proteases produced in cells as inactive precursors (pro-caspase) containing common structural elements: a pro-domain, a large and a small subunits and a linker region. The active site cysteine is harbored within a conserved QACXG motif in the large subunit. The caspase is activated by proteolysis that occurs at aspartate residues, residing between the pro-domain and the large subunit and within the linker region. The active caspase is a tetramer made of two large/small subunit heterodimers each with an active site.

Aspartate cleavage sites are found between the pro-domain and the large subunit as well as within the inter-domain linker. Caspase activation occurs by proteolytic cleavage of the linker region, thus allowing the large and small subunits to assemble into a functionally active heterodimer [Wilson *et al*, 1994; Nunez & Del Peso, 1998; Wolf & Green, 1999]. Initiator caspases have a long pro-domain, which contain either a CARD (caspase-2 and -9) or a

DED (caspase-8 and -10) domain [Slee *et al*, 1999]. Interaction of either the DED or CARD with corresponding regions in other initiator caspases or adaptor proteins facilitates clustering and auto-proteolysis of initiator caspases. Once activated, initiator caspases act in a hierarchical manner to cleave and activate death effector caspases. Subsequently, activated effector caspases can activate remaining initiator caspases. This system of activation enables rapid caspase mobilization and cascade amplification [Wolf & Green, 1999].

The downstream caspases induce cleavage of protein kinases, cytoskeletal proteins, DNA repair proteins, inhibitory subunits of endonucleases, and finally, destruction of "housekeeping" cellular functions. Caspases also affect cytoskeletal structure, cell cycle regulation, and signalling pathways, ultimately leading to the morphologic manifestations of apoptosis, such as DNA condensation and fragmentation, and membrane blebbing [Thornberry & Lazebnik, 1998; Kumar, 2007].

1.3. Regulators of Apoptosis

At the molecular level, the intrinsic pathway is primarily governed by a series of proteins belonging to two distinct groups [Hengartner, 2000]: those of the Bcl-2 family and those of the Inhibitors of Apoptosis Proteins (IAPs) family.

1.3.1. Bcl-2 Family Proteins

The bcl-2 gene was first discovered in human B-cell lymphomas where, by chromosomal translocations, it was moved into juxtaposition with strong enhancer elements in the immunoglobulin heavy-chain locus [Tsujimoto *et al*, 1985]. Bcl-2 gene has been established to be a proto-oncogene that prolongs cell survival by inhibiting apoptosis. Subsequent studies have demonstrated that Bcl-2 can prevent or delay apoptosis induced by a large variety of stimuli in many cell types [Hockenbery *et al*, 1990; Willis *et al*, 2003; Thomadaki & Scorilas, 2006; Zinkel *et al*, 2006]. However, the exact mechanism of its protective action remains unclear. Several hypotheses have been proposed to explain the anti-apoptotic function of Bcl-2. Bcl-2 may prevent the release of the mitochondria activators of the cytosolic caspases [Thomadaki & Scorilas, 2006]. The association of Bcl-2 with the Apaf-1 may prevent the cytochrome *c* release and the activation of the two effector caspases, caspase-9 and -3. Also, Bcl-2 might act by modulating the collapse of the mitochondrial transmembrane potential that occurs during apoptosis [Hockenbery *et al*, 1990; Kroemer *et al*, 2007].

Members of the Bcl-2 family are characterized by the presence of distinct conserved sequence motifs known as Bcl-2 homology (BH) domains designated BH1, BH2, BH3 and BH4, which correspond to α-helical segments [Adams & Cory, 2007] (Figure 5). This family members are either anti- or pro-apoptotic. Generally, the anti-apoptotic members (such as Bcl-2, Bcl-x_L, Mcl-1, A1, Bcl-W) display sequence homology in all four BH domains [Adams & Cory, 2007], whereas the pro-apoptotic members (such as Bax,

Bak, Bcl-x_S, Bok) have homologous BH1-3 domains [Puthalakath & Strasser, 2002; Adams & Cory, 2007] (Figure 5).

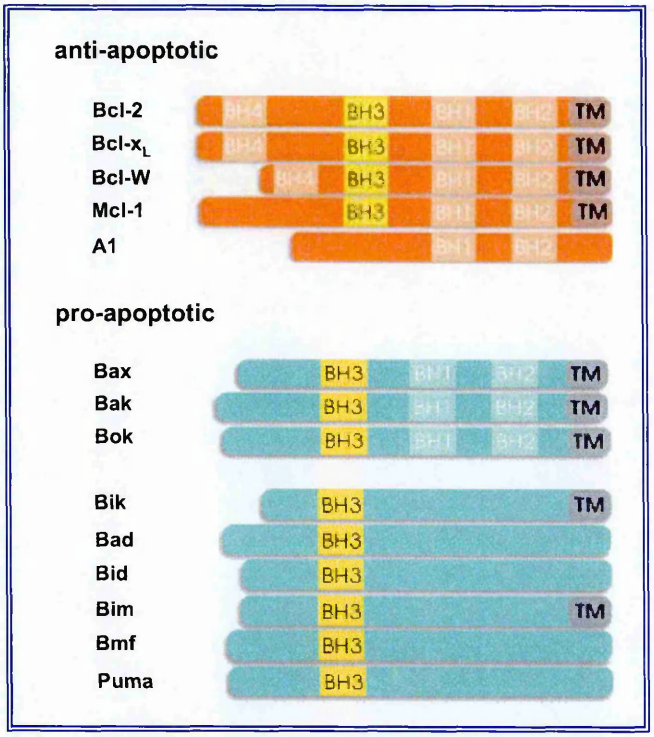

Figure 5. The Bcl-2 protein family.

Most anti-apoptotic Bcl-2 family members express four Bcl-2 homology domains (BH) as well as a putative transmembrane domain (TM) responsible for their preferred localization at inner membranes. The pro-apoptotic Bcl-2 family members can be divided into two groups: *i*, the Bax sub-family (Bax, Bak, Bok) resemble Bcl-2 closely in structure and possess three out of four BH domains; *ii*, the more distantly related 'BH3-only' proteins only share one BH3 domain with all other Bcl-2 family members. [Adapted from Ranger *et al*, 2001]

Pro-apoptotic Bcl-2 family members, upon activation by apoptotic stimuli, are capable of forming heterodimers with anti-apoptotic members. Deletion and mutagenesis studies show that the BH3 domains among pro-apoptotic members are critical for their pro-apoptotic and heterodimerization function [Opferman & Korsmeyer, 2003]. Thus, the α-helical BH3 domain serves as a

critical death domain among pro-apoptotic members. The hypothesis that the BH3 domain of pro-apoptotic members may be required and sufficient for mediating pro-apoptotic function is supported by the discovery of a third subset of the pro-apoptotic members of the Bcl-2 family (such as Bid, Bad, Bik, Bim, Bmf, Puma) that have sequence homology only in the BH3 domains [Huang & Strasser, 2000] (Figure 5).

Different Bcl-2-like proteins have different cytoplasmic distributions. Both Bcl-2 and Bcl-x_L have a carboxy-terminal membrane insertion sequence, and the majority of these proteins are found to be associated with mitochondrial membranes, endoplasmic reticulum, and nucleus [Jacobson *et al*, 1993; Wolter *et al*, 1997; Minn *et al*, 1998]. In their inactive state, the pro-apoptotic members, Bad, Bax and Bid have primarily a cytoplasmic location. However, upon activation, they translocate to the mitochondria [Wolter *et al*, 1997; Goping *et al*, 1998; Khaled *et al*, 1999; Ruffolo *et al*, 2000]. Bid and Bik can directly induce mitochondria to release cytochrome *c*, and they may also act to inhibit the anti-apoptotic actions of Bcl-2 and Bcl-x_L via the formation of heterodimers [Shimizu *et al*, 2000].

Several different cellular mechanisms exist to modulate the activity of both the pro- and anti-apoptotic function of Bcl-2 proteins. The dimerization state of Bcl-2 family members affects their activity [Korsmeyer, 1999]. One function of the anti-apoptotic Bcl-2 and Bcl-x_L is to dimerize with pro-apoptotic Bax to neutralize its activity. As a heterodimer, Bax is inactive, but once free to dimerize with itself, Bax is able to induce apoptosis [Gross *et al*, 1998; Minn *et al*, 1998]. Altering the expression levels of pro- and anti-apoptotic family members can either promote or inhibit apoptosis [Adams & Cory, 2007]. In

fact, when the amount of Bcl-2 is greater than or equal to the amount Bax, a given cell is protected from apoptosis. However, when the amount of Bax exceeds the amount Bcl-2, a cell is more prone to undergo apoptosis. Moreover, Bcl-2 proteins can be altered by phosphorylation [Ito *et al*, 1997; Maundrell *et al*, 1997; Thomadaki & Scorilas, 2006]. In its un-phosphorylated state, Bad dimerizes with Bcl-2 and Bcl-x_L, neutralizing their anti-apoptotic activity (and allowing Bax to self-associate) [Yang *et al*, 1995]. However, when Bad is phosphorylated, it is sequestered by a protein, and therefore cannot interact with and neutralize Bcl-2 and Bcl-x_L [Zha *et al*, 1998; Korsmeyer, 1999]. The function of Bcl-2 family members can be altered by cleavage. During Fas-mediated apoptosis, caspases have been shown to cleave both Bcl-2 and Bcl-x_L [Clem *et al*, 1998; Fujita *et al*, 1998]. The cleaved products are no longer protective, and in fact become pro-apoptotic [Clem *et al*, 1998; Fujita *et al*, 1998]. Bid is another Bcl-2 protein that is activated by caspase cleavage. While the full-length protein is inactive, after caspase-8-mediated cleavage, Bid induces cytochrome *c* release from the mitochondria [Li *et al*, 1998; Luo *et al*, 1998; Gross *et al*, 1999].

Finally, the conformation of Bcl-2 proteins modifies their activity. The best evidence for this mechanism comes from studies of Bax [Khaled *et al*, 1999]. In its inactive state, Bax exists in a conformation in which it is resistant to protease cleavage. However, upon activation and translocation to mitochondria, the amino-terminal region of this protein becomes susceptible to protease cleavage, suggesting that a conformational change has occurred [Khaled *et al*, 1999].

1.3.2. Inhibitor Apoptosis Proteins (IAPs) Family

The Inhibitors of Apoptosis Proteins (IAPs) family are a group of anti-apoptotic proteins that are conserved in several species [Deveraux & Reed, 1999]. These proteins characterized by one or more 70–80 amino-acid baculoviral IAP repeat (BIR) domains. The BIR domain is a characteristic cysteine-and histidine-rich protein folding domain that chelates zinc and forms a compact globular structure consisting of four or five α-helices and a variable number of antiparallel β-pleated sheets. The core of a BIR domain consists of the variable consensus sequence, C(X)2 C(X)6 (X)3 D(X)5 H(X)6 C, where X is any amino acid [Deveraux & Reed, 1999]. They were first discovered in baculoviruses, a group of viruses specific to insects [Birnbaum *et al*, 1994] and proteins containing BIR domains have been identified in a wide range of eukaryotic species, including the fission yeast *Schizosaccharomyces pombe*, the budding yeast *Saccharomyces cerevisiae*, the nematode *Caenorhabditis elegans*, the fly *Drosophila melanogaster*, and several mammalian species including mice, rats, chickens, pigs, and humans [Deveraux & Reed, 1999].

The first mammalian IAP homologue to be identified was neuronal apoptosis inhibitory protein (NAIP) (Figure 6), which was isolated during a positional cloning effort to identify the causative gene for spinal muscular atrophy [Roy *et al*, 1995]. In contrast to the baculoviral IAPs, which possess two BIR domains and a carboxy-terminal RING zinc-finger, NAIP encodes three BIR domains and a very large and unique carboxy-terminus containing a nucleotide-binding oligomerization domain [Koonin & Aravid, 2000].

Subsequent to the identification of NAIP, the IAP family expanded with the identification of cellular IAP1 (cIAP1, hIAP2), cIAP2 (hIAP1), and X-chromosome-linked IAP (XIAP) (Figure 6), all of which contain three BIR domains and a carboxy-terminal RING finger [Rothe *et al*, 1995; Duckett *et al*, 1996; Liston *et al*, 1996; Uren *et al*, 1996]. Finally were identified survivin (with a single BIR and the carboxy-terminal coiled-coil domain) [Ambrosini *et al*, 1997], Livin or ML-IAP (with a single BIR and the carboxy-terminal RING finger) [Lin *et al*, 2000; Vucic *et al*, 2000; Kasof & Gomes, 2001], the testis-specific IAP (Ts-IAP, with a single BIR and the carboxy-terminal RING finger) [Lagace *et al*, 2001; Richter *et al*, 2001], and the Apollon/BRUCE (with a single BIR and the carboxy-terminal ubiquitin-conjugating enzyme) [Hauser *et al*, 1998; Verhagen *et al*, 2001] (Figure 6).

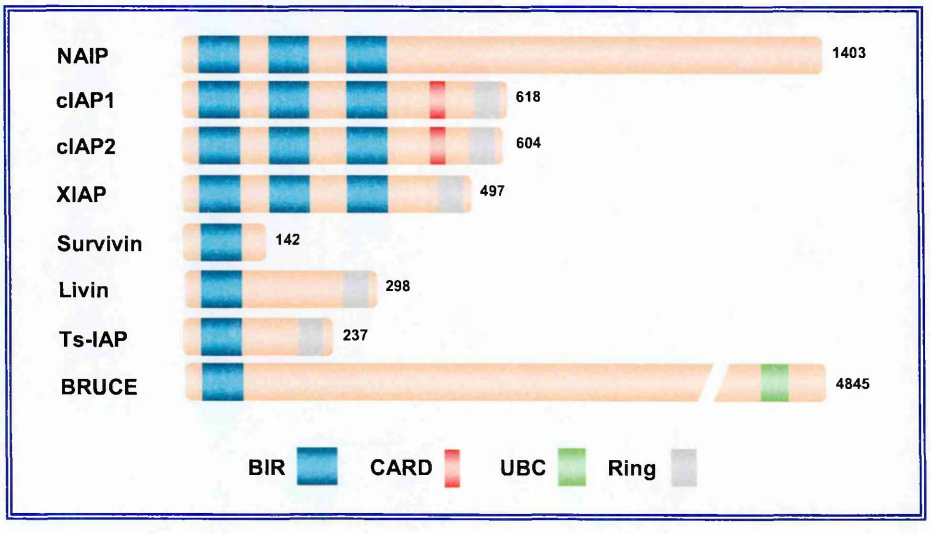

Figure 6. Schematic structure of the domains of the mammalian IAP family.
The first mammalian IAP homologue, NAIP, encodes three BIR domains and a very large and unique carboxy-terminus containing a nucleotide-binding oligomerization domain; cIAP1, cIAP2 and XIAP contain three BIR domains and a carboxy-terminal RING finger; survivin contains a single BIR and the carboxy-terminal coiled-coil domain; Livin and Ts-IAP encode a single BIR and carboxy-terminal RING finger; and BRUCE contains a single BIR and an UBC motif.

The characterization of IAP proteins suggests that they function as suppressor of cell death in a variety of tissue culture systems, including triggers of both the endogenous and exogenous pathways of apoptosis [LaCasse *et al*, 1998; Deveraux & Reed, 1999; Wright & Duckett, 2005]. It was subsequently shown that the IAPs could directly inhibit the activity of several recombinant caspases *in vitro* [Deveraux *et al*, 1997; Roy *et al*, 1997; Maier *et al*, 2002], and structure-function studies of IAP family proteins have demonstrated a requirement for at least one BIR domain for suppression of apoptosis, although other domains found within some IAPs may also be required under certain circumstances. Several of the mammalian, fly, and viral IAPs have a RING domain located near their carboxyl termini (Figure 6). The necessity for the RING domain for suppression of apoptosis appears to depend on cellular context. In fact, some reports have indicated that the baculoviral IAPs require both amino-terminal BIR domains and the carboxy-terminal RING domain for their anti-apoptotic function in insect cells [Clem & Miller, 1994; Harvey *et al*, 1997]. By contrast, the human proteins cIAP1, cIAP2, and XIAP have been reported to retain anti-apoptotic function in the absence of their carboxy-terminal RING domains [Deveraux *et al*, 1997; Roy *et al*, 1997; Takahashi *et al*, 1998].

The BIR domains of the IAPs are the most fully characterized functional units of the IAPs. Each BIR domain folds into a functionally independent structure that chelates a zinc ion and consists of a globular head and an unstructured tail derived from the amino-terminal 'linker' region located upstream of the individual BIR domains. Specific interactions with initiator (caspase-9) and effector (caspase-3 and -7) caspases have been mapped to

individual BIR domains. As a general rule, the IAPs containing multiple BIRs employ the third BIR domain to inhibit caspase-9, and the second BIR domain functions to inhibit caspase-3 and -7 [Roy *et al*, 1997; Takahashi *et al*, 1998; Maier *et al*, 2002]. As regards single BIR-containing proteins, Ts-IAP inhibits caspase-9 [Richter *et al*, 2001], while the survivin and livin inhibit caspase-3, -7 and -9 [Lin *et al*, 2000; Vucic *et al*, 2000; Kasof & Gomes, 2001; Shin *et al*, 2001].

Among the mammalian IAPs that are known to be involved in apoptosis, X-linked IAP (XIAP) has been characterized extensively (Figure 7).

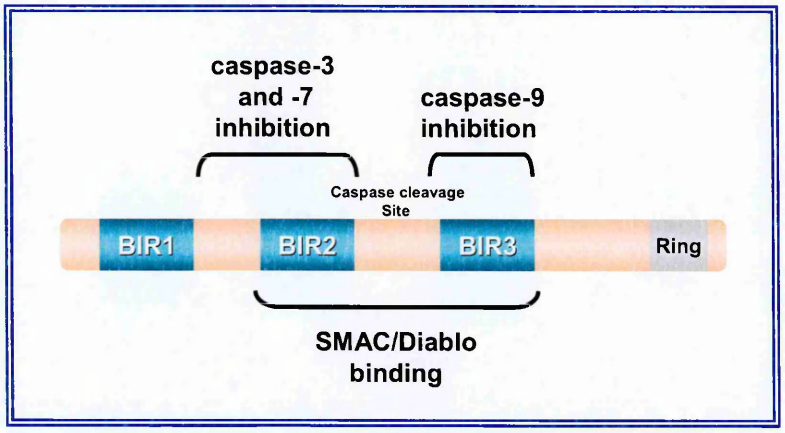

Figure 7. Map of XIAP activities and interactions.
XIAP contains three BIR domains and a C-terminal RING motif. BIR2 binds to and inhibits active caspase-3 and caspase-7, whereas BIR3 potently targets active caspase-9. No specific function has been identified for the BIR1 domain. SMAC/Diablo peptide, released from mitochondria during apoptosis, binds to a highly conserved surface groove on the BIR3 domain of XIAP, and re-activates the processed initiator and effector caspases.

This protein contains three BIR domains and a C-terminal RING motif. The second BIR domain (BIR2) specifically binds to and inhibits active caspase-3 and caspase-7, whereas BIR3 potently targets active caspase-9 [Shi, 2002]. No specific function has been identified for the BIR1 domain of XIAP. The

linker segment that immediately precedes the BIR2 domain of XIAP binds to the active site of effector caspase-3 and caspase-7, hence, preventing substrate binding and subsequent catalysis. By contrast, the BIR3 domain of XIAP employs a different method to inhibit the initiator caspase, caspase-9. Caspase-9 becomes catalytically active through a conformational change when bound by Apaf-1, and thus appears to be unique among the caspases in that there is no absolute requirement for proteolytic activation. In addition to its ability to proteolytically process caspase-3, caspase-9 can undergo a self-cleavage event in the linker region between the p20 and p10 subunits. The XIAP BIR3 domain directly binds caspase-9 via this newly exposed amino terminus and the interaction is stabilized through additional contacts with the enzyme. Using purified caspase-9 and XIAP BIR3, in the absence of Apaf-1 and cytochrome *c*, it was demonstrated that this interaction prevents caspase-9 homodimerization and stabilizes the enzyme in an inactive state similar to its monomeric form [Shiozaki *et al*, 2003]. It has been proposed that a similar change in caspase-9 morphology occurs within the apoptosome complex as a consequence of XIAP binding. Caspase-9 can also undergo further cleavage catalysed by caspase-3. This proteolytic event further increases the enzymatic activity of caspase-9, and was proposed to remove the peptide sequence that binds XIAP [Srinivasula *et al*, 2001].

In the intrinsic cell death pathway, the key event leading to the activation of caspases is the release of several pro-apoptotic proteins from the intermembrane space of mitochondria into the cytosol [Wang, 2001]. One such protein is SMAC/Diablo [Du *et al*, 2000; Verhagen *et al*, 2000]. The newly synthesized SMAC/Diablo protein contains 239 amino acids. Its N-

terminal 55 residues encode the mitochondrial-targeting sequence and are proteolytically removed in the mature SMAC/Diablo protein [Du *et al*, 2000]. This cleavage results in the exposure of four hydrophobic amino acids, Ala-Val-Pro-Ile, at the N-terminus of mature SMAC/Diablo. This tetrapeptide represents the founding member of a family of IAP-binding motifs in mammals and fruit flies [Shi, 2002]. Structural analysis reveals that this tetrapeptide motif binds to a highly conserved surface groove on the BIR3 domain of XIAP [Liu *et al*, 2000; Wu *et al*, 2000] (Figure 7). The interactions between SMAC/Diablo and IAPs requires that the N-terminus of the tetrapeptide is exposed, which explains why only the mature form of SMAC/Diablo is functional in cells. Before apoptosis, accidental activation of either caspase-9 or caspase-3 and caspase-7 might not lead to cell death because of the inhibitory effect of IAPs. During apoptosis, SMAC/Diablo is released from mitochondria and re-activates the processed initiator and effector caspases by relieving IAP-mediated inhibition.

1.4. Apoptosis & Cancer

In cancer cells, the growth equilibrium, determined as the ratio between the rate of cell proliferation and incidence of apoptosis, is uncontrolled, and the increase in abnormal proliferation of cancer cells causes tumour invasion and metastatic potential [Olopade *et al*, 1997].

The goal of most cancer therapies, including radiotherapy, chemotherapy, immunotherapy and gene therapy is the reduction or elimination of cancer

cells. Drug resistance is a major problem that limits the success of the treatment. In fact, most tumours are intrinsically resistant to chemotherapy prior to treatment. Other tumours, initially sensitive, recur and are resistant not only to the initial therapeutic agents, but also to other drugs not used in the treatment. Drug resistance, whether intrinsic or acquired, is believed to cause treatment failure in over 90% of patients with metastatic cancer, and resistant micrometastic tumour cells may also reduce the effectiveness of chemotherapy in the adjuvant setting.

Cancer cell resistance to chemotherapy can occur at many levels, including increased drug efflux and decreased drug influx, drug inactivation, alterations in drug target, processing of drug-induced damage. Apoptosis pathways are also extremely related to drug sensitivity and resistance. Apoptosis in tumour cells plays a critical role in chemotherapy-induced tumour cell killing thus suggesting that blockade of the apoptosis-inducing pathway could be another mechanism for multidrug resistance [Kim *et al*, 2002]. Several studies have demonstrated that high Bcl-2 expression in cancers (particularly lymphomas) correlates with poor response to chemotherapy [Campos et al, 1993; Hermine et al, 1996; Bonetti et al, 1998; Schmitt et al, 2000; Reed & Pellecchia, 2005; Adams & Cory, 2007]. However, other studies have shown either no correlation between Bcl-2 expression and drug response [Colleoni et al, 1999; Bottini et al, 2000; Sjostrom et al, 2002; Adams & Cory, 2007], or an association between Bcl-2 and good prognosis [Fontanini et al, 1995; Sjostrom et al, 2002; Adams & Cory, 2007]. Some clinical studies have also demonstrated a correlation between Bax expression and response to chemotherapy [Krajewski et al,

1995; Kymionis et al, 2001; Adams & Cory, 2007]; however, such an correlation was not confirmed in other studies [Campos et al, 1993; Paradiso et al, 2001; Adams & Cory, 2007]. It has been also demonstrated that NAIP XIAP, cIAP1,and cIAP2, diminish apoptosis triggered by a number of agents including camptothecin and menadione *in vitro* [Liston *et al*, 1996]. However, it has been found that expression of cIAP1, cIAP2, and XIAP did not predict response to chemotherapy in patients with advanced non-small cell lung cancer [Ferreira *et al*, 2001]. Finally, silencing of Apaf-1 has been reported in melanoma cell lines and clinical samples [Soengas *et al*, 2001]. The Apaf-1-deficient melanoma cells exhibited diminished apoptosis in response to doxorubicin [Soengas *et al*, 2001].

Resistance to apoptosis causes a decrease in the sensitivity of cancer cells to drugs, resulting in the failure of chemotherapy. Since the induction of apoptosis following chemotherapy is associated with the activation of pro-apoptotic genes and the suppression of anti-apoptotic genes, attenuation of pro-apoptotic genes and increases in anti-apoptotic genes causes resistance to apoptosis [Kaufmann & Vaux, 2003]. Thus, targeting apoptosis-related genes may lead to new strategies to increase the therapeutic effect of cancer chemotherapy. *In vitro* studies have shown that targeting death receptors with recombinant death ligands or agonistic antibodies can induce apoptosis and/or enhance chemotherapy-induced apoptosis [Petak *et al*, 2000; Fan *et al*, 2004; Longley et al, 2004; Wu *et al*, 2004]. Most pre-clinical studies are focused on local administration of rFasL, or the use of FasL-expressing vectors as gene therapy [Timmer *et al*, 2002]. However, it has been developed a non-hepatotoxic agonistic Fas antibody [Timmer *et al*, 2002],

suggesting that it is possible to develop less toxic Fas antibodies. Apoptosis mediated by Fas can be inhibited by cytoplasmic factors, including c-FLIP, which binds to the DISC and inhibits caspase-8 activation [Krueger *et al*, 2001]. Moreover, c-FLIP overexpression has been found to inhibit death receptor-mediated apoptosis in a number of *in vitro* studies [Hu *et al*, 1997; Irmel *et al*, 1997; Srinivasula *et al*, 1997]. Small RNA interfering targeting of c-FLIP dramatically sensitises a panel of colon cancer cell lines to 5-FU, oxaliplatin, and CPT-11 [Galligan *et al*, 2005], suggesting an important role for c-FLIP in regulating colon cancer cell chemosensitivity. A promising clinical approach may be to target the TRAIL receptors, as TRAIL has been shown to exert marked anticancer activity without systemic toxicity in mice [Ashkenazi *et al*, 2002]. Approaches for targeting TRAIL receptors are currently being tested in the clinic.

At mitochondrial level, *in vitro* studies have demonstrated that down-regulation of Bcl-2 and Bcl-X_L using antisense techniques sensitises cells to chemotherapy [Teixeira *et al*, 1995; Zangemeister-Wittke *et al*, 2003; Hayward *et al*, 2004; Adams & Cory, 2007], whereas loss of Bax expression has been found to decrease chemosensitivity [Zhang *et al*, 2000; Adams & Cory, 2007]. An antisense oligonucleotide against Bcl-2 (oblimersen) has been in phase III clinical trials for melanoma, CLL and multiple myeloma, as well as in phase II clinical trials for several other cancers [Cummings *et al*, 2004; Gleave & Monia, 2005], but the results in the clinic are not very promising [Fesik, 2005]. Recently antisense oligonucleotides have been used to reduce IAP protein levels in cancer cells. Down-regulation of XIAP protein levels induced apoptosis in chemoresistant ovarian cancer cells [Sasaki et al,

2000] and increased doxorubicin activity in bladder cancer [Bilim *et al*, 2003]. An antisense oligonucleotide targeting XIAP are now in phase I clinical trials [McManus *et al*, 2004].

2. SURVIVIN

The mammalian IAP survivin is a bifunctional protein that facilitates tumour cell evasion from apoptosis and promotes mitotic progression [Altieri & Marchisio, 1999].

Survivin was discovered in 1997 by hybridisation screening of a human genomic library with the cDNA of the effector cell protease receptor-1 (EPR-1) [Ambrosini *et al*, 1997]. Survivin has a particular relationship to EPR-1: in fact its sequence is complementary to and in the reverse orientation of EPR-1.

2.1. Protein Structure of Survivin

The *survivin* human gene spans 14.7 kb, and is located on the telomeric position of chromosome 17 at band q25 [Ambrosini *et al*, 1998]. It comprises three introns and four exons, a TATA-less proximal promoter, and approximately 200 nt GC-rich regions upstream of exon 1 [Ambrosini *et al*, 1997]. The gene encodes a 16.5 kDa protein of 142 amino acids. The amino-terminal portion of survivin consists of three α helices (residues 14-21, 31-41, 68-80) and 3 β-sheets (residues 43-45, 55-58, 61-64), which closely resemble the BIR domain that is conserved in the IAP family [Ambrosini *et al*, 1997; Chantalat *et al*, 2000] (Figure 8). Differently from other IAPs, survivin contains only one BIR and a carboxy-terminus coiled-coil, but no RING finger or other identifiable domain [LaCasse *et al*, 1998].

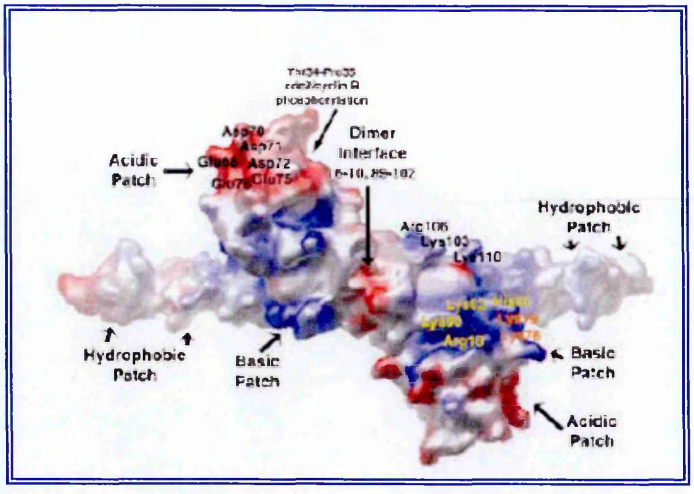

Figure 8. Representation of survivin protein structure.
The amino-terminal portion of survivin consists of three α helices (residues 14-21, 31-41, 68-80) and 3 β-sheets (residues 43-45, 55-58, 61-64), which closely resemble the BIR domain. Differently from other IAPs, survivin contains only one BIR and a carboxy-terminus coiled-coil, but no RING finger or other identifiable domain. [Adapted from Verdecia *et al*, 2000]

Crystal structure analysis of survivin revealed that it exists as a dimer, with the two BIR domains forming a "bow-tie-shape" [Chantalat *et al*, 2000] (Figure 9). The carboxy-terminal helix is not involved in the dimerization of survivin but extends outward from the entwined BIR structure [Chantalat *et al*, 2000].

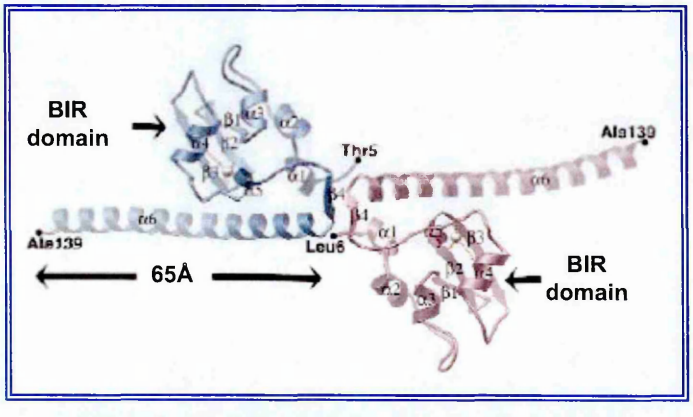

Figure 9. Representation of the survivin dimer.
[Adapted from Verdecia *et al*, 2000]

The survivin gene is subjected to alternative splicing (Figure 10). Human survivin gene has four dominant (1, 2, 3, and 4) and two hidden (2B and 3B) exons. Alternative splicing of its pre-mRNA produces four different mRNAs, which encode four distinct proteins, survivin, survivin-2B, survivin-ΔEx3 [Mahotka *et al*, 1999], and survivin-3B [Badran *et al*, 2004] (Figure 10).

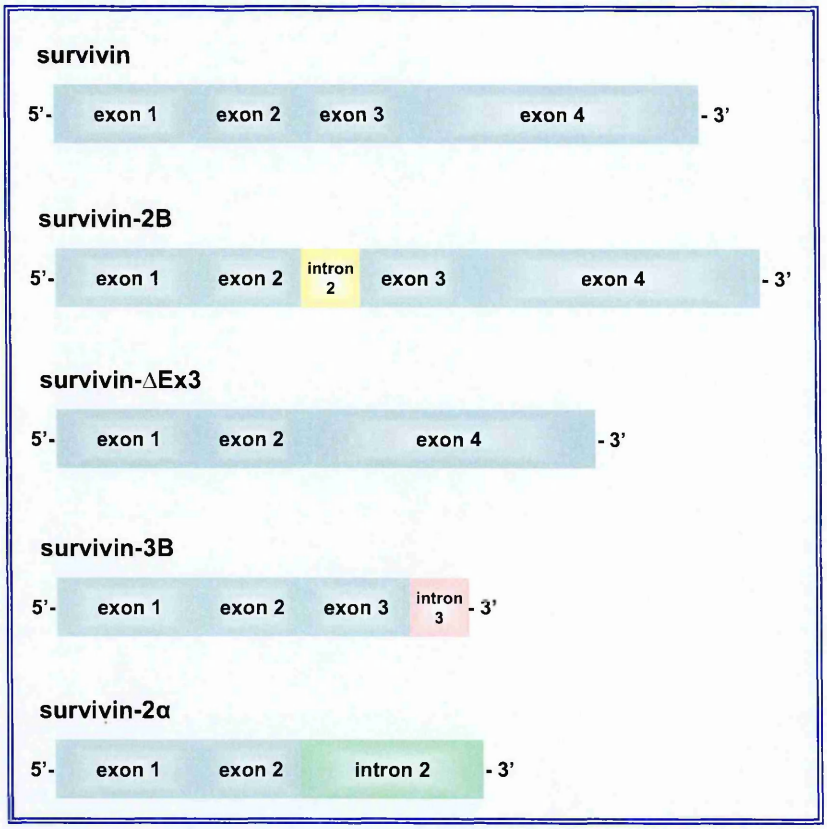

Figure 10. Schematic representation of the alternative splicing variants of survivin.

Human survivin gene has four dominant (1, 2, 3, and 4) and two hidden (2B and 3B) exons. Alternative splicing of its pre-mRNA produces different mRNAs, which encode five distinct proteins, survivin, survivin-2B, survivin-ΔEx3, survivin-3B, and survivin 2α.

Survivin (142 aa) is derived from exons 1-4; survivin-2B (167 aa) has an additional 23 aa derived from a 69-bp cryptic exon (2B) within intron 2, which is spliced into survivin mRNA in frame between exons 2 and 3 (Figure 10);

survivin-ΔEx3 (137 aa) is derived from exons 1, 2, and 4, a frameshift read-through variant due to exon 3 escape (Figure 10); and the survivin-3B (120 aa) consists of the N-terminal 113 aa of survivin (coded by exons 1, 2, and 3) plus seven new aa sequences at carboxy-terminal tail encoded by a DNA sequence (exon 3B) from intron 3 (Figure 10). Recently, an additional splice variant, survivin 2α, has been identified [Caldas *et al*, 2005]. Structurally, the transcript consists of 2 exons: exon 1 and exon 2, as well as a 3' 197 bp region of intron 2 (Figure 10). Acquisition of a new in-frame stop codon within intron 2 results in an open reading frame of 225 nucleotides, predicting a truncated 74 amino acid protein [Caldas *et al*, 2005a].

Little is known about the differential functions of survivin alternative splice forms, which are generally expressed at lower levels than the wild-type survivin. However, it has been reported that the expression of survivin-2B is predominant in some neuroblastoma with a good prognosis, but it is expressed at low levels in most malignant tissues [Islam *et al*, 2000]. In renal cell carcinomas (RCC), while the expression levels of survivin and survivin-ΔEx3 did not show a decrease in late tumour stages in comparison with the early and intermediate tumour stages in 57 clinical RCC samples, survivin-2B expression was significantly decreased in late tumour stages [Mahotka *et al*, 2002a], indicating a possible unfavourable role of these splicing variant in the development of this tumour type. In gastric cancer, the expression of survivin-ΔEx3, survivin-2B, and survivin (dominant transcript) was found in clinical samples, irrespective of their histological type, grade, or stage [Krieg *et al*, 2002; Meng *et al*, 2004]. However, survivin-2B expression was significantly decreased in later tumour stage in comparison with early stage

[Krieg *et al*, 2002; Meng *et al*, 2004], and inversely correlated with tumour differentiation and invasion [Meng *et al*, 2004]. The expression of survivin and survivin-ΔEx3 remained unchanged in different stages of cancer [Krieg *et al*, 2002], and the expression level of survivin-ΔEx3 is inversely correlated with apoptotic index [Meng *et al*, 2004]. It was also reported that survivin-2B expression was dominant in benign brain tumours in comparison with the malignant ones [Yamada *et al*, 2003], and that survivin-ΔEx3 expression was prominent in comparison with survivin-2B expression in survivin-expressing acute lymphocytic leukaemia and chronic lymphocytic leukaemia patient bone marrow samples [Nakagawa *et al*, 2004].

Preliminary data would suggest that heterodimerisation of survivin with survivin-ΔEx3 is essential for the inhibition of mitochondrial-dependent apoptosis [Caldas *et al*, 2005b], further suggesting a possible anti-apoptotic role for survivin-ΔEx3. In addition, the different subcellular localisation of survivin-ΔEx3 (in nucleus) and survivin-2B (in cytoplasm) [Mahotka *et al*, 2002b] suggests their potential different functions. These observations indicate that survivin-ΔEx3 and survivin-2B may play an opposing role in tumour progression and tumorigenesis. Moreover, it has been demonstrated in exogenous expression assays that survivin 2α attenuates the anti-apoptotic activity of survivin [Caldas *et al*, 2005a]. More recently, it was reported that despite their ability to interact with wild-type survivin, alternative splice isoforms such as survivin-ΔEx3 and survivin-2B do not play a role in mitosis since they do not localize with the chromosomal passenger complex *in vivo* as a consequence of their reduced affinity for the survivin partner Borealin [Noton *et al*, 2006]. Moreover, these splice variants cannot rescue

cell proliferation inhibited by RNAi-mediated survivin depletion [Noton *et al*, 2006].

Survivin exhibits cell cycle-dependent expression at mitosis. This requires canonical CDE/CHR boxes in the proximal survivin promoter [Kobayashi *et al*, 1999; Badie *et al*, 2000] acting as G_1-repressor elements to shut down gene transcription in interphase cells [Kobayashi *et al*, 1999]. Survivin levels are regulated by rapid changes in protein stability. Poly-ubiquitination on multiple Lys residues and proteasomal-dependent destruction has been proposed as a mechanism to maintain low levels of survivin in interphase cells [Zhao *et al*, 2000], thus further enhancing cell cycle periodicity. In addition, mitotic phosphorylation of survivin on Thr34 by $p34^{cdc2}$-cyclin B1 has been associated with increased survivin stability at metaphase [O'Connor *et al*, 2002]. It has been suggested that this pathway is dominant in normal cells and constitutes the primary function of survivin in adult tissues [Yang *et al*, 2004; Altieri, 2006].

Other non-cell-cycle-dependent mechanisms driving *survivin* gene transcription independent of mitosis have been described, which involve tissue patterning circuits (Wnt/β-catenin) [Kim *et al*, 2003], cytokine activation (STAT3) [Gritsko *et al*, 2006], costimulatory messages (OX-40) [Song *et al*, 2005] and pleiotropic signaling mechanisms (AkT, NFkB) [Mitsiades *et al*, 2002] that are operative during development and generally up-regulated in cancer cells [Vogelstein & Kinzler, 2004] and can explain survivin overexpression in the large majority of human tumours. It has been recently suggested that these non-cell-cycle-dependent pathways are dominant in tumours. This hypothesis also relies on the fact that a transgenic mouse

model expressing the green fluorescent protein reporter gene under the control of the minimal survivin promoter demonstrated that expression of survivin in development and tumour formation is largely independent of cell-cycle-dependent transcription of the survivin gene at mitosis [Xia & Altieri, 2006]. The fraction of survivin produced through these non-cell-cycle–dependent mechanisms mediates apoptosis inhibition through intermolecular cooperation with cofactors including the hepatitis B virus X interacting protein [Marusawa *et al*, 2003], a target of the oncogenic viral HBX protein, and XIAP [Dohi *et al*, 2004a].

2.2. Survivin & Inhibition of Apoptosis

Survivin plays an important role in the suppression of apoptosis by either directly or indirectly inhibiting the activity of caspases (Figure 11).

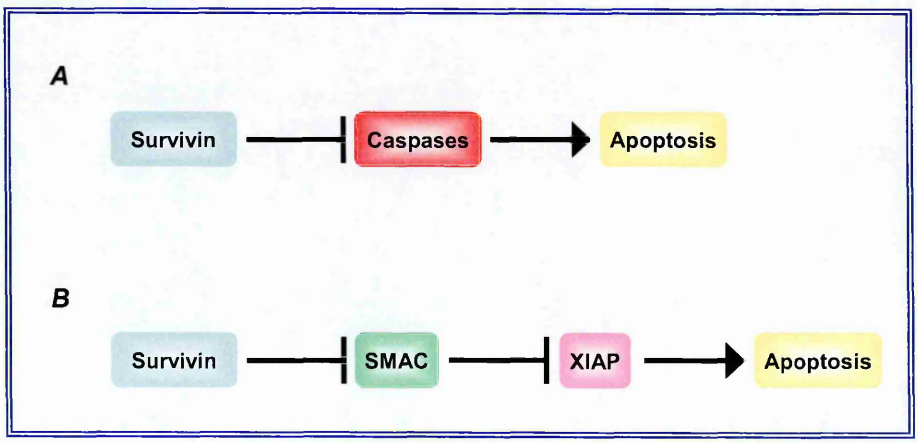

Figure 11. The role of survivin in the apoptosis pathways.
Survivin may regulate apoptosis (**A**) directly inhibiting the caspases responsible for induction and execution of apoptosis; (**B**) indirectly inhibiting caspase function by regulating SMAC/Diablo.

The IAP family members have been shown to suppress apoptosis by direct inhibition of caspases [Deveraux & Reed, 1999] via the BIR domains [Miller, 1999] (Figure 11A). The structure of survivin has been compared to another IAP family member, XIAP (Figure 7). XIAP inhibits caspase-3 and caspase-7 via a linker region between the first two BIR domains, and also binds to and inhibits caspase-9 through its third BIR (BIR3) domain [Sun *et al*, 1999]. The BIR domain of survivin appears closely related in three-dimensional structure to the BIR3 domain of XIAP, suggesting the possibility that survivin binds caspase-9 [Shi, 2000]. The interaction between survivin and caspase-9, and the functional implications of this interaction, have been studied through mutagenesis. Loss of phosphorylation at Thr^{34} on the T34A mutant of survivin results in dissociation of an immunoprecipitable survivin-caspase-9 complex on the mitotic apparatus, allowing caspase-9 dependent apoptosis [O'Connor *et al*, 2000].

Survivin may also inhibit caspase activity indirectly (Figure 11B). There is evidence of an indirect regulation of caspase activity by survivin in the mitochondrial pathway of apoptosis. Haepatocytes of heterozygous survivin knockout mice contain low basal levels of activated pro-caspase-8, Bid, pro-caspase-9, and pro-caspase-3, and have increased susceptibility to Fas-induced apoptosis [Conway *et al*, 2002]. Fas-induced apoptosis is associated with release of cytochrome *c* and up-regulation of survivin in the mitochondria as well as in the nucleus and cytosol [Conway *et al*, 2002]. Upon Fas stimulation in cell culture, survivin has been shown to interact with cdk4, which releases p21 from its complex with cdk4 [Suzuki *et al*, 2000] making it possible for p21 to complex with caspase-3, the initial step in inactivating

caspase-3 in the mitochondria. In addition, overexpression of a second mitochondrial- derived activator of caspases, SMAC/Diablo, increases Apo-2L/TRAIL-induced caspase-3 activity, and down-regulates the activity of survivin and other IAPs such as XIAP and cIAP1 [Guo *et al*, 2002]. SMAC/Diablo is released from mitochondria into the cytosol along with cytochrome *c* during execution of the mitochondrial apoptosis pathway. SMAC/Diablo can promote apoptosis by binding to and suppressing the inhibitory effects of the IAP proteins [Du *et al*, 2000]. Survivin may possibly function to inhibit caspase activity indirectly via binding to and sequestering SMAC/Diablo, thus preventing SMAC/Diablo binding to other IAPs [Du *et al*, 2000] (Figure 11B).

The mechanism of caspase-3 inhibition by survivin remains controversial. There are reports indicating that purified survivin directly binds to caspase-3 and inhibits its activity *in vitro* [O'Connor *et al*, 2000; Shin *et al*, 2001]. However, the survivin protein lacks the linker region found in other IAP members that is responsible for their interaction with caspase-3 [Sun *et al*, 1999].

Moreover, subcellular compartmentalization of survivin in mitochondria seems to play a role in the anti-apoptotic function of the protein. Specifically, the existence of a mitochondrial pool of survivin was recently reported, and it was found that, in response to cell death stimulation, mitochondrial survivin is rapidly discharged and released into the cytosol, where it prevents caspase activation and inhibits apoptosis [Dohi *et al*, 2004b]. In addition, survivin was not seen in mitochondria in normal tissues, suggesting that mitochondrial survivin is exclusively associated with tumour transformation [Dohi *et al*,

2004b]. A very recent study found that survivin has a nuclear export signal and that in cancer cells the anti-apoptotic and mitotic roles of survivin can be separated through mutation of its NES, which abrogates the cytoprotective activity of the protein but still allows mitosis to proceed [Colnaghi *et al*, 2006].

2.3. Survivin & Cell Division

During the cell cycle, survivin localizes to various components of the mitotic apparatus [Vagnarelli & Earnshaw, 2004] (Figure 12).

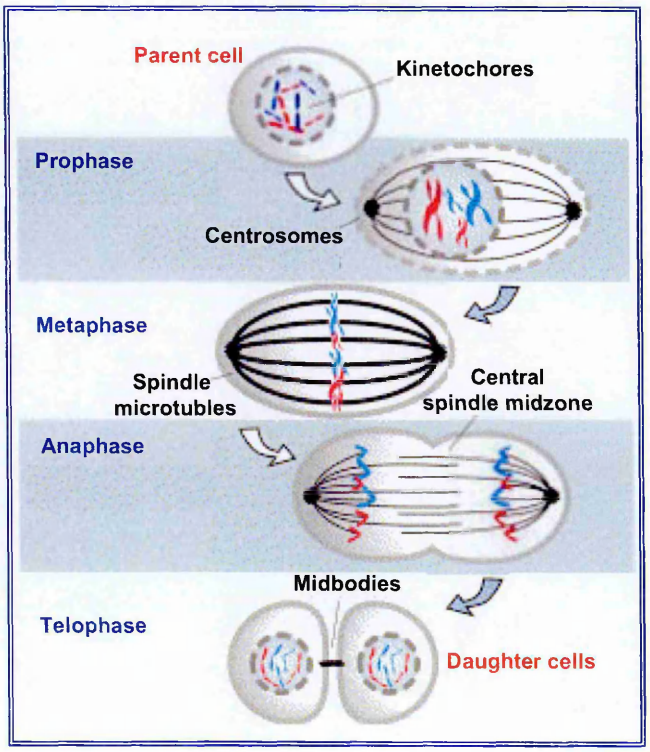

Figure 12. The role of survivin in the cell cycle.
Survivin is detected on centromeres at prophase/metaphase, in the spindle midzone during anaphase/telophase, but is no longer detected by the end of telophase. Survivin has been found to be localized to kinetochores until metaphase: to the spindle midzone in anaphase and in the cleavage plane during telophase and cytokinesis.

Survivin is first detected on centromeres at prophase/metaphase; it is present in the spindle midzone during anaphase/telophase, but is no longer detected by the end of telophase [Li *et al*, 1998; Uren *et al*, 2000]. Moreover, survivin is localized to kinetochores until metaphase, then to the spindle midzone in anaphase and in the cleavage plane during telophase and cytokinesis [Skoufias *et al*, 2000].

In summary, survivin exists in two immunohistochemically distinct pools, with a nuclear pool localised to kinetochores of metaphase chromosomes and to the central spindle midzone at anaphase, and a cytosolic pool associated with interphase microtubules, centrosomes, spindle poles and mitotic spindle microtubules at metaphase and anaphase [Fortugno *et al*, 2002]. The microtubule-associated pool appears to be quantitatively predominant and functionally relevant. These findings, together with the phenotype of knockout mice (which is characterised by a catastrophic defect of microtubule assembly, with absence of mitotic spindle, formation of multinucleated cells and 100% embryonic lethality [Uren *et al*, 2000]), are consistent with a critical role of survivin in mitosis to preserve the mitotic apparatus and to allow normal mitotic progression. In fact, it has been demonstrated that survivin down-regulation causes pleiotropic cell-division defects [Li *et al*, 1999; Chen *et al*, 2000]. Moreover, forced expression of survivin in HeLa epithelial carcinoma cells profoundly influenced microtubule dynamics and also caused stabilization of microtubules against nocodazole-induced depolymerization, thus indicating that survivin may facilitate evasion from checkpoint mechanisms of growth arrest and, consequently, promote resistance to drugs targeting the mitotic spindle [Giodini *et al*, 2002].

Additional evidence indicates that survivin also participates in the regulation of chromosome segregation [Kallio *et al*, 2001], and that the protein cooperates together with the chromosomal passenger proteins INCENP and Aurora-B to perform its mitotic duties [Carvalho *et al*, 2003].

2.4. Regulation of Survivin Function

A critical requisite for survivin function was identified in the phosphorylation on threonine 34 [O'Connor *et al*, 2000]. The only kinase recognized to phosphorylate survivin is $p34^{cdc2}$-cyclinB1, a cyclin-dependent kinase that is only active during certain points in the cell cycle [O'Connor *et al*, 2000]. The $p34^{cdc2}$-cyclin B1 was shown, *in vivo*, to physically associate with survivin and to phosphorylate survivin on Thr^{34} during mitosis. A direct link between survivin and $p34^{cdc2}$-cyclin B1 was independently confirmed using array technology in gene-profiling studies of large-cell non-Hodgkin's lymphoma; it was associated with an activated B-cell phenotype and unfavourable disease progression [Kuttler *et al*, 2002]. Mutants of $p34^{cdc2}$-cyclin B1 prevent survivin phosphorylation, and the enzyme can be co-immunoprecipitated with survivin in cells that have been synchronized in mitosis. Although other members of the cdc2 family of kinases may also associate with survivin [Suzuki *et al*, 2000], they are active only during certain cell cycle transitions, and thus the activity of survivin as an apoptosis-blocking protein is likely restricted to dividing cells. The p53-dependent repression of cdc2 expression has been demonstrated during G_2-arrest

[Passalris *et al*, 1999], suggesting the hypothesis that p53 loss is associated with greater phosphorylation of survivin and thus more complete suppression of apoptosis.

Expression of non-phosphorylatable survivin $Thr^{34}\rightarrow Ala$ prevented phosphorylation of endogenous survivin, resulting in apoptosis of various cancer cell types [O'Connor *et al*, 2000], and suppressed cell growth *in vivo* [Grossman *et al*, 2001; Mesri *et al*, 2001]. Moreover, inhibitors of cyclin-dependent kinases (cdk) such as flavopiridol or the more $p34^{cdc2}$-specific inhibitor, purvalanol A, were tested in tumour cells arrested at mitosis with paclitaxel, which induces hyperphosphorylation of survivin on Thr^{34} [Zaffaroni *et al*, 2002]. Sequential administration of cdk inhibitors resulted in escape from the mitotic block imposed by paclitaxel, marked activation of mitochondrial-dependent apoptosis and anticancer activity *in vivo* [O'Connor *et al*, 2002].

A physical interaction with the molecular chaperone heat shock protein 90 (Hsp90), which involves the Hsp90 ATPase domain and the survivin BIR domain, was shown to be essential for the stability and function of survivin. In fact, targeted antibody-mediated disruption of the survivin-Hsp90 complex in cancer cells resulted in proteasomal degradation of survivin, mitochondrial-dependent apoptosis, and mitotic arrest [Fortugno *et al*, 2003].

2.5. Survivin Expression in Normal & Tumour Tissues

One of the most significant features of survivin is its differential expression in cancer versus normal tissues. Survivin expression in normal tissues is developmentally regulated and the protein was found to be absent or low in most terminally differentiated tissues [Ambrosini *et al*, 1997]. However, recent studies tend to attribute a role to survivin in regulating the function of normal adult cells [Fukuda *et al*, 2006] including vascular endothelial cells [Mesri *et al*, 2001], polymorphonuclear cells [Altznauer *et al*, 2004], T cells [Xing *et al*, 2004], erythroid cells [Gurbuxani *et al*, 2005], and haematopoietic progenitor cells [Fukuda & Pelus, 2001]. Moreover, survivin expression was reported in adult liver cells [Deguki *et al*, 2002], gastrointestinal tract mucosa [Chiou *et al*, 2003] and ovarian granulosa cells [Wang *et al*, 2004]. However, although survivin is expressed in normal tissues characterized by self-renewal and proliferation, its expression is significantly lower than in transformed cells. In fact, several studies have demonstrated strong survivin expression in most human solid tumour types and haematologic malignancies [Altieri, 2003]. Expression of survivin has also been detected in a variety of benign and preneoplastic lesions including polyps of the colon, breast adenomas, Bowen's disease and hypertrophic actinic keratosis [Altieri, 2003], suggesting that re-expression of survivin may occur early during malignant transformation or following a disturbance in the balance between cell proliferation and cell death. The up-regulation of survivin at the transcriptional level in human tumours has been confirmed in genomewide searches, which indicated survivin as the fourth top 'transcriptome' in cancers of various histology

[Velculescu *et al*, 1999]. Moreover, global deregulation of the *survivin* gene mediated by oncogenes such as STAT3 [Gritsko *et al*, 2006], E2F [Jiang *et al*, 2004], and activated H-Ras [Sommer *et al*, 2003; Fukuda & Pelus, 2004], or by loss of tumour suppressors like wild type p53 [Hoffman *et al*, 2002] or the adenomatous polyposis coli protein [Zhang *et al*, 2001], seems to be responsible for the enhanced expression of survivin in tumours.

Growing evidence suggests that survivin expression in cancer cells is associated with clinicopathologic variables of aggressive disease and may represent an important prognostic marker for patient outcome. In fact, several studies on different types of solid tumours and haematologic malignancies showed that high levels of the protein were predictive of tumour progression in terms of either disease-free or overall survival [Altieri, 2003]. In several neoplasms the association with tumour progression was corroborated in the context of a comprehensive analysis of gene-expression profiling by DNA microarray or PCR-based assay. As it is possible to immunohistochemically distinguish two intracellular pools of survivin, a nuclear and a cytosolic one, the prognostic significance of the protein has been analyzed in some studies as a function of its intracellular localization, and inconsistent and sometimes contrasting results have been obtained regarding the prognostic value of nuclear survivin expression [Fengzhi *et al*, 2005]. The different prognostic value of survivin may reflect differences in methods to detect its expression and/or a differential expression of survivin splice variants.

2.6. Survivin as a Determinant of Treatment Resistance

Considering that apoptosis is the primary mode of cell death induced by several classes of chemical and physical agents commonly used in cancer therapy, it has been hypothesized that survivin expression/up-regulation could be crucial in determining the chemo- and radio-sensitivity profiles of tumour cells. This possibility is supported by several experimental evidences demonstrating that survivin is able to counteract a broad range of different apoptotic stimuli.

Giodini *et al* [2002] first reported that infection of HeLa cells with an adenoviral vector expressing survivin suppressed apoptosis induced by taxol. Successively, studies performed on human ovarian carcinoma cell lines and clinical specimens clearly indicated that survivin is involved in regulating cell sensitivity to taxanes. Specifically, the OAW42 and IGROV-1 human ovarian cancer cell lines were transfected with the human survivin cDNA. Stable transfection with survivin cDNA was able to protect these cells from the cytotoxic effects induced by paclitaxel and taxotere, with IC_{50} values for the survivin-transfectant cell populations 4-6-fold those of the control cells [Zaffaroni *et al*, 2002]. Zhang *et al* [2005] showed that forced expression of wild type survivin in human prostate cancer cell lines increased the resistance to taxol *in vitro* and *in vivo*. In addition, in the clinical setting, in advanced ovarian cancer patients receiving a paclitaxel+platinum-based regimen, the overexpression of the anti-apoptotic protein correlated with a lower clinical or pathologic complete remission rate (with respect of those

treated patients where survivin expression was found to be low or absent) [Zaffaroni *et al*, 2002].

It has been reported that taxol-induced microtubule stabilization and mitotic arrest increase the expression of survivin, which engenders a cell survival pathway to counteract taxol-induced apoptosis [O'Connor *et al*, 2002]. Interestingly, using a taxol-resistant ovarian cancer cell clone, PTX10, with a β-tubulin mutation at the taxol binding site, Zhou *et al* [2004] found that taxol treatment failed to induce mitotic arrest and survivin expression. However, the finding that taxol induced an apoptotic response in these cells suggests that mitotic arrest is not strictly required for taxol-induced apoptosis. It is also possible that the mitotic survival pathway is not the only one by which cancer cells counteract taxol-induced apoptosis. In fact, Ling *et al* [2004] reported that induction of survivin by taxol in MCF-7 cells is an early event and is independent of taxol-mediated G_2/M arrest, suggesting a role for survivin in taxol resistance not only during mitosis but outside of the mitotic checkpoint as well. There is evidence that the mTOR pathway, which constitutes a sensor network for stress conditions, is involved in resistance to paclitaxel by increasing survivin levels [Vaira *et al*, 2006]. In fact, it has been recently reported that IGF-1-mediated mTOR activation in prostate cancer cells positively modulated survivin levels by favoring stabilization and translation of a survivin mRNA pool, and that mTOR inhibition with rapamycin, alone or in combination with paclitaxel, abolished survivin increase. Consistent with a critical reduction of the anti- apoptotic threshold maintained by survivin, the paclitaxel plus rapamycin combination was more

effective than either treatment in reducing cell viability of in the presence of IGF-1 [Vaira *et al*, 2006].

An increase in survivin expression has also been reported in prostate cancer [Nomura *et al*, 2005] and thyroid cancer [Tirro *et al*, 2006] cell lines permanently resistant to cisplatin as well as in colorectal cancer cells resistant to TRAIL [van Geelen *et al*, 2004]. Zhang *et al* [2005] showed that survivin mediates resistance to anti-androgen therapy with flutamide in prostate cancer cells. Specifically, these authors suggested that up-regulation of survivin via insulin-like growth factor-1/AKT signaling during androgen blockade may be one of the mechanisms by which prostate cancer cells develop resistance to anti-androgens. Paik *et al* [2004] showed that survivin was one of the sixteen genes predictive of recurrence in tamoxifen-treated breast cancer patients.

Regarding the role of survivin in determining the response of human tumour cells to radiation, Asanuma *et al* [2000] first reported that survivin acts as a constitutive radio-resistance factor in pancreatic cancer cells. Specifically, in a panel of established cell lines they found an inverse relationship between survivin mRNA expression and *in vitro* sensitivity to X-irradiation. Moreover, they demonstrated that survivin mRNA expression was increased by sublethal doses of X-irradiation, which would suggest that the protein also acts as an inducible radioresistance factor. Rodel *et al* [2003] also showed an inverse correlation between survivin expression and apoptotic response to irradiation in a panel of colorectal carcinoma cell lines. More recently, in a translational study of 59 rectal cancer patients treated with a combination of radiotherapy and chemotherapy, the same authors

reported that increased survivin expression was associated with a significantly increased risk of local tumour recurrence [Rodel *et al*, 2005]. It is worthy of note that survivin can contribute to radiation resistance also by promoting the survival of tumour vascular endothelial cells. In fact, induction of vascular endothelial apoptosis was recently shown to be a major determinant of overall tumour response to radiotherapy [Garcia-Barros *et al*, 2003]. Radiation may induce tumour cells to secrete cytokines such as vascular endothelial growth factor, which in turn could inhibit radiation-induced apoptosis of vascular endothelial cells by up-regulating survivin expression, as already demonstrated for drug-induced apoptosis [Tran *et al*, 2002].

3. SURVIVIN-DIRECTED CANCER THERAPY

In recent years considerable efforts have been made to validate survivin as a new target in cancer therapy. In this context, a collection of different approaches to counteract survivin in tumour cells, including antisense oligonucleotides, ribozymes, small interfering RNAs (siRNAs) and dominant-negative mutants, as well as cyclin-dependent kinase inhibitors, have been proposed with the dual aim to inhibit tumour growth potential and to enhance tumour cell response to apoptosis-inducing anticancer agents (Figure 13).

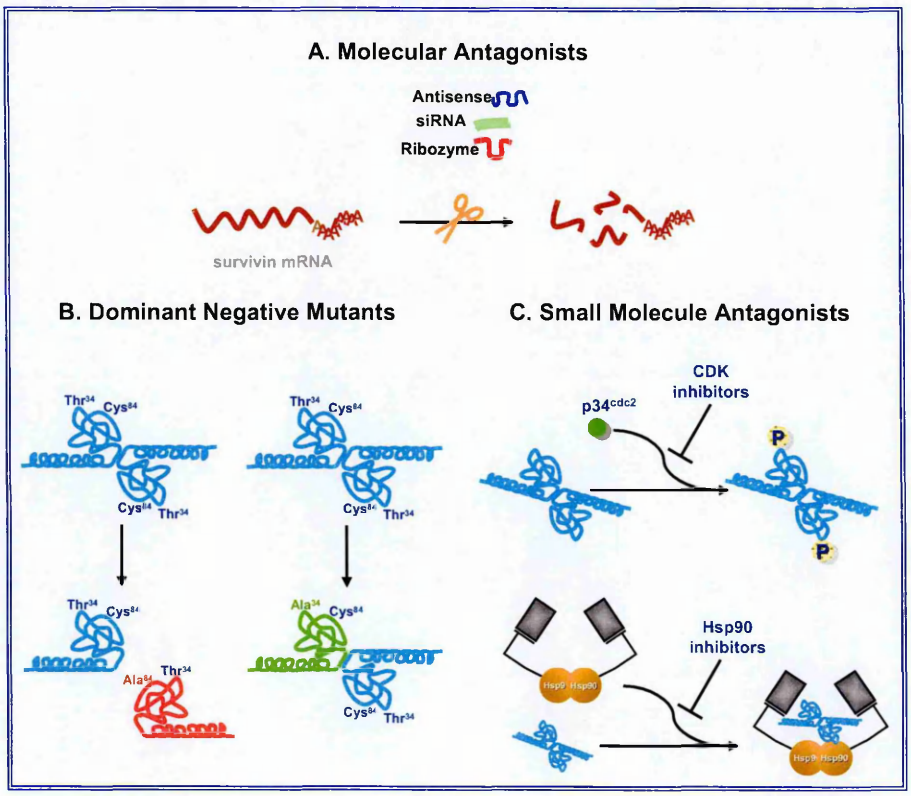

Figure 13. Summary of the current strategies for survivin targeting in cancer therapy.

A, Molecular antagonists able to target survivin mRNA and inhibit translation; **B**, Dominant negative mutants able to inhibit survivin dimerization or survivin activation; **C**, Small molecule antagonists able to inhibit survivin phosphorylation on Thr^{34} residue (CDK inhibitors) or to counteract survivin-Hsp90 interaction (Hsp90 inhibitors). In B and C, the wild type protein is reported in its dimeric arrangement [Muchmore *et al*, 2000].

3.1. Molecular Antagonists

A number of technologies have been used in an attempt to down-regulate gene expression. At present, there are three well documented genetic approaches being pursued to affect the ablation of defective gene production (Figure 14).

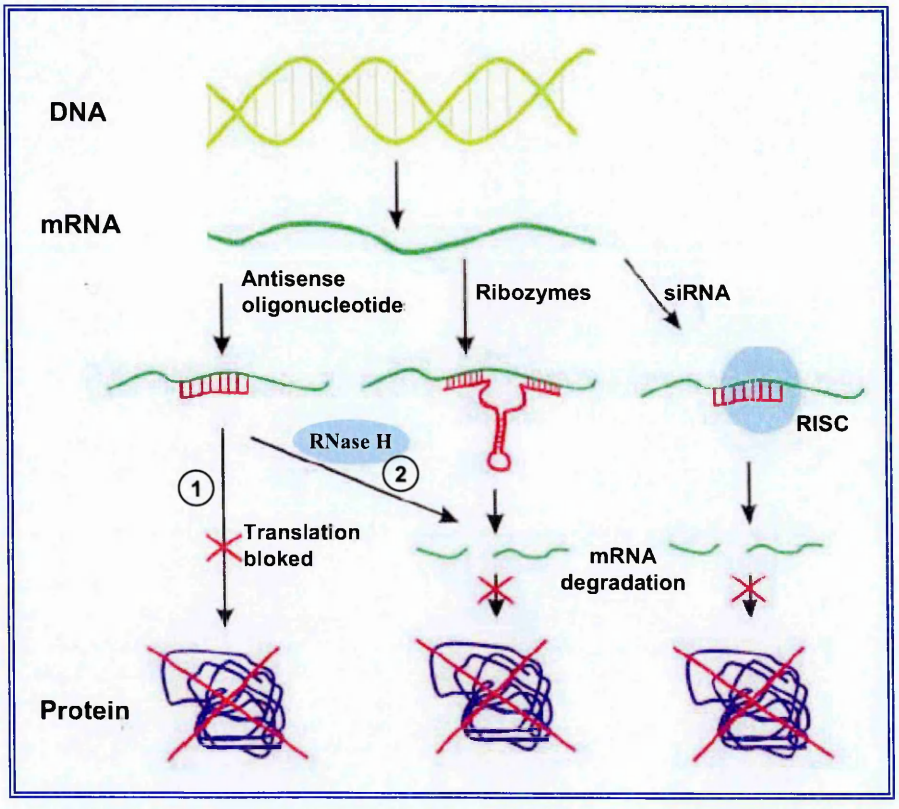

Figure 14. Schematic representation of the most exploited antisense approaches.

Antisense oligonucleotides block translation (occupancy mechanism) (**1**) or induce the degradation (RNase H-meduated mechanism) (**2**) of the mRNA. Catalytic nucleic acids (ribozymes and DNA enzyme) lead to mRNA degradation through a cleavage mechanism. siRNA, the effectors molecules of the RNA interference pathway after being recruited into RISC complex induce degradation of the target mRNA [Adapted from Kurreck *et al*, 2003].

The use of antisense RNA or deoxyoligonucleotides [Milligan et al, 1993; Crook & Bennet, 1996; Pan & Clawson, 2006], serve primarily to block gene expression by interfering with RNA translation. Ribozyme and DNA enzyme are catalytically active oligonucleotides that not only bind, but can also cleave, their target RNA in a highly sequence-specific manner [Sun et al, 1997; Welch et al, 1998; Rossi, 1999]. In recent years, considerable progress has been made through the development of novel chemical modifications to stabilize oligonucleotides against nucleolytic degradation and enhance their target affinity. In addition, RNA interference has been established as a third, highly efficient method of suppressing gene expression in mammalian cells by the use of 21–23-mer small interfering RNA (siRNA) molecules [Elbashir et al, 2001].

3.1.1. Antisense Oligonucleotides

Among the anticancer approaches, antisense-based strategies, first developed as a powerful means for target validation, represent a useful tool to inhibit specific gene expression for therapeutic purposes [Kurreck, 2003]. In fact, several antisense oligonucleotides (AS-ONs) are being tested in clinical trials on patients with cancer or other diseases [Dean & Bennet, 2003; Kureck, 2003]. Antisense oligomers are nucleic acid-related molecules that target a given RNA within cells in a sequence-specific manner, through Watson-Crick base pairing. The modality of action of AS-ONs can be distinguished in two main mechanisms (Figure 15).

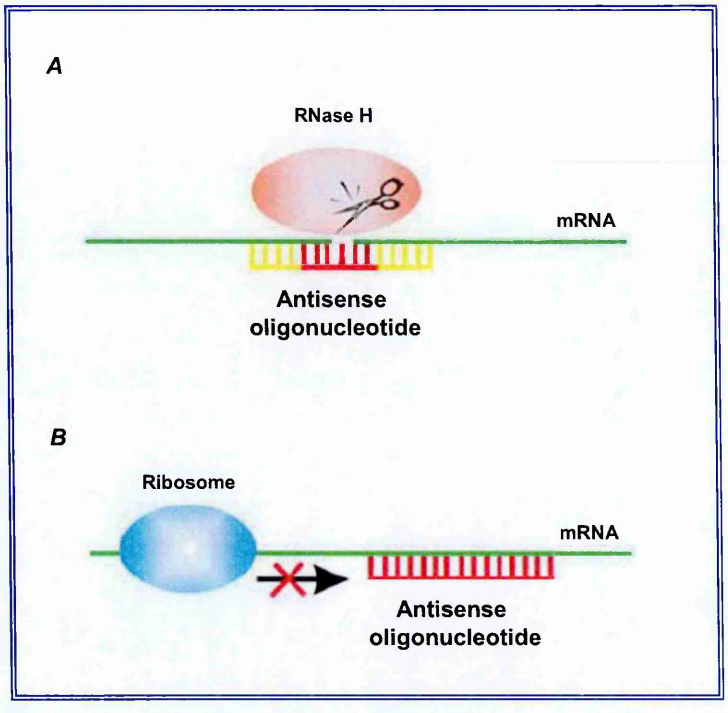

Figure 15. Mechanisms of action of antisense oligonucleotides.
A, RNase H cleavage induced by antisense oligonucleotides; **B**, Translational arrest by blocking the ribosome. [Adapted from Kurreck *et al*, 2003].

The modality of action defined as cleavage mechanism leads to degradation of the RNA target through the oligomer-mediated recruitment of RNase H (a family of ubiquitously expressed enzymes that cleaves the RNA strand of an RNA/DNA heteroduplex) or RNase L. Conversely, the modality of action, defined as a non-RNA-cleaving mechanism, is based on a steric block of RNA transcription/translation mediated by oligonucleotides that do not recruit endonucleases, such as peptide nucleic acids (PNAs) and 2'-alkyl oligomers (i.e. occupancy mediated mechanism) [Crooke, 1999].

One of the major challenges for antisense approaches is the stabilization of oligonucleotides, which as unmodified oligodeoxynucleotides are rapidly degraded in biological fluids by nucleases. A vast number of chemically

modified nucleotides have been used in antisense experiments. In general, three types of modifications of ribonucleotides can be distinguished (Figure 16): analogs with unnatural bases, modified sugars (especially at the 2' position of the ribose) or altered phosphate backbones. A variety of heterocyclic modifications have been described, which can be introduced into AS-ONs to strengthen base-pairing and thus stabilize the duplex between AS-ONs and their target mRNAs.

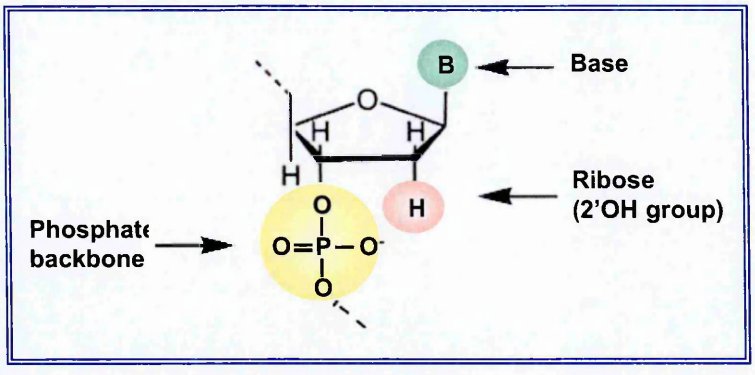

Figure 16. Sites for chemical modifications of ribonucleotides. Three types of modifications of ribonucleotides can be distinguished: analogs with unnatural bases (B), modified sugars or altered phosphate backbones. [Adapted from Kurreck *et al*, 2003].

Phosphorothioate oligodeoxynucleotides (PTO) are the major representatives of first generation DNA analogs, which are widely employed in clinical trials [Crooke, 1999] (Figure 17). In the PTO molecule, one of the nonbridging oxygen atoms of the phosphodiester linkage is replaced by a sulfur atom, which enhances resistance to nuclease action. The mechanism of action of these oligomers relies on RNase H activation. The major disadvantage of PTO is their binding to certain proteins, particularly those that interact with polyanions such as heparin-binding proteins [Brown *et al*,

1994; Rockwell *et al*, 1998]. The reason for this nonspecific interaction is not yet fully understood, but it may cause cellular toxicity [Levin, 1999] and reduce their therapeutic index [Pirollo *et al*, 2003].

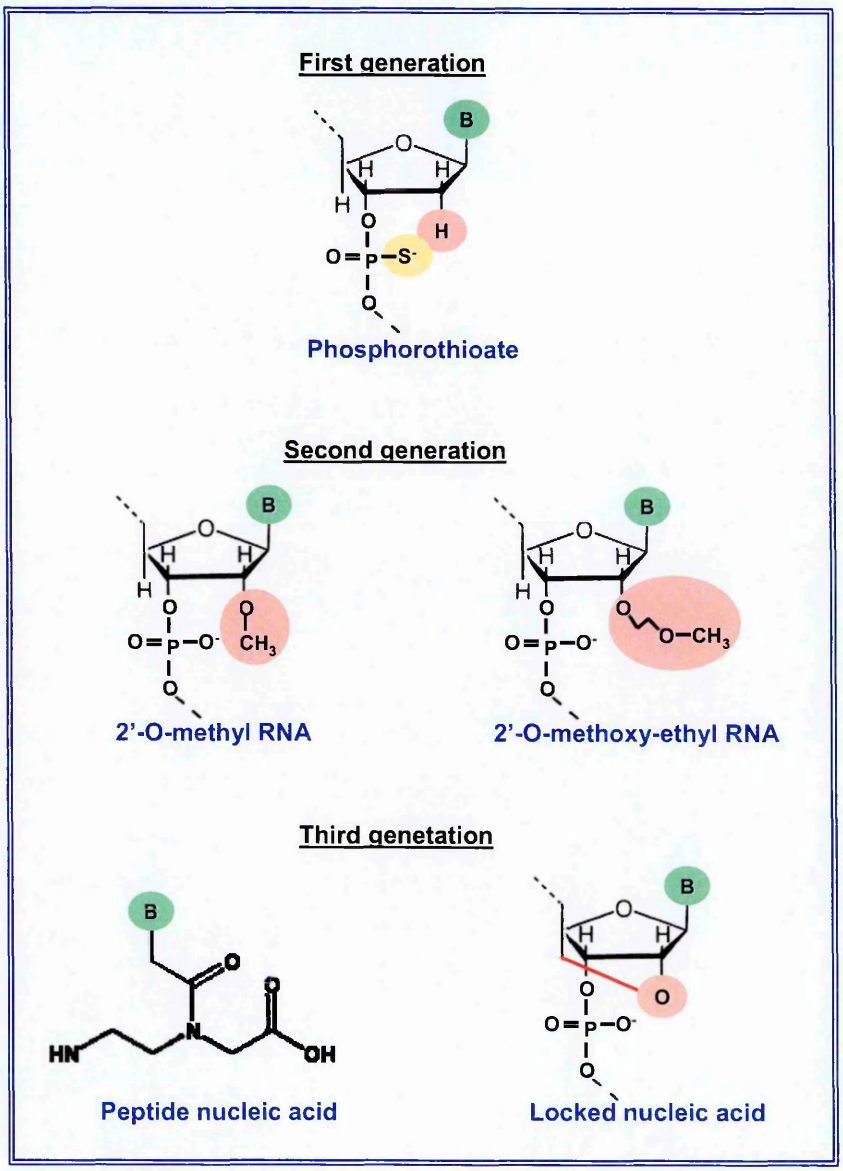

Figure 17. Example of the antisense oligonucleotides chemically modified.
'B' denotes one of the base adenine, guanine, cytosine or thymine.

The problems associated with PTO are to some degree solved in second generation oligonucleotides containing nucleotides with alkyl modifications at

the 2' position of the ribose. 2'-O-methyl and 2'-O-methoxy-ethyl RNA (Figure 17) are the most important members of this class. Such oligomers are less toxic than PTO and possess enhanced stability and binding affinity to the target with respect to their analogous RNA or DNA counterparts. However, 2'-O-alkyl oligomers do not activate RNase H to induce the cleavage of the target RNA, and their antisense effect is a consequence of the occupancy-mediated mechanism [Crooke, 1999; Dean & Bennet, 2003; Kureck, 2003] (Figure 15).

In recent years a variety of modified nucleotides have been developed to improve properties such as target affinity, nuclease resistance and pharmacokinetics. Peptide nucleic acids (PNAs) belong to the third generation of antisense oligonucleotides and are the most intensively studied DNA analogs [Kurreck, 2003]. In PNAs, the phosphate backbone is replaced by a pseudopetide linkage composed of N-(2-aminoethyl) glycine units (Figure 17). The uncharged nature of the PNA internucleotide backbone increases the stability of the PNA/nucleic acid duplex and affords greater resistance to protease and nuclease than unmodified ODNs [Gambari, 2001] but does not lead to degradation of the RNA target by recruiting RNase H. The Watson-Crick base-pairing rules are strictly observed in hybrids of PNA and nucleic acids [Egholm *et al*, 1993; Smulevitch *et al*, 1996; Gambari, 2001]. Moreover, PNAs are better at discriminating between base-pair mismatches [Egholm *et al*, 1993; Gambari, 2001] and are less likely to bind to proteins through non-sequence-specific interactions than PTOs. The lack of electrostatic repulsion between the two strands in a PNA/nucleic acid duplex also leaves the melting temperature largely independent of the salt

concentration. Their favourable properties have led to the use of PNAs for different applications in oncology. A number of experiments with permeabilised cells, isolated nuclei and also intact cells has demonstrated the potential of PNA in antigene or antisense applications to down-regulate the transcription or translation of cancer-related genes. PNA invasion of the DNA double helix to form a stable PNA-DNA hybrid was found to effectively block gene transcription [Ray & Norden, 2000; Knauert & Glazer, 2001; Pooga *et al*, 2001]. The N3'-P5' phosphoroamidates (NPs) are another example of a modified phosphate backbone, in which the 3'-OH group of the sugar residue is replaced by a 3'-NH group [Kurreck, 2003] (Figure 17). Such a modification confers to the oligonucleotide high binding affinity to the target RNA and a greater nuclease resistance. One of the most promising candidates of chemically modified nucleotides developed in the last few years is locked nucleic acid (LNA), a ribonucleotide containing a methylene bridge that connects the 2'-oxygen of the ribose with the 4'-carbon [Braasch & Corey, 2001; Vester B & Wengel J, 2004; Karkare S & Bhatnagar, 2006] (Figure 17). Introduction of LNA into a DNA oligonucleotide induces a conformational change of the DNA/RNA duplex towards the A-type helix [Bondensgaard *et al*, 2000] and therefore prevents RNase H cleavage of the target RNA.

3.1.1.1. Cellular Uptake of Antisense Oligonucleotides

An important hurdle for successful antisense applications is the cellular uptake of the molecules. In cultured cells, internalization of naked DNA is usually inefficient, due to the charged oligonucleotides having to cross a hydrophobic cell membrane. A number of methods have therefore been developed for *in vitro* and *in vivo* delivery of oligonucleotides [Huges *et al*, 2001; Liang *et al*, 2002]. By far the most commonly and successfully used delivery systems are liposomes and charged lipids, which can either encapsulate nucleic acids within their aqueous center or form lipid–nucleic acid complexes as a result of opposing charges (Figure 18). These complexes are usually internalized by endocytosis. For efficient release of the ONs from the endosomal compartment, many transfection reagents contain helper lipids that disrupt the endosomal membrane and help to set the oligonucleotides free. A number of macromolar delivery systems have been developed recently that mediate a highly efficient cellular uptake and protect the bound oligonucleotides against degradation in biological fluids.

Further polymers for the delivery of AS-ONs consist of amino acids or sugars. Evidence has been provided, however, that the structural properties of a peptide conjugated to an oligonucleotide do not significantly alter its ability to cross mammalian plasma membranes [Oehlke *et al*, 2002]. Therefore, aspects other than improved translocation across the membrane are likely to be responsible for enhanced biological activity of peptide-oligonucleotide derivatives.

Another strategy for effective targeting of AS-ONs to specific tissues or organs is receptor-mediated endocytosis. For this purpose, oligonucleotides are conjugated to antibodies or ligands that are specifically recognized by a certain receptor, which mediates their uptake into target cells. For example, coupling of a radioactively labelled PNA to a transferrin receptor monoclonal antibody made the antisense agent transportable through the blood–brain barrier [Shi *et al*, 2000].

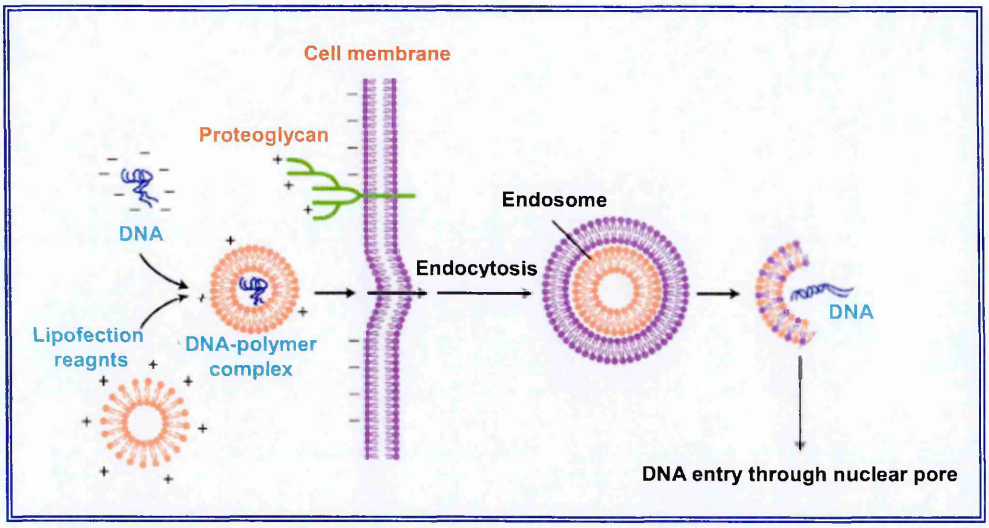

Figure 18. The method of entry of DNA–polymer complexes.
DNA and polymer are mixed to form complexes that are overlaid onto a monolayer of cells. Uptake occurs by endocytosis. The mechanism of release from the endosome still remain unclear. Transport to the nucleus occurs by active transport through the nuclear pore complex and represents the major barrier for the efficient uptake of foreign DNA. [Adapted from Parker *et al*, 2003]

3.1.1.2. Survivin Inhibition by Antisense Oligonucleotides

The use of antisense to ablate expression of endogenous survivin mRNA and protein has consistently shown promising results in several independent studies (Figure 13A).

Grossman *et al* [1999] first demonstrated that transfection of survivin antisense triggered spontaneous apoptosis in the absence of other stimuli in YUSAC2 and LOX human melanoma cell lines. Successively, several studies dealing with the use of survivin antisense oligonucleotides, delivered to the cells as chemically synthesized molecules or through the use of expression vectors, consistently showed that specific inhibition of survivin mRNA and protein could reduce cell proliferation and induce caspase-dependent apoptosis in established cell lines of different tumour origins including lung, bladder, head and neck, and thyroid cancers, sarcomas and lymphomas [Ansell *et al*, 2004; Cao *et al*, 2004; Fuessel *et al*, 2004; Sharma *et al*, 2005; Du *et al*, 2006]. Moreover, down-regulation of survivin was shown to sensitise human tumour cells to cytotoxic drugs such as etoposide and cisplatin [Sharma *et al*, 2005], as well as ionizing radiation [Sah *et al*, 2006]. Antisense-mediated survivin knockdown also caused inhibition of tumour growth in xenograft models [Ansell *et al*, 2004; Cao *et al*, 2004] and sensitised lung cancer xenografts to radiotherapy [Cao *et al*, 2004]. Kanwar *et al* [2001] demonstrated that survivin inhibition resulted in increased sensitivity to immunotherapy in murine EL-4 thymic lymphoma. Specifically, tumours injected with plasmids encoding survivin antisense were significantly inhibited in their growth. Such growth delay was further enhanced by concomitant injection of the T-cell costimulator B7-1.

Supported by a favorable safety profile, the first antisense oligonucleotide, LY2181308 (ISIS 23722, Lilly and Co, and ISIS Pharmaceuticals Inc), already entered the clinic and is currently undergoing phase I trials in patients with advanced cancers.

3.1.2. Ribozymes & siRNAs

3.1.2.1. Ribozymes

Ribozymes are small RNA molecules that possess specific endonucleolytic activity and catalyze the hydrolysis of specific phosphodiester bonds, resulting in cleavage of RNA target sequences [Puerta-Fernandez *et al*, 2003]. In nature, existing catalytic RNAs include hammerhead, hairpin, hepatitis delta virus (HDV) and Varkud Satellite (VS) RNA, group I and group II introns [Khan & Lal, 2003] and the RNA subunit of RNase P [Khan & Lal, 2003]. In addition, recent structural and chemical analyses strongly suggest that ribosomal RNA is an enzyme [Cech, 2000]. Similarly, there is evidence that the RNA component of the spliceosome may also have enzymatic properties [Collins & Saville, 1990].

The discovery of ribozymes and fundamental studies on the mechanisms of self-splicing have revealed details on the catalytic core and the secondary and tertiary structure of RNA folding leading to ribozyme-mediated cleavage of RNA. Ribozymes were initially believed to be metalloenzymes requiring divalent metal ions for catalysis and it was thought that all ribozymes operate through a similar mechanism of action. However, a unique RNA hairpin was shown to behave like a ribozyme in the absence of divalent metal ions [Earnshaw & Gait, 1998; Murray *et al*, 1998; Burke, 2002].

The specificity of the cleavage is determined by Watson-Crick base-pairing between ribozymes and nucleotides near the cleavage site of the target RNA. By altering substrate recognition sequences, several

intramolecular cis-cleaving ribozymes can be designed to cleave any RNA in trans. Theoretically, these trans-cleaving ribozymes can be designed to cleave any RNA species in a sequence-specific manner by incorporating the flanking sequences complementary to the target. After the cleavage reaction, the substrate is accessible to ribonucleases, a step that guarantees its permanent inactivation and offers a considerable advantage over the simple physical blockage obtained with complementary oligodeoxynucleotides.

Ribozymes are grouped into two classes on the basis of their size: the large and the small ribozymes. The large group contains group I and II introns, and the RNA subunit of RNase P. Group I and II introns are found in bacteria and in the organelles of higher plants, fungi and algae [Lal & Hall, 1997; Khan *et al*, 2000; Woodson, 2002]. These introns are spliced out of their hnRNA by a two-step mechanism. In the first step of splicing, the 5'-spliced site is attacked by the 3'-OH of the external guanosine group (group I). Whereas, in group II intron it is attacked by the 2'-OH of the internal adenosine residue or by a hydroxide ion. In the second step, the 3'-OH of the 3'-end of the upstream exon attacks the 3'-spliced site to produce the splicing products. RNase P is an endonuclease that generates the mature 5'-ends of tRNAs. In bacterial RNase P, the RNA subunit (RNase P ribozyme) has catalytic activity and the protein component is thought to act only to facilitate the binding of the anionic RNase P ribozyme to its substrate. During the cleavage of RNase P ribozyme, a scissile-site phosphate is attacked by a hydroxide ion to leave a 3'-oxygen and produce a 5'-phosphate terminus [Chen *et al*, 1994; Kirsebom, 2001].

The class of small ribozymes comprises hammerhead, HDV (hepatitis delta-viroid) hairpin and VS ribozymes. Each of the naturally existing ribozymes catalyse the endonucleolytic cleavage of RNA via a mechanism that involves nucleophilic attack by a 2'-OH group on the phosphorus of the neighbouring phosphodiester bond, generating 5'-OH and 2',3'-cyclic phosphate termini. The cleavage reaction catalysed by these ribozymes appears to proceed with the inversion of the configuration at the phosphorus atom, suggesting a direct in-link attack with development of a pentacoordinate transition or intermediate state [Stage-Zimmermann & Uhlenbeck, 1998].

The smallest of the naturally occurring catalytic RNAs that were identified to date are the hammerhead ribozymes (Figure 19), which were found in several plant virus satellite RNAs, viroids and as transcripts of a nuclear satellite DNA (a riboprotein particle of about 12 S in oocytes of Triturus) [Foster & Sympson, 1987].

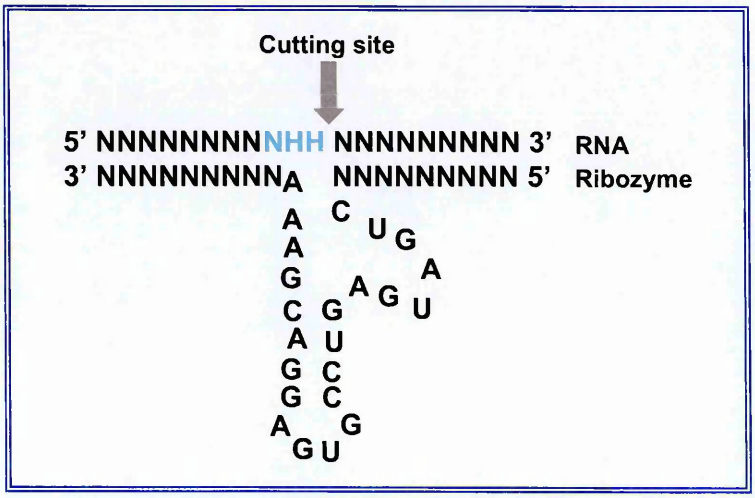

Figure 19. Structure of a hammerhead ribozyme.
The hammerhead ribozyme consists of a highly conserved catalytic core, which cleaves substrate RNA at NHH triplets 3' to the second H, where N is any nucleotide and H is any nucleotide but guanidine. [Adapted from Sun *et al*, 2000]

A large number of studies have been performed to provide a better understanding of the mechanism of ribozyme-mediated catalysis. In general, a minimal kinetic description for one turnover of hammerhead ribozyme reaction (Figure 20) involves assembly of ribozyme and substrate, cleavage of the phosphodiester bond, generating a product with a cyclic phosphate terminus and a product with a hydroxyl terminus that remains bound to the ribozyme, and release of the products. A Michaelis-Menten mechanism has been established by using multiple- and single-turnover conditions for the formation of the ribozyme-substrate complex and its subsequent conversion to products [Perreault *et al*, 1990; Hammann C & Lilley, 2002]. Under multiple-turnover conditions, the substrate is in excess of the ribozyme so that the ribozyme can catalyse the cleavage of several substrate molecules. The catalytic rate constant, k_{cat}, is a measure of the rate-limiting step, which can be cleavage, conformational transitions of the ribozyme-substrate complex, or product release. When a ribozyme with six bases in each arm was used in kinetic analysis, k_{cat} and K_M were within typical values of 1–2 min^{-1} and 20–200 nM, respectively. Extension of the helical arms generally results in an increased stability and markedly decreased k_{cat} [Hertel *et al*, 1994]. Under single-turnover conditions, the ribozyme is in excess of the substrate, and such conditions are normally used for cleavage of long mRNA substrate. Cleavage rates are generally several orders of magnitude lower, compared with the rates obtained for short substrate [Heidenreich *et al*, 1994]. The presence of Mg^{2+} is essential for the cleavage, and convincing evidence suggested that Mg^{2+} not only assists in RNA folding but also participates directly in the cleavage mechanism [Dahm & Uhlenbeck, 1991].

The hammerhead ribozyme consists of a highly conserved catalytic core, which cleaves substrate RNA at NHH triplets 3' to the second H, where N is any nucleotide and H is any nucleotide but guanidine [Kore *et al*, 1998] (Figure 19). One assumption is that the inability to cleave 3' of G is due to an unfavourable interaction with C3 in the core [Baidya & Uhlenbeck, 1997; Blount KF & Uhlenbeck, 2005]. NMR studies have confirmed that this base pair exists and that it stabilizes the ground state ribozyme-substrate complex [Simmore *et al*, 1998]. However, an additional contribution to the lack of cleavage comes from destabilizing the transition state. Various pyrimidine nucleoside analogues have been used as H [Baidya *et al*, 1997]. Although all such modifications had no effect on binding of the substrates to the ribozyme, cleavage occurred more slowly than when H was cytidine. Comparative studies revealed that the reaction rate (k_{cat}) decreases in the following order: AUC, GUC>GUA, AUA, CUC>AUU, UUC, UUA>GUU, CUA>UUU, CUU. This indicates that functional groups at the cleavage site are important for transition state formation.

In addition to the catalytic core, a particular cleavage site in a target RNA can be specifically recognized by creating, in the hammerhead ribozyme recognition arms, flanking sequences complementary to specific target RNA molecules.

It has been demonstrated the possibility to prepare ribozyme libraries that are targeted to multiple mRNA substrates by randomizing the sequences of the recognition arms. Such libraries can be used as knock down libraries to interfere with the activities of several gene products. Ribozymes can be screened and target genes that appear responsible for a particular phenotype can be identified by introducing a ribozyme library into cells. Isolation of cells

with the phenotype of interest allows the rescue of the ribozyme of interest. Moreover, the examination of DNA database allows rapid identification of the gene responsible for the phenotype of interest using the sequence of the rescued ribozyme. Such a methodology has been recently used to identify genes involved in cell migration and invasion, two processes that are essential features of tumour metastasis [Suyama *et al*, 2003a; Suyama *et al*, 2003b].

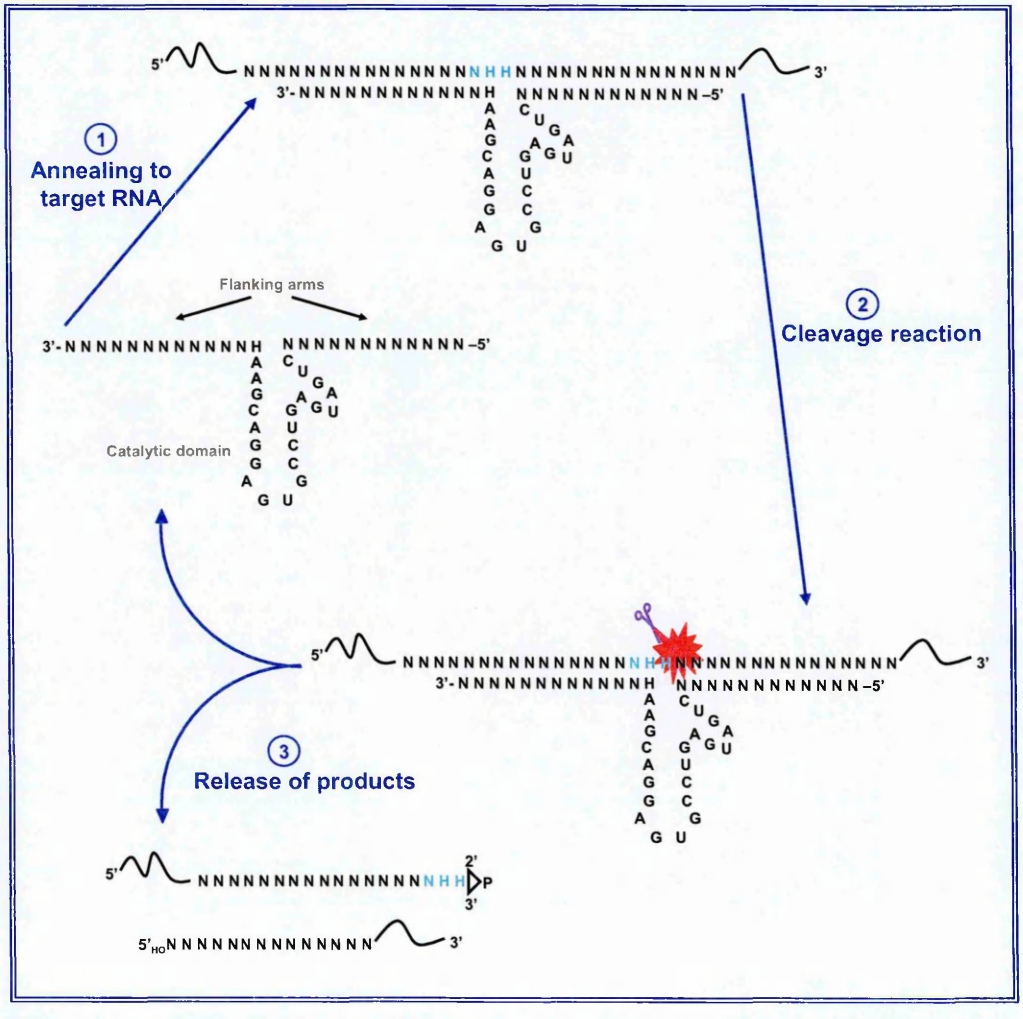

Figure 20. Schematic representation of the catalytic cycle for a hammerhead ribozyme.

The ribozyme binds through the flanking arms to its RNA substrate, via Watson-Crick interactions (**1**). Once the ribozyme-substrate complex has formed, the cleavage reaction mediated by the catalytic domain of the enzyme leads to cleavage of the phosphorodiester linkage located at the 3' end of a NHH consensus sequence (**2**). Release of the products make the ribozyme available for another cycle of the reaction (**3**). [Adapted from Zaffaroni & Folini, 2004]

Owing to their ability to efficiently inhibit specific gene expression, ribozymes have been used to validate a number of disease-related (mainly cancer-related) genes as potential targets for new therapeutic interventions.

3.1.2.2. Small Interfering RNA (siRNAs)

RNA interference (RNAi) is a natural mechanism of sequence-specific, post-transcriptional gene silencing. RNAi may play an important role in protecting the genome against instability caused by transposons and repetitive sequences, and it represents an evolutionary conserved anti-viral defense pathway in animals and plants [Elbashir *et al*, 2002]. Moreover, RNAi has emerged as a powerful mechanism for sequence-specific modulation of gene expression and seems to provide a higher potency than conventional antisense strategies, presumably because it relies on natural site-directed cleavage machinery [Elbashir *et al*, 2002].

In mammalian cells RNAi can be triggered by several double-stranded RNAs (dsRNA) or dsRNA domain-containing molecules. Endogenously expressed dsRNA domains are converted into the nucleus by specific ribonucleases in the form of precursors that are successively processed in the cytoplasm to give rise to micro RNAs (miRNAs). The miRNAs are believed to bind to sites that have partial sequence complementarity in the 3' untranslated region of their target mRNA, causing repression of translation and inhibition of protein synthesis [Dykxhoorn *et al*, 2003; Izquierdo *et al*, 2005]. By contrast, exogenously-introduced dsRNA (e.g. viral genome) are

processed in the cytoplasm by the endoribonuclease Dicer into small duplex RNAs, the 21-23 nucleotide-long terminal effectors molecule, known as small interfering RNAs (siRNA), characterized by a 2-3 nucleotide overhang at the 3' terminus [Dykxhoorn *et al*, 2003; Izquierdo *et al*, 2005] (Figure 21).

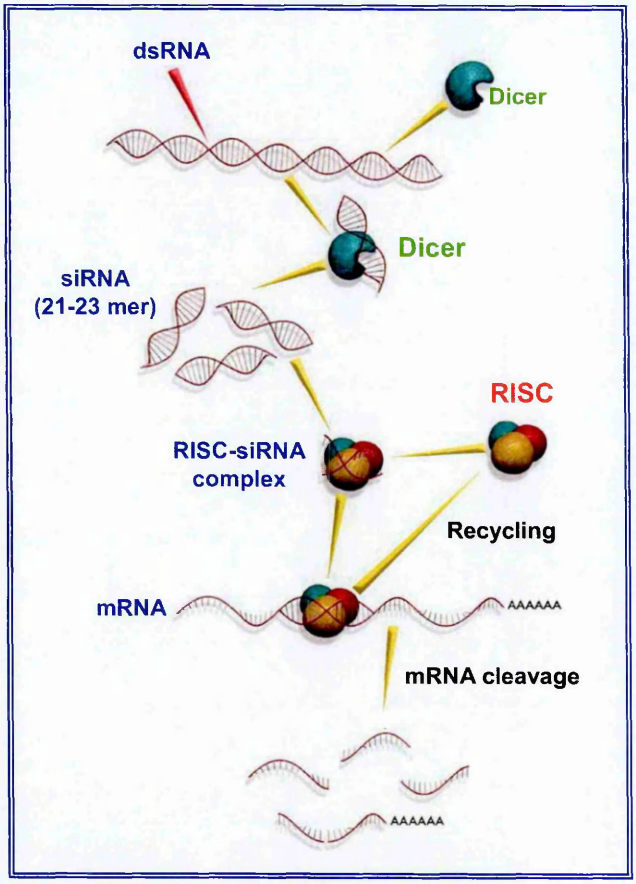

Figure 21. Gene silencing by RNAi.
When dsRNA enters the cell, it is recognised by the enzyme complex Dicer and cleaved to yield siRNA. The siRNAs then bind to a multiprotein complex to form the RISC. Activation of the RISC is accompanied by the unwinding of the siRNA duplex, and one strand of the siRNA then guides RISC to cleave the target mRNA.

The resulting siRNAs are then assembled to form an RNA/protein complex, referred to as the RNA-induced silencing complex (RISC)

(Figure 21). The double-stranded siRNA is then unwound, leaving the antisense strand to guide RISC to its homologous target mRNA for endonucleolytic cleavage. The target mRNA is cleaved in the centre of the duplex region arising from the annealing of the antisense strand of siRNA and the target mRNA, a process that ultimately results in the target degradation.

Different effectors molecules have been identified as inductors of gene expression silencing in mammalian cells through the activation of the RNAi pathway. Specifically, short hairpin RNAs (shRNAs) are transcribed from plasmid- or viral-based vectors as a pre-siRNA in which the sense and antisense strands are linked by a short spacer. The pre-siRNA is then predicted to form a 19-nucleotide-long stem-loop structure, the terminal effectors shRNA. Short hairpin RNAs are usually coded downstream of an RNA polymerase III promoter (e.g. U6 small nucleolar RNA or human RNase H1 promoters) although the use of inducible or tissue-specific RNA polymerase II promoters has been described [Dykxhoorn *et al*, 2003; Izquierdo *et al*, 2005]. By contrast, pre-synthesized siRNA are RNA duplexes formed by two complementary single strands. In this case, a siRNA may be obtained by the annealing of two in vitro transcribed 21-nucleotide-long single strands leaving two nucleotides unpaired at the 3' terminus [Dykxhoorn *et al*, 2003; Izquierdo *et al*, 2005] or as preformed duplexes, usually provided by specialized companies.

To date the siRNA technology has been validated in several mammalian experimental models but its therapeutic usefulness for human diseases is still under intensive investigation. In fact, although the effect of siRNAs on gene

expression has been demonstrated to be rapid and persistent (days/weeks), the main limitation to be overcome before such technology will be exploited in the clinical practice is represented by the selectivity for the target RNA, delivery and stability inside cells, similarly to ribozyme- and antisense-based approaches.

3.1.2.3. Ribozyme & siRNA Delivery Systems

The most challenging aspect of the use of ribozymes and siRNAs for therapeutic purposes is delivering these molecules to their site of action, the RNA target located within the cytoplasm or nucleus. Delivery requires that the oligonucleotide survive local or systemic administration long enough to bind to the target cells, cross the cytoplasmic membrane or become released from an endosomal/lysosomal vesicle, pass through the nuclear membrane, and be able to functionally hybridise to the target RNA.

There are two approaches to deliver ribozymes and siRNAs to cells for the successful inhibition of gene expression. One is exogenous delivery where the presynthesised molecules are delivered directly to cells. The other is endogenous delivery, which provides the gene encoding the ribozyme and siRNA, as part of a vector, to the cells where transcription generates the ribozyme and siRNA.

3.1.2.3.1. Exogenous Delivery

Exogenous delivery, at first glance, looks simple, straightforward and attractive. Presynthesised ribozymes can be delivered directly to cells or administered to an animal. This mode of application is identical to that of the antisense oligonucleotides method. Given the amount of accumulated experience, it is not surprising that most of the delivery techniques used in the ribozyme field are adopted from the AS-ODN strategy. Exogenous delivery requires stabilization of oligonucleotides against nuclease degradation. This is particularly true for ribozymes, which are rapidly degraded by RNases. AS-ODNs are customarily protected by incorporation of phosphorothioates, but ribozymes demand modification of the 2'-OH group, which the RNases also require for cleavage. Stabilization should not compromise catalytic activity of the ribozyme, thus the choice of derivative and its placement are crucial. In general, poor uptake is a challenge for exogenous delivery of ribozymes to cells in culture. Significant improvement can be achieved with the help of carrier such as cationic liposomes.

Chemically synthesized or *in vitro* transcribed siRNAs are probably the most easy and direct approach to induce RNA interference in mammalian cells. 21-nucelotide RNAs specific to the mRNA target are synthesized and annealed *in vitro* by heating to 90°C followed by slow cooling to 37°C. Such RNA duplexes are transfected into cells by generating liposomes incubated with cationic lipids, electroporation, covalent binding to hydrophobic carrier molecules or covalent coupling to cell penetrating peptides [Wadhwa *et al*, 2004]. The defence interferon system against viruses, however, is very

sensitive to the presence of double-stranded RNA, and under certain conditions, siRNA can activate the interferon system complicating the interpretation of the experiments. The removal of the 5'-triphosphate end when siRNA is synthesized *in vitro* using phage T7 RNA polymerase, instead of chemical methods, is important to avoid the interferon response in mammalian cells [Izquierdo *et al*, 2005]. High doses should also be avoided because they will again induce interferon *in vivo* and in some instances may cause unexpected and divergent changes in the levels of untargeted proteins [Izquierdo *et al*, 2005].

3.1.2.3.2. Endogenous Delivery

The search for ways to introduce genes into cancer cells led to significant improvements in viral and nonviral vector development (Table II).

3.1.2.3.2.1. Viral Delivery

A number of viral delivery systems are available for gene delivery of DNA or oligonucleotides into mammalian cells, either *in vitro* or *in vivo* (Table II). The most common vector systems are based on retroviruses, adeno-associated virus (AAV), adenovirus, and herpes simplex virus (HSV) [Boulaiz *et al*, 2005; Tan *et al*, 2006]. Other viral vectors are based on lentiviruses, human citomegalovirus (CMV), Epstein-Barr virus (EBV), poxviruses, negative-strand RNA viruses (influenza virus), alphaviruses, and herpesvirus

saimiri [Boulaiz *et al*, 2005; Tan *et al*, 2006]. Moreover extremely interesting appears the construction of a hybrid adenoviral/retroviral vector, which has successfully been used for *in vivo* gene transduction [Barquiner *et al*, 2004; Ghosh *et al*, 2004; Warrington & Herzog, 2006].

Table II. Description of the main gene delivery systems.

Vectors	Characteristics	Disadvantages
Viral Delivery		
Retroviruses	Relatively high titers (10^6-10^7 cfu/ml) Broad cell tropism Stable gene expression No toxic effect on infected cells Total insert capacity in the virion in the range of 10 kb Only infection of dividing cells	Random insertion of viral genome, which may possibly result in mutagenesis Possibility of replication virus formation by homologous recombination
Lentiviruses	Infection of nondividing cells Broad cell tropism Stable gene expression Total insert capacity in the virion in the range of 10 kb	Serum conversion to HIV-1 Possible proviral insertional mutagenesis in target cells
Adenoviruses	Very high titers (10^{10} pfu/ml) Transiently high levels of gene expression Total insert capacity in the vector in the range of 10 kb Infection of nondividing cells	Host immune response Not suitable for long-term expression due to the lack of integration into host genome Complicate vector genome
Adeno-associated viruses (AAV)	Infection of nondividing cells Viral integration specific for human chromosome 19 (only for wild-type AAV) No toxic effect on infected cells Nonpathogenic for infected cells	Difficult to obtain high titers of pure viruses Limited capacity for foreign genes (about 4 kb) Lack of specific integration for recombinant AAV vector
Nonviral Delivery		
Cationic liposomes	Not infectious No limit to the size of DNA Low degree of toxicity	Non specific targeting Low transfection efficiency Difficult *in vivo* application

Adenovirus, a class of DNA viruses, can successfully deliver genes to the nucleus. However, these viruses provide only transient expression of the gene and generate a strong antibody response, thus the infected cells are rapidly removed and repeated application is not possible [Ali *et al*, 1994; Relph *et al*, 2005; Young *et al*, 2006]. Adeno-associated virus is an alternative vector for ribozyme delivery [Bertrand *et al*, 1997; Lewin & Hauswirth, 2001]. It is appealing for several reasons. It is non-pathogenic and does not require dividing cells to integrate the gene into the host genome.

Retroviruses are among the most efficient tools for gene transduction of mammalian cells. For this reason, they were successfully used in the early gene therapy clinical trials for the treatment of inherited genetic diseases and cancer [Young *et al*, 2006; Rodrigues *et al*, 2007]. A number of different retroviruses are in use as gene delivery vehicles. The most common retroviral vector is based on the amphotropic Moloney murine leukaemia virus (MoMuLV) [Shinnick *et al*, 1981]. This system is particularly suitable for efficient *in vitro* cell transduction: the amphotropic MoMuLV has a broad cell tropism, it can be produced at relatively high titers (10^6-10^7 iu/ml), and allows for long-term transgene expression because of the viral integration in the host chromosomal DNA. Another important feature of retroviruses is that although they do not elicit immune responses in the host, they are susceptible to rapid degradation by the complement [Takeuchi *et al*, 1994]. This is a major limitation for *in vivo* retroviral-mediated gene transfer.

The viral RNA encodes 3 genes called gag, pol and env which encode the capsid core proteins (gag), reverse transcriptase, integrase and protease (pol) and the envelope antigens (env) (Figure 22). Gag (Group specific

Antigens) is the precursor to the internal structure of the retrovirus also known as the "core". It gives rise to four different polypeptides. The three common to all retroviruses are the capsid (the largest protein composed of 200–270 amino acids, the matrix (derived from the amino terminus of the Gag gene, is a membrane associated protein), and the nucleocapsid (a 60-90 amino acid protein that binds the viral RNA). Pol gives rise to three polypeptides: the protease, the reverse transcriptase (with RNase H activity) and integrase. Finally, Env gives rise to two polypeptides: the transmembrane "spike" protein (gp41 in HIV) and the knob-like surface protein gp120. Together these form the surface antigen gp160 characteristic to retroviruses. These proteins are initially inserted into the host cell membrane and are acquired by the virus particle at a later stage during budding.

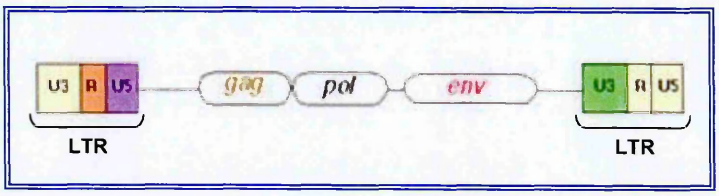

Figure 22. Schematic representation of the genomic organisation of a retroviruse.
The retroviral genome is flanked by a long terminal repeat sequence (LTR) and encodes 3 genes which encode the capsid core proteins (gag), reverse transcriptase, integrase and protease (pol) and the envelope antigens (env).

The retroviral genome is flanked by a long terminal repeat sequence (LTR) (Figure 22). This region contains all signals necessary for gene expression, including the enhancer, promoter, transcription initiation, transcription terminator and polyadenylation signal. The size of the LTR varies

considerably among the different retroviruses. The integrated provirus has two LTRs; the 5' LTR normally acts as an RNA polymerase II promoter whereas the 3' LTR functions as the terminator sequence. An LTR is composed of three elements: U3, R and U5 regions. U3 includes most of the transcriptional control elements and carries the promoter/enhancer sequence. It is the unique, non-coding region of 75–250 nucleotides which is in the first part of the genome to be reverse transcribed, forming the 3' end of the provirus genome. R region is usually a short (18–250 nucleotide) sequence that provides the sequence homology for strand transfer during reverse transcription of the RNA genome. Finally, U5 region carries the poly A-site and, together with the R region, determines the poly A addition. It is a unique non-coding region of 200-1,200 nucleotides that forms the 5' end of the provirus after reverse transcription. Both U3 and U5 regions contain the Att sites required for integration.

The key factor in using a retrovirus as a gene delivery vehicle is biosafety. The main goal of the vector design is to ensure that a replication incompetent virus is generated. Separation of the packaging function from the genetic material to be transferred makes this possible. A basic retroviral vector contains the *cis*-acting elements required for replication as a virus, but lacks some or all of the viral genes, which are replaced by foreign coding sequences. For a retroviral vector to replicate as a virus, it is necessary to provide the missing viral gene(s) in *trans*. Moreover, retroviral particles are difficult to concentrate, as they are fragile and can be destroyed during the precipitation. This problem can be circumvented by pseudotyping the retroviral core with the G glycoprotein of vesicular stomatitis virus (VSV-G).

This envelope stabilizes the retroviral particles, which can then be easily concentrated by ultracentrifugation of the retroviral supernatant [Romano *et al*, 1999]. Engineered cell lines that express the viral genes from heterologous promoters are used to produce vector virus. These genetically-engineered cell lines are called *packaging* or *helper* cells. There are various packaging cell lines that can be used to generate retroviruses; the choice of packaging cells depends on the host range or tropism of the desired virus (Figure 23).

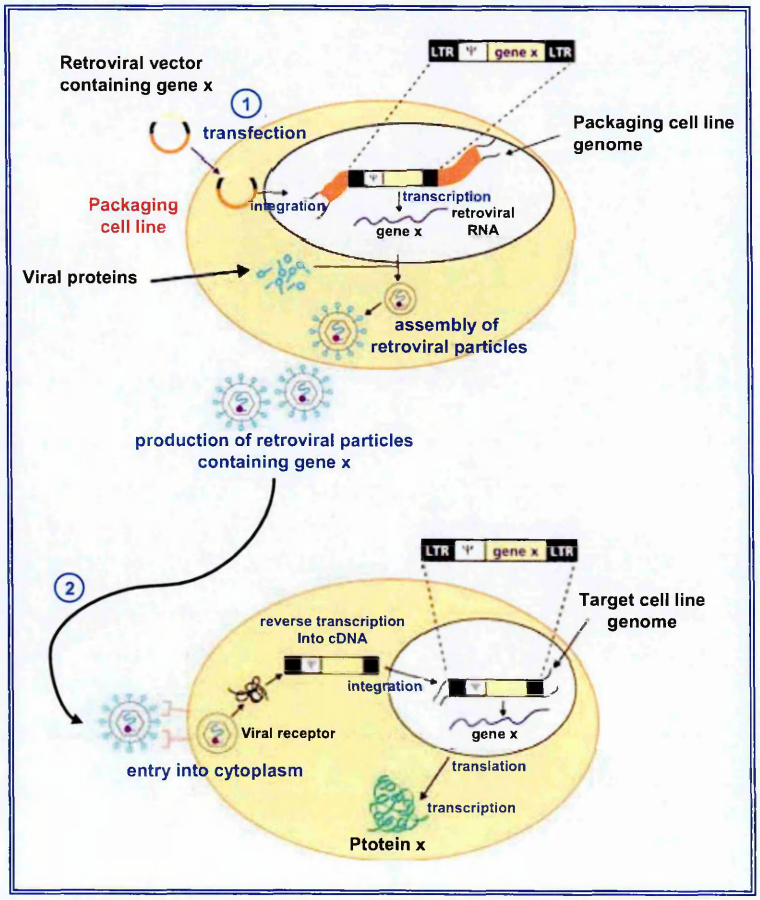

Figure 23. Production of an infectious retroviral particle and infection of a target cell.

A replication-incompetent vector encoding a gene of interest (x) is introduced into a pakaging line (**1**). This cell line encodes the proteins necessary for production of viral particles. The viral transcript is pakaged into viral particles, which are thus budded from the pakaging cell. The replication-incompetent retroviral vector interacts with a host-cell receptor and enters into the target cell (**2**), where the virus reverse transcribes its RNA genome and integrates it into the host genome.

3.1.2.3.2.2. Nonviral Delivery

As an alternative to viral vectors, several DNA-based plasmid vectors for transient and stable expression of ribozymes and siRNA have been developed [Brummelkamp *et al*, 2002; Sui *et al*, 2002].

Nonviral gene delivery makes use of lipo/polyfection reagents such as liposomes, cationic lipids, or cationic polymers complexed with the foreign DNA for transfection [Azzam & Domb, 2004; Tiera, 2006] (Figure 18), or physical methods such as microinjection, gene gun delivery, or the use of uncomplexed, "naked" plasmid DNA. All these methods are less efficient than viral transduction and there are viability complications due to toxicity as well as evidence that unmethylated plasmid DNA amplified in bacteria is immunogenic [Deng *et al*, 1999; Loisel *et al*, 2001]. However, there are few restrictions on the size of the gene of interest.

Briefly, the plasmid carries the genetic information required to express a foreign protein or ribozyme or siRNA: all the necessary sequences for subcloning the gene of interest, elements needed for bacterial propagation and amplification of the plasmid as well as eukaryotic promoters, poly(A) signals and antibiotic resistance genes for selection of stable cell lines. Newer features of plasmids allow for a choice of episomal or extra-chromosomal maintenance, integration, site-specific integration, and the ability to turn gene expression on or off. DNA–polymer complexes enter cells either by charge-mediated interactions with proteoglycans or by receptor-mediated endocytosis. Either method results in delivery to lysosomes followed by release and transport to the nucleus. DNA transport across the

nuclear membrane through the nuclear pores requires active transport, is limited to particles 100 nm in size, and is the major barrier to overcome in nonviral gene delivery [Tachibana *et al*, 2001].

The key principles for nonviral delivery systems are to avoid undesirable interactions with surface proteins and the extracellular matrix, and to avoid self-aggregation. Thus, the DNA and reagent must complex, preferably in a predictable ratio, and the DNA must condense or the particle will be too large to pass through the nuclear pore. Furthermore, the complex should allow endolysosomal release, but not inhibit downstream cellular processes, that is, transcription and translation.

3.1.3. Survivin Inhibition by Ribozymes & siRNAs

As an alternative antisense strategy for survivin inhibition (Figure 13A), Choi *et al* [2003] developed two hammerhead ribozymes able to cleave the human survivin mRNA at nucleotide position +279 and +28 and cloned them into a replication-deficient adenoviral vector. These authors showed that survivin down-regulation increased the apoptotic response to etoposide in transduced MCF-7 breast cancer cells.

Several studies on experimental human tumour models have demonstrated the feasibility of the use of the small interfering RNAs approach for the inhibition of cancer-related genes including survivin (Figure 13A).

Carvalho *et al* [2003] first used RNAi to specifically repress survivin in HeLa cells. These authors showed that survivin was no longer detectable in cultures 60 hours after transfection with specific siRNAs and that survivin-depleted cells were delayed in mitosis and accumulated in prometaphase with misaligned chromosomes. Several studies dealing with the use of chemically synthesized siRNAs or plasmid/viral vectors encoding short hairpin RNAs showed that RNAi-mediated survivin knockdown was able to reduce tumour cell proliferative potential and induce caspase-dependent apoptosis in a variety of human tumour cell models [Lens *et al*, 2003; Beltrami *et al*, 2004;Yang *et al*, 2004; Ai *et al*, 2006; Nakao *et al*, 2006; Jiang *et al*, 2006], as well as to decrease the formation of new tumours and the growth of already established lesions in nude mice [Jiang *et al*, 2006; Li *et al*, 2006]. Survivin down-regulation also induced an enhanced apoptotic response of tumour cells of different histologic origin to several stimuli, including treatment with vincristine [Jiang *et al*, 2006], doxorubicin [Li *et al*, 2006; Yonesaka *et al*, 2006], TNF-alpha [Li *et al*, 2006] and APO2L/TRAIL [Nakao *et al*, 2006], and caused radio-sensitisation of a sarcoma cell line expressing wild-type p53 [Kappler *et al*, 2005]. Finally, Coma *et al* [2004] demonstrated that transfection of endothelial cells with survivin-specific siRNAs induced a marked increase in the rate of apoptosis, a dose-dependent inhibition of their migration on vitronectin, and a decrease in capillary formation.

3.2. Gene Therapy

Two main gene therapy approaches targeting survivin have been successfully developed. One is based on the use of plasmids or viral vectors to deliver dominant-negative survivin mutants to tumour cells (Figure 13B) and the second involves the use of the *survivin* gene promoter to drive the expression of cytotoxic genes in tumour cells [Lo *et al*, 2005].

3.2.1. Dominant Negative Mutants

Two mutations in survivin have been characterized for what appears to be a dominant negative effect on the function of the endogenous molecule (Figure 13B).

Grossman *et al* [1999] first demonstrated that transfection of YUSAC2 and LOX melanoma cell lines with a mutant carrying a cysteine 84→alanine (Cys84Ala) mutation in the survivin BIR domain increased the apoptotic index and enhanced the sub-G_1 apoptotic cell fraction in both tumour models. More recently, Tu *et al* [2005] showed that adeno-associated viral vector-mediated transfer of the survivin mutant Cys84Ala induced apoptosis and mitotic catastrophe in colon cancer cells, inhibited angiogenesis and tumour growth in a colon cancer xenograft model *in vivo*, and strongly enhanced the antitumour activity of 5-fluorouracil. By using a phosphorylation-defective survivin threonine 34→alanine (Thr34→Ala) mutant, Grossman *et al* [2001] demonstrated the induction of spontaneous apoptosis in different melanoma

cell lines as well as an increased apoptotic response following cisplatin treatment. Conditional expression of Thr34→Ala in these cells prevented tumour formation upon subcutaneous injection in 13 of 15 CB.17 severely combined immunodeficient (SCID) mice. Such treatment also caused a significant reduction (60-70%) in the growth rate of already established tumours and enhancement of apoptosis [Grossman *et al*, 2001]. Mesri *et al* [2001] investigated the effect of a replication-deficient adenovirus encoding the survivin Thr34→Ala dominant-negative mutant (pAd-T34A) in human tumour cells of various origin *in vitro* and *in vivo*. They showed that infection with pAd-T34A caused enhanced spontaneous and paclitaxel-induced apoptosis in cell lines of different tumour origin while not affecting the growth of proliferating normal human cells not expressing survivin. *In vivo* experiments on the MCF-7 human breast cancer xenograft model demonstrated that pAd-T34A was able to suppress *de novo* tumour formation, inhibit the growth of already established tumours by approximately 40%, and reduce intraperitoneal tumour dissemination. Moreover, tumours infected with pAd-T34A showed massive apoptosis and loss of proliferating cells. Very recently, using a recombinant fusion protein containing the TAT transduction domain and the Thr34→Ala dominant-negative mutant (TAT-Surv-T34A), Yan *et al* [2006] observed an induction of caspase-dependent apoptosis in melanoma cells. Moreover, repeated intraperitoneal injection of TAT-Surv-T34A resulted in a marked reduction of the growth and mass of established subcutaneous tumours in mice.

3.2.2. The *Survivin* Gene Promoter

The second gene therapy approach involves the use of the *survivin* gene promoter to drive the expression of cytotoxic genes in tumour cells [Lo *et al*, 2005]. It was shown that when coupled to the pro-apoptotic protein Bik, administration of the suicidal construct as a DNA-liposome formulation suppressed the growth of human lung cancer *in vitro* and *in vivo* [Chen *et al*, 2004]. Van Houdt *et al* [2006] showed recently that *survivin* promoter-based conditionally replicative adenoviruses (CRAds), composed of *survivin* promoter-regulated E1 gene expression and an RGD-4C capsid modification, efficiently replicated within and killed a variety of established glioma cell lines but were inactive in a normal liver culture. Moreover, *survivin* promoter-based CRAds significantly inhibited the growth of glioma xenografts *in vivo*.

3.3. Small Molecule Antagonists

3.3.1. Cyclin-Dependent Kinase (CDK) Inhibitors

If survivin phosphorylation on Thr by $p34^{cdc2}$ is required for cancer cell viability, it should be possible to target this step with a more generally applicable pharmacological approach (Figure 13C). Indeed, kinase inhibitors and in particular antagonists of cdk have emerged as promising anticancer drugs for their ability to disrupt a number of cell proliferation and cell survival pathways [Davies *et al*, 2002]. In particular, the flavone cdk inhibitor of

$p34^{cdc2}$, flavopiridol, is has been explored in the clinic for its ability to induce apoptosis in various tumour cell types [Senderowicz, 2003].

Flavopiridol (NSC 649890, L86-8275 or HMR 1275) is a semisynthetic small molecular derivative of rohitukine, an alkaloid isolated from Dysoxylum binectariferum (Figure 24). Initially, flavopiridol demonstrated potent effects on cell proliferation (IC50=66 nM) in 60 National Cancer Institute human tumour cell lines, with no obvious tumour-type selectivity [Day & Grant, 2003]. Antitumour effect has also been observed in xenograft models of various tumour-types treated with this compound [Day & Grant, 2003]. Flavopiridol is a potent small molecule inhibitor of multiple cdks, including cdk1 (cdc2), cdk2, cdk4, cdk6, and cdk7 [Senderowicz & Sausville, 2000]. It inhibits cdks by binding to their ATP-binding pocket [Senderowicz & Sausville, 2000]. Flavopiridol also causes transcriptional repression of cyclin D1 [Senderowicz & Sausville, 2000]. By inhibiting cyclin H-cdk7, it inhibits the phosphorylation of cdks at threonine 160/161 [Senderowicz & Sausville, 2000]. These activities result in the arrest of the cell cycle in the G_1/S or G_2/M and mediate the anti-proliferative effect of flavopiridol in tumour cells. Flavopiridol has also been shown to induce apoptosis, to inhibit transcription and to have anti-angiogenic activity [Day & Grant, 2003].

As a member of the first generation of cdk inhibitors, flavopiridol is not particularly selective for a specific cdk. However, more selective cdk inhibitors have since been developed. Several of these compounds are being evaluated for antitumour activity in preclinical model systems. Purine-based cdk inhibitors display greater selectivity for cdks 1, 2 and probably 5, but exhibit no inhibitory activity toward cdks 4 and 6. Some of these inhibitors

have been reported to exert potent antitumour activity, including olomucine, roscovitine, and purvalanols.

Purvalanol A and B, are olomucine derivatives (Figure 24) which exhibit potent and selective inhibition of cdks 1 and 2. *In vitro* studies demonstrated that purvalanol inhibits cell growth (IC_{50}=2.5 μM) and induces G_2/M arrest. These effects are linked to inhibition of cdk1 and p42/p44 mitogen-activated protein kinase, both of which have been identified as intracellular targets of purvalanol [Day & Grant, 2003]. Administration of purvalanol did not appear to trigger extensive activation of caspases; however, induction of apoptosis might be highly dependent upon the concentration of cdk inhibitors [Day & Grant, 2003].

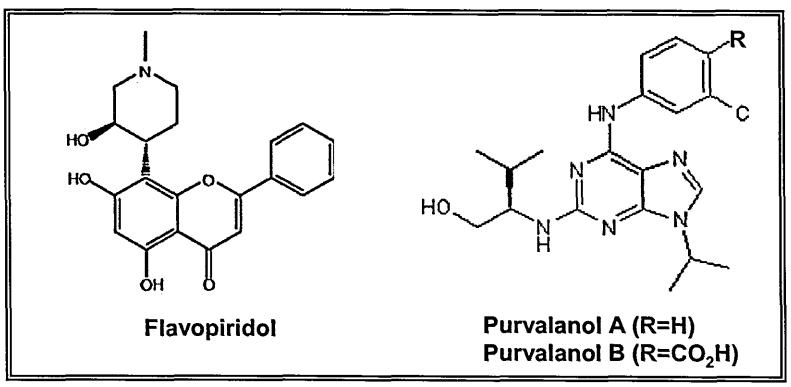

Figure 24. Structure of small-molecule direct cdk modulators.

In the context of a strategy focused on pharmacologic inhibition of mitotic phosphorylation of survivin on Thr34 to accelerate protein destruction and counteract its function [O'Connor *et al*, 2002], cdk inhibitors such as flavopiridol or the more $p34^{cdc2}$-specific inhibitor, purvalanol A, were tested in tumour cells arrested at mitosis with paclitaxel, which induces

hyperphosphorylation of survivin on Thr^{34} [Zaffaroni *et al*, 2002]. Sequential administration of cdk inhibitors resulted in escape from the mitotic block imposed by paclitaxel, marked activation of mitochondrial-dependent apoptosis, and anticancer activity *in vivo* [O'Connor *et al*, 2002].

3.3.2. Hsp90 Inhibitors

A structure-based rational screening for antagonists of the survivin-Hsp90 complex identified a cell-permeable peptidomimetic derived from the survivin sequence Lys^{79}-Leu^{87}, shepherdin [Plescia *et al*, 2005]. In addition to counteracting survivin-Hsp90 interaction, the molecule inhibited Hsp90 chaperone function by competing with ATP binding. Specifically, shepherdin was able to destabilize several Hsp90 client proteins (including Akt, cdk6 and telomerase) and to induce cell death via apoptotic and non-apoptotic mechanisms in cell lines of different tumour types. The cytotoxicity of shepherdin was seen to be independent of the proliferative activity of the cell model, concomitant overexpression of other cytoprotective factors such as Bcl-2, and p53 status. Moreover, shepherdin appeared to be selective in its antitumour activity since it did not affect viability of normal cells or tissues, including haematopoietic progenitors. Systemic administration of shepherdin *in vivo* was safe and well tolerated and inhibited the growth of already established prostate and breast cancers without inducing systemic or organ toxicity. Moreover, immunohistochemical analysis of Hsp90 client proteins carried out in tumours samples at the end of shepherdin treatment showed a

nearly complete loss of Akt levels and severely attenuated survivin expression [Plescia *et al*, 2005]. The clinical development of shepherdin with respect to its optimal formulation and pharmacokinetic profile is currently under way through the National Cancer Institute (NCI) Rapid Access to Intervention Development (RAID) program.

Since the shepherdin residues between Lys^{79} and Gly^{83} were shown to be essential for Hsp90 binding, a new five-residue peptide containing the Lys^{79}-Gly^{83} sequence (called shepherdin[79-83]) was successively synthesized [Gyurkocza *et al*, 2006]. The oligopeptide inhibited the formation of the survivin-Hsp90 complex and competed with ATP binding to Hsp90. Cell-permeable shepherdin[79-83] induced rapid killing in different types of human acute myeloid leukaemia cell lines and in patient-derived AML peripheral blasts but not in normal mononuclear cells. Moreover, when systemically delivered, shepherdin[79-83] abolished the growth of AML xenograft tumours without systemic or organ toxicity [Gyurkocza *et al*, 2006]. We have recently used shepherdin as a scaffold to rationally identify low-molecular-weight compounds that may act as structurally novel Hsp90 inhibitors. Through a combined structure- and dynamics-based computational design strategy, the nonpeptidic small molecule 5-aminoimidazole-4-carboxamide-1-β-D-ribofuranoside (AICAR) was selected to bind the Hsp90 N-terminal domain, mimicking the chemical and conformational properties of shepherdin. AICAR was shown to destabilize several Hsp90 client proteins *in vivo*, including survivin, and to exhibit anti-proliferative and pro-apoptotic activity in multiple tumour cell lines, while not affecting proliferation of normal human fibroblasts [Meli *et al*, 2006].

3.3.3. Other Small Molecules

Additional small molecules that target survivin have been developed and some of them are currently being evaluated in clinical trials. One of those that directly affect survivin expression, tetra-O-methyl nordihydroguaiaretic acid (M(4)N), was shown to suppress Sp1-dependent *survivin* gene transcription and activate the mitochondrial apoptotic pathway in transformed cells [Chang *et al*, 2004]. Moreover, M(4)N suppressed the growth of human xenograft tumours following systemic treatment [Park *et al*, 2005]. However, considering that the compound is a global transcription inhibitor, both survivin-dependent and survivin-independent pathways are thought to be responsible for drug-induced cell death in tumours [Huang *et al*, 2006].

YM155 is a small molecule that selectively inhibits *survivin* gene transcription and protein expression in several tumour cell lines. It showed marked anti-proliferative activity (in the nanomolar range) in a broad spectrum of human tumour cell lines and induced tumour regression in lymphoma, prostate cancer and non-small cell lung cancer xenografts [Mita *et al*, 2006]. Moreover, preliminary evidence of the clinical activity of the compound was derived from a phase I open-label study in which 41 patients with different tumour types were treated with 7-day continuous intravenous infusion of YM155 and objective responses were observed in 3 patients with non-Hodgkin's lymphoma [Mita *et al*, 2006]. The compound is currently being evaluated in a phase II study for patients with stage III and stage IV melanoma.

Other small molecules currently in the clinic were shown to indirectly affect survivin expression. Some of them, including STAT3 [Turkson, 2004] and T-cell factor [Emami *et al*, 2004] antagonists, caused the suppression of *survivin* gene transcription, whereas others, such as the ErbB2 antagonist lapatinib [Xia *et al*, 2006], markedly inhibited survivin expression by acting at the post-translational level through the promotion of the ubiquitin-proteasome-mediated degradation of the protein [Xia *et al*, 2006].

Overall, these data clearly validate survivin as a good target for cancer therapy thus indicating that interfering with survivin expression/activity by means of novel strategies may provide a viable approach to kill cancer cells selectively. Moreover, the notion that this factor plays a crucial role also in tumour angiogenesis would suggest that its targeting can increase the overall tumours treatment response not only through direct interference with the apoptotic pathways in cancer cells but also by favouring the apoptotic involution of newly formed tumour vasculature.

Chapter 2

AIMS OF THE STUDY

Apoptosis is a physiological process by which unwanted or useless cells are eliminated during development and other normal biological processes. Resistance to apoptotic stimuli is a hallmark feature of various malignancies including cancer. One of the mechanisms through which tumour cells acquire resistance to apoptosis is by overexpression of Inhibitor of Apoptosis Proteins (IAPs), a group of anti-apoptotic proteins that interact with and inhibit the enzymatic activity of caspases. Survivin is a structurally unique member of the IAP family, which is involved in control of cell division and inhibition of apoptosis. This protein is undetectable in most terminally differentiated normal tissues but is selectively expressed in the most common human neoplasms and associated with clinical tumour progression. Survivin also appears to be involved in tumour cell resistance to some anticancer agents as well as ionising radiation. It has been reported that survivin inhibition by use of the oligonucleotide antisense, mutant dominant negative, ribozyme and small interfering RNA, renders tumour cells more susceptible to treatment with chemotherapeutic agents and ionising radiation. On the basis of these findings, survivin has been proposed as a promising therapeutic target for novel anticancer therapies.

The present study is aimed **to develop different approaches to induce a specific inhibition of survivin expression/activity in human cancer cells** with the final aim **to sensitise tumour cells to the effects of apoptosis-inducing anticancer agents**.

Specifically, we proposed to inhibit:

- ✓ survivin expression through the use of hammerhead ribozymes and small interfering RNA targeting different portions of survivin mRNA;
- ✓ survivin activity through the use of specific cdk inhibitors.

The knock down phenotype arising from the exposure of tumour cells to different inhibitors was evaluated in terms of cell proliferative and tumorigenic potential, susceptibility to activate programmed cell death and chemosensitivity profile.

Chapter 3

MATERIAL & METHODS

1. GENERAL PROCEDURES

1.1. Drugs

Cisplatin was obtained from Pharmacia-Upjohn (Milan, Italy). Topotecan was purchased from Smith-Kline Beecham Pharmaceuticals (King of Prussia, PA, USA). Temozolomide was obtained from Schering Plough Inc (Madison, NJ, USA). Paclitaxel was purchased from Sigma (Milan, Italy). The 17-allylamino-17-demethoxy-geldanamycin (17-AAG) was kindly provided by Dr E. Sausville (NCI, Bethesda, MA, USA). Purvalanol A was purchased from Tocris (Bristol, United Kingdom). NU6140 was kindly provided by Prof D.R. Newell (University of Newcastle, Newcastle upon Tyne, United Kingdom).

1.1.1. Cisplatin Preparation

To obtain a 1 mg/ml cisplatin stock solution, 10 ml of PBS were added to cisplatin powdered stock and the drug was completely dissolved by vigorous vortexing immediately before use.

1.1.2. Topotecan Preparation

To obtain a 1 mg/ml topotecan stock solution, 10 ml of sterile water were added to topotecan powdered stock and the drug was completely dissolved,

stored at -20°C and diluted in complete culture medium immediately before use.

1.1.3. Temozolomide Preparation

To obtain a 1 mg/ml temozolomide stock solution, 10 ml of DMSO were added to temozolomide powdered stock and the drug was completely dissolved, stored at -20°C and diluted in complete culture medium immediately before use.

1.1.4. Paclitaxel Preparation

To obtain a 1 mg/ml paclitaxel stock solution, 10 ml of DMSO were added to paclitaxel powdered stock and the drug was completely dissolved, stored at -20°C and diluted in complete culture medium immediately before use.

1.1.5. 17-AAG Preparation

To obtain a 1 mg/ml 17-AAG solution, 10 ml of DMSO were added to the powder stock and the drug was completely dissolved, stored at -20°C and diluted in complete culture medium immediately before use.

1.1.6. Purvalanol A Preparation

To obtain a 1 mg/ml purvalanol A stock solution, 10 ml of DMSO were added to purvalanol A powdered stock and the drug was completely dissolved, stored at -20°C and diluted in complete culture medium immediately before use.

1.1.7. NU6140 Preparation

To obtain a 1 mg/ml NU6140 stock solution, 10 ml of DMSO were added to NU6140 powdered stock and the drug was completely dissolved, stored at -20°C and diluted in complete culture medium immediately before use.

1.2. Human Tumour Cell Lines

The melanoma cell line (JR8) was kindly supplied by Dr. Zupi (Experimental Chemotherapy Laboratory, Regina Elena Cancer Institute, Rome, Italy). The cell lines derived from untreated patients with prostate carcinoma (DU145 and PC-3) and uterine cervix carcinoma (HeLa), were purchased from American Type Culture Collection (ATCC, Rockville, MD, USA). The ovarian cancer cell lines, OAW42/e and OAW42/Surv were previously obtained after transfection of the OAW42 parental cell line (purchased from ATCC) with the empty pCI-neo vector and the pCI-neo

expression vector carrying the full-length human survivin cDNA (pCI-surv) [Zaffaroni *et al*, 2002].

1.2.1. Human Tumour Cell Lines Growth Conditions

All cell lines were maintained as monolayers in 25-cm^2 flasks (Corning-Costar Italia, Milan, Italy) at 37°C in a 5% CO_2 humidified atmosphere in an air incubator (Heraeus Sepatech, Milan, Italy).

JR8, DU145 and PC-3 were maintained in RPMI-1640 medium (Cambrex Italia, Milan, Italy), supplemented with 10% (v/v) FBS, 2 mM L-glutamine, and 0.1% (v/v) gentamycin, at a density of 0.6 x 10^5 cells per 25-cm^2 flask. HeLa cells were cultured using D-MEM/F12 medium (Cambrex), supplemented with 10% (v/v) FBS, 2 mM L-glutamine and 0.1% (v/v) gentamycin, at a density of 0.8 x 10^5 cells per 25-cm^2 flask. OAW42/e and OAW42/Surv were maintained D-MEM/F12 medium (Cambrex), supplemented with 10% (v/v) FBS, 2 mM L-glutamine, 0.25 units/ml insulin, 0.1% (v/v) gentamycin, 1 mg/ml G418, at a density of 1 x 10^5 cells per 25-cm^2 flask.

All tumour cells were cultured as follow: at set time points, specific growth medium was removed from the 25-cm^2 flask and the cell monolayer was washed twice with 5 ml 37°C-heated PBS. One ml of a Trypsin-EDTA solution (Cambrex) was then added to each flask. After a 5 minutes-incubation at 37°C with gentle shaking, cell detachment was checked under the microscope (Nikon TMS, Folabo, Buccinasco, Italy) and trypsin activity was blocked by addition of 5 ml of complete medium. Five ml-suspension

containing detached cells was transferred in a sterile 15 ml conical tube (Falcon-Becton Dickinson Italia, Milan, Italy) and centrifuged at 1,500 rpm for 5 minutes at room temperature in a Varifuge 3.OR centrifuge (Heraeus Sepatech). Cell pellet was then carefully resuspended in 5 ml of growth medium and a small aliquot (100 µl) was transferred in a plastic 20 ml-vial (Falcon-Becton Dickinson) containing 10 ml of the isoton solution (azide-free balanced electrolyte solution; Coulter Scientific, Luton, United Kingdom). Single-cell suspension was checked under the microscope in a Burker camera, and the number of detached cells was calculated by counting in a particle counter (Coulter Counter, Coulter Scientific).

Frozen stocks of human tumour cell lines were prepared as follows. Cells in logarithmic growth phase were detached from the flasks and counted as previously described. The percentage of viable cells was also determined by Trypan blue dye exclusion test by mixing, in a 0.5 ml clean conical tube (Eppendorf Italia, Milan, Italy) 5 µl of detached cells suspension, 45 µl of PBS and 50 µl of Trypan blue dye (Sigma). Five µl of Trypan blue dye-stained cell suspension were placed onto a Burker camera and checked under the microscope. The number of viable cells generally exceeded 95%. After counting, the cell suspension was centrifuged at 1,500 rpm for 5 minutes at 4°C. The supernatant was removed and the cell pellet was carefully resuspended in 4°C-cold freezing medium [D-MEM/F12 medium supplemented with 40% (v/v) FBS] at a density of 5 x 10^6 viable cells/ml. One ml of such a cell suspension was then transferred in a 2 ml sterile Nalgene tube (Nalgene Company, Rochester, NY, USA) and placed on ice. One ml of cryoprotective medium [basal EAGLE'S medium with HANKS' BBSS and

15% (v/v) dimethylsulfoxide (DMSO)] (Cambrex) was added to each tube and after a gentle resuspension, the tube was placed onto a Cryo 1°C Freezing Container (Nalgene) and stored at –80°C for the initial freezing step. After 16-24 hours, frozen cells were removed from the freezing container and stored under liquid nitrogen vapours in the Barnstead/Thermolyne containers (Barnstead/Thermolyne, Dubuque, IO, USA).

For cell thawing, frozen cells were incubated in a 37°C water bath (PBI International Italia, Milan, Italy), transferred into a sterile 15 ml conical tube containing 10 ml of complete growth medium and centrifuged at 1,500 rpm for 5 minutes at room temperature. The cell pellet was then resuspended in 15 ml of growth medium and cells were seeded in a 25-cm^2 flask.

1.3. Nucleic Acids Quantification

Concentration and quality of solutions containing DNA, RNA or oligonucleotides were determined by spectrophotometric analysis as follows. In two clean 1.5 ml tube (Eppendorf), a suitable volume of nucleic acid-containing solution (generally, 5 and 10 µl) was gently mixed with RNase- or DNase-free distilled water to a final volume of 200 µl to obtain a 1:40 and 1:20 dilutions. As the blank sample, a third clean tube containing 200 µl of RNase- or DNase-free distilled water was also prepared. The content of each tube was transferred into quartz cuvettes (Perkin-Elmer Italia, Monza, Italy), the cuvettes were then placed onto a Lambda 11/Bio spectrophotometer (Perkin-Elmer) and absorbance values at 260 nm (A_{260nm}) and 280 nm

(A_{280nm}) of wave length were measured. The A_{260nm} and A_{280nm} values obtained with the blank sample were subtracted from the absorbance values obtained with the nucleic acid-containing samples, and DNA, RNA or oligonucleotide concentration was then calculated using these formulae:

µg/ml of DNA = (A_{260nm}) x (DILUTION FACTOR) x (50 µg/ml)

µg/ml of RNA = (A_{260nm}) x (DILUTION FACTOR) x (40 µg/ml)

µg/ml of oligonucleotide = (A_{260nm}) x (DILUTION FACTOR) x (30 µg/ml)

The nucleic acid concentration was expressed as the mean of the values (µg/ml) obtained in the two independently-prepared and –measured dilutions.

The quality of nucleic acid solutions was evaluated by calculating the A_{260nm}/A_{280nm} ratio. It is well known that for both DNA and oligonucleotide, a ratio of 1.8-2 was indicative of a good-quality preparation, whereas high quality RNA solutions are characterised by a A_{260nm}/A_{280nm} ratio of 2.

1.4. Protein Concentration Determination

Protein concentration was determined according to Bradford [1976].

1.4.1. Calibration Curve Preparation

Solutions of bovine serum albumin (BSA) (0.001 µg/µl, 0.0025 µg/µl, 0.005 µg/µl, 0.01 µg/µl, 0.025 µg/µl and 0.05 µg/µl) were prepared by dissolving powdered BSA (Sigma) in distilled water. In a 1.5 ml tube, 250 µl

of each BSA solution were mixed with 150 µl of distilled water and 100 µl of Biorad Protein assay dye (Biorad, Milan, Italy). In the blank sample, 400 µl of distilled water were mixed with 100 µl of Biorad Protein assay dye. Samples were rapidly transferred into disposable 96 well plate (Corning-Costar) and the absorbance at 595 nm wave length of each calibration point was measured using a microtiter plate reader (PBI International). The absorbance value corresponding the blank sample was then subtracted from the values obtained in the BSA-containing samples. Each calibration sample was run in triplicate.

1.4.2. Protein Concentration Quantification

Concentration of extracted proteins was determined by mixing in a 1.5 ml tube 5 µl of protein extracts with 95 µl of Biorad Protein assay dye and distilled water to a final volume of 500 µl. Samples were rapidly transferred into 96 well plate and the absorbance at 595 nm wave length was measured in the spectrophotometer plate reader. From the calibration curve, it was possible to determine the protein concentration of each sample. Also in this case, each sample was run in triplicate.

1.5. Agarose Gel Preparation

All agarose gel electrophoresis experiments were carried out using Hoefer horizontal electrophoresis units (Amersham-Pharmacia Biotech Italia, Cologno Monzese, Italy).

Gels of different sizes and percentages (w/v = grams of powdered agarose per 100 ml of running buffer) were prepared in clean glass bottles by mixing suitable amounts of powdered agarose (Sigma) in 1x TAE [0.04 M Tris-Acetate (Sigma), 0.001 M EDTA (Sigma)] or 1x TBE [0.09 M Tris-Borate (Sigma), 0.002 M EDTA] running buffers. Agarose was dissolved by heating in a microwave, cooled to about 50°C, transferred onto the casting tray and, after the insertion of a clean comb, left to polymerise at room temperature. When polymerisation was completed, the comb was removed and solidified agarose gel was transferred into the running tray and submerged with running buffer.

1.6. SDS-Polyacrylamide Gel Preparation

All SDS-polyacrylamide gels used for protein separation (8 centimetres high/ 10 centimetres length/ 1 millimetres thick) were prepared as described by Laemmli [1970] and run in a Hoefer SE 600 vertical electrophoresis slab unit (Amersham). Resolving gel (10 ml) was prepared in a 15 ml conical tube (Falcon-Becton Dickinson) by mixing a suitable volume of 40% (w/v) polyacrylamide stock solution (acrylamide:N,N'-methylenebisacrylamide

molar ratio = 29:1) (Sigma) with 0.1 ml of 10% (w/v) SDS solution (Sigma) [final concentration = 0.1% (w/v)], 2.5 ml of 1.5 M Tris-HCl pH 8.8 solution (Sigma) (final concentration = 375 mM), 100 µl of 10% (w/v) APS (Sigma) [final concentration = 0.1% (w/v)] and 6 µl of TEMED (Sigma) [final concentration = 0.06% (v/v)], and subsequently poured into the gap between glass plates (previously washed with absolute ethanol) leaving sufficient space for the stacking gel. The poured resolving polyacrylamide gel solution was immediately and carefully overlaid with 0.1% (w/v) SDS solution (the overlay prevents oxygen from diffusing into the gel and inhibiting polymerisation) and the gel was placed in a vertical position at room temperature to polymerise. When polymerisation was complete (within 20-40 minutes), the overlay was poured off and the top of the gel was carefully washed several times with distilled water to remove any unpolymerised acrylamide. The stacking gel (2 ml) containing 5% (w/v) polyacrylamide (acrylamide:N,N'-methylenebisacrylamide molar ratio = 29:1), 0.1% (w/v) SDS, 125 mM Tris-HCl pH 6.8, 0.1% (w/v) APS and 0.1% (v/v) TEMED was prepared in a 15 ml conical tube and poured directly onto the surface of the polymerised resolving gel. A clean comb was immediately inserted into the stacking gel solution and the gel was placed in vertical position to polymerise. When polymerisation was complete, the comb was removed, the wells were washed with distilled water to remove any unpolymerised acrylamide and the gel was mounted in the electrophoresis apparatus containing TGS running buffer [25 mM Tris base, 250 mM Glycine (Sigma), 0.1% (w/v) SDS, pH 8.3] in both upper and lower buffer reservoirs.

1.7. Non-Denaturating Polyacrylamide Gel Preparation

Non-denaturing polyacrylamide gels (16 centimetres high/16 centimetres length/1.5 millimetres thick) were prepared and run in a Hoefer SE 600 vertical electrophoresis slab unit (Amersham).

Polyacrylamide gel solution (30 ml) containing 10% (w/v) polyacrylamide (acrylamide : N,N'-methylenebisacrylamide molar ratio = 19:1), 0.5x TBE buffer, 0.07% (w/v) APS and 0.035% (v/v) TEMED, was prepared in a 50 ml conical tube and subsequently poured into the gap between glass plates (previously washed with absolute ethanol). A clean comb was immediately inserted and the gel was placed in vertical position to polymerise. When polymerisation was completed, the comb was removed, the wells were washed with 0.5x TBE buffer to remove any unpolymerised acrylamide and the gel was mounted in the electrophoresis apparatus containing 0.5x TBE running buffer in both upper and lower reservoirs.

1.8. Preparation of the Plasmid Vectors

To obtain a permanent and stable source of pRc/CMV (Invitrogen, San Diego, CA, USA), pCI-neo (Promega Italia, Milan, Italy) and pCLXSN (Imgenex, San Diego, CA, USA) vectors carrying ribozyme and survivin sequences, the following procedures were performed.

1.8.1. Preparation of Competent JM109 E. Coli Cells for Transformation

Fifty µl of sterile JM109 E. coli cellular suspension (Promega) were mixed, in a sterile 50 ml conical tube, with 10 ml of sterile LB medium [1% (w/v) Bacto-Tryptone (Invitrogen), 0.5% (w/v) Bacto-Yeast extract (Invitrogen), 1% (w/v) NaCl (Sigma), pH 7.0] and allowed to grow in a 37°C-heated shaking incubator (GFL3031; Folabo) at 225 rpm over night. One ml of such liquid bacterial culture was then transferred into a sterile 500 ml bottle containing 100 ml of sterile LB medium and the bottle was placed into the 37°C-heated shaking incubator at 225 rpm.

To harvest bacterial cells in logarithmic growth phase, 2 hours later, 1 ml of liquid culture was transferred, under a laminar flow, in a disposable cuvette and the absorbance at 600 nm of wave length was read on the spectrophotometer. E. coli concentration in the liquid culture was calculated by considering that 1 A_{600nm} unit corresponds to about 8 x 10^6 bacterial cells/ml. When A_{600nm} of the liquid culture reached 0.3 units (corresponding to 240 x 10^6 cells/ml; 24 x 10^9 cells in 100 ml) the bacterial suspension was transferred, under a laminar flow, in two ice-cold sterile 50 ml conical tubes and the cell growth was stopped by placing the tubes on ice for 15 minutes. E. coli cells were pelleted by a 3,000 rpm centrifugation at 4°C for 10 minutes and, after the removal of LB medium, cell pellets were pooled in the same tube by gentle resuspension in 10 ml of ice-cold sterile 0.1 M $CaCl_2$ solution (Sigma). After addition of 40 ml of ice-cold sterile 0.1 M $CaCl_2$ solution, bacterial suspension was incubated on ice for 30 minutes and subsequently centrifuged at 3,000 rpm for 10 minutes at 4°C. The supernatant was then

removed and the cell pellet was carefully resuspended in 5 ml of an ice-cold sterile 0.1 M $CaCl_2$-15% (v/v) glycerol (Sigma) solution. Such a bacterial suspension was incubated on ice for 24 hours. At the end of incubation, the bacterial suspension was mixed by gentle pipetting, divided in 500 µl-aliquots (4.8×10^9 cells/ml; 2.4×10^9 cells in each 500 µl-aliquot) in sterile 0.5 ml Nalgene tubes, frozen by snap freezing in liquid nitrogen and stored at -80°C.

Fifty µl (240×10^6 cells) of freshly-prepared competent cells were transformed with 50 ng of a DNA vector able to confer ampicillin resistance and 1/100,000 (dilution factor, 10^5) of the bacterial suspension was plated as described in the 2.1.9.2 section. Transformation efficiency, calculated on the basis of the formula

(NUMBER OF COLONIES) x (10^3) x (DILUTION FACTOR) / 50 ng

was expressed as the number of colony forming units (CFU) per µg of plasmid DNA. Generally, 10^6-10^8 CFU per µg of plasmid DNA were indicative of a good preparation of competent bacterial cells.

1.8.2. Transformation of Bacteria

In an ice-cold 10 ml Falcon 2059 tube (Falcon-Becton Dickinson), 240×10^6 of competent bacterial cells (50 µl; section 2.9.1) were diluted to a final volume of 100 µl with 0.1 M $CaCl_2$ and 50 ng (5 µl) of purified vector were then added. The mixture was gently mixed by tapping and the tube was chilled on ice for 30 minutes, incubated for 90 seconds at 42°C in a water

bath and for 2 minutes on ice. After a 5-minute incubation at room temperature, 900 µl of LB medium were added and tube was placed into a 37°C-heated shaking incubator at 225 rpm for 2 hours. The tube was then centrifuged at 3,000 rpm for 5 minutes at room temperature, 950 µl of supernatant LB were removed and bacterial cell pellet was resuspended in the remaining 50 µl, plated onto 90-mm dish (Corning-Costar) containing selective solid LB medium [liquid LB medium, 1.5% (w/v) agar (Invitrogen), 50 µg/ml ampicillin (Mead-Johnson, Rome, Italy)] and incubated over night at 37°C. Each colony, representing ampicillin-resistant/transformed growing bacterial cells, was picked-up with a sterile disposable loop, dissolved in a 50 ml conical tube containing 10 ml of liquid LB medium supplemented with ampicillin (50 µg/ml final concentration) and allowed to grow over night at 37°C with 225 rpm shaking.

1.8.3. Small Scale Preparation of Plasmid DNA ("miniprep")

To confirm the presence of plasmids in ampicillin-resistant liquid culture, 8 ml of the bacterial suspension were used for "miniprep" by using Qiagen Plasmid Mini Kit (Qiagen, Hilden, Germany) according to the manufacturer's instructions. Plasmid DNA concentration was determined spectrophotometrically as described in the section 1.3.

Electrophoretic analysis was performed on 1% (w/v) agarose mini gel prepared and run in 1x TAE buffer. About 500 ng of extracted and original DNA vectors were loaded and separated at 90 volt (SE300 power supply;

Amersham) at room temperature for 1 hour in the presence of 500 ng of λ-*BstEII* molecular weight marker (Sigma). DNA fragments were visualised by placing the gel onto the UV-transilluminator (260 nm wave length) (Biorad) after a 30-minutes staining with 1 µg/ml ethidium bromide (Invitrogen)-1x TAE buffer staining and a 30-minute 1x TAE buffer destaining.

1.8.4. Storage of Vector-Transformed Bacteria

In a 2 ml sterile Nalgene tube, 1.6 ml of ampicillin-resistant liquid bacterial culture and 0.4 ml of sterile pure glycerol (final concentration (v/v) = 20%) were mixed by a vortex mixer and frozen by snap freezing in liquid nitrogen and stored at -80°C.

1.8.5. Large Scale Preparation of Plasmid DNA ("maxiprep")

By means of a sterile spatula, frozen bacterial cells were scraped from the 2 ml sterile Nalgene tube and dissolved in 10 ml of 50 µg/ml ampicillin containing-LB medium (contained in a 50 ml conical tube) and allowed to grow at 37°C in a shaking incubator at 225 rpm. After 8 hours, 10 ml liquid culture was mixed with 100 ml of fresh 50 µg/ml ampicillin containing-LB medium into a 500 ml glass bottle and cells were left to grow over night at 37°C and 225 rpm.

Bacterial cells were pelleted by a 30-minute centrifugation at 4,000 rpm at 4°C and, after removal of LB medium, plasmid DNA was purified with the

Qiagen Plasmid Maxi Kit (Qiagen) according to the manufacturer's instructions.

Concentration and quality of the plasmid DNA were evaluated as described in the section 1.3.

2. SPECIFIC PROCEDURES

2.1. Design and Synthesis of Ribozymes Targeting Survivin mRNA

The ribozyme design was performed by an *in silico* approach using the already described, home-developed computing method [Mercatanti *et al*, 2002], which predicts the regions of the survivin mRNA (GeneBank Accession N. NM_001168.1) endowed with the most probable conformational accessibility. Many NHH consensus cleavage triplets (N= any nucleotide, H= A, C, U) lie within these accessible regions, therefore they were recognized to be suitable targets for hammerhead ribozymes. A series of catalytic ribozyme sequences were correspondingly deduced. The final analysis accounting for the correct structure-activity relationship enabled us to select the hammerhead ribozyme addressed to the CUA_{110} triplet located on the survivin mRNA. The ribozyme sequence, Rz (Figure 25), was synthesized by *in vitro* transcription. A mutant ribozyme (mutRz) obtained by deleting the G_{12} from the catalytic core (as indicated by the circled letter in Figure 25) and an irrelevant ribozyme (CTR) directed against the FIV primer bonding site, were designed and synthesized to obtain the negative controls. Single-stranded synthetic DNA oligonucleotides encoding active and control ribozymes were obtained from MWG Biotech (Ebersberg, Germany). The oligonucleotide sequences were the following:

Rz+ 5'-AGCTTCTTGAATGCTGATGAGGCCGAAAGGCCGAAAGAGATGT-3'

Rz- 5'-CTAGACATCTCTTTCGGCCTTTCGGCCTCATCAGCATTCAAGA-3'

mutRz+ 5'-AGCTTCTTGAATGCTGATGAGGCCGAAAGGCCAAAGAGATGT-3'

mutRz- 5'-CTAGACATCTCTTTGGCCTTTCGGCCTCATCAGCATTCAAGA-3'

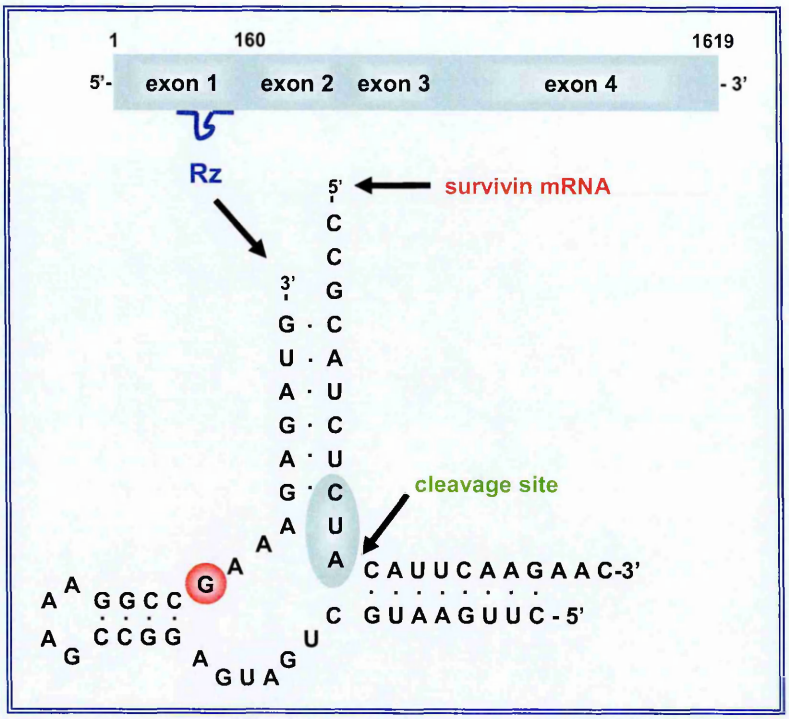

Figure 25. Ribozyme structure.

Schematic representation of base pairing of the Rz ribozyme with its RNA target site obtained from survivin mRNA. The cleavage site is indicated by an arrow. The mutant ribozyme mutRz, which was used as control throughout the study, was obtained by deleting the G_{12} from the catalytic core of the active ribozyme.

2.1.1. Annealing of Complementary Pairs of Oligonucleotides

In a microcentrifuge tube, the complementary oligonucleotides were mixed together at a 1:1 molar ratio. The oligonucleotide mixture was then diluted to a final concentration of 1 pmol/µl with a phosphate buffer containing salt [10 mM Tris, 1 mM EDTA, 50 mM NaCl (pH 8.0) or 100 mM sodium phosphate, 150 mM NaCl, 1 mM EDTA (pH 7.5)]. The oligonucleotides were incubated at 95°C for 5 minutes, and then the heat was gradually reduce until the oligonucleotides have reached room temperature. The double-stranded DNA probe was stored at -20°C. Annealing of the complementary

oligonucleotides produced two fragments with *HindIII* and *XbaI* protruding ends.

2.1.2. Synthesis of Ribozyme-Expressing Plasmid Vectors

2.1.2.1. Digestion of the pRC/CMV Plasmid Vector

In a 1.5 ml tube, an aliquot containing 30 µg of pRC/CMV plasmid was mixed with 60 units of *HindIII* and *XbaI* restriction enzymes (Promega), 1x digestion buffer specific for both enzymes (Buffer E) (Promega) and distilled water to a final volume of 100 µl. The mixture was then incubated at 37°C in a water bath. After 1 hour, the reaction was stopped by addition of 5 µl of 0.5 M EDTA, pH 8. The digestion of the vector template was verified as described in the 1.8.3. section by loading about 200 ng of digested vector with the same amount of undigested plasmid DNA and 500 ng of λ-*BstEII* molecular weight marker.

2.1.2.2. Purification of *HindIII/XbaI*-Digested pRC/CMV Vector

Digestion mixture was diluted to a final volume of 400 µl with distilled water. An equal volume of phenol (Sigma)/chloroform/isoamilic alcohol (Carlo Erba Reagenti, Milan, Italy) solution [25:24:1, (v/v/v)] was then added. The tube was extensively mixed by tapping and centrifuged at 12,000 rpm at 4°C for 5 minutes, then the aqueous upper phase, containing plasmid DNA, was recovered and placed in a clean 1.5 ml tube and an equal volume of

chloroform/isoamilic alcohol solution [24:1, (v/v)] was added. After mixing, the tube was centrifuged and the aqueous upper phase was recovered and placed in a clean 1.5 ml conical tube. To precipitate plasmid DNA, the aqueous phase was mixed with sodium acetate, pH 5.2 (Sigma), (0.3 M final concentration) then, after addition of 2 volumes of -20°C-cold 100% ethanol, the solution was mixed for a few seconds using the vortex and placed for 1 hour at -80°C. The sample was then centrifuged at 12,000 rpm at 4°C for 30 minutes, and, after ethanol removal, pelleted DNA was washed twice with 70% (v/v) ethanol and dried for 3 minutes with a speed-vacuum centrifuge (Heraeus). Dried plasmid vector was then dissolved in distilled water and quantified spectrophotometrically.

2.1.2.3. Cloning of the Ribozyme Sequences into the pRC/CMV Vector

In a 1.5 ml tube, 10 µl of each fragment was mixed with 3 µl digested plasmid, 4 µl 5x ligation buffer, 1 µl T4 DNA ligase, and sterile distilled water to a final volume of 20 µl. Tubes were incubated overnight at 16°C. The resulting plasmids were named pRc/Rz and pRc/mutRz. A permanent and stable source of the plasmids were obtained as described in 1.8.2. and 1.8.4. sections.

2.1.3. Synthesis of VA1-Fusion Ribozymes

2.1.3.1. Digestion of the pBS-VA1 Plasmid Vector

In a 1.5 ml tube, 30 µg of pBS-VA1 plasmid [Prislei *et al*, 1997] was mixed with 60 units of *HindIII* and *XbaI* restriction enzymes (Promega), 1x digestion buffer specific for both enzymes (Buffer E) (Promega) and distilled water to a final volume of 100 µl. The mixture was then incubated at 37°C in a water bath. After 1 hour, the reaction was stopped by addition of 5 µl of 0.5 M EDTA, pH 8. The digestion of the vector template was verified as described in the 1.8.3 section by loading about 200 ng of digested vector with the same amount of undigested plasmid DNA and 500 ng of λ-*BstEII* molecular weight marker. The mixture was then purified and quantified as described in the 2.1.2.2. section.

2.1.3.2. Cloning of the Ribozyme Sequences into the pBS-VA1 Vector

In a 1.5 ml tube, 10 µl of each fragment was mixed with 3 µl digested plasmid, 4 µl 5x ligation buffer, 1 µl T4 DNA ligase, and sterile distilled water to a final volume of 20 µl. Tubes were incubated overnight at 16°C.

2.1.3.3. Digestion of the VA1-Ribozyme Cassette

In a 1.5 ml tube, 30 µg of VA1-ribozyme cassette was mixed with 60 units of *EcoRI* and *HindIII* restriction enzymes (Promega), 1x digestion buffer specific for both enzymes (Buffer H) (Promega) and distilled water to a final volume of 100 µl. The mixture was then incubated at 37°C in a water bath. After 1 hour, the reaction was stopped by addition of 5 µl of 0.5 M EDTA, pH 8. The digestion of the template was verified as described in the 1.8.3 section by loading about 200 ng of digested vector with the same amount of undigested plasmid DNA and 500 ng of λ-*BstEII* molecular weight marker.

2.1.3.4. Blunting of the VA1-Ribozyme Cassette

In a 1.5 ml tube, 0.1 pmol of VA1-ribozyme cassette was mixed with 1 µl of T4 DNA polymerase (Promega), 1x of reaction buffer (Promega) and distilled water to a final volume of 10 µl. The mixture was then incubated 5 minutes at 70°C followed by 5 minutes at 37°C. The reaction was stopped by addition of DNA dilution buffer to bring the DNA concentration to 1 µg/50 µl. The mixture was then purified and quantified as described in the 2.1.2.2. section.

2.1.3.5. Digestion of the pCLXSN Plasmid Vector

In a 1.5 ml tube, 30 µg of pCLXSN plasmid was mixed with 60 units of *NheI* restriction enzyme (Promega), 1x digestion buffer specific for both

enzymes (Buffer H) (Promega) and distilled water to a final volume of 100 µl. The mixture was then incubated at 37°C in a water bath. After 1 hour, the reaction was stopped by addition of 5 µl 0.5 M EDTA, pH 8. The digestion of the vector template was verified as described in the 1.8.3 section by loading about 200 ng of digested vector with the same amount of undigested plasmid DNA and 500 ng of λ-*BstEII* molecular weight marker. The mixture was then purified and quantified as described in the 2.1.2.2. section.

2.1.3.6. Cloning of the VA1-Ribozyme Cassette into the pCLXSN Vector

In a 1.5 ml tube, 10 µl of each VA1-ribozyme cassette was mixed with 3 µl digested plasmid, 4 µl 5x ligation buffer, 1 µl T4 DNA ligase, and sterile distilled water to a final volume of 20 µl. Tubes were incubated overnight at 16°C. The resulting plasmids were named pCLXSN/Rz and pCLXSN/CTR. A permanent and stable source of the plasmids were obtained as described in 1.8.2. and 1.8.4. sections.

2.2. *In Vitro* Catalytic Activity

2.2.1. *In Vitro* Ribozyme Transcription

2.2.1.1. Linearization of the pRc/Rz and pRc/mutRz Plasmids

In a 1.5 ml tube, 30 µg of pRc/Rz and pRc/mutRz plasmids were mixed with 60 units of *XbaI* restriction enzyme (Promega), 1x specific digestion

buffer (Buffer E) (Promega) and distilled water to a final volume of 100 µl. The mixture was then incubated at 37°C in a water bath. After 1 hour, the reaction was stopped by addition of 5 µl 0.5 M EDTA, pH 8. The linearization of the vector template was verified as described in the 1.8.3. section by loading about 200 ng of digested vector with the same amount of undigested plasmid DNA and 500 ng of *λ-BstEII* molecular weight marker. The mixtures were then purified and quantified as described in the 2.1.2.2. section.

2.2.1.2. *In Vitro* Transcription of Ribozymes

In a 0.5 ml tube, 20 µg of the resulting linear templates were *in vitro* transcribed in 0.2 ml of a reaction mixture composed of 260 units recombinant RNAsin ribonuclease inhibitor (Promega), 0.25 mM each of ribonucleotide triphosphates, 5 mM DTT, 1x transcription buffer (40 mM Tris-HCl, pH 8, 8 mM $MgCl_2$, 2 mM spermidine), and 200 units T7 RNA polymerase (Takara, Shuzo Co., Otsu Shiga, Japan). The reaction mixtures were incubated for 2 hours at 37°C and then treated with 20 units RQ1 RNase-free DNase (Promega) for 20 minutes at 37°C. The products were then purified and quantified as described in the 2.1.2.2. section.

2.2.2. Synthesis of the Synthetic Substrate

2.2.2.1. Linearization of the pCI-Surv Plasmid

In a 1.5 ml tube, 30 µg of pCI-surv plasmid was mixed with 60 units of *StyI* restriction enzyme (Promega), 1x specific digestion buffer (Buffer H) (Promega) and distilled water to a final volume of 100 µl. The mixture was then incubated at 37°C in a water bath. After 1 hour, the reaction was stopped by addition of 5 µl 0.5 M EDTA, pH 8. The linearization of the vector template was verified as described in the 1.8.3. section by loading about 200 ng of digested vector with the same amount of undigested plasmid DNA and 500 ng of *λ-BstEII* molecular weight marker. Digestion mixtures were then purified as described in the 2.1.2.2. section.

2.2.2.2. *In Vitro* Transcription of the Synthetic Substrate

In a 0.5 ml tube, 10 µg (6.25 pmoles) of *StyI*-linearised vector was *in vitro* transcribed in a solution containing 260 units recombinant RNAsin ribonuclease inhibitor (Promega), 0.25 mM each of ribonucleotide triphosphates, 5 mM DTT, 1x transcription buffer (40 mM Tris-HCl, pH 8, 8 mM $MgCl_2$, 2 mM spermidine), 200 units T7 RNA polymerase (Takara), and 10 µCi [γ-^{32}P]-ATP (800 Ci/mmole) (Amersham). The reaction mixtures were incubated for 2 hours at 37°C and then treated with 20 units RQ1 RNase-free DNase (Promega) for 20 minutes at 37°C. Labelled DNA was purified and recovered as described in the 2.1.2.2. section with some modifications.

Labelled DNA pellet was washed 4 times with 70% ethanol; the dried DNA pellet was dissolved in distilled water (50 µl) and cpm corresponding to 1 µl of this DNA solution was evaluated by "Cerenkov counting" at the β-counter (Tri-Carb Liquid Scintillation Analyzer; Camberra-Packard Italia, Milan, Italy). Assuming a DNA recovery of 50% after purification steps, a solution at a concentration of 100 ng/µl with a specific activity of 50,000-100,000 cpm/ng was generally obtained.

2.2.3. *In Vitro* Cleavage Reaction

The synthetic ^{32}P-substrate RNA (10 nM) was mixed with 10-1000 nM Rz or with 1000 nM mutRz in 50 mM Tris-HCl, pH 7.5. The mixtures were heated for 5 minutes at 90°C, cooled at 37°C, and then incubated in the presence of 50 mM $MgCl_2$. The cleavage reactions were performed at 37°C for 120 minutes. Reactions were stopped by adding an equal volume of stop solution (95% formamide, 20 mM EDTA, 0.05% bromophenol blue, 0.02% xylene cyanol FF). Products were resolved on a 5% polyacrylamide/7 M urea gel and the results were quantified by densitometric analysis.

2.3. Transfection of Cells with the Ribozyme Expression Vectors

After harvesting in logarithmic growth phase, JR8 cells were seeded in 6-well plates (Corning-Costar) in 2 ml of fresh media at a density yielding approximately 50% confluency at the time of transfection. The plates were

then incubated at 37°C in a 5% CO_2 humidified atmosphere in the air incubator for 24 hours. In a 0.5 ml tube, 5 µg of pRc/Rz vector (or pRc/mutRz vector) were complexed with 30 µg of DOTAP (N-(1-(2,3 dioleoyloxy) propyl)-N,N,N-trimethylammoniummethyl sulphate) (Boehringer Mannheim, Mannheim, Germany). The reaction mixtures were incubated for 20 minutes at 37°C and then added to the wells. Twenty-four hours after transfection the culture medium containing the DOTAP/DNA mixture was replaced by a selection medium containing G418 to a final concentration of 2 mg/ml. The transfected cells were exposed to G418 for 1 month for the selection of different cellular clones. Two polyclonal populations, JR8/Rz and JR8/mutRz cells expressing the active and the mutant ribozymes respectively, were selected for the study.

2.4. Transduction of Cells with the Ribozyme Expression Vectors

2.4.1. Transfection of HEK293gp cells

Twenty-four hours prior to transfection, HEK293gp packaging cells (constitutively expressing *gag* and *pol* genes) [Somia *et al*, 2000] were seeded in 4 ml of fresh media at a density of 2 x 10^6 cells in 6-well plates (Corning-Costar). Just prior to transfection, the medium was removed and the fresh growth medium was gently added. In a 0.5 ml tube, 5 µg of plasmid vector (pCLXSN/Rz or pCLXSN/CTR) was complexed with 5 µg of VSV-G-encoding plasmid, 36 µl of 2 M $CaCl_2$, 300 µl of 2x HeBS and sterile distilled water to a final volume of 600 µl. This solution was then added to the cells

and the plate was gently swirled to ensure uniform mixing. After 6 hours incubation at 37°C in a 5% CO_2 humidified atmosphere, the transfection cocktail was washed out and replaced with fresh medium. The viral particle-containing supernatants were collected 24, 48 and 72 hours after transfection and filtered through a 0.45-µm filter.

2.4.2. Infection of Prostate Cancer Cells

Twenty-four hours prior to transfection, DU145 and PC-3 prostate cancer cells were seeded in 4 ml of fresh media at a density of 1 x 10^6 cells in 6-well plates (Corning-Costar). Just prior to transfection, the medium was removed and replaced with 1 ml of viral particle-containing supernatants, 1 ml of fresh complete media and polybrene (8 µg/ml). The cells were cultured for 72 hours in the presence of the virus and then maintained in RPMI medium supplemented with G418 for 1 month and four polyclonal cell populations, two expressing the anti-survivin ribozyme (DU145/Rz and PC-3/Rz) and two expressing the control ribozyme (DU145/CTR and PC-3/CTR), were selected for the study.

2.5. Reverse Transcriptase-PCR Analysis of Ribozyme Expression

Ribozyme expression in parental (JR8, DU145 and PC-3), transfected (JR8/Rz and JR8/mutRz) and infected (DU145/Rz, PC-3/Rz, DU145/CTR and PC-3/CTR) cells was evaluated by RT-PCR analysis.

2.5.1. Cell Preparation

Cells in logarithmic growth phase were detached from the flasks by means of sterile Trypsin-EDTA solution, transferred into a sterile a 15 ml conical tube and pelleted by a 5-minute centrifugation at 1,500 rpm at 4°C. Single-cell suspension was obtained by resuspending cell pellets in 10 ml of sterile PBS; the suspension was checked under the microscope, and a small aliquot (100-500 µl) was transferred in the isoton solution and counted in the particle counter.

An aliquot of cell suspensions containing about 5-10 x 10^6 cells was then transferred in a sterile 1.5 ml tube, cells were pelleted by a 30-second centrifugation at 12,000 rpm at 4°C. After removal of PBS, cell pellets were washed twice with 1 ml of sterile PBS. At the end of the last wash, PBS was removed and total RNA was extracted from the cells.

2.5.2. Total RNA Isolation

All extraction and manipulation steps were performed under sterile conditions using Diethylpirocarbonate (DEPC) (Sigma)-treated or 'RNase-free' certified chemicals and plastic disposable materials.

Total cellular RNA was obtained from fresh or frozen cell pellets by means of the Trizol Reagent (Invitrogen) according to the manufacturer's instructions. The amount of extracted RNA was determined spectrophotometrically.

Quality of isolated RNA was checked by gel electrophoresis analysis carried out by using a 1% (w/v) agarose mini gel (10 centimetres length/6 centimetres wide) prepared in 1x TAE buffer. An aliquot corresponding to about 1 µg of extracted ribonucleic acid was mixed in a RNase-free 0.5 ml tube with an equal volume of sequencing gel loading buffer [95% (v/v) Formamide (Sigma), 20 mM EDTA pH 8, 0.05% (w/v) bromophenol blue and 0.05% (w/v) xylene cyanol (Sigma)], heated at 100°C for 3 minutes (to completely destroy possible RNA secondary structures), chilled on ice for further 3 minutes and loaded. RNA samples were run at a constant voltage of 90 volts for 1 hour at room temperature. The gel was then stained for 30 minutes at room temperature with gentle shaking in the ethidium bromide staining solution (1 µg/ml ethidium bromide prepared in 1x TAE buffer) and destained for further 30 minutes at room temperature with gentle shaking in 1x TAE buffer. RNA was visualised by means of the UV transilluminator and photographed on a 667 Polaroid film (Polaroid LtD-St. Albans, United Kingdom). The presence of well defined and visible bands corresponding to both 28S and 18S ribosomal RNA was indicative of a good RNA preparation.

Total RNA extracted from each cell line was stored at -80°C as 1 µg aliquots.

2.5.3. Synthesis of First Strand cDNA by Reverse Transcriptase Reaction

Total RNA extracted from each cell line was reverse transcribed by using RNA PCR Core Kit (Perkin-Elmer). In a RNase-free 0.5 ml reaction tube

(Perkin-Elmer), 1 µg of total RNA was mixed with 2.5 µM random hexamers, 20 units of RNase inhibitor, 2.5 mM $MgCl_2$, 1mM each dNTP, 1x PCR buffer (10 mM Tris-HCl pH 8.3, 50 mM KCl), 50 units of MuLV reverse transcriptase and RNase-free water to a final volume of 20 µl. Tubes were incubated at room temperature for 15 minutes (to allow annealing between random hexamers and RNA). First strand cDNA synthesis and MuLV reverse transcriptase inactivation were then obtained by a 42°C-incubation for 30 minutes and a 5-minute heating at 95°C, respectively, in a hot-bonnet thermal cycler (MJ Research/M-Medical-Florence, Italy). Samples were stored at 4°C until they were used in PCR reactions.

2.5.4. PCR Reactions

To analyze ribozyme expression, the resultant cDNAs were amplified using T7 (5'-TAA TAC GAC TCA CTA TAG GGA GA-3') and SP6 (5'-CG ATT TAG GTG ACA CTA TAG-3') or VA1 sense (5'-GGG CAC TCT TCC GTG GTC-3') and VA1 anti-sense (5'-AAA GGA GCG CTC CCC CGT TG-3') primers in melanoma and prostate cancer cells, respectively. All primers used were synthesised and supplied in lyophilised form by MWG Biotech. For each primer, 100 µM stock solution was prepared by dissolving the lyophilised primer in an opportune volume of 1x TE pH 8 (10 mM Tris-HCl, 1 mM EDTA) by extensive vortexing. The successive dilutions were prepared in distilled water.

The vectors pRc/Rz, pRc/mutRz, pCLXSN/Rz and pCLXSN/CTR were used as controls for the correct fragment size during PCR amplification.

The PCR amplification was performed using the RNA PCR Core Kit (Perkin-Elmer) as follows. In DNase-free 0.5 ml PCR reaction tubes, 125 ng of total RNA reverse transcribed in first strand cDNA (or plasmid vector) were mixed with 1 μM T7 and SP6 (or VA1 sense and antisense) primers, 0.625 units of AmpliTaq DNA polymerase, 1x PCR buffer, 2 mM $MgCl_2$ and DNase-free water to a final volume of 25 μl. Tubes were then placed in a hot-bonnet thermal cycler and PCR products were obtained performing 1 cycle at 95°C for 5 minutes followed by 30 cycles each formed by a denaturation step of 1 minute at 95°C, an annealing step of 1 minute at 47°C for T7/SP6 primers (62°C for VA1 sense and antisense) and an extension step of 1 minute at 72°C followed by a final extension cycle of 5 minutes at 72°C.

It is important to stress that these experimental conditions were selected on the basis of preliminary experiments to ensure that the PCR was still in the exponential phase when the reaction was stopped.

2.5.5. Gel Electrophoresis and Densitometric Quantification of PCR Products

Twenty-five μl PCR solution were mixed with 5 μl 6x gel loading buffer (0.25% (w/v) of both bromophenol blue and xylene cyanol, 30% (v/v) glycerol in distilled water) and samples were loaded onto 3% (w/v)-1x TAE buffer agarose gel. Electrophoretic separation was performed at 90 volts in 1x TAE

buffer and was stopped when bromophenol blue dye reached the bottom of the gel. Agarose gel was then stained for 30 minutes at room temperature with gentle shaking in the ethidium bromide-1x TAE buffer staining solution and destained for a further 30 minutes at room temperature with gentle shaking in 1x TAE buffer. PCR products were visualised on the UV-transilluminator and photographed on a 665 Polaroid film. Negative copy of the film was developed by using 18% (w/v) sodium sulphite (Sigma) according to the manufacturer's instructions and it was used for densitometric quantification of the PCR products by means of a HP ScanJet IIcx/t scanner (HewlettPackard Italia, Milan, Italy) and IQ software (Molecular Dynamics Ltd., Kemsing, United Kingdom).

2.6. Small Interfering RNA Design

Four different siRNAs (siRNA2 [Carvalho *et al*, 2003], siRNA3, siRNA7 and siRNA10) targeting specific consensus sequences (5'-AA(N_{19})UU-3', where N is any nucleotide) within the survivin mRNA were designed by using the siRNA target finder tool (http://www.ambion.com/techlib/misc/siRNA_ finder) (Figure 26). A blast search (http://www.ncbi.nlm.nih.gov/BLAST) for selected siRNA sequences was performed to ensure that only a single gene was targeted. A scramble siRNA, made of a sequence with no significant homology to any known human mRNA, was used as control (siRNActr) throughout the study (Figure 26) [Elbashir *et al*, 2001].

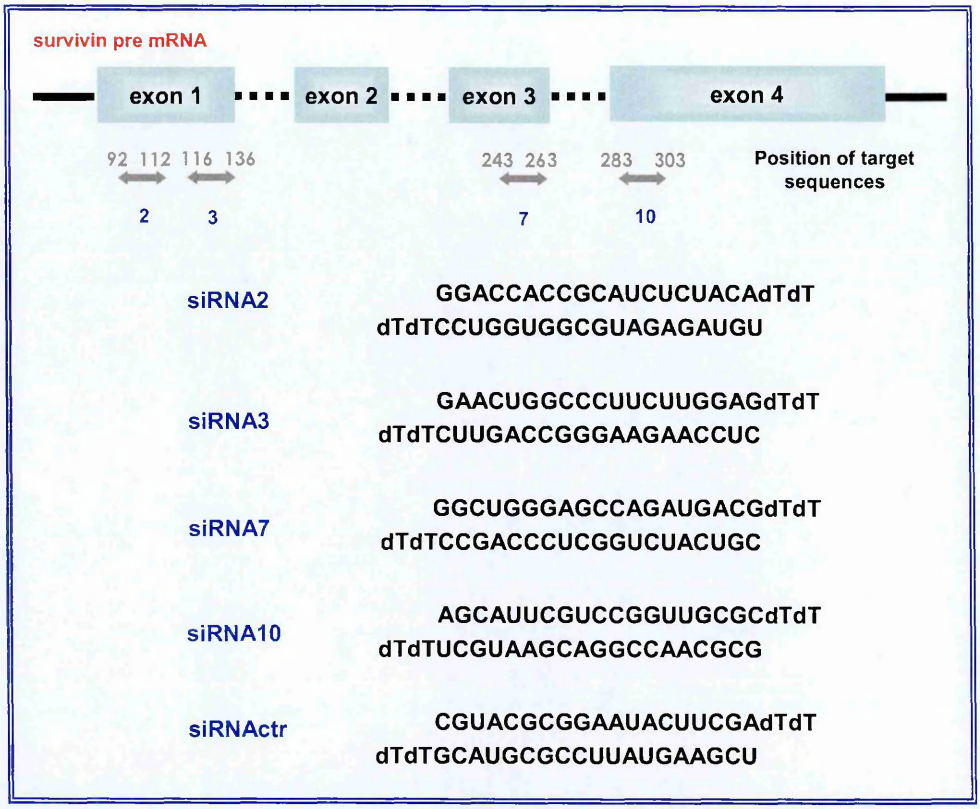

Figure 26. Structures of siRNAs.

Schematic representation of the survivin pre-mRNA and location of each target sequence in survivin mRNA (GeneBank accession n. NM_001168.1). The scramble siRNA (siRNactr) denotes a siRNA that had no significant homology to any known human mRNA [Elbashir *et al*, 2001] and was used to control the specificity of the RNAi reaction.

All siRNAs were purchased from MWG Biotech as preformed and purified duplexes, made of 19 ribonucleotides with two extra thymidine bases forming a 3' overhang on both strands (Figure 26). Each siRNA was resuspended in water and the stock solutions (20 μM) were stored at 4°C until use.

2.7. Transfection of Prostate Cancer Cells with siRNAs

The day before transfection, prostate cancer cells were seeded at a density of 2.5-5.0 x 10^5 per 25 cm^2 flask. A given amount of each siRNA was diluted in 50 µl of Opti-MEM® I reduced serum medium (Invitrogen). The Lipofectamine2000™ (Lipo2000) was diluted in 50 µl of Opti-MEM® I medium and incubated for 5 minutes at room temperature. After the incubation, the diluted siRNA was combined with the diluted Lipo2000 (total volume is 100 µl) and incubated for 20 minutes at room temperature to allow the siRNA:Lipo2000 complexes to form. The mixtures were then applied to the cells in a final volume of Opti-MEM® I medium giving a final siRNA concentration of 100 nM. After incubation for 8 hours at 37°C, RPMI-1640 medium supplemented with serum was added. Cells were then cultured for an additional 24-48 hours at 37°C before further analysis.

2.8. Expression of Survivin and Apoptosis-Related Proteins

The expression of survivin and some of the most important proteins involved in the control of apoptosis was determined by Western blot analysis.

2.8.1. Protein Extract Preparation

Cells in logarithmic growth phase were detached from the flasks by means of Trypsin-EDTA solution, transferred in a 15 ml conical tube and pelleted by

a 5-minute centrifugation at 1,500 rpm at 4°C. To obtain a single-cell suspension, cell pellets were dissolved by repeated pipetting in 10 ml of PBS. Cell suspension was checked under the microscope, and a small aliquot (100 µl) was transferred in the isoton solution and counted in the particle counter.

An aliquot of cell suspension containing about 5 x 10^6 cells was then transferred in a 1.5 ml conical tube and cells were pelleted by a 15-second centrifugation at 12,000 rpm at 4°C. After removal of PBS, cell pellets were again washed twice with PBS. At the end of the last wash, PBS was removed and cells were resuspended by gentle pipetting in 50 µl of ice-cold lysis buffer [1% Nonidet P-40, 10 mM NaF, 1 mM NaV_3O_4, 1 mM $NaPPO_4$, 10 µg/ml leupeptin, 10 µg/ml aprotinin, 1 mM AEBSF, 1x PBS]. Cell suspensions were incubated on ice for 30 minutes. The homogenates were then centrifuged 5 minutes at 12,000 rpm at 4°C and supernatants containing the protein extracts were transferred in a clean 0.5 ml conical tubes.

Protein concentration was determined as described in section 1.4, and protein extracts were stored at -80°C as 50 µg aliquots.

2.8.2. Immunoprecipitation

For the assessment of the Thr^{34}-phosphorylated form of survivin, 100 µg of precleared, detergent-solubilized protein extracts were mixed with 50 µl of a 20% (v/v) protein A-Sepharose slurry (Amersham) 50:50 protein A slurry (Sigma) and immunoprecipitated with the anti-human survivin antibody

(20 µg/ml). The formation of immune complexes was carried out by a 4°C-incubation on a shaking platform. The protein A-Sepharose/anti-survivin antibody/survivin ternary immune complexes were then collected to the bottom of the tube by a 12,000 rpm-centrifugation for 2 minutes at 4°C. After the supernatant phase removal, immune complexes pellets were washed twice with 100 µl of lysis buffer.

2.8.3. Western Blot Analysis

Equivalent amounts of cellular extracts were fractionated, blotted onto solid support and immunoassayed to qualitatively evaluate the expression of survivin protein and apoptosis-related proteins.

2.8.3.1. SDS-Polyacrylamide Gel Electrophoresis

An 12% (w/v) polyacrylamide resolving gel was used to obtain the separation of survivin, Bcl-2, Bcl-x_L, Bax, caspase-3, caspase-9, Akt and cdk6. An aliquot of cellular extracts containing 40 µg of proteins were mixed with 20 µl of colour markers for SDS-PAGE and protein transfer spanning a molecular weight range of 6.5-205 KDa (Sigma) in a 1.5 conical tube. An equal volume of 2x SDS loading buffer (100 mM Tris-HCl pH 6.8, 4% (w/v) SDS, 0.2% (w/v) bromophenol blue (Sigma), 20 (v/v) glycerol and 200 mM DTT) was then added. Tubes were heated at 100°C for 5 minutes, chilled on

ice for an additional 5 minutes, centrifuged at 4°C at 12,000 rpm for 5 seconds and loaded onto the SDS-PAGE system.

Proteins were fractionated running the gel at constant voltage (150 volt) by means of a Biorad 200/2.0 power supply (Biorad). The run was stopped when the 6.8 KDa band of the colour marker reached the bottom of the gel.

2.8.3.2. Transfer of Fractionated Proteins into Nitrocellulose Filter

Protein blotting was performed in an electrophoresis protein transfer unit (Biorad). When the SDS-PAGE was approaching the end of its run, four pieces of Whatman 3MM (Whatman International LtD., Maidstone, United Kingdom) and one piece of nitrocellulose filter (Hybond ECL, Amersham) to the exact size of the resolving gel were cut and soaked for at least 5 minutes in transfer buffer [50 mM Tris base, 100 mM Glycine, 0.01% (w/v) SDS, 20% (v/v) methanol (Carlo Erba Reagenti), pH 7.5]. At the end of the run, the glass plates holding the SDS-polyacrylamide gel were removed from the electrophoresis tank, the glass plates were opened and, by means of a scalpel, the stacking gel was removed. The resolving gel was placed exactly on the top of nitrocellulose filter and then sandwiched between two pairs of transfer buffer wetted-Whatman 3MM papers. Possible air bubbles trapped were displaced by repeated rolling with a pipette tip. The sandwich was then placed between two transfer buffer wetted-porous pads and two plastic supports and the entire construction was immersed in the electrophoresis transfer tank containing transfer buffer with the nitrocellulose filter placed

toward the anode. Transfer of the protein from the gel to nitrocellulose membrane was carried out at room temperature for 2 hours at 70 volt (constant voltage) by means of a Biorad 200/2.0 power supply.

2.8.3.3. Immunological Detection of Nitrocellulose-Immobilised Proteins

At the end of the transfer, the nitrocellulose filter was recovered from the sandwich and, in order to verify the correct protein blotting, it was stained for 5 minutes in a clean tray containing a Ponceau S red dye solution (Sigma) with gentle agitation at room temperature. When the bands of proteins were visible, the filter was destained with several washes of distilled water at room temperature. To completely destain the Ponceau S red dye bound to the proteins, nitrocellulose slices were washed three times for 20 minutes at room temperature on a shaking platform with blocking solution [5% (w/v) dried-nonfat milk (Regilait, Barcelona, Spain), 0.1% (v/v) Tween-20 (Sigma) and PBS]; filter slices were then incubated at room temperature on a shaking platform in blocking solution to mask potential nonspecific antibodies binding sites and, thus, to reduce general background. After 1 hour, blocking solution was removed and filters were incubated over night at 4°C on a shaking platform with the specific antibody-containing solution. Detection of proteins of interest was achieved by using polyclonal antibodies anti-survivin, Bcl-2, Bcl-x_L, Bax, Akt and cdk6 (Abcam Ltd, Cambridge, United Kingdom) or monoclonal antibodies anti-caspase-3, caspase-9 and β-actin (Abcam), diluted in blocking solution. At the end of the over night incubation, primary

antibodies were removed and filter slices were washed 3 times for 20 minutes with T-PBS wash solution [0.1% (v/v) Tween-20 in PBS] at room temperature on a shaking platform. Nitrocellulose filters were then incubated at room temperature on a shaking platform with the secondary anti-mouse or anti-rabbit Ig horseradish peroxidase-linked whole antibodies (Amersham) diluted 1:1000 in blocking solution. After a 1-hour hybridisation, secondary antibodies were removed and filter slices were washed three times for 20 minutes at room temperature on a shaking platform with T-PBS wash solution followed by a rapid wash with PBS. Antibodies bound to proteins of interest on nitrocellulose slices were detected by means of the enhanced chemoluminescence system (ECL) (Amersham) according to the manufacturer's instructions using Hyperfilm MP films (Amersham).

2.9. Evaluation of Survivin Gene Expression by RT-PCR Analysis

The expression of survivin gene in cancer cells was quantified by RT-PCR analysis.

2.9.1. Cell Preparation

Cells were detached from the flasks by means of sterile Trypsin-EDTA solution, transferred into a sterile a 15 ml conical tube and pelleted by a 5-minute centrifugation at 1,500 rpm at 4°C. Single-cell suspension was obtained by resuspending cell pellets in 10 ml of sterile PBS, the suspension

was checked under the microscope, and a small aliquot (100 µl) was transferred in the isoton solution and counted in the particle counter.

An aliquot of cell suspensions containing about 5-10 x 10^6 cells was then transferred in a sterile 1.5 ml tube, cells were pelleted by a 15-second centrifugation at 12,000 rpm at 4°C. After removal of PBS, cell pellets were washed twice with 1 ml of sterile PBS. At the end of the last wash, PBS was removed and total RNA was extracted from the cells.

2.9.2. Total RNA Extraction

All extraction and manipulation steps were performed under sterile conditions using DEPC-treated or RNase-free certified chemicals and plastic disposable materials.

Total cellular RNA was obtained from fresh or frozen cell pellets by means of the Trizol Reagent (Invitrogen) according to the manufacturer's instructions. The amount of extracted RNA was determined spectrophotometrically. Quality of isolated RNA was checked by gel electrophoresis analysis carried out by using a 1% (w/v) agarose mini gel (10 centimetres length/6 centimetres wide) prepared in 1x TAE buffer. An aliquot corresponding to about 1 µg of extracted ribonucleic acid was mixed in a RNase-free 0.5 ml tube with an equal volume of sequencing gel loading buffer [95% (v/v) Formamide (Sigma), 20 mM EDTA pH 8, 0.05% (w/v) bromophenol blue and 0.05% (w/v) xylene cyanol (Sigma)], heated at 100°C for 3 minutes (in order to completely destroy possible RNA secondary

structures), chilled on ice for further 3 minutes and loaded. RNA samples were run at a constant voltage of 90 volts for 1 hour at room temperature. The gel was then stained for 30 minutes at room temperature with gentle shaking in the ethidium bromide staining solution (1 µg/ml ethidium bromide prepared in 1x TAE buffer) and destained for further 30 minutes at room temperature with gentle shaking in 1x TAE buffer. RNA was visualised by means of the UV transilluminator and photographed on a 667 Polaroid film. The presence of well defined and visible bands corresponding to both 28S and 18S ribosomal RNA was indicative of a good RNA preparation.

Total RNA extracted from each cell line was stored at -80°C as 1 µg aliquots.

2.9.3. Synthesis of First Strand cDNA by Reverse Transcription Reaction

Total RNA extracted from each cell line was reverse transcribed by using RNA PCR Core Kit (Perkin-Elmer). In a RNase-free 0.5 ml reaction tube (Perkin-Elmer), 1 µg of total RNA was mixed with 2.5 µM random hexamers, 20 units of RNase inhibitor, 2.5 mM $MgCl_2$, 1 mM each dNTP, 1x PCR buffer (10 mM Tris-HCl pH 8.3, 50 mM KCl), 50 units of MuLV reverse transcriptase and RNase-free water to a final volume of 20 µl. Tubes were incubated at room temperature for 15 minutes (to allow annealing between random hexamers and RNA). First strand cDNA synthesis and MuLV reverse transcriptase inactivation were then obtained by a 42°C-incubation for 30

minutes and a 5-minute heating at 95°C, respectively, in a hot-bonnet thermal cycler. Samples were stored at 4°C until they were used in PCR reactions.

2.9.4. PCR Reactions

Primers used were synthesised and supplied in lyophilised form by MWG Biotech:

survivin sense 5'-AGCCCTTTCTCAAGGACCAC-3'

survivin antisense 5'-TGACAGATAAGGAACCTGCA-3'

β-actin sense 5'-GGGAATTCAAAACTGGAACGGTGAAGG-3'

β-actin antisense 5'-GGAAGCTTATCAAAGTCCTCGGCCACA-3'

For each primer, 100 µM stock solution was prepared by dissolving the lyophilised primer in an opportune volume of 1x TE pH 8 (10 mM Tris-HCl, 1 mM EDTA) by extensive vortexing. The successive dilutions were prepared in distilled water.

Non-competitive quantitative PCR amplification was performed using the RNA PCR Core Kit (Perkin-Elmer) as follows. In DNase-free 0.5 ml PCR reaction tubes, 125 ng of total RNA reverse transcribed in first strand cDNA were mixed with 1 µM sense and antisense survivin primers, 0.1 µM sense and antisense β-actin primers, 0.625 units of AmpliTaq DNA polymerase, 1x PCR buffer, 2 mM $MgCl_2$ and DNase-free water to a final volume of 25 µl. Tubes were then placed in a hot-bonnet thermal cycler and both 864 bp survivin and 620 bp β-actin PCR products were obtained performing 1 cycle

at 95°C for 2 minutes followed by 30 cycles each formed by a denaturation step of 1 minute at 95°C, an annealing step of 30 seconds at 62°C and an extension step of 30 seconds at 72°C followed by a final extension cycle of 7 minutes at 72°C.

It is important to stress that these experimental conditions were selected on the basis of preliminary experiments to ensure that the PCR was still in the exponential phase when the reaction was stopped.

2.9.5. Gel Electrophoresis and Densitometric Quantification of PCR Products

Twenty-five µl of PCR solution were mixed with 5 µl of 6x gel loading buffer (0.25% (w/v) of both bromophenol blue and xylene cyanol, 30% (v/v) glycerol in distilled water) and samples were loaded onto 3% (w/v)-1x TAE buffer agarose gel. Electrophoretic separation was performed at 110 volts in 1x TAE buffer and was stopped when bromophenol blue dye reached the bottom of the gel. Agarose gel was then stained for 30 minutes at room temperature with gentle shaking in the ethidium bromide-1x TAE buffer staining solution and destained for a further 30 minutes at room temperature with gentle shaking in 1x TAE buffer. PCR products were visualised on the UV-transilluminator and photographed on a 665 Polaroid film. Negative copy of the film was developed by using 18% (w/v) sodium sulphite (Sigma) according to the manufacturer's instructions and it was used for densitometric quantification of the PCR products by means of a HP ScanJet IIcx/t scanner

(HewlettPackard) and IQ software (Molecular Dynamics). The relative expression level of survivin was normalised to that of β-actin.

2.10. The Cytotoxic Activity of Different Drugs on Cell Lines

2.10.1. Colony Formation Assay

After harvesting in logarithmic growth phase, melanoma cell clones, HeLa, OAW42/e and OAW42/Surv cells were plated in plastic dishes (Corning-Costar) in 5 ml of fresh media at a different density (ranging from 250 to 2000 cells/dish) depending on the drug concentration to be used.

Immediately before cell treatment, drug stock solutions were diluted in specific growth media and cells were exposed to cisplatin (1.0-20 μg/ml) for 1 hour, topotecan (1.0-10 ng/ml) for 24 hours, temozolomide (0.1-10 μg/ml) for 24 hours, or to paclitaxel (1.0-10 nM), NU6140 and purvalanol A (1.0-10 μM), singly administrated or in combination. For the paclitaxel and cdk inhibitors combination, two schedules were tested: a) a 24-hour paclitaxel treatment followed by a 24-hour incubation with NU6140 or purvalanol A; b) a 24-hour NU6140 or purvalanol A treatment followed by a 24-hour incubation with paclitaxel. Control cells were exposed to 1% (v/v) DMSO. At the end of the different treatments, drug-containing medium was removed from each well, cells were washed with PBS and incubated at 37°C in a 5% CO_2 humidified atmosphere for 10 days to form colonies.

Colonies consisting of at least 50 cells were stained with crystal violet in 70% v/v ethanol/water and counted under the microscope. Each

experimental point was run four times. The colony-forming efficiency was calculated from the number of colonies counted and the number of morphologically intact single cells seeded.

The *in vitro* effect of drugs was expressed in terms of IC_{50}, i.e, the concentration able to inhibit clonogenic cell survival by 50%. The plating efficiency (PE) was calculated from the number of colonies counted and the number of cells seeded. The surviving fraction (SF) was calculated as follows:

SF = (PE of treated sample)/(PE of control).

2.10.2. Cell Proliferation Assay

After harvesting in logarithmic growth phase, DU145 and PC-3 cells were seeded in 6-well plates (Corning-Costar) in 2 ml of fresh media at 40 x 10^3 cells/well. Plates were then incubated at 37°C in a 5% CO2 humidified atmosphere in the air incubator for 24 hours.

Immediately before cell treatment, cisplatin stock solution was diluted in specific growth media and cells were treated with increasing concentrations of cisplatin (1.0-20 µg/ml) for 1 hour. At the end of the treatment, drug-containing medium was removed from each well, cells were washed with PBS and incubated at 37°C in a 5% CO_2 humidified atmosphere for 3 days.

To assess siRNA-mediated inhibition of cell proliferation, prostate cancer cells were transfected with 100 nM of each siRNA as described in the 2.7 section. In combination experiments, following an 8-hour transfection with

siRNA2, cells were exposed for 72 hours to different concentrations (from 5 to 500 ng/ml) of 17-AAG (previously reconstituted in sterile DMSO and then diluted with sterile water to the final dose). Cells were then harvested immediately at the end of treatment (day 3), or after an additional 4 days in drug-free medium (day 7).

At the end of treatments, medium was removed from each well, cells were washed three times with PBS (3 ml/well) and detached from the plates by a 5-minute incubation at 37°C with Trypsin-EDTA solution (1 ml/well). Trypsin activity was stopped by addition of a 10% (v/v) FBS-PBS solution (5 ml/well) and cells were transferred in the isoton solution. Single-cell suspensions were obtained by repeated pipetting, checked under the microscope and counted in a particle counter. Cell viability was determined by the Trypan blue dye exclusion test. Each experimental sample was run in triplicate and the results were expressed as percentage variation in the number of viable cells in treated compared to control cells.

2.11. The Cytotoxic Activity of Ionising Radiation on Cell Lines

2.11.1. Irradiation

After harvesting in logarithmic growth phase, melanoma cells were irradiated at room temperature using a 137Cs γ-irradiator (IBL-437, Oris, France) at a dose rate of 7.2 Gy/min. Immediately after irradiation or 72 hours after irradiation, cells were processed for colony formation or apoptosis experiments, respectively, as outlined below.

2.11.2. Clonogenic Assay

After treatment with 1-10 Gy ionizing radiation, melanoma cells were plated at appropriate concentrations in plastic dishes (ranging from 250 to 2000 cells/dish) and incubated at 37°C in an atmosphere of 5% CO_2 and 95% air for 10 days. Colonies consisting of at least 50 cells were stained with crystal violet in 70% v/v ethanol/water and counted under the microscope. The colony-forming efficiency was calculated from the number of colonies counted and the number of morphologically intact single cells seeded. The surviving fractions of treated cells relative to unirradiated cells were determined, and the data were fitted to the multitarget single-hit model of cell inactivation:

$$S/S0 = 1-(1 - e^{-D/D0})^n$$

where S/S0 is the surviving fraction and D is the dose (Gy). The parameters *n* and D_0 were calculated using ELMAT software (kindly provided by Dr. Benassi, Regina Elena Cancer Institute, Rome, Italy). Triplicate determinations of each radiation dose were performed and an intra-experiment average was calculated. The points shown on the clonogenic survival curves are the inter-experiment averages (and their relative standard deviations) calculated from at least three intra-experiment averages.

2.12. Cell Cycle Analysis

Fresh cells (1 x 10^6, 0.5 ml) were fixed by a drop-to drop addition of cellular suspension to 4.5 ml of -20°C cold 70% ethanol present in a 5 ml Nalgene tube. Fixed cells were stored at -20°C until they were subjected to flow cytometric analysis.

Immediately before analysis, fixed cells were collected by a 1,500 rpm-centrifugation at 4°C for 5 minutes, transferred into a 1.5 ml tube and washed twice with 0.5 ml of PBS. Cell pellets were then resuspended in 0.5 ml of the solution A [50 µg/ml propidium iodide (Sigma), 50 mg/ml RNase A and 0.05% (v/v) Nonidet P-40] and stained at 4°C. After 30 minutes, drug-induced cell cycle perturbations were assessed by analysing the stained cellular suspension with a FACScan flow cytometer (Becton Dickinson, Sunnyvale, CA, USA). At least 30,000 events were read and the percentages of cells in $G_{0/1}$, S and G_2/M phases were evaluated on DNA plots by CellFit software (Becton Dickinson) according to the SOBR model (Becton Dickinson).

2.13.Apoptosis Analysis

Each experimental sample was split into various aliquots (containing an appropriate number of cells) for the different apoptosis assays. Cells aliquots destined to be used in assays for which fresh cells were not required were collected by a 12,000 rpm-centrifugation at 4°C for 30 seconds and frozen by snap freezing in liquid nitrogen and stored at -80°C.

2.13.1. Evaluation of Apoptotic Morphology by Fluorescent Microscopy

Untreated and treated cells were stained with solution A (1 ml for 1 x 10^6 cells) as described in the 3.12 section. An aliquot of 30,000 stained cells was cytocentrifuged onto a glass slide for 3 minutes at 500 rpm (Cytospin 3) (Shandon Italia, Milan, Italy) at room temperature and, a cover slide was then placed on the top of cells and glass slides were observed under fluorescence microscopy (excitation wave length = 588 nm, emission wave length = 610 nm) by using a fluorescence miscroscope. The percentage of apoptotic cells was determined by scoring at least 500 cells in each sample.

2.13.2. The Terminal dUTP Nick-End Labeling (TUNEL) Assay

Cells (1 x 10^6) were washed in cold PBS and centrifuged at 200 g for 5 minutes and then fixed in 1 ml 4% paraformaldehyde pH 7.4 for 45 minutes at room temperature. After rinsing with PBS, cells were permeabilized in a solution of 0.1% Triton X-100 in sodium 0.1% citrate for 2 minutes on ice. Cell suspension was centrifuged at 200 g for 5 minutes and washed with PBS. Cell pellet was resuspended in 50 µl of the TUNEL reaction mixture (Boehringer Mannheim) and incubated for 1 hour at 37°C in the dark. After rinsing with PBS, the pellet was suspended in PBS and analyzed by a FACScan flow cytometer (Becton Dickinson). The results were expressed as the percentage of TUNEL-positive cells in the overall cell population.

2.13.3. Evaluation of Caspase-9 and Caspase-9 Catalytic Activity

Cell pellet (2 x 10^6) was washed with cold PBS, resuspended in 100 µl of chilled lysis buffer (caspase-9/Mch6 or caspase-3/cpp32 fluorometric assay kit, MBL, Japan) and incubated on ice for 20 minutes. The pellet was centrifuged for 15 minutes at 14,000 rpm at 4°C and the clear supernatant was transferred in a 1.5 ml conical tube. One hundred µl of 2x Reaction Buffer (MBL) and 10 µl of the specific fluorogenic substrate (leu-glu-his-asp-7-amino-4-trifluoromethylcoumarin, LEHD-AFC, for caspase-9 and N-acetyl-Asp-Glu-Val-Asp-aldehyde-7-amino-4-methylcoumarin, Ac-DEVD-AMC, for caspase-3) were added and incubate at 37°C for 1 hour. At the end of incubation, samples were transferred to a 96-well plate and the hydrolysis of the specific substrates for caspase-9 and caspase-3 was monitored by spectrofluorometry using an excitation wavelength of 400 nm and an emission wavelength of 505 nm.

2.14. Detection of Telomerase Activity

2.14.1. Protein Extract Preparation

Cell pellet was resuspended by gentle pipetting in 200 µl of ice cold 1x CHAPS lysis buffer (Intergen Co., Oxford, United Kingdom) [10 mM Tris-HCl, pH 7.5, 1 mM $MgCl_2$, 1 mM EGTA, 0.1 mM benzamidine, 0.5% CHAPS, 5 mM mercaptoethanol, and 10% glycerol], and leaved on ice for 30 minutes. The lysate was then centrifuged at 12,000 rpm for 20 minutes at 4°C and

160 µl of supernatant were collected into a clean eppendorf tube, making sure no traces of pellet were withdrawn. Protein concentration was determined as described in section 1.4, and protein extracts were stored at -80°C as 0.5 µg/µl aliquots.

2.14.2. Labeling of the TS Primer

In RNase-free 0.5 ml PCR reaction tubes, 10 µl of the TS primer oligonicleotide (5'-AATCCGTCGAGCACAGAGTT-3') were mixed with 25 µCi [γ-^{32}P]-ATP, 5 units of T4 polynucleotide kinase, 1x kinase buffer, RNase-free water to a final volume of 20 µl. Tubes were then placed in a hot-bonnet thermal cycler for 20 minutes at 37°C followed by 5 minutes at 85°C.

2.14.3. The Telomere Repeat Amplification Protocol (TRAP) Assay

One µg (2 µl) of protein extract was used to assess telomerase activity by the polymerase chain reaction (PCR)-based telomeric repeats amplification protocol (TRAP) assay by means of the TRAPeze kit (Intergen). Specifically, the master mix was prepared by mixing 1x TRAP reaction buffer, 1x dNATs mix, 2 µl ^{32}P-TS primer, 1 µl TRAP primer mix, 2 units Taq polymerase and RNase-free water to a final volume of 48 µl. Two µl of the protein extract (or control sample) were mixed with 48 µl of the master mix and the tubes were incubated for 30 minutes at 30°C.

The enzyme activity products were amplified by PCR performing 1 cycle at 94°C for 2 minutes followed by 30 cycles each formed by the first step of 10 seconds at 94°C, the second step of 25 seconds at 50°C and the last step of 30 seconds at 72°C, followed by a final cycle of the first step of 15 seconds to 94°C, the second step of 25 seconds to 50°C and the last step of 1 minute to 72°C.

Each reaction product was amplified in the presence of a 36-bp internal TRAP assay standard. A TSR8 quantiation standard (which serves as a standard to estimate the amount of product extended by telomerase in a given extract) was included for each set of TRAP assays.

2.14.4. Polyacrylamide Gel Electrophoresis

The enzyme activity products were resolved in 10% (w/v) polyacrylamide-0.5x TBE buffered non-denaturing gel, prepared as described in the 1.7 section.

Ten µl of loading 6x gel loading buffer were then added to each 50 µl-reaction mixture and 30 µl of the samples were loaded onto the gel. Electrophoretic run was performed at a constant voltage of 180 volts for 45 minutes then at 300 volts for 1 hour and 45 minutes. When the xylene cyanol runs 75% of the gel length, electrophoresis was stopped and the polyacrylamide gel was detached from the glass plates by means of Whatman 3MM papers. After that a sheet of Saran Wrap was placed on the top, the gel was dried at 80°C for 20 minutes, placed in a Hypercassette with

intensifying screens and autoradiographed by exposure to X-ray film over night at -80°C.

2.14.5. Quantification of Telomerase Activity

Quantitative analysis was performed with the Image-QuanT software (Molecular Dynamics), which allowed densitometric evaluation of the digitized image. Telomerase activity was quantified by measuring the signal of telomerase ladder bands, and the relative telomerase activity was calculated as the ratio to the internal standard using the following formula:

$$[(X - X_0)/C] \times [(R - R_0)/Cr]^{-1}$$

where X is the untreated sample, X_0 is the RNase-treated sample, C is the internal control of untreated samples, Cr is the internal control of TSR8, R is the TSR8 quantitation control and R_0 is the negative control.

2.15. *In Vivo* Studies

All procedures requiring the use of animals were carried out according to the United Kingdom Coordinating Committee on Cancer Research Guidelines [Workman *et al*, 1998] and approved by the Ethics Committee for Animal Experimentation of the Istituto Nazionale per lo Studio e la Cura dei Tumori (Milan, Italy). Male and female athymic Swiss nude mice supplied from Charles River Laboratories (Calco, Italy) were randomly distributed into

treatment groups and housed in groups of four to five in polypropylene cages with stainless steel wire lids and heat treated chips (Cellu-Dri; Shepherd Specialty Papers, Kalamazoo, USA), with access to food (Lab Rodent Diet 5001; PMI Nutrition International Inc., St. Louis, USA) and water ad libitum. The animal rooms were maintained on a 12-hours light:dark cycle (6 a.m. to 6 p.m.) at 23 ± 1°C with 30–50% relative humidity.

2.15.1. Tumour Injection

Cells from *in vitro* cultures of JR8, JR8/mutRz or JR8/Rz were intramuscularly injected into the right hind leg of female mice (10^7 cells/mouse). For each cell line, half of the group (5-8 mice) was left untreated and half was treated with topotecan. Topotecan was dissolved in sterile, distilled water and delivered in a volume of 10 ml/kg body weight. The drug was administered orally at the dose of 10 mg/kg every seventh day for four times (q7dx4), starting the day after cell injection. In a second set of the experiments, exponentially growing DU145/CTR and DU145/Rz cells were injected subcutaneously (10^7 cells/mouse) into the right flank of the male mice (9 mice/group).

The mice were inspected daily to establish tumour take (i.e. the ratio between the number of growing tumours over the total number of tumour-injected mice), the time of tumour appearance and the tumour volume. Tumour growth was followed by measuring tumour diameters with a Varnier caliper.

Tumour volume was calculated according to the formula:

$$TV\ (mm^3) = d^2 \times D/2$$

where d and D are the shortest and longest diameter, respectively.

2.15.2. Reverse Transcriptase-PCR Analysis of Ribozyme Expression

2.15.2.1. RNA Isolation from Tissues

Animals were sacrified 60 days after tumour cell inoculation with carbon dioxide anesthesia followed by cervical dislocation. Tumours were removed, fixed in 10% formalin and then stored at -80°C. All extraction and manipulation steps were performed under sterile conditions using DEPC-treated chemicals and plastic disposable materials.

Frozen tissues were homogenised using Brinkman Tissuemizer (Haereus) for 30 to 60 seconds and total RNA was obtained by means of the Trizol Reagent (Invitrogen) according to the manufacturer's instructions. The amount of extracted RNA was determined spectrophotometrically. Quality of isolated RNA was checked by gel electrophoresis analysis carried out by using a 1% (w/v) agarose mini gel prepared in 1x TAE buffer. RNA was visualised by means of the UV transilluminator and photographed. Total RNA extracted was stored at -80°C as 1 µg aliquots.

2.15.2.2. RT-PCR Reaction and Gel Electrophoresis

Total RNA extracted from tissues was reverse transcribed by using RNA PCR Core Kit (Perkin-Elmer) as described in the 2.5.3 section.

To analyze ribozyme expression, the resultant cDNAs were amplified using T7 (5'-TAA TAC GAC TCA CTA TAG GGA GA-3') and SP6 (5'-CG ATT TAG GTG ACA CTA TAG-3') primers and the PCR amplification was performed as described in the 2.5.4. section. PCR products were obtained performing 30 cycles of PCR (at 95°C for 1 minute, 47°C for 1 minute, and 72°C for 1 minute), followed by a 7-minutes extension step at 72°C. PCR products were then verified by agarose gel electrophoresis. Vectors pRc/Rz and pRc/mutRz were used during PCR amplification as control for the correct fragment size.

2.16.Statistical Analysis

Statistical evaluation of data was generally done with two-tailed Student's *t* test. The Fisher exact text was used to compare tumour take between animal groups. *P* values <0.05 were considered statistically significant.

The type of interaction between the cytotoxic effects of siRNA2 and 17-AAG was analyzed as previously described [Silvestrini *et al*, 1997]. For the evaluation, the agents were assumed to provide independent effects. For a given concentration of 17-AAG, we observed a survival fraction of cells (SFa); likewise, for siRNA2 transfection, we observed SFb. For the combined

treatment (siRNA2 transfection followed by 17-AAG exposure) we observed SFab. The results obtained were expressed according to the following criteria: SFab = SFa x SFb indicates additive effect; SFab < SFa x SFb indicates supra-additive effect; SFab > SFa x SFb indicates subadditive effect.

The method described by Chou & Talalay [1984] was used to determine the nature of the interaction between NU6140 or purvalanol A and paclitaxel. Drugs were always combined at a constant ratio of paclitaxel and NU6140 or purvalanol A concentrations (i.e. 1:1000). The interaction of drugs was quantified by determining a combination index (CI). CI values of less than or greater than 1 indicated synergy or antagonism, respectively, whereas a CI value of 1 indicates additivity.

Chapter 4

RESULTS

1. RIBOZYME-MEDIATED DOWN-REGULATION OF SURVIVIN EXPRESSION SENSITISES HUMAN MELANOMA CELLS TO DRUG AND RADIATION TREATMENT

Cutaneous melanoma is the most aggressive form of skin tumours and its incidence is increasing more rapidly than that of any other cancer [Grossman & Altieri, 2001]. In contrast to localized melanoma, which has a good prognosis after adequate surgery, disseminated disease is characterized by a very poor clinical outcome, which is not modified by conventional anticancer treatments [Becker *et al*, 2000]. Although not yet fully elucidated, the basis of melanoma resistance to chemotherapy seems to rely on dysregulation of apoptosis [Satyamoorthy *et al*, 2001; Soengas & Lowe, 2003]. In fact, it has been shown that cells within melanoma lesions are characterized by an inherently low level of spontaneous apoptosis [Mooney *et al*, 1995]. Moreover, defects at multiple levels of the two major apoptotic pathways have been found in melanoma cells, including altered death receptor signalling [Thomas & Hersey, 1998], increased levels of anti-apoptotic proteins belonging to the Bcl-2 family such as Bcl-2, Bcl-x_L and Mcl-1 [Tang *et al*, 1998], inactivation of the apoptosis effector Apaf-1 [Soengas *et al*, 2001], and overexpression of members of the inhibitors of apoptosis protein (IAP) family such as ML-IAP and survivin [Vucic *et al*, 2000; Grossman *et al*, 1999]. In particular, survivin expression has been detected in almost all invasive and metastatic melanomas but not in normal skin melanocytes [Grossman *et al*, 1999].

Considering that apoptosis is the major mode of cell kill by many chemotherapeutic agents and radiation, it appears reasonable that the

inability to undergo programmed cell death is a major mechanism of the chemo- and radio-resistance of melanoma. As a consequence, the genes that control apoptosis provide interesting new targets for the rational development of strategies aimed at increasing the susceptibility of melanoma cells to chemical and physical treatments. In this context, it has been demonstrated that down-regulation of Bcl-2 and Mcl-1 by antisense oligonucleotides sensitised human melanoma to dacarbazine in cell culture as well as in SCID mouse xenotransplantation models [Jansen *et al*, 1998; Thallinger *et al*, 2003]. Moreover, in the clinical setting, sensitisation of malignant melanoma to dacarbazine by concomitant Bcl-2 antisense therapy was confirmed in a phase I-II study in patients with Bcl-2-expressing advanced melanoma [Jansen *et al*, 2000]. Again, reduction of Bcl-x_L protein expression by a specific antisense oligonucleotide significantly increased the *in vitro* sensitivity of melanoma cells to cisplatin [Heere-Ress *et al*, 2002]. Using a different approach dealing with the recovery of Apaf-1 expression by treatment with the demethylating agent 5'-aza-2'-deoxycytidine, Soengas *et al* [2001] were able to enhance the *in vitro* sensitivity of Apaf-1-negative melanoma cells to doxorubicin.

The possibility to modulate the chemosensitivity of melanoma and other tumour cell types by targeting survivin has been also actively pursued in the last years. It has been previously demonstrated by Grossman *et al* [1999] that transfection of melanoma cells with survivin antisense was able to increase the fraction of spontaneous apoptosis. The same research group reported that the forced expression of a phosphorylation-defective survivin mutant (Thr34→Ala) in melanoma cell lines, besides triggering apoptosis,

enhanced the level of programmed cell death induced by in vitro treatment with the chemotherapeutic agent cisplatin [Grossman *et al*, 2001a]. A number of additional studies carried out in experimental models of other tumour types showed that targeting of survivin by antisense oligonucleotides or dominant negative mutants resulted in an increased sensitivity to anticancer agents including taxol [Mesri *et al*, 2001; O'Connor *et al*, 2002], etoposide [Olie *et al*, 2001], doxorubicin [Wall *et al*, 2003] and 5-fluorouracil [Yamamoto *et al*, 2002]. Moreover, a possible role of survivin as a molecular determinant of radiation response in tumour cells has been recently proposed by Asanuma *et al* [2000], who reported evidence suggesting that this protein acts as a constitutive and inducible radio-resistance factor in pancreatic cancer cell lines.

In the present study, we proposed to assess the effect of attenuation of survivin expression, accomplished through a ribozyme-mediated strategy, in the response of human melanoma cells to chemotherapeutic agents and ionising radiation.

1.1. *In Vitro* Catalytic Activity of the Anti-Survivin Ribozyme

The catalytic potential of the Rz ribozyme was assessed as the ability to cleave an internally ^{32}P-labeled synthetic RNA substrate obtained by cloning a portion of the human survivin mRNA. The size of the substrate was 362-nucleotides, and the cleavage reaction (the cleavage site is indicated by the arrow in Figure 25) was expected to produce two fragments of 236 and

126 nucleotides, respectively. Experiments performed by incubating 10 nM of labelled RNA substrate with increasing concentrations (from 10 to 1000 nM) of the Rz ribozyme for 120 minutes at 37°C (Figure 27) resulted in a decrease of the full-length substrate and accumulation of the expected cleavage products.

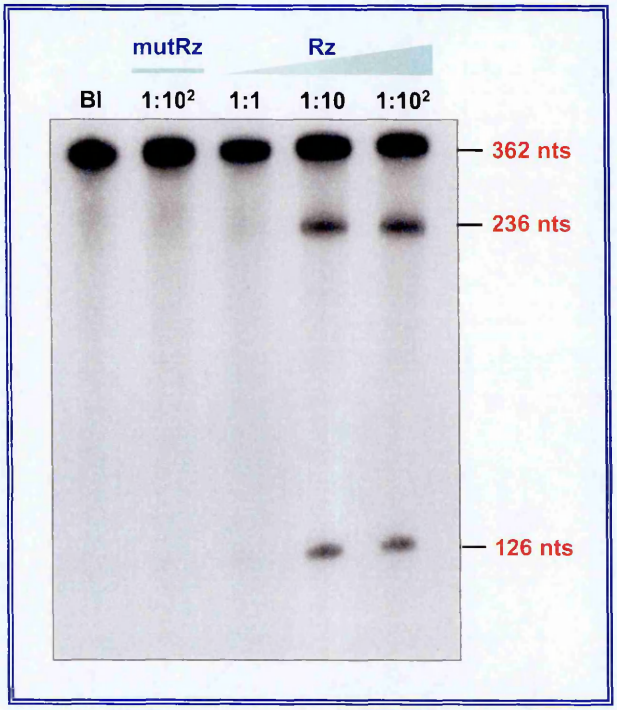

Figure 27. ***In vitro*** **catalytic activity.**
The synthetic ^{32}P-substrate was incubated with 10-1000 nM Rz or 100-1000 nM mutRz for 120 minutes at 37°C. (BL: ^{32}P-substrate RNA incubated without the ribozyme).

The efficiency of cleavage was dependent on the substrate/ribozyme ratio, with the cleavage products being detectable at a ratio of 1:10. As expected, the mutRz ribozyme, carrying a mutation (i.e., deletion of G_{12}) in the catalytic core of the Rz ribozyme, did not induce any cleavage in the synthetic RNA (Figure 27).

1.2. Ribozyme-Mediated Attenuation of Survivin Expression in JR8 Melanoma Cells

To evaluate the effect of the ribozyme in intact cells, the JR8 human melanoma cell line inherently over-expressing survivin was transfected with pRc/Rz and pRc/mutRz vectors containing the sequence coding for the active Rz ribozyme and the catalytically inactive mutRz ribozyme, respectively. The transfectants were treated with G418 for 1 month, and the G418-resistant clones were selected and screened for survivin expression by Western blotting. To rule out the possibility that attenuation of survivin expression was simply due to clonal divergence, we used two polyclonal populations of transfectants proven to endogenously express the active (JR8/Rz cells) or the mutant (JR8/mutRz cells) ribozyme (Figure 28).

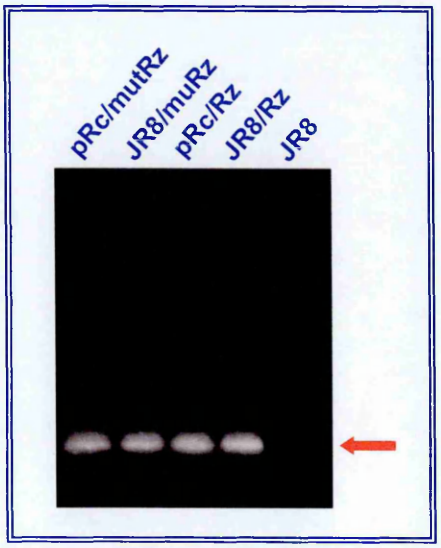

Figure 28. Ribozyme expression in JR8 melanoma cell clones.

Ribozyme expression was detected by RT-PCR in JR8 parental cells and cell clones transfected with the active ribozymes (JR8/Rz cells) or with the mutant ribozyme (JR8/mutRz cells). Lanes pRc/Rz and pRc/mutRz indicate plasmids used as controls for the size of each fragment during PCR amplification.

JR8/Rz cells were characterized by a markedly lower survivin protein level (-60 ± 8%) than JR8 parental cells, as assessed by Western blot analysis in four independent cultures. Conversely, a very modest reduction (-13 ± 7%) in survivin expression was observed in mutRz cells (Figure 29). No appreciable differences were found among the different melanoma cell lines in the expression of other proteins involved in the control of apoptosis, such as Bcl-2 and Bax (Figure 29).

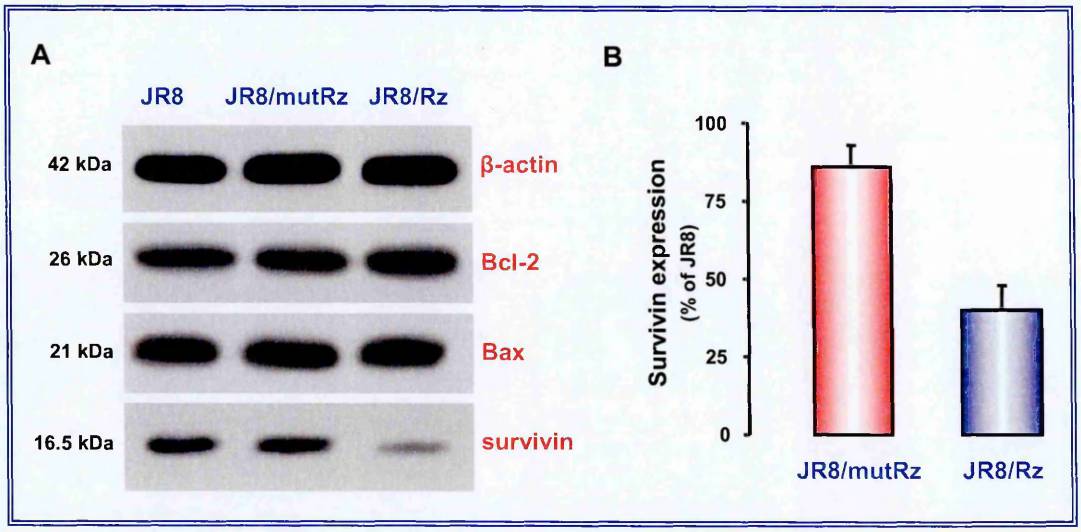

Figure 29. Survivin expression in melanoma cell clones.
(**A**) A representative Western blotting experiment illustrating the expression of survivin and other apoptosis-related proteins in JR8, RZ and mutRZ cells. β-actin was used as control for loading. (**B**) Densitometric quantification of band intensities for survivin. Data represent mean values ± sd of three independent experiments.

Attenuation of survivin expression did not appreciably affect the growth potential of melanoma cells. In fact, only a modest increase in the doubling time of JR8/Rz cells compared to JR8 and JR8/mutRz cells was observed (29 ± 3h vs 24 ± 3h and 25 ± 4h, respectively).

1.3. Survivin Inhibition Sensitises JR8 Melanoma Cells to Drug-Induced Apoptosis

To determine whether the level of survivin expression is associated with the chemosensitivity of melanoma cells, JR8/Rz and JR8/mutRz cell lines were analyzed for their clonogenic cell survival profiles after exposure to different concentrations of the topoisomerase-I inhibitor topotecan for 24 hours (Figure 30). Transfection with the active ribozyme sequence did not appreciably modify the plating efficiency of JR8/Rz cells compared to JR8/mutRz cells (10.2 ± 1.5% and 13.4 ± 2.1%, respectively).

A dose-dependent reduction in cell survival was observed in both cell lines following topotecan exposure. However, JR8/Rz cells showed enhanced sensitivity to the drug compared to JR8/mutRz cells. The concentration of the drug that inhibited cell proliferation by 50% (IC_{50}) was calculated by computer-assisted extrapolation. Specifically, a curve of drug concentration versus mean percent inhibition was constructed. Using the formula for the slope of the line between the two drug doses that bracketed (above and below) 50% inhibition, the IC_{50} was calculated. A significantly ($p<0.01$) lower topotecan IC_{50} was observed in JR8/Rz than JR8/mutRz (1.86 ± 0.44 ng/ml vs 6.76 ± 0.53 ng/ml) (Table III).

In parallel, we assessed the susceptibility of melanoma cells as a function of the level of survivin expression to other DNA-interacting agents currently used in the treatment of melanoma patients. Specifically, we observed an increased sensitivity of JR8/Rz cells compared to cells expressing the mutant ribozyme to a 1-hour cisplatin exposure, as indicated by the significantly

(p<0.05) lower IC_{50} (1.36 ± 0.40 µg/ml vs 2.9 ± 0.30 µg/ml) (Table III). Conversely, JR8/Rz and JR8/mutRz cells showed a comparable sensitivity to a 24-hours exposure to temozolomide (IC_{50}: 5.81 ± 0.39 µg/ml vs 6.29 ± 0.29 µg/ml) (Table III).

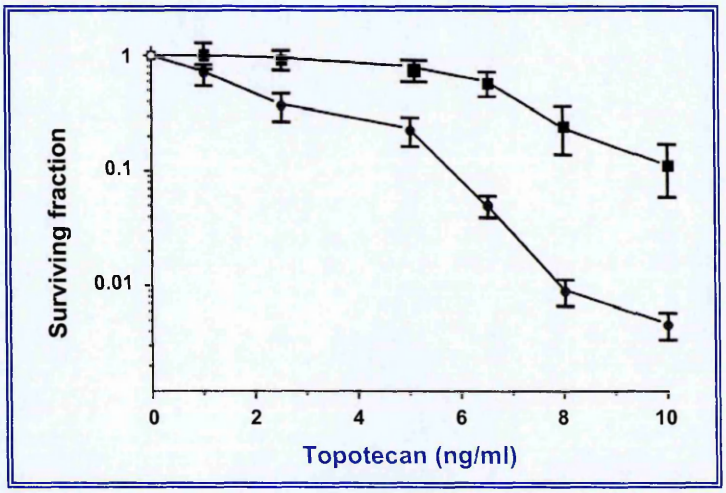

Figure 30. Clonogenic cell survival curves obtained after exposure of melanoma cell clones to topotecan.
JR8/Rz (●) and JR8/mutRz (■) cells were treated with topotecan for 24 hours and then incubated at 37°C for 10 days. Colonies consisting of at least 50 cells were stained with crystal violet and counted under the microscope. Data represent mean values ± sd of three independent experiments. (The IC_{50} values were calculated from the dose-response curves by graphical extrapolation.)

Table III. Cytotoxic activity of topotecan, cisplatin and temozolomide in melanoma cell clones.

Cell line	Topotecan IC_{50} (ng/ml)	Cisplatin IC_{50} (µg/ml)	Temozolomide IC_{50} (µg/ml)
JR8/mutRz	6.76 ± 0.53	2.9 ± 0.30	6.29 ± 0.29
JR8/Rz	1.86 ± 0.44	1.36 ± 0.40	5.81 ± 0.39

Drug activity is expressed in terms of concentration able to inhibit clonogenic cell survival by 50% (IC_{50}). Values represent the mean ± sd of three independent experiments.

To investigate whether the increased cytotoxic activity of cisplatin and topotecan observed in JR8/Rz cells was mediated by an enhanced susceptibility of cells to undergo programmed cell death as a consequence of survivin inhibition, we examined the induction of apoptosis in the two cell lines. Specifically, the number of cells with apoptotic nuclei was determined by fluorescence microscopy 72 hours after a 1-hour exposure to 10 µg/ml cisplatin or 24-hours exposure to 10 ng/ml topotecan (Figures 31). Spontaneous apoptosis was observed in a small fraction of cells in both cell lines (0.5 ± 0.2% and 1.0 ± 0.2% of the overall cell population in JR8/mutRz and JR8/Rz cells, respectively). Conversely, a significantly (p<0.01) higher apoptotic response to drugs was appreciable in JR8/Rz than in JR8/mutRz cells (27.7 ±2.3% vs 4.8 ± 1.7% for cisplatin; 26.4 ± 2.6% vs 9.8 ± 1.3% for topotecan) (Figure 31).

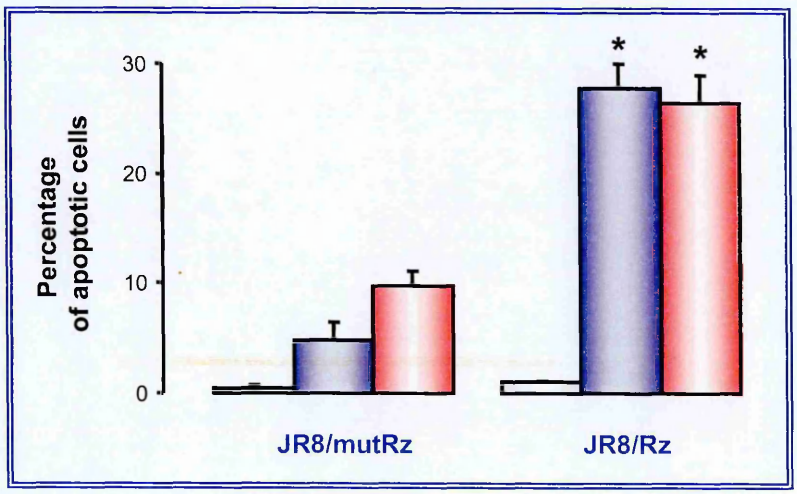

Figure 31. Induction of apoptosis in melanoma cell clones exposed to topotecan and cisplatin.

The percentage of cells with an apoptotic morphology with respect to the overall population as assessed by fluorescence microscopy in untreated cells (empty column) and in cells exposed to topotecan (blue column) or cisplatin (red column). Data represent mean values ± sd of three independent experiments. *p<0.01, Student's t test.

To obtain mechanistic insights into the apoptotic pathway activated by lowering survivin expression, we evaluated the *in vitro* catalytic activity of caspase-9 and caspase-3 in the two melanoma cell lines. JR8/Rz and JR8/mutRz cells were characterized by a similar basal level of caspase activity as assessed by hydrolysis of specific fluorogenic substrates (Figure 32).

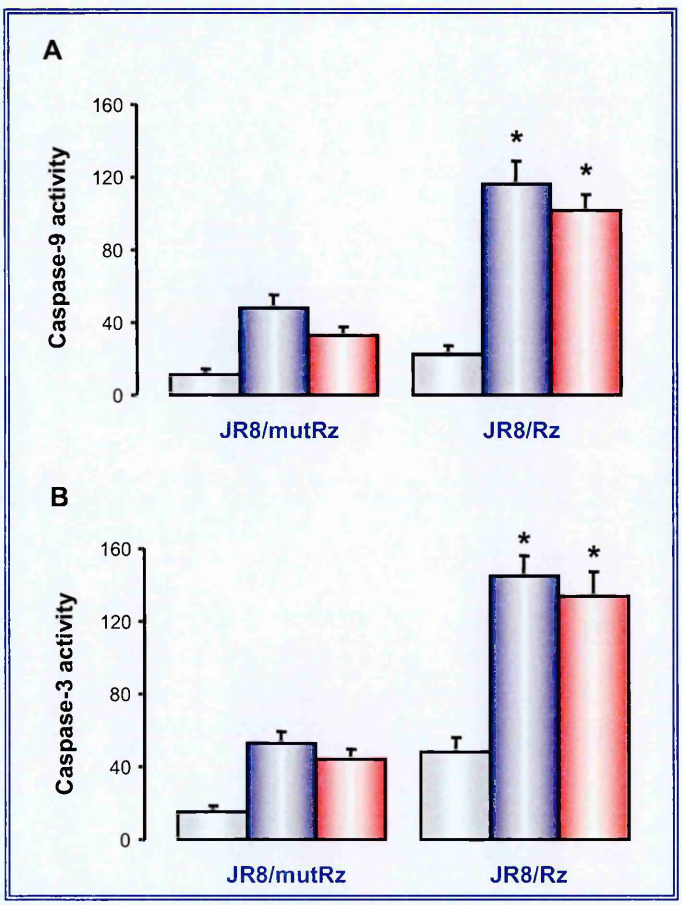

Figure 32. Caspase activation in melanoma cell clones treated with topotecan and cisplatin.

Caspase-9 (**A**) and caspase-3 (**B**) catalytic activity was determined by hydrolysis of specific fluorogenic substrates in untreated cells (empty column) and in topotecan- (blue column) and cisplatin- (red column) treated cells. Data are expressed as relative fluorescence units (r.f.u.) and represent mean values ± sd of three independent experiments. *$p<0.05$, Student's t test.

Treatment with cisplatin and topotecan increased the activation of caspase-9 and caspase-3 in both cell lines. However, the catalytic activity of both enzymes was significantly ($p<0.05$) higher (two–fold and three-fold in the case of caspase-9 and caspase-3, respectively) in the JR8/Rz than in the JR8/mutRz drug-treated cells (Figure 32).

1.4. Survivin Inhibition Enhances the Antitumour Activity of Topotecan *in Vivo*

The effect of survivin inhibition on the antitumour activity of topotecan was studied in athymic nude mice after injection of melanoma cells expressing the active or the mutant ribozyme. The endogenous presence of the ribozymes in tumours grown in the animal was confirmed by RT-PCR (Figure 33).

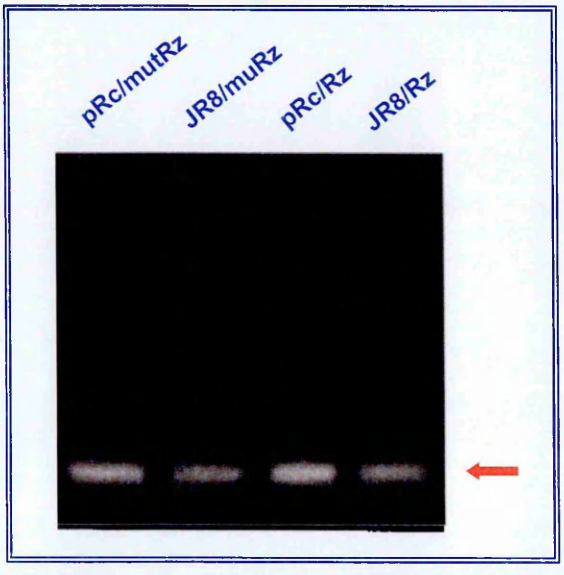

Figure 33. Ribozyme expression in tumours grown in nude mice.
Ribozyme expression was detected by RT-PCR in tissue samples obtained from tumours originating from JR8 cells transfected with the active ribozyme (JR8/Rz) or with the mutant ribozyme (JR8/mutRz). Lanes pRc/Rz and pRc/mutRz indicate plasmids used as controls for the size of each fragment during PCR amplification.

The drug (10 mg/kg) was administered orally every seventh day for 4 times (q7dx4), starting from the day after cell injection. Although JR8/Rz cells retained a reduced expression of survivin compared to JR8/mutRz cells after xenografting in mouse, survivin inhibition did not appreciably modify tumour take or growth in untreated animals. Specifically, at day 12 after cell injection, tumours were present in 5/7 and 3/8 mice receiving JR8/mutRz and JR8/Rz cells, respectively (Table IV), and tumour growth curves of the two groups of mice were similar and superimposable to that observed for JR8 parental cells (Figure 34; Table V).

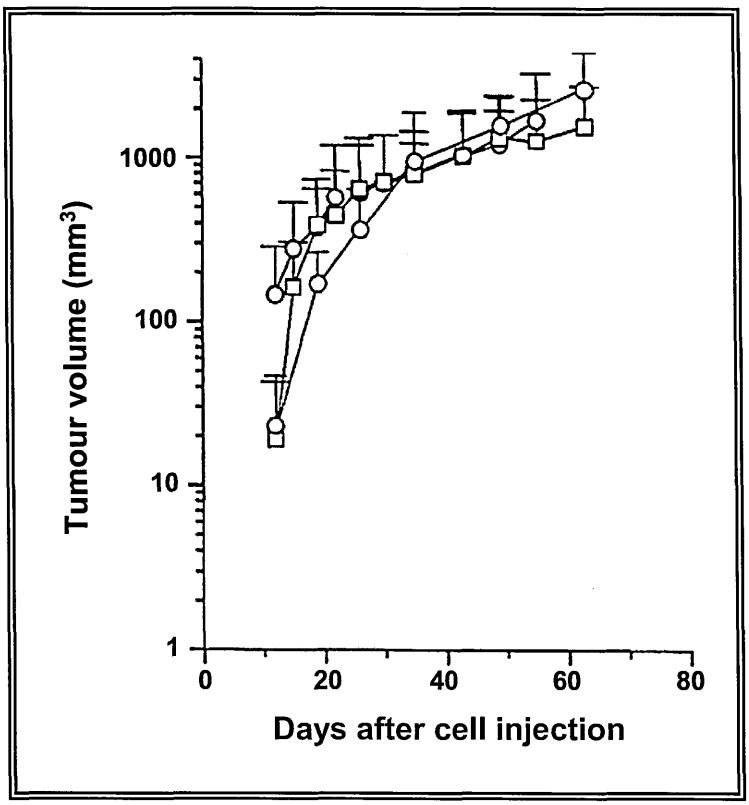

Figure 34. Growth curves of JR8, JR8/mutRz and JR8/Rz melanoma cells in athymic nude mice.

Cells were intramuscularly injected into the right hind leg of mice (10^7 cells/mouse) at day 0. JR8 (○), JR8/mutRz (●) and JR8/Rz (□) cells.

Table IV. Effects of oral topotecan on tumorigenicity (tumour take[a]) of JR8/mutRz and JR8/Rz melanoma cells in nude mice.

Days[b]	JR8/mutRz		JR8/Rz			
	12	49	12	49	63	104
Controls	5/7	5/7	3/8	5/8	6/8	---
Topotecan	1/5	4/5	0/8	0/8[c]	3/8	4/8

[a]Tumour take, i.e. number of growing tumours/total number of tumour-injected mice.
[b]Day 0: 10^7 cells were i.m. injected into the right hind leg. Topotecan treatment: 10 mg/kg, q7dx4 from day 1.
[c]p=0.0128 vs control mice; Fisher exact test.

Table V. Effect of survivin inhibition on the growth[a] of melanoma cells in nude mice.

Days[b]	12	15	19	22	26	30	35	43	49	56	63
JR8											
# 1	25		50		50		294		648		729
# 2	25		216		750		1224		1690		2475
# 3	25		198		384		908		1527		2156
# 4	28		245		384		700		1352		1690
# 5	50		196		567		1368		2250		2944
# 6	25		196		416		750		1521		1960
# 7	25		216		650		1029		2156		2352
# 8	28		221		56		800		1521		1960
JR8/mutRz											
# 1	60	198	500	527	698	752	853	988	1420	1520	
# 2	288	550	650	1268	1008	1008	1352	1568	1460	1268	
# 3	288	408	486	1372	1800	1800	2304	2890	3240	3978	
# 4	50	88	256	221	256	300	405	750	1352	3240	
# 5	--	--	--	--	--	--	--	--	--	--	
# 6	352	700	726	793	802	844	902	1002	1130	1180	
# 7	--	--	--	--	--	--	--	--	--	--	
JR8/Rz											
# 1	--	405	968	968	1352	2025	1862	2250	2475	2816	2475
# 2	50	221	486	847	1268	1004	1268	1568	2250	2025	3240
# 3	--	--	--	--	--	--	--	--	--	--	196
# 4	--	--	--	--	--	--	--	--	--	--	--
# 5	50	196	787	787	787	908	869	1152	1521	1666	1764
# 6	--	--	--	--	--	--	--	--	--	--	--
# 7	--	196	365	446	550	550	1080	1852	2475	1859	2475
# 8	50	288	500	500	1183	1183	1183	1372	1800	1800	2176

[a]expressed as tumour volume (calculated according to the formula: TV (mm3) = d2 x D/2, where d and D are the shortest and longest diameter, respectively) in individual animals.
[b]Day 0: 10^7 cells were i.m. injected into the right hind leg.

In JR8/mutRz tumours, topotecan treatment initially retarded tumour growth (Figure 35; Table IV & VI). In fact, at day 12 the tumour was present in only 1/5 mice. However, at later intervals, tumours grew in most of the treated mice (4/5), and no difference was evident in tumour take or volume between treated and untreated mice. In contrast, topotecan was very effective in increasing the latency and reducing the take rate and growth of JR8/Rz tumours. In fact, at day 49 after cell injection, tumours had not yet appeared in topotecan-treated mice, whereas they were present in 5/8 control mice (p=0.0128). Again, at day 63, when control mice were sacrificed for tumour burden, tumours were present in only 3/8 treated mice. Topotecan-treated mice were kept under observation for more than 100 days, but tumour take did not increase over 50% (4/8 at day 104).

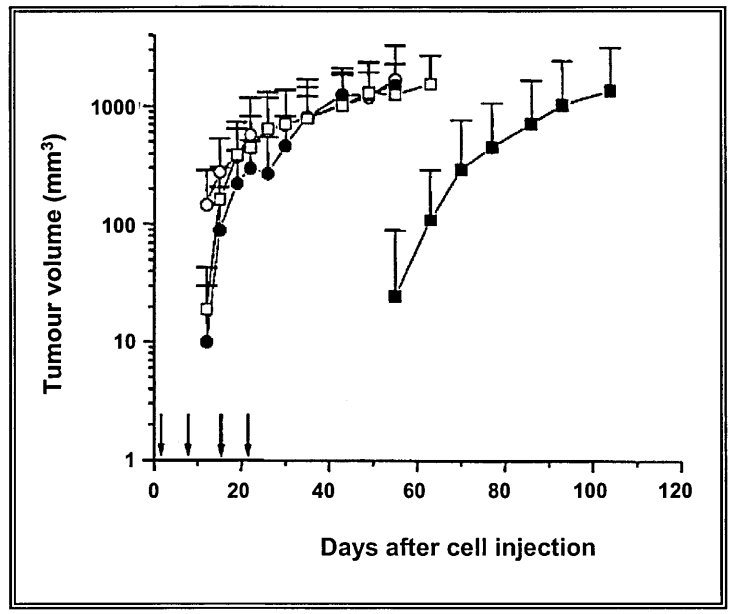

Figure 35. Effect of ribozyme-mediated survivin inhibition on the anti-tumorigenic activity of oral topotecan in melanoma xenografts.

Cells were intramuscularly injected into the right hind leg of mice (10^7 cells/mouse) at day 0. Treatment consisted of 10 mg/kg, q7dx4 from day 1. Control JR8/mutRz (O), topotecan-treated JR8/mutRz (●), control JR8/Rz (□) and topotecan-treated JR8/Rz cells (■).

Table VI. Effect of oral topotecan on the growth[a] of melanoma cells in nude mice.

Days[b]	12	15	19	22	26	30	35	43	49	56	63	70	77	86	93	104
JR8/mutRz																
#1	--	--	--	--	--	--	--	--	--	--						
#2	--	--	136	405	390	600	908	1224	1224	1521						
#3	--	320	550	600	787	908	1002	1332	1521	2138						
#4	--	50	50	126	88	87	1080	1960	1890	1960						
#5	50	75	320	365	162	726	1080	1764	1960	1960						
JR8/Rz																
#1	--	--	--	--	--	--	--	--	--	--	--	--	--	--	--	--
#2	--	--	--	--	--	--	--	--	--	--	352	1470	1568	2560	3971	4800
#3	--	--	--	--	--	--	--	--	--	--	--	--	--	--	--	--
#4	--	--	--	--	--	--	--	--	--	--	50	365	666	1352	1913	2560
#5	--	--	--	--	--	--	--	--	--	195	486	486	1372	1500	2432	3564
#6	--	--	--	--	--	--	--	--	--	--	--	--	--	--	--	--
#7	--	--	--	--	--	--	--	--	--	--	--	50	50	50	50	136
#8	--	--	--	--	--	--	--	--	--	--	--	--	--	--	--	--

[a]expressed as tumour volume (calculated according to the formula: TV (mm3) = d2 x D/2, where d and D are the shortest and longest diameter, respectively) in individual animals.
[b]Day 0: 10^7 cells were i.m. injected into the right hind leg. Topotecan treatment: 10 mg/kg, q7dx4 from day 1.

1.5. Ribozyme-Mediated Survivin Inhibition Sensitises JR8 Melanoma Cells to Ionising Radiation

To determine whether the level of survivin expression is associated with the radio-sensitivity of melanoma cells, the different cell lines were analyzed for their clonogenic cell survival profiles after exposure to different doses of γ-irradiation (Figure 36). Transfection with the active ribozyme sequence did not appreciably modify the plating efficiency of JR8/Rz cells compared to JR8 and JR8/mutRz cells (8.7 ± 0.9% vs 9.8 ± 1.0% and 9.6 ± 1.3%, respectively).

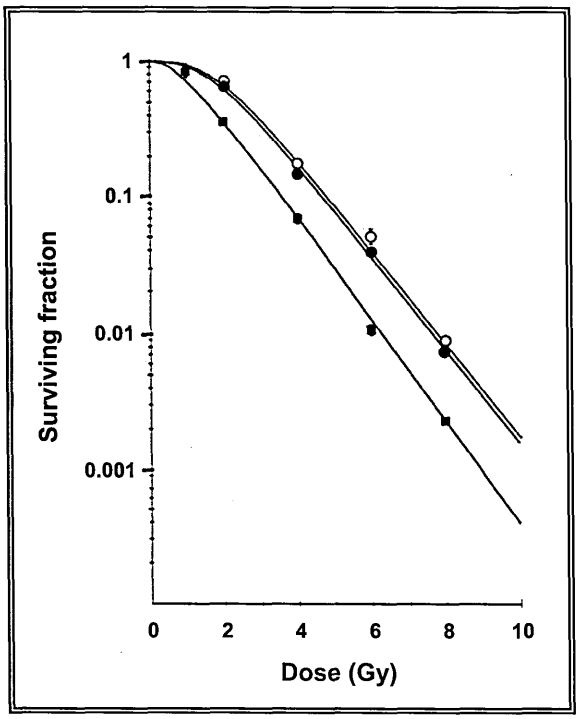

Figure 36. Clonogenic cell survival curves obtained after γ-irradiation of melanoma cell clones.
JR8 (O), JR8/Rz (■) and JR8/mutRz (●) cells were irradiated and then incubated at 37°C for 10 days. Colonies consisting of at least 50 cells were stained with crystal violet and counted under the microscope. Data represent mean values ± sd of three independent experiments.

A radiation dose-dependent reduction in cell survival was observed in all cell lines (survival curve parameters are reported in Table VII). However, cells expressing the active ribozyme showed enhanced radio-sensitivity compared to parental cells. Specifically, the surviving fractions of JR8/Rz cells were significantly ($p<0.01$) lower than those observed for JR8 at all radiation doses starting from 2 Gy. Such radio-sensitisation seemed to be a consequence of the decreased survivin levels in cells expressing the active ribozyme rather than non-specific effects of the expression vector itself. In fact, the survival curve obtained after irradiation of JR8/mutRz cells

expressing the catalytically inactive ribozyme was superimposable to that obtained for irradiated JR8 parental cells (Figure 36).

Table VII. Survival curve parameters of melanoma cell.

Cell lines	D_0	n	SF2
JR8	1.29 ± 0.02	4.83 ± 0.45	0.68 ± 0.03
JR8/mutRz	1.27 ± 0.02	4.19 ± 0.38	0.70 ± 0.08
JR8/Rz	1.15 ± 0.01	2.32 ± 0.16	0.36 ± 0.02

The colony-forming efficiency was calculated from the number of colonies counted and the number of morphologically intact single cells seeded. The parameters n and D_0 were calculated using ELMAT software. Values represent the mean ± sd of three independent experiments.

To investigate whether the increased cytotoxic activity of γ-irradiation observed in the active ribozyme transfectant cells was mediated by an enhanced susceptibility of cells to undergo programmed cell death as a consequence of survivin inhibition, we examined the extent of apoptosis induction in the different cell lines 48 and 72 hours after exposure to different radiation doses. For this purpose the percentage of cells with an apoptotic nuclear morphology was determined by fluorescence microscopy after cell staining with propidium iodide and calculated in relation to the total cell population (Figure 37). Spontaneous apoptosis was observed in a small fraction (always <2%) of cells in the different cell lines, and γ-irradiation consistently induced a dose-dependent increase in the percentage of apoptotic cells in the different clones.

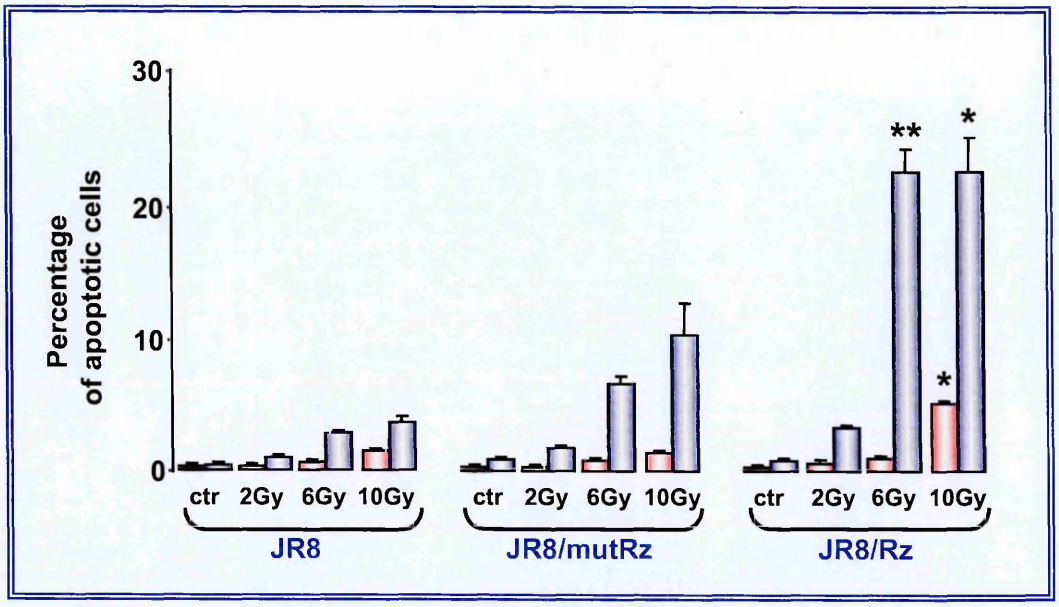

Figure 37. Induction of apoptosis in melanoma cell clones exposed to γ-irradiation.

The percentage of cells with an apoptotic morphology with respect to the overall population was assessed by fluorescence microscopy 48 hours (red column) and 72 hours (blue column) after exposure to different radiation doses. Data represent mean values ± sd of three independent experiments. *p<0.05, **p<0.01, Student's t test.

However, in cells expressing the active ribozyme, the extent of radiation-induced programmed cell death was higher than that observed in JR8/mutRz cells and in JR8 parental cells. (Figure 37). Specifically, such a difference was statistically significant at 48 hours (p<0.05) and 72 hours (p<0.01) after exposure to 10 Gy and at 72 hours after exposure to 6 Gy (p<0.01).

The caspase-3 catalytic activity, as assessed by hydrolysis of the fluorogenic substrate Ac-DEVD-AMC, was markedly higher in the JR8/Rz than in the JR8/mutRz cells and in JR8 parental cells after 10 Gy exposure (Figure 38).

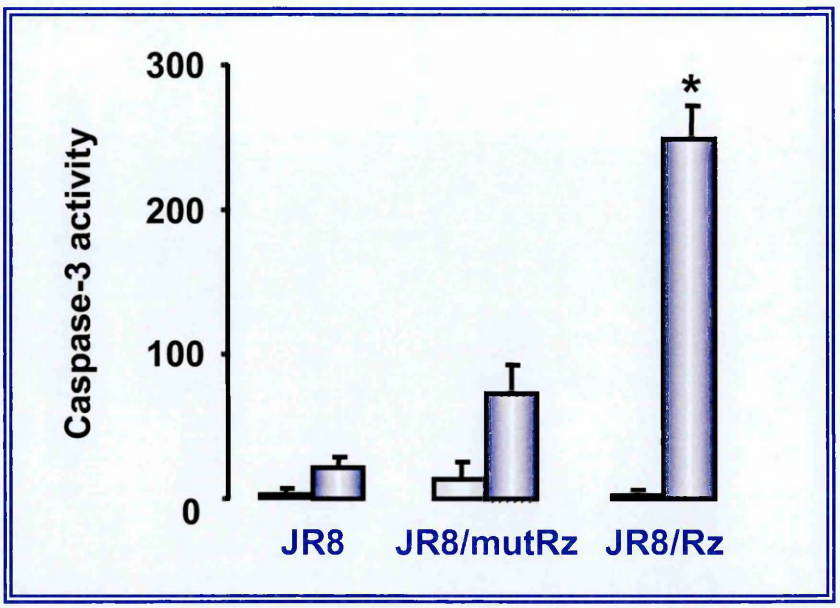

Figure 38. Caspase activation in melanoma cell clones exposed to γ-irradiation.

Caspase-3 catalytic activity was determined by hydrolysis of the fluorogenic substrate Ac-DEVD-AMC 72 hours after exposure to 10 Gy in unirradiated control cells (empty column) and γ-irradiated cells (blue column). Data are expressed as relative fluorescence units (r.f.u.) and represent mean values ± sd of three independent experiments. *p<0.05, Student's t test.

2. RIBOZYME-MEDIATED INHIBITION OF SURVIVIN EXPRESSION INCREASES SPONTANEOUS AND DRUG-INDUCED APOPTOSIS AND DECREASES THE TUMORIGENIC POTENTIAL OF HUMAN PROSTATE CANCER CELLS

Prostate cancer is the most frequently diagnosed tumour and the second leading cause of cancer-related death among men in Western countries [Dennis & Resnick, 2000]. Whereas more than 80% of tumours are initially responsive to androgen ablation, metastatic disease inevitably progresses to an androgen-independent state that is largely refractory not only to hormonal manipulation but also to chemotherapy and radiotherapy [Daskivich & Oh, 2006; Swanson, 2006; Sowery *et al*, 2007]. Accordingly, androgen-independent progression is the main obstacle to survival in patients with advanced disease, and this emphasizes the need for novel therapeutic strategies targeting the molecular determinants of treatment resistance of advanced prostate cancer. Several lines of evidence suggested that one of the main events associated with the conversion to an androgen-independent phenotype is increased resistance to apoptosis [Denmeade *et al*, 1996; Howell, 2000], mainly due to up-regulation of anti-apoptotic genes, including Bcl-2, Bcl-x_L and Mcl-1 [Krajewska *et al*, 1996]. Moreover, it has been described to be selectively expressed in the most common human neoplasms, including prostate cancer [McEleny *et al*, 2002], and to be associated with clinical tumour progression [Altieri, 2001]. As a consequence, the identification of points in the apoptotic pathway at which dysregulation occurs could open new therapeutic opportunities for this malignancy.

As an alternative strategy to target the survivin pathway we developed a Moloney-based retroviral vector expressing a hammerhead ribozyme directed against the 3' end of the CUA_{110} triplet in survivin mRNA, encoded as a chimeric RNA within adenoviral VA1 RNA. Here we assessed the effects of the ribozyme-mediated inhibition of survivin expression on the spontaneous and drug-induced apoptosis and on the tumorigenic potential of androgen-independent human prostate cancer cells.

2.1. Construction of a Retroviral Vector for Targeted Intracellular Expression of an Anti-Survivin Ribozyme and Transduction of Prostate Cancer Cells

The hammerhead ribozyme coding sequence was cloned as a substitute to a portion of the central domain of the adenovirus type 2 *VA1* gene, a region that does not influence transcription by RNA polymerase III or cellular localization of the RNA in the cytoplasm [Cagnon & Rossi, 2000; Mendoza-Maldonado *et al*, 2002]. As a control, we also inserted in the VA1 construct an irrelevant ribozyme targeting the feline immunodeficiency virus (FIV) primer binding site. To attain high-efficiency expression of the VA1-ribozyme cassettes, Moloney-based retroviral vectors were constructed, in which the VA1-ribozyme cassette was encoded in the 3' long terminal repeat (LTR). After transduction, a double copy vector was obtained, with the ribozyme-expressing cassettes at both LTRs.

Two androgen-independent human prostate cancer cell lines, DU145 and PC-3, were transduced with the viral vectors and treated *in vitro* with G418 for 1 month. G418-resistant clones were selected and screened for survivin expression by Western blotting. To rule out the possibility that attenuation of survivin expression was simply due to clonal divergence, we used polyclonal populations proven to endogenously express the anti-survivin (DU145/Rz and PC-3/Rz cells) or control (DU145/CTR and PC-3/CTR cells) ribozyme (Figure 39).

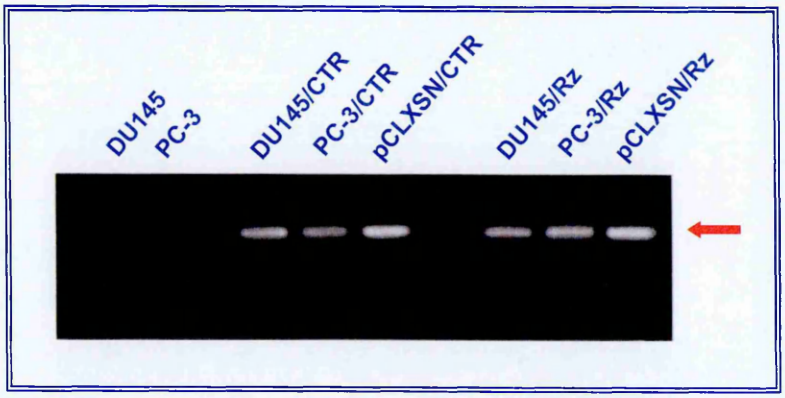

Figure 39. Ribozyme expression in prostate cancer cells.
Ribozyme expression was detected by RT-PCR in DU145 and PC-3 parental cells and cell clones transduced with the anti-survivin ribozyme (DU145/Rz and PC-3/Rz) or with the control ribozyme (DU145/CTR and PC-3/CTR). pCLXSN/CTR and pCLXSN/Rz plasmids were used as controls for the correct size of each fragment during PCR amplification.

Specifically, DU145/Rz and PC-3/Rz cells were characterized by a markedly lower survivin protein level (-90 ± 8% and -68 ± 5%, respectively) than DU145/CTR and PC-3/CTR cells (Figure 40), as assessed in three independent western blot experiments.

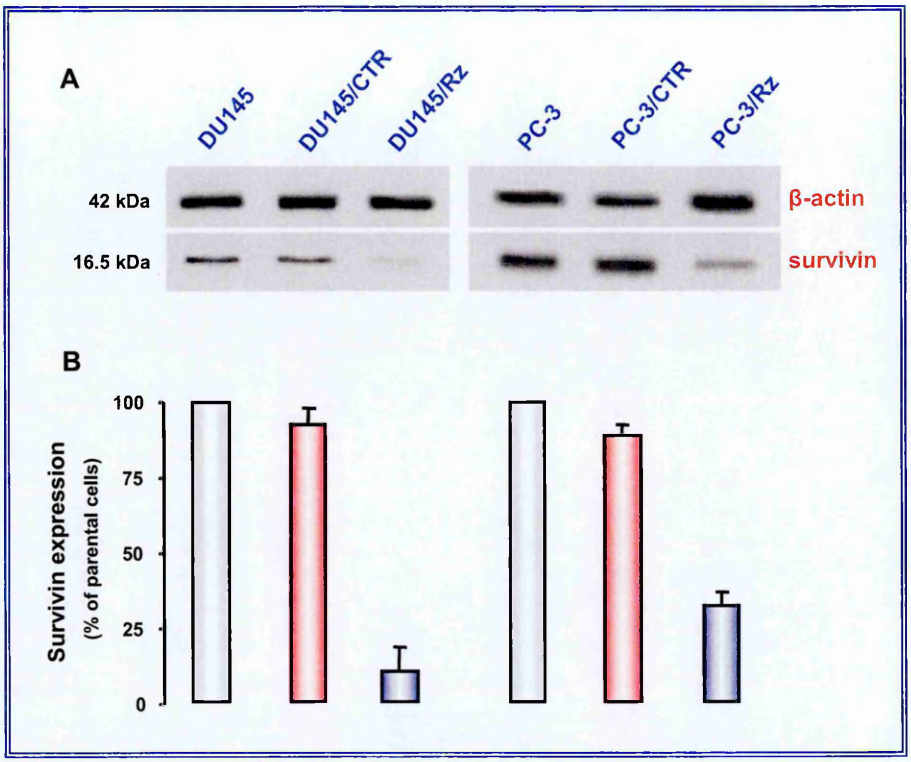

Figure 40. Survivin expression in prostate cancer cells.
(**A**) A representative Western blotting experiment illustrating the expression of survivin in DU145, DU145/CTR, DU145/Rz, PC-3, PC-3/CTR and PC-3/Rz cells. β-actin was used as control for loading. (**B**) Densitometric quantification of band intensities for survivin. Data represent mean values ± sd of three independent experiments.

Attenuation of survivin protein expression markedly affected the *in vitro* growth potential of DU145/Rz cells, as demonstrated by the significantly ($p<0.01$) longer doubling time than DU145/CTR cells (48 ± 4h vs 26 ± 3h). Consistent with the role of survivin in the proper execution of mitosis [Giodini *et al*, 2002], we observed that the almost complete ribozyme-mediated inhibition of survivin induced aberrant mitotic progression in DU145/Rz cells with the appearance of a fraction of polyploid cells characterized by a more than 4N DNA content (Figure 41A). This finding was consistently observed in four cell samples collected at different intervals of growth in culture.

Conversely, a very modest increase in the doubling time of PC-3/Rz compared to PC-3/CTR cells (30 ± 3h vs 24 ± 3h) was observed, and the presence of polyploid cells was undetectable in the PC-3/Rz cell population (Figure 41B).

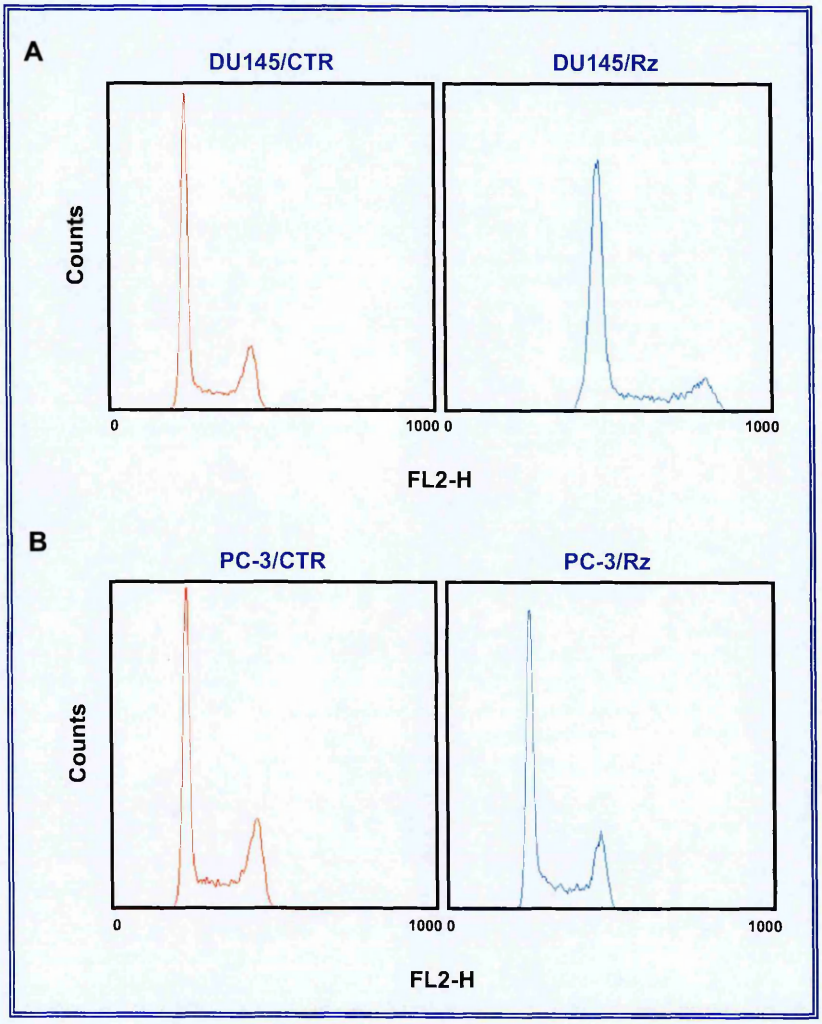

Figure 41. Effect of survivin inhibition on cell cycle progression.
Cell cycle analysis of DU145/CTR and DU145/Rz (**A**), PC-3/CTR and PC-3/Rz (**B**), was carried out by flow cytometry on cells stained with propidium iodide.

2.2. Ribozyme-Mediated Survivin Inhibition Enhances Spontaneous and Drug-Induced Apoptosis in Prostate Cancer Cells

Down-regulation of survivin in ribozyme-expressing prostate cancer cells was associated with an increased rate of spontaneous apoptosis in both cell lines. Specifically, a more marked DNA fragmentation was observed in cells expressing the anti-survivin ribozyme, as indicated by the percentage of TUNEL-positive cells, which was 20% in DU145/Rz and 17% in PC-3/Rz compared to only 2% and 3% in DU145/CTR and PC-3/CTR cells, respectively (Figure 42A). At the molecular level, ribozyme-mediated inhibition of survivin expression in DU145/Rz cells resulted in proteolytic processing of caspase-9 and caspase-3, which coincided with a significantly increased catalytic activity of both enzymes. Specifically, caspase-9 and caspase-3 activity, as assessed by *in vitro* hydrolysis of specific fluorogenic substrates (LEMD-AFC for caspase-9 and Ac-DEVD-AMC for caspase-3) was 12-fold ($p<0.05$) and 10-fold ($p<0.01$) higher, respectively, in DU145/Rz than in DU145/CTR cells (Figure 42B). Although to a lower extent, increased caspase-9 and caspase-3 catalytic activity (10-fold; $p<0.01$ and 3-fold; $p<0.02$, respectively) was also observed in PC-3/Rz compared to PC-3/CTR cells (Figure 42B).

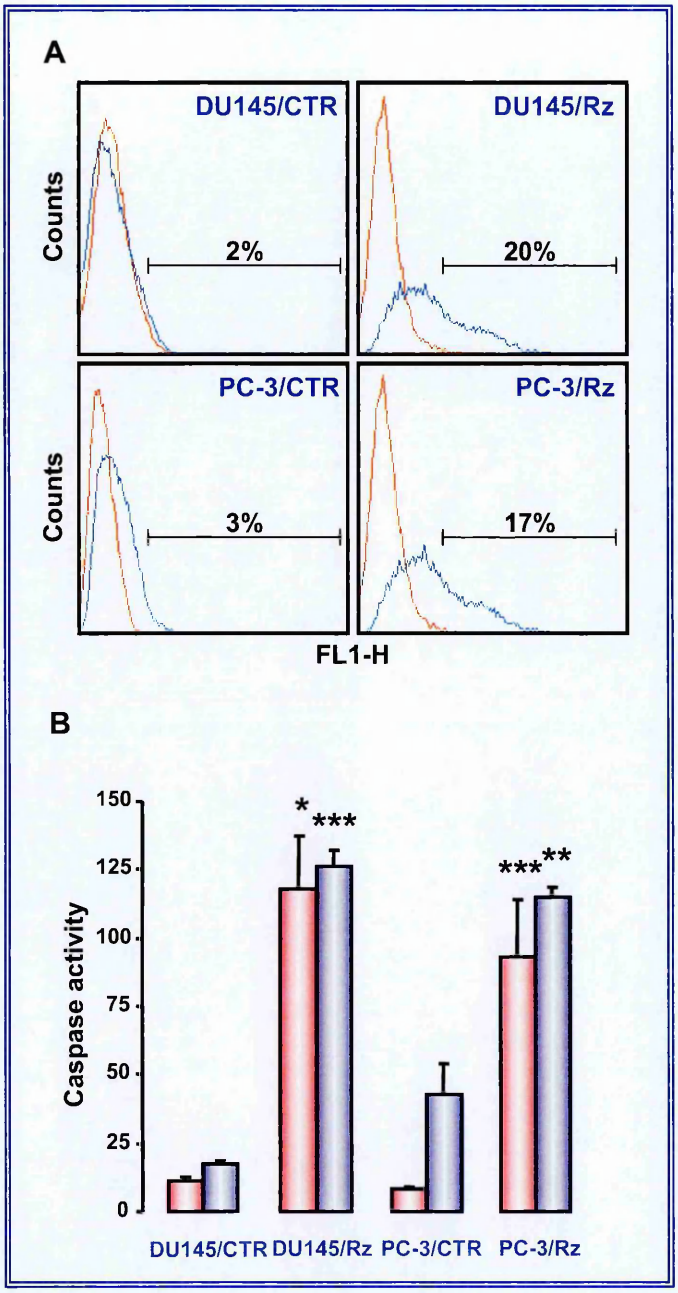

Figure 42. Induction of spontaneous apoptosis in prostate cell clones.

(**A**) TUNEL analysis of spontaneous apoptosis in DU145/CTR, DU145/Rz, PC-3/CTR and PC-3/Rz cells was carried out by flow cytometry. Red lines represent the negative control incubated in the absence of terminal transferase; blue lines represent the samples incubated with TUNEL reaction mixture. The percentage of TUNEL-positive cells in each sample is reported. (**B**) Caspase-9 (red column) and caspase-3 (blue column) catalytic activity was determined by hydrolysis of the specific fluorogenic substrates. Data are expressed as relative fluorescence units (r.f.u.) and represent mean values ± sd of three independent experiments. *p<0.05, **p<0.02, ***p<0.01, Student's t test.

To evaluate whether or not inhibition of survivin expression influences the susceptibility of prostate cancer cells to undergo programmed cell death after exposure to anticancer agents, we treated DU145/Rz and DU145/CTR cells with increasing concentrations of cisplatin. DU145/Rz cells showed enhanced sensitivity to the drug compared to DU145/CTR cells, as indicated by the significantly ($p<0.05$) lower concentration required to inhibit cell proliferation by 50% (IC_{50}: 3.17 ± 0.39 µg/ml vs 8.25 ± 0.98 µg/ml).

We then assessed the effect of cisplatin (10 µg/ml) on caspase-3 activity 72 hours after treatment. Drug exposure enhanced caspase-3 activity in both cell clones; however, in DU145/Rz cells expressing the anti-survivin ribozyme the enzyme's catalytic activity was significantly ($p<0.01$) higher than that in DU145/CTR cells (Figure 43).

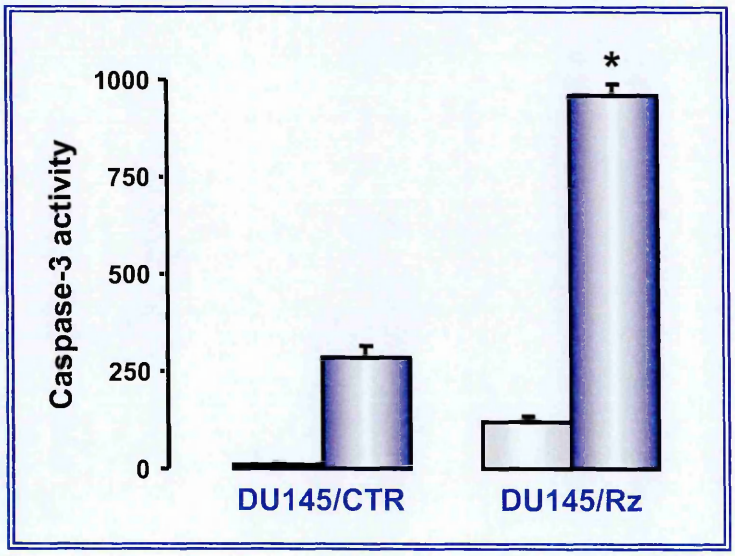

Figure 43. Caspase activation in prostate cell clones exposed to cisplatin.

Caspase-3 catalytic activity was determined by hydrolysis of the fluorogenic substrate Ac-DEVD-AMC in untreated cells (empty column) and in cisplatin-treated cells (blue column). Data represent mean values ± sd of three independent experiments. *$p<0.01$, Student's t test.

2.3. Effect of Survivin Inhibition on Tumorigenic Potential of Prostate Cancer Cells

The effect of ribozyme-mediated inhibition of survivin expression on tumour growth *in vivo* was studied in a xenograft prostate cancer model. Subcutaneous injection of DU145/CTR cells into athymic nude mice induced tumour growth in 9 of 9 xenografted mice. Tumours were measurable after 6 days from injection (mean size: 87 ± 25 mm3) and increased with time. Conversely, when xenografted in athymic mice DU145/Rz cells were unable to form growing tumours during the entire observation period (50 days) (Figure 44).

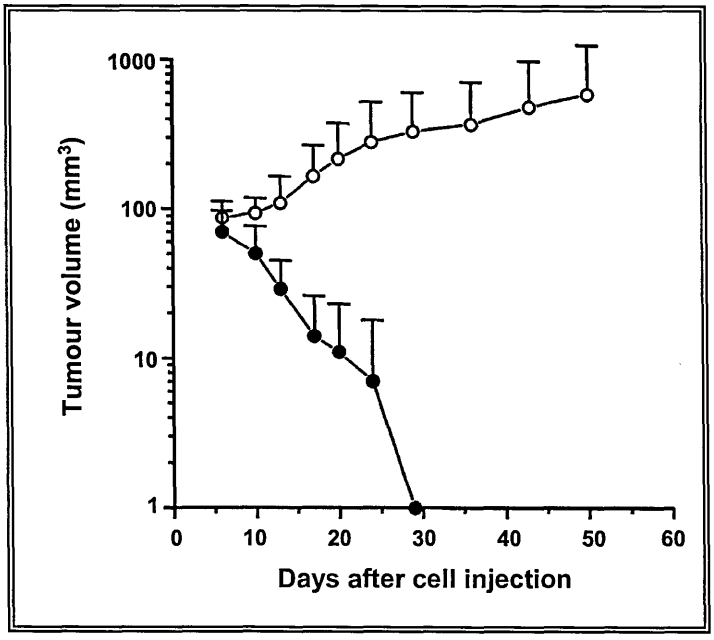

Figure 44. Effect of ribozyme-mediated survivin inhibition on the tumorigenic potential of human prostate cancer cells.

Exponentially growing DU145/CTR (○) and DU145/Rz (●) cells were injected subcutaneously (10^7 cells/mouse) into the right flank of male athymic nude mice.

3. SILENCING OF SURVIVIN GENE BY SMALL INTERFERING RNAS PRODUCES SUPRA-ADDITIVE GROWTH SUPPRESSION IN COMBINATION WITH 17-ALLYLAMINO-17-DEMETHOXY-GELDANAMYCIN IN HUMAN PROSTATE CANCER CELLS

It has recently been demonstrated that the association of survivin with the heat shock protein 90 (Hsp90) is required for its stability and function [Fortugno *et al*, 2003]. Targeted antibody-mediated disruption of the survivin-Hsp90 complex in cancer cells resulted in proteasomal degradation of survivin, mitochondrial-dependent apoptosis and mitotic arrest [Fortugno *et al*, 2003]. Hsp90 plays a central role in the cellular stress response, which is constitutively up-regulated in cancer cells to enhance adaptation to environmental challenges [Isaacs *et al*, 2003]. Specifically, Hsp90 is involved in the stabilization and conformational maturation of a number of proteins belonging to signal transduction pathways, which are deregulated in cancers and contribute to all major components of the malignant phenotype [Richter & Buchner, 2001].

The identification of survivin as a new client protein for Hsp90 links the cellular stress response to the dual cell viability/mitotic checkpoint maintained by survivin. While the survivin-Hsp90 association may promote proliferation of tumour cells by elevating their anti-apoptotic threshold, it may also suggest new opportunities for the design of novel anticancer strategies. In this context, combined approaches aimed at interfering with different levels of the survivin-Hsp90 connection could be particularly useful.

Here we evaluated the effect of small interfering RNA (siRNA)-mediated silencing of survivin on the proliferative potential of human androgen-independent prostate cancer cells and their sensitivity to the first-in-class Hsp90 inhibitor 17-allylamino-17-demethoxy-geldanamycin (17-AAG).

3.1. Silencing of Survivin Gene by siRNAs in Prostate Cancer Cells

Since strong positional effects on the function of siRNAs have been demonstrated [Ryther *et al*, 2005], we tested the effectiveness of four 21-mer siRNAs targeting different portions within exons 1-3 of survivin mRNA (Figure 26) to silence survivin gene expression in the DU145 androgen-independent prostate cancer cell line. RT-PCR experiments carried out in DU145 cells collected at different intervals after a 8-hours transfection with 100 nM of each survivin-specific siRNA showed a reduction of survivin mRNA as compared to Lipo2000-exposed cells (Figure 45). Such inhibition ranged from 39% to 60%, depending on the different siRNAs, at 24 hours after transfection and was still appreciable to a similar extent at 48 hours (Figure 45). Survivin mRNA down-regulation was paralleled by a reduction in survivin protein abundance that ranged from 38% to 75% at 24 hours and remained almost constant at 48 hours (Figure 46).

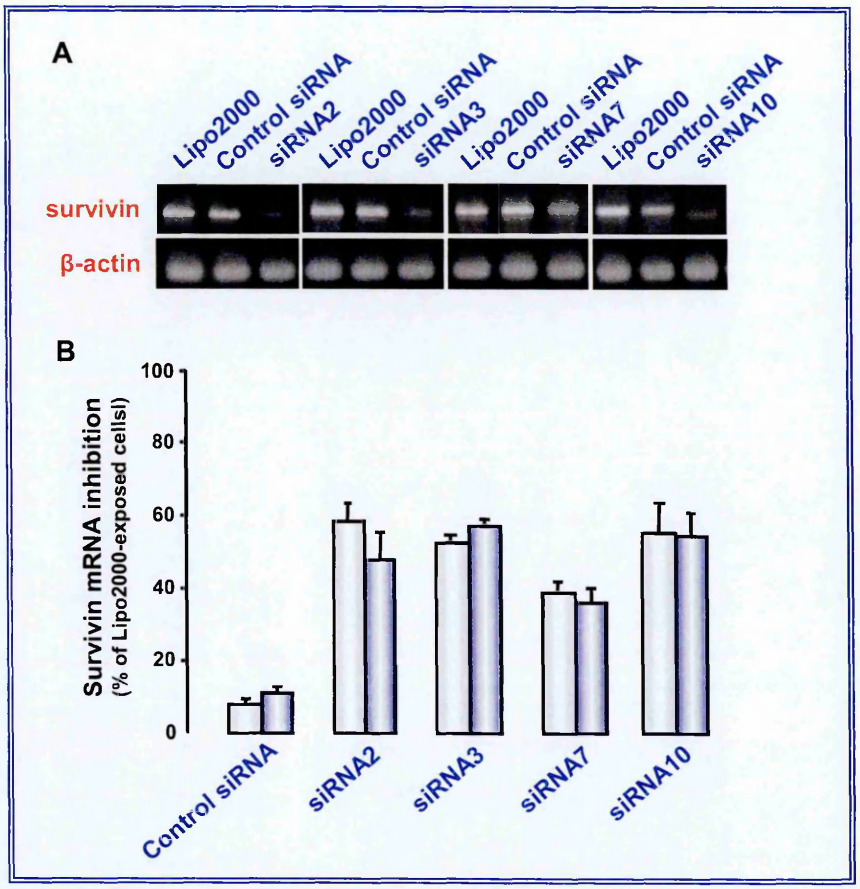

Figure 45. Survivin mRNA expression in DU145 cells.

(**A**) A representative RT-PCR experiment illustrating survivin mRNA expression in DU145 cells at 24 hours after transfection with the different siRNAs (100 nM). β-actin was used as control for loading. (**B**) Densitometric of survivin mRNA expression levels at 24 hours (empty column) and 48 hours (blue column) after transfection. Data are expressed as percentage inhibition of survivin expression compared to Lipo2000-exposed cells and represent mean values ± sd of three independent experiments.

Transfection of DU145 cells with 100 nM of a control, unrelated siRNA caused modest inhibition (around 10% compared to Lipo2000-exposed cells) of survivin mRNA expression at both time points considered (Figure 45). A slightly stronger inhibitory effect (around 25%) on survivin protein expression was consistently observed in cells transfected with the control siRNA (Figure 46).

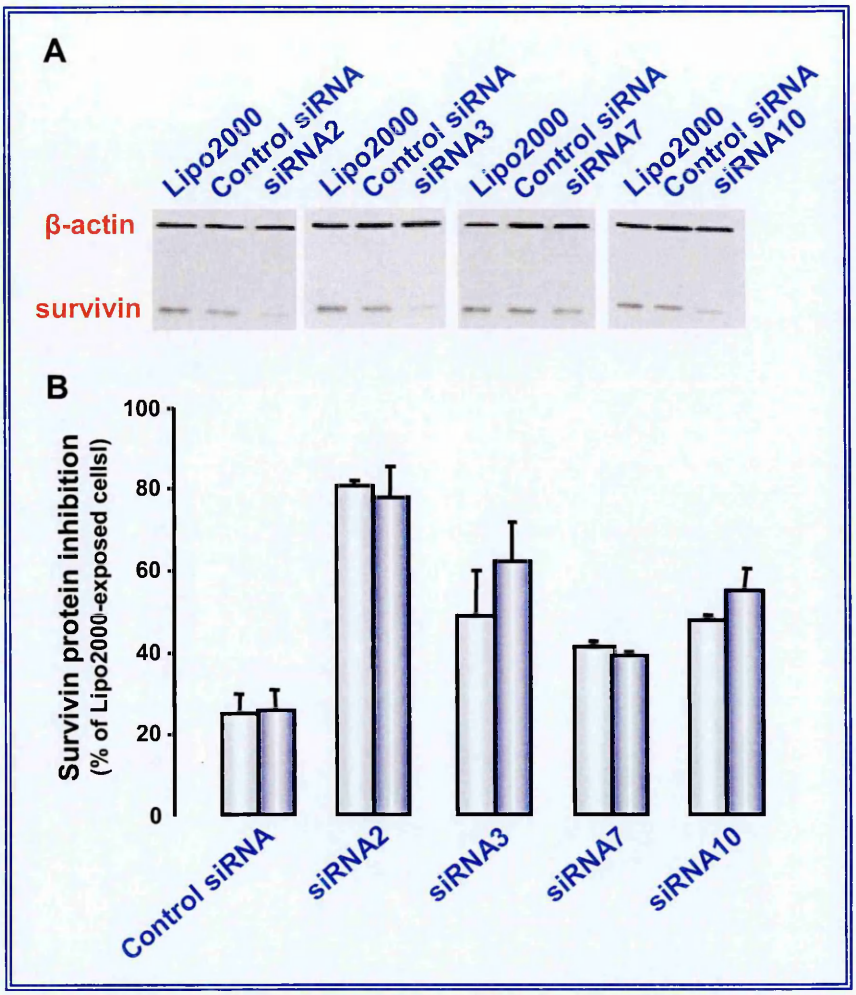

Figure 46. Survivin protein expression in DU145 cells.

(**A**) A representative Western blotting experiment illustrating survivin protein expression in DU145 cells at 24 hours after transfection with the different siRNAs (100 nM). β-actin was used as control for loading. (**B**) Densitometric of survivin protein expression levels at 24 hours (empty column) and 48 hours (blue column) after transfection. Data are expressed as percentage inhibition of survivin expression compared to Lipo2000-exposed cells and represent mean values ± sd of three independent experiments.

Transfection of DU145 cells with a survivin-specific siRNA, siRNA2, failed to appreciably affect the expression of other anti-apoptotic proteins including XIAP and Bcl-x_L (Figure 47). As already reported [Chaudary *et al*, 2001], no Bcl-2 expression was observed in these cells (Figure 47).

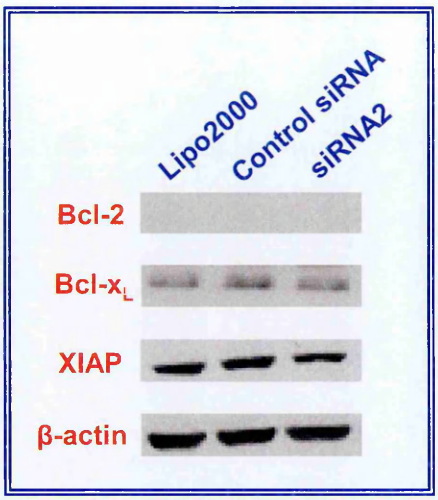

Figure 47. Effect of siRNA-mediated silencing of survivin on the expression of the other anti-apoptotic proteins.

A representative Western blot experiment illustrating the expression of other anti-apoptotic proteins in DU145 cells at 24 hours after transfection with 100 nM siRNA2.

3.2. siRNA-Mediated Silencing of Survivin Gene Causes Cell Proliferation Decline and Apoptosis Induction in Prostate Cancer Cells

Transfection with the three survivin-specific siRNAs (siRNA2, 3 and 10) able to induce the greatest inhibition of survivin expression also resulted in significant (p<0.01) and time-dependent decline of DU145 cell proliferation compared to Lipo2000-exposed cells, which was appreciable starting from 24 hours after transfection (ranging from 47% to 55% with respect to Lipo2000-exposed cells) and increased at 48 hours (ranging from 65% to 73%) (Figure 48). Conversely, transfection with the control, unrelated siRNA only induced a modest inhibitory effect on cell proliferation (Figure 48).

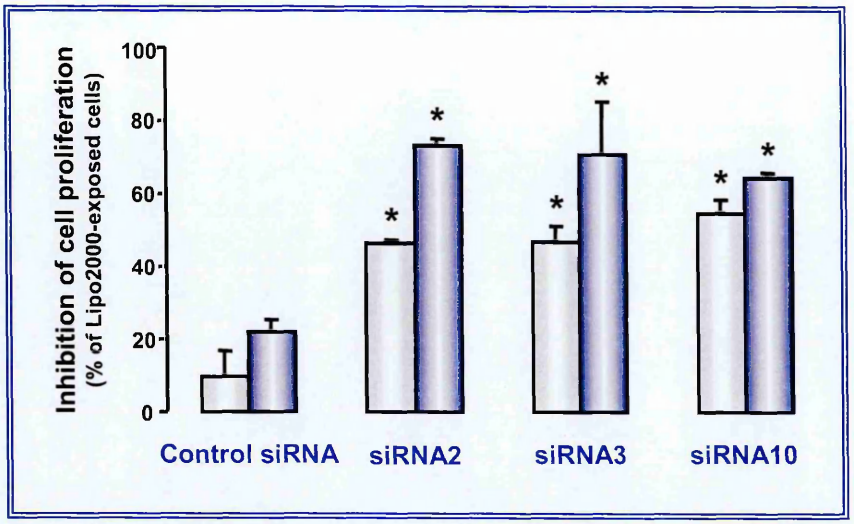

Figure 48. Effects of siRNA-mediated survivin down-regulation on *in vitro* growth of DU145 cells.

Data are expressed as percentage values of cell growth in DU145 cells at 24 (empty column) and 48 hours (blue column) after transfection with 100 nM control siRNA or survivin-specific siRNAs (siRNA2, 3 and 10), as compared to that of control cells exposed to lipofectamine alone. Data represent mean values ± sd of three independent experiments. * $p<0.01$, Student's t test.

To test whether the cytotoxic effect consequent to survivin down-regulation was due to the induction of apoptosis, we assessed by flow cytometry the presence of an apoptotic sub-$G_{0/1}$ peak 48h after transfection of DU145 with the different siRNAs. No sub-$G_{0/1}$ peak was observed in Lipo2000-exposed cells, whereas a peak accounting for 6.5% of the overall cell population was present in DU145 cells transfected with the control siRNA (Figure 49). However, the extent of sub-$G_{0/1}$ peaks was markedly increased in cells transfected with the survivin-specific siRNAs 2, 3 and 10, and ranged from 25% to 40% of the overall cell population (Figure 49).

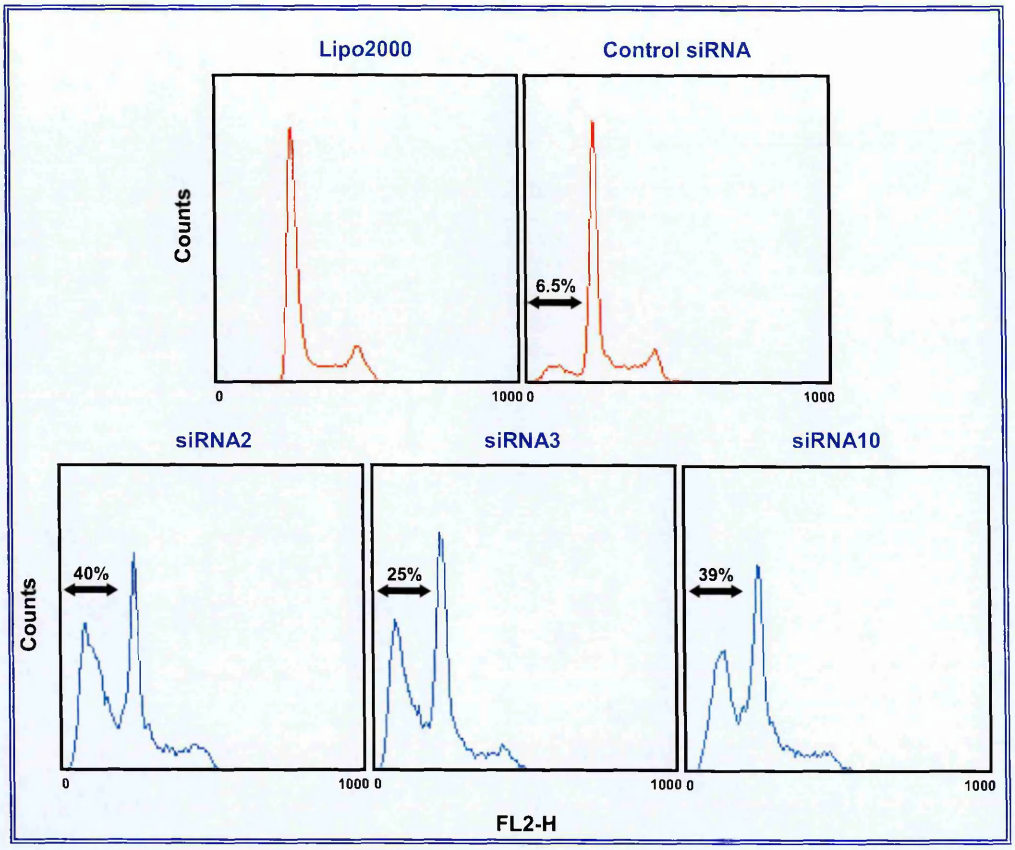

Figure 49. Effects of siRNA-mediated survivin down-regulation on the apoptotic rate of DU145 cells.

Flow cytometric analysis of DU145 cells at 48 hours after transfection with different siRNAs. The percentage of the sub-$G_{0/1}$ population is reported in each histogram.

At the molecular level, siRNA-mediated inhibition of survivin expression in DU145 cells coincided with a significantly (p<0.01) increased catalytic activity of caspase-9. Specifically, the enzyme's activity was three-four-fold higher in DU145 cells transfected with survivin-specific siRNAs than in those exposed to Lipo2000. Conversely, transfection of cells with the control, unrelated siRNA did not appreciably modify the extent of caspase-9 activity (Figure 50).

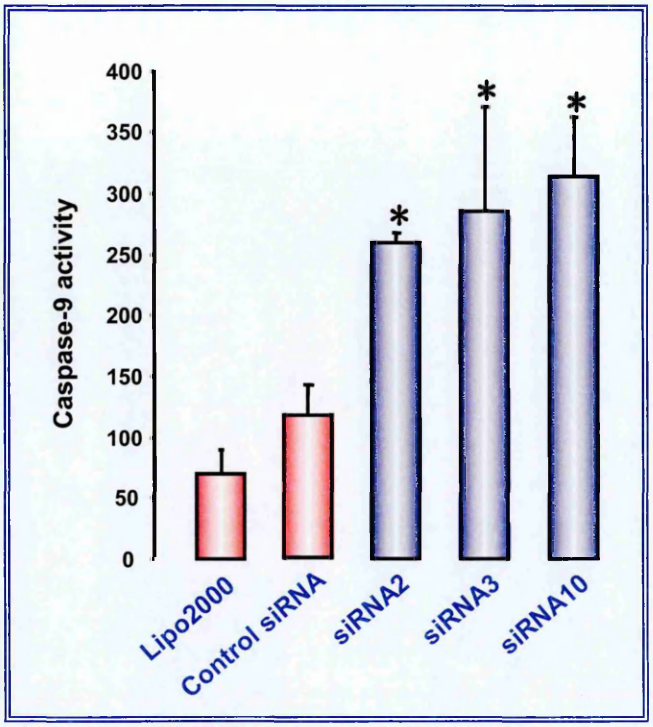

Figure 50. Effects of siRNA-mediated survivin down-regulation on the apoptotic rate of DU145 cells.
Caspase-9 catalytic activity as determined by hydrolysis of the fluorogenic substrate LEHD-AFC in Lipo2000-exposed cells and in cells transfected with different siRNAs. Data are expressed as relative fluorescence units (r.f.u) and represent the mean values ± sd of three independent experiments. * $p<0.01$, Student's t test.

3.3. siRNA-Mediated Silencing of the Survivin Gene Increases the Sensitivity of Prostate Cancer Cells to 17-Allylamino-17-Demethoxy-Geldanamycin

To test whether the basal level of survivin in the tumour cell population plays a role in determining the in vitro response to Hsp90 inhibitors, we examined the effect of siRNA-mediated survivin down-regulation on cell sensitivity to 17-AAG in DU145 cells. A 72-hours exposure to different drug

concentrations (from 5 to 50 ng/ml) induced a dose-dependent decline of DU145 cell proliferation (Figure 51) as well as a decrease in the expression/activity of Hsp90 client proteins including Akt, cdk6 (Figure52A) and telomerase (Figure 52B). The extent of the 17-AAG cytotoxic activity was enhanced in cells transfected with siRNA2. Specifically, at all drug concentrations tested, the sequential treatment (8-hours siRNA2 transfection followed by 72-hours 17-AAG exposure) induced an inhibitory effect on cell proliferation greater than that expected by simple additivity of the effects of the two agents, which was appreciable both at the end of treatment and at 7 days (Figure 51).

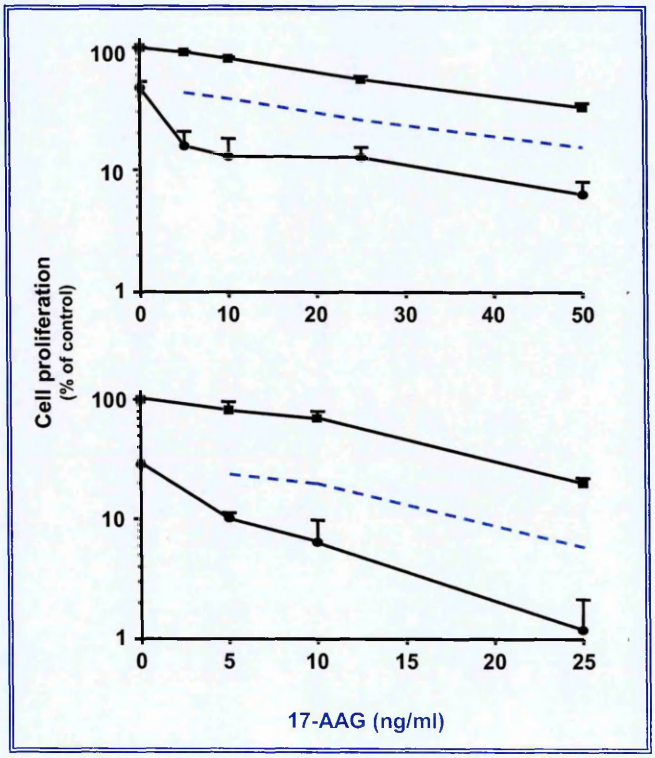

Figure 51. Dose-response survival curves of DU145 cells exposed to siRNA in combination with 17-AAG.

Dose-response survival curves of DU145 cells exposed to 17-AAG alone for 72 hours (■) or to combined treatment (8-hours transfection with 100 nM siRNA2 followed by 72-hours exposure to 17-AAG) (•) and obtained at the end of treatment (3 days; top) or at 7 days (bottom). Mean plots ± sd of three independent experiments are reported. The dashed line indicates the expected curve for an additive effect of the two agents in combination.

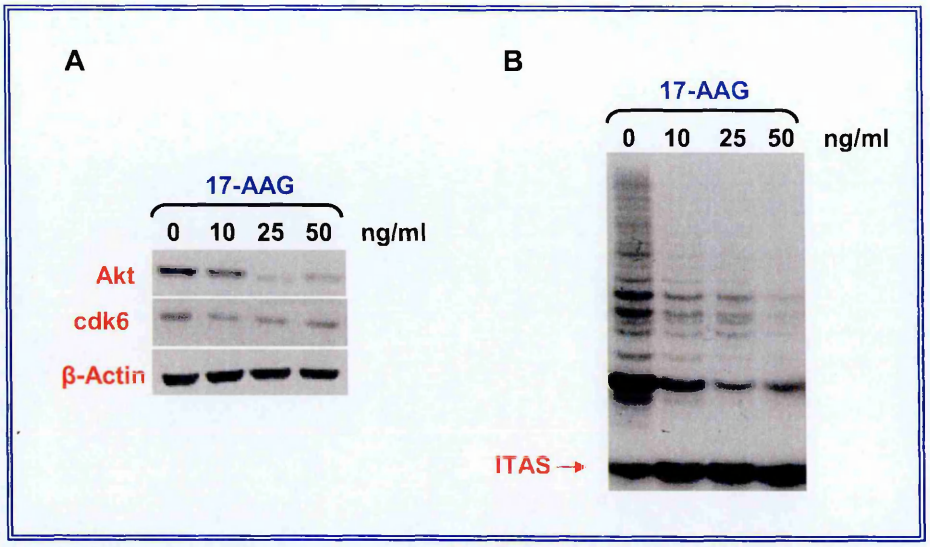

Figure 52. Effects of siRNA-mediated survivin down-regulation combined with 17-AAG treatment on the expression/activity of Hsp90 client proteins.

Representative Western blot **(A)** and TRAP assay **(B)** experiments illustrating the expression of Akt and cdk6 proteins and telomerase catalytic activity in DU145 cells after a 72-hours exposure to 17-AAG.

Exposure of cells to 17-AAG alone did not appreciably affect survivin expression up to 100 ng/ml, whereas a marked and dose-dependent inhibition of protein expression was observed at the two highest drug concentrations (500 and 1000 ng/ml) (Figure 53). Sequential treatment with siRNA2 and 17-AAG consistently caused a strong decrease of survivin expression, which was almost superimposable to that observed after transfection of cells with siRNA2 alone (Figure 53). However, it was not possible to evaluate the cytotoxic effect of the sequential treatment at 17-AAG concentrations able to down-regulate survivin, since an almost complete inhibition of cell proliferation (around 99%) was found after a 3-days exposure to 500 ng/ml of drug. The cytotoxic effect of 17-AAG in DU145 cells transfected with the control siRNA was superimposable to that observed in cells exposed to 17-AAG alone.

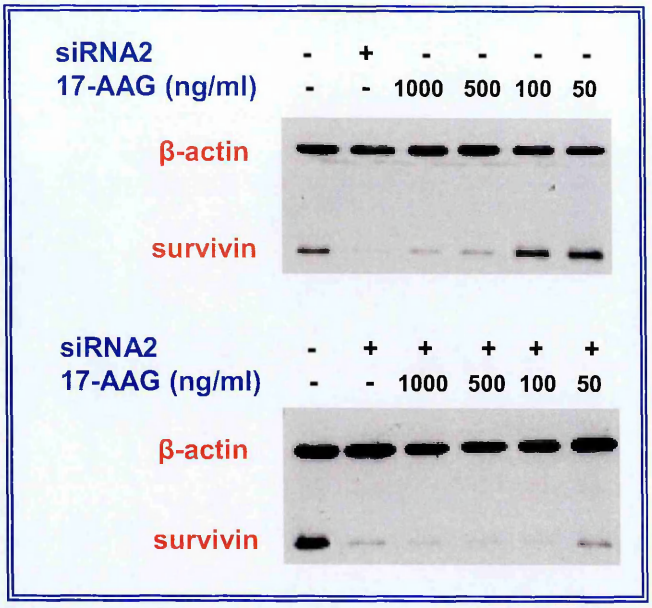

Figure 53. Survivin protein expression in DU145 cells after exposure to siRNA and 17-AAG.

Representative Western blot experiments illustrating the expression of survivin in DU145 cells after exposure to siRNA2 and 17-AAG, singly administered (top) or in sequence (bottom).

To gain insight into the molecular basis responsible for the increased sensitivity to 17-AAG observed in siRNA2-transfected DU145 cells, we evaluated the *in vitro* catalytic activity of caspase-9 following single and combined treatments (Figure 54). Exposure to 17-AAG increased the enzyme's activation compared to that observed in control (no-drug) cells. However, the caspase-9 catalytic activity was consistently and significantly ($p<0.02$) higher in cells exposed to the combined treatment (8-hours siRNA2 transfection followed by 72-hours 17-AAG exposure) than in those treated with the drug alone, and such enhancement was greatest (2.8-fold) at the highest 17-AAG concentration (Figure 54).

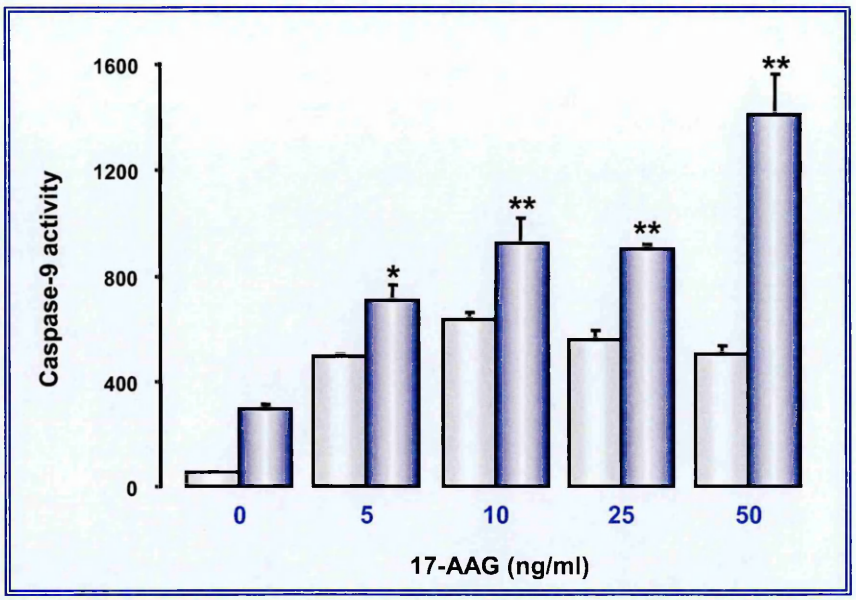

Figure 54. Caspase activation in DU145 cells after exposure to siRNA and 17-AAG.

Caspase-9 catalytic activity was determined by hydrolysis of the fluorogenic substrate Ac-DEVD-AMC in DU145 cells exposed to 17-AAG alone (empty column) or to the combined treatment (blue column). Data represent the mean values ± sd of three independent experiments. * $p<0.02$; ** $p<0.01$; Student's t test.

To evaluate the effect of survivin down-regulation on 17-AAG sensitivity in a second prostate cancer cell line, we transfected PC-3 cells with 100 nM siRNA2. Such transfection induced a marked inhibition of survivin protein expression as compared to Lipo2000-exposed cells, which was appreciable starting from 24 hours after transfection and remained stable at 48 hours (Figure 55). Moreover, the extent of inhibition (around 70-80%) was comparable to that obtained in DU145 cells after transfection with the same survivin-specific siRNA. Transfection of PC-3 cells with siRNA2 failed to appreciably modify the expression of other anti-apoptotic proteins such as XIAP, Bcl-2 and Bcl-x_L (Figure 55).

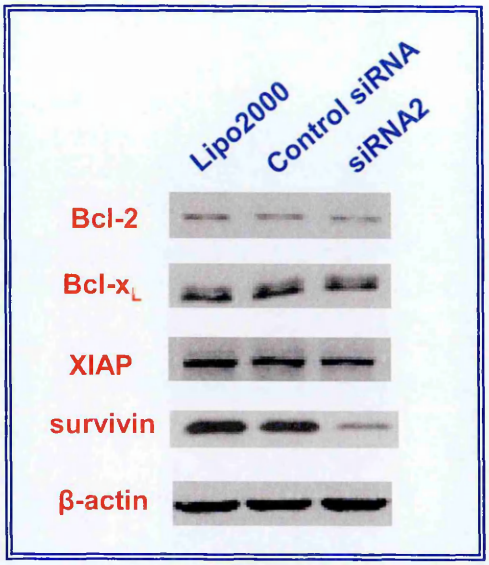

Figure 55. Survivin protein expression in PC-3 cells.
Representative Western blot experiments illustrating the expression of survivin and other anti-apoptotic proteins in PC-3 cells at 24 hours after transfection with siRNA2 (100 nM).

PC-3 cells were considerably more resistant to 72-hours exposure to 17-AAG than DU145 cells (Figure 56), as indicated by the 13-fold higher IC_{50} value (410 ± 20 ng/ml vs 31 ± 2 ng/ml, respectively). However, 17-AAG cytotoxic activity was enhanced in cells transfected with siRNA2 and, in accord with that observed in DU145 cells, the sequential treatment induced an inhibitory effect on cell proliferation (appreciable at the end of treatment and at 7 days) greater than that expected by simple additivity of the effects of the two agents when the drug was used at concentrations ranging from 100to 500 ng/ml. Conversely, no potentiating effect was observed when the highest 17-AAG concentration (1000 ng/ml) was used in sequence with siRNA2 (Figure 56). 17-AAG alone induced an appreciable inhibition of survivin expression only when used at 1000 ng/ml, whereas a markedly decreased

survivin abundance was consistently observed in cells exposed to siRNA2-17AAG sequential treatment independently of drug concentration (Figure 57).

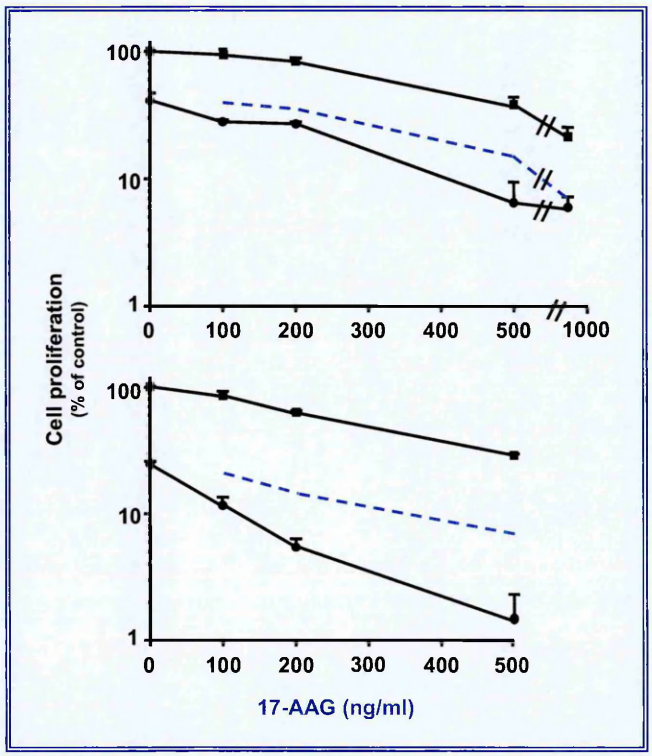

Figure 56. Dose-response survival curves of PC-3 cells exposed to siRNA in combination with 17-AAG.

Dose-response survival curves of PC-3 cells exposed to 17-AAG alone for 72 hours (■) or to combined treatment (8-hours transfection with 100 nM siRNA2 followed by 72-hours exposure to 17- AAG) (•) and obtained at the end of treatment (3 days; top) or at 7 days (bottom). Mean plots ± sd of three independent experiments are reported. The dashed line indicates the expected curve for an additive effect of the two agents in combination.

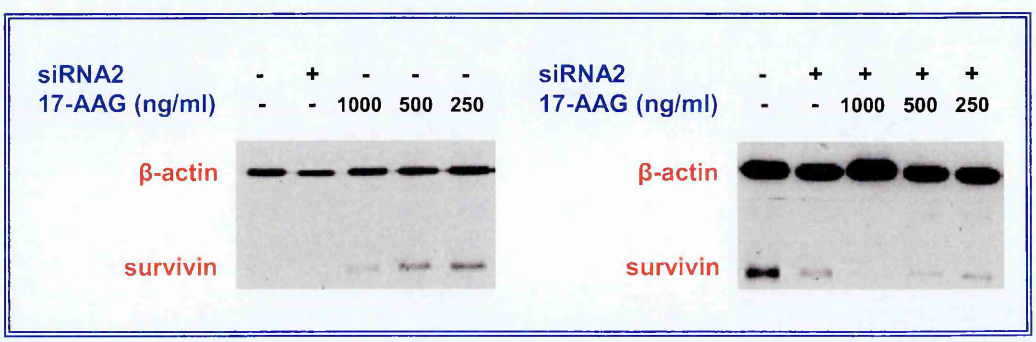

Figure 57. Survivin protein expression in PC-3 cells after exposure to siRNA and 17-AAG.

A representative Western blot experiment illustrating the expression of survivin in PC-3 cells after exposure to siRNA2 and 17-AAG, singly administered (left) or in sequence (right).

4. POTENTIATION OF PACLITAXEL-INDUCED APOPTOSIS BY THE NOVEL CYCLIN-DEPENDENT KINASE INHIBITOR NU6140: A POSSIBLE ROLE FOR SURVIVIN DOWN-REGULATION

Cell progression through the cell cycle is controlled by serine/threonine cyclin-dependent kinases (cdk) that form complexes with cyclins and operate in distinct phases of the cell cycle [Sherr, 1996; Morgan, 1997]. Aberrant control of cdks is a central feature of the molecular pathology of cancer [Kamb, 1995; Vogt & Reed, 1998; Pavletich, 1999]; hence cdks and their related pathways represent attractive targets in the development of anticancer therapeutics. Small molecule cdk inhibitors, including flavopiridol, roscovitine, UCN-01 and purvalanol A (Figure 58), which act by competing with ATP for binding at the catalytic site of the kinases, have been generated [Senderowicz, 2003]. In addition to arresting cell-cycle progression through the inhibition of multiple cdks [Senderowicz, 2003], some of these inhibitors exhibit a variety of activities, including induction of apoptosis [Meijer *et al*, 1997], promotion of cell differentiation [Lee *et al*, 1999], interference with transcription [Rickert *et al*, 1996; Chao *et al*, 2000] and anti-angiogenic effects [Melillo *et al*, 1999]. Furthermore, the possibility of enhancing the activity of conventional chemotherapeutic agents and radiation by combination with cdk inhibitors has also been shown [Schwartz *et al*, 1997; Motwani *et al*, 1999; Shah & Schwartz, 2000; Schwartz *et al*, 2001; Shapiro *et al*, 2001; Jung *et al*, 2003]. The purine-based cdk inhibitor NU6140 (4-(6-cyclohexylmethoxy-9*H*-purin-2-ylamino)-*N,N*-diethyl-benzamide) (Figure 58) was derived from NU6102 (6-cyclohexylmethoxy-2-(4'-

sulfamoylanilino)purine), a potent and selective CDK2 inhibitor developed using structure-based drug design [Davies *et al*, 2002], as a cdk inhibitor with greater cellular potency.

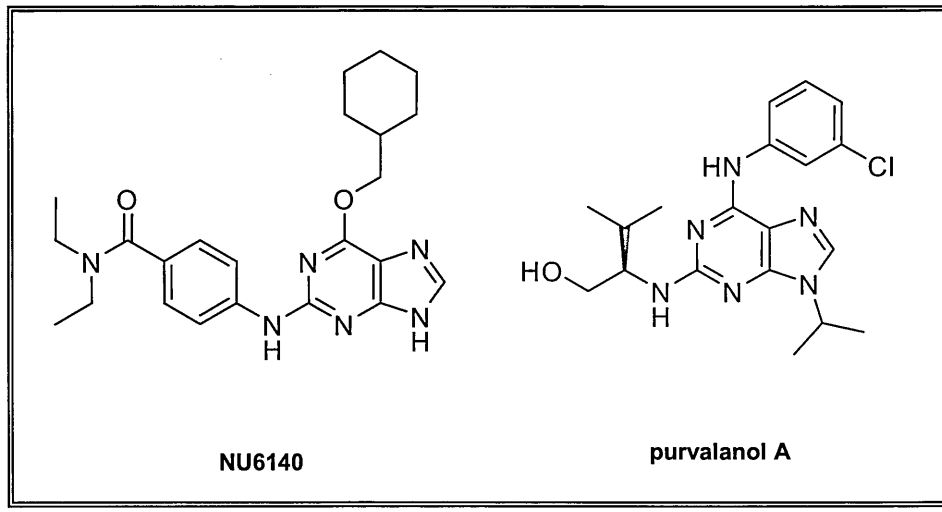

Figure 58. Chemical structure of NU6140 and purvalanol A.

Survivin is expressed in a cell cycle-dependent manner and during mitosis it localizes to various components of the mitotic apparatus and associates with microtubules of the mitotic spindle [Giodini *et al*, 2002]. Its expression is controlled at transcriptional [Li & Altieri, 1999] and post-translational [O'Connor *et al*, 2000] levels. In this context, it has been demonstrated that cdk1-mediated phosphorylation of survivin on Thr^{34} is essential for the cytoprotective function of the protein [O'Connor *et al*, 2000]. Moreover, previous evidence indicated that targeting survivin by means of Purvalanol A, resulted in an increased sensitivity to paclitaxel in HeLa cells [O'Connor *et al*, 2002].

In this study we investigated the cellular effects of the novel cdk inhibitor NU6140 in relation to inhibition of cell proliferation and cell cycle progression, and ability to potentiate the apoptotic response to paclitaxel, in HeLa cells, in comparison to purvalanol A.

4.1. Effect of Cdk Inhibitors, Alone or in Combination with Paclitaxel, on Tumour Cell Growth

Clonogenic survival assays were performed to assess the anti-proliferative activity of NU6140 and purvalanol A, alone or in combination with paclitaxel. In a preliminary set of experiments, HeLa cervical carcinoma cells were treated with increasing concentrations of each cdk inhibitor alone. A concentration-dependent decline in cell survival was observed after treatment with both compounds, although NU6140 was somewhat more potent than purvalanol A as indicated by the three-fold lower concentration required to kill 50% of cells (IC_{50} values: 2.3 ± 0.2 μM vs 8.7 ± 0.4 μM, respectively) (Figure 59; Table VIII).

We further assessed the cytotoxic effects of the cdk inhibitors in combination with paclitaxel. HeLa cells were treated with paclitaxel for 24 hours followed by a 24 hours-exposure to NU6140 or purvalanol A, and the opposite sequence was also tested. Both cdk inhibitors cooperated with paclitaxel to inhibit clonogenic cell survival (Table VIII). Specifically, sequential treatment with paclitaxel followed by each cdk inhibitor was more effective than the reverse treatment sequence, and induced an inhibitory

effect on surviving fraction greater than that expected by simple additivity of the effects of the two drugs (Table VIII). However, the most marked effect was obtained with the paclitaxel-NU6140 combination.

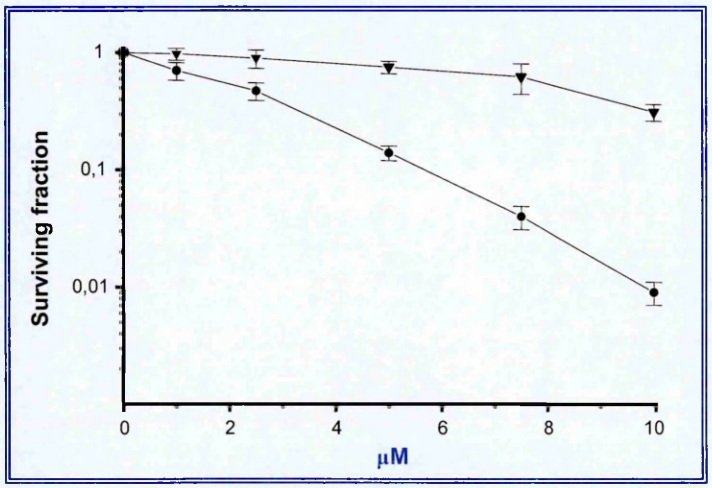

Figure 59. Clonogenic cell survival curves obtained after exposure of HeLa cells to cdk inhibitors.

HeLa cells were treated with NU6140 (●) and purvalanol A (▼) for 24 hours and then incubated at 37°C for 10 days. Colonies consisting of at least 50 cells were stained with crystal violet and counted under the microscope. Data represent mean values ± sd of three independent experiments.

A marked effect of the paclitaxel-NU6140 combination on the surviving fraction was also confirmed in OAW42/e ovarian cancer cells. Conversely, a subadditive effect of the paclitaxel-NU6140 combined treatment was found in OAW42/Surv cells ectopically expressing survivin (Table IX).

Table VIII. Cytotoxic effect of NU6140 and purvalanol A against HeLa cells as single agents and in combination with paclitaxel.

Agent/Combination	Concentration	Surviving fraction Observed (O)	Surviving fraction Expected[a] (E)	E/O ratio [b]	C.I. [c]	I[d]
Paclitaxel (nM)	1	0.76				
	2.5	0.34				
	5	0.12				
NU6140 (μM)	1	0.70				
	2.5	0.47				
	5	0.14				
Purvalanol A (μM)	1	0.97				
	2.5	0.89				
	5	0.75				
Paclitaxel (nM)	1					
+ NU6140 (μM)	1	0.50	0.53	1.06	1.14	0.96
	2.5					
	2.5	0.05	0.16	3.2	0.47	0.77
	5					
	5	0.002	0.02	10	0.29	0.71
Paclitaxel (nM)	1					
+ Purvalanol A (μM)	1	0.62	0.74	1.19	0.90	0.80
	2.5					
	2.5	0.18	0.30	1.7	0.60	0.80
	5					
	5	0.02	0.09	4.5	0.44	0.93
NU6140 (μM)	1					
+ Paclitaxel (nM)	1	0.64	0.53	0.87	1.51	1.43
	2.5					
	2.5	0.09	0.16	1.78	0.76	0.84
	5					
	5	0.012	0.02	1.67	0.45	0.97
Purvalanol A (μM)	1					
+ Paclitaxel (nM)	1	0.66	0.74	1.12	0.95	0.92
	2.5					
	2.5	0.18	0.30	1.67	0.70	0.83
	5					
	5	0.03	0.09	3.00	0.53	1.09

[a] calculated as the product of the surviving fractions observed for individual drugs;
[b] (surviving fraction observed) / (surviving fraction expected)
[c] Combination index according to Chou & Talalay [1984]
[d] Isobologram analysis according to Berenbaum [Berenbaum, 1989]

Table IX. Cytotoxic effect of NU6140 against OAW42/e and OAW42/Surv cells as single agent and in combination with paclitaxel.

Agent/Combination	Concentration	Surviving fraction Observed (O)	Surviving fraction Expected[a] (E)	E/O ratio [b]	C.I. [c]
OAW42/e					
Paclitaxel (nM)	1	0.81			
	2.5	0.56			
	5	0.14			
NU6140 (μM)	1	0.83			
	2.5	0.29			
	5	0.17			
Paclitaxel (nM)	1				
+ NU6140 (μM)	1	0.82	0.67	2.09	1.33
	2.5				
	2.5	0.08	0.16	2.00	0.57
	5				
	5	0.0023	0.023	10	0.36
NU6140 (μM)	1				
+ Paclitaxel (nM)	1	0.43	0.67	1.55	0.95
	2.5				
	2.5	0.13	0.16	1.23	0.74
	5				
	5	0.014	0.023	1.64	0.60
OAW42/Surv					
Paclitaxel (nM)	1	0.99			
	2.5	0.90			
	5	0.75			
NU6140 (μM)	1	0.89			
	2.5	0.30			
	5	0.18			
Paclitaxel (nM)	1				
+ NU6140 (μM)	1	0.85	0.88	1.03	1.19
	2.5				
	2.5	0.30	0.27	0.90	1.28
	5				
	5	0.16	0.13	0.81	1.34
NU6140 (μM)	1				
+ Paclitaxel (nM)	1	0.87	0.88	1.01	1.25
	2.5				
	2.5	0.32	0.27	0.84	1.33
	5				
	5	0.18	0.13	0.72	1.40

[a] calculated as the product of the surviving fractions observed for individual drugs;
[b] (surviving fraction observed) / (surviving fraction expected)
[c] Combination index according to Chou & Talalay [1984].

4.2. Effects of Cdk Inhibitors on Cell Cycle Progression and Apoptosis

Flow cytometric analysis of propidium iodide-stained HeLa cells showed that a 24-hours treatment with NU6140 and purvalanol A resulted in a concentration dependent decrease in the number of cells in the G_1 phase, and a concomitant increase in the sub-G_1 apoptotic cell population (Figure 60A). Moreover, chromatin condensation and DNA fragmentation, which are common features of apoptosis, were detected by fluorescence microscopy after staining with propidium iodide of HeLa cells treated with NU6140 and purvalanol A. The percentage of cells with an apoptotic nuclear morphology, as determined on the overall cell population, increased in a concentration-dependent fashion after treatment with both inhibitors (Figure 60B).

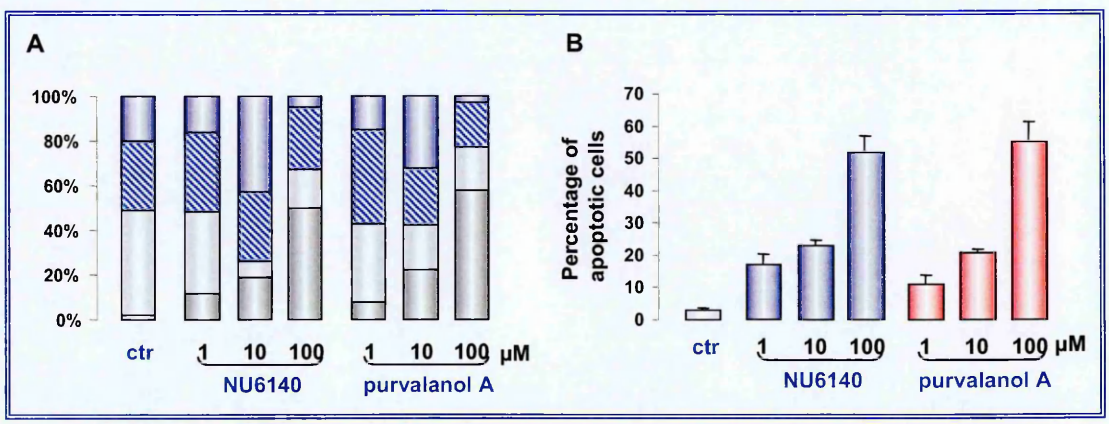

Figure 60. Effect of NU6140 and purvalanol A on cell cycle and apoptosis.
HeLa cells were exposed to 1% (v/v) DMSO (control cells) or 1, 10, 100 µM NU6140 and purvalanol A. (**A**) Cell cycle distribution was assessed by flow cytometry on cells stained with propidium iodide. The percentage of cells in sub-G_1 (grey column), G_1 (empty column), S (hatched column) and G_2/M phase (blue column) are shown. Data represents the means of the three independent experiments; sd were always within 5%. (**B**) The percentage of cells with an apoptotic morphology was assessed by fluorescence microscopy. Data represent mean values ± sd of three independent experiments.

At the molecular level, treatment with NU6140 and purvalanol A resulted in a concentration-dependent increase in the catalytic activity of capase-9 and capase-3, as assessed by the *in vitro* hydrolysis of specific fluorogenic substrates (Figure 61).

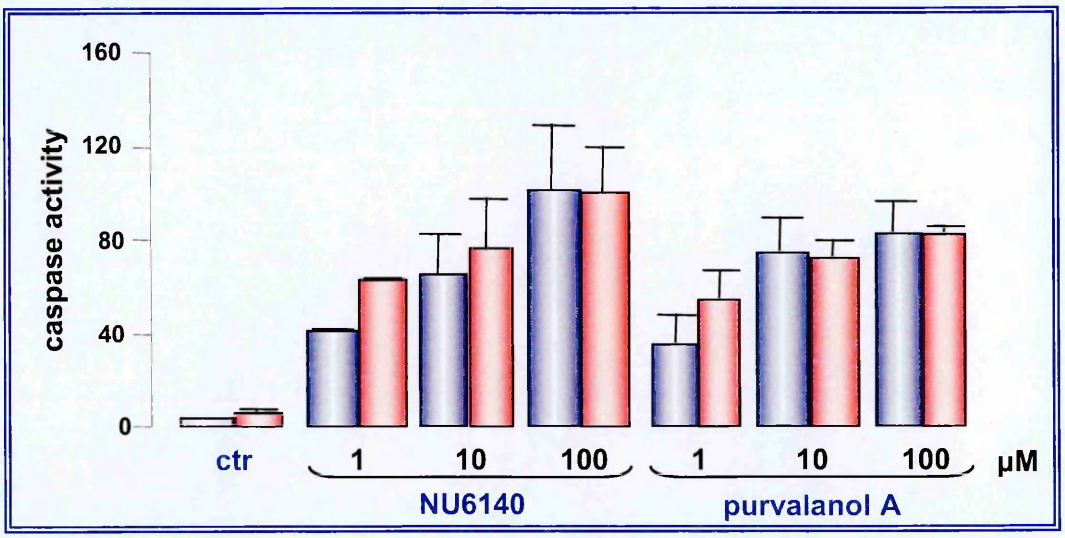

Figure 61. Caspase activation in HeLa cells after exposure to NU6140 and purvalanol A.

Caspase-9 (blue column) and caspase-3 (red column) catalytic activity was determined by hydrolysis of the fluorogenic substrate LEHD-AFC and Ac-DEVD-AMC AMC respectively, in cells exposed to 1% (v/v) DMSO (control cells) or treated with 1, 10, 100 µM of NU6140 and purvalanol A for 24 hours. Data are expressed as relative fluorescence units (r.f.u.) and represent mean values ± sd of three independent experiments.

4.3. Effects of Cdk Inhibitors on Survivin Expression

To investigate the mechanisms by which NU6140 and purvalanol A induced apoptosis, we evaluated the expression of the anti-apoptotic gene survivin in cancer cells after drug exposure. Treatment of HeLa cells with NU6140 or purvalanol A induced a concentration-dependent decrease in the levels of survivin protein (Figure 62). A NU6140-induced inhibition of survivin

expression was also seen in OAW42/e and OAW42/Surv cells. However, in OAW42/Surv cells, which displayed a 2.5-fold higher basal level of survivin protein compared to OAW42/e cells, the protein abundance was consistently higher than in parental cells also after exposure to different NU6140 concentrations (Figure 62). Conversely, exposure to NU6140 failed to modulate the expression of other anti-apoptotic proteins, such as Bcl-2 and Bcl-x_L, in all three cell lines (Figure 62).

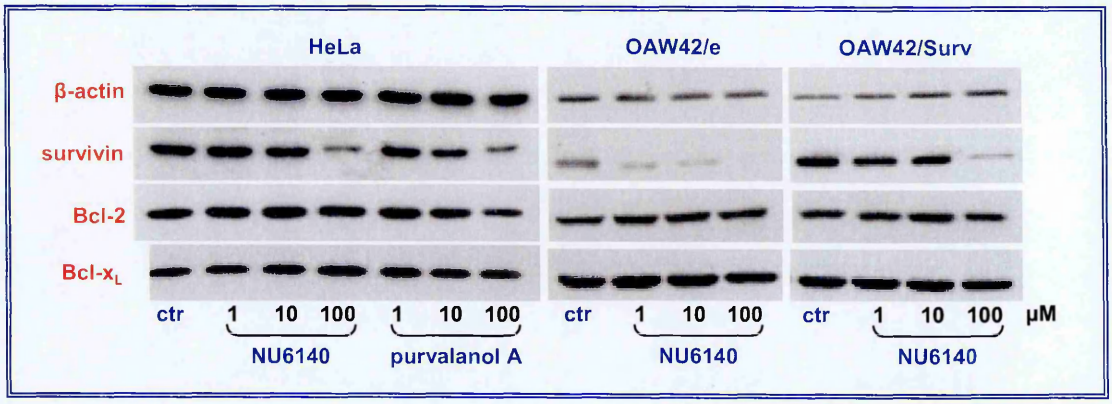

Figure 62. Down-regulation of survivin protein by cdk inhibitor treatment.
Tumour cells were exposed to 1% (v/v) DMSO (control cells) or treated with 1, 10, 100 μM of NU6140 and purvalanol A for 24 hours. Survivin, Bcl-2 and Bcl-x_L protein expression was assessed by Western blot. β-actin was used as a control for loading.

Furthermore, RT-PCR analysis in HeLa cells demonstrated that survivin mRNA levels were reduced by both cdk inhibitors (Figure 63), suggesting that NU6140 and purvalanol A modulate survivin expression at the transcriptional level.

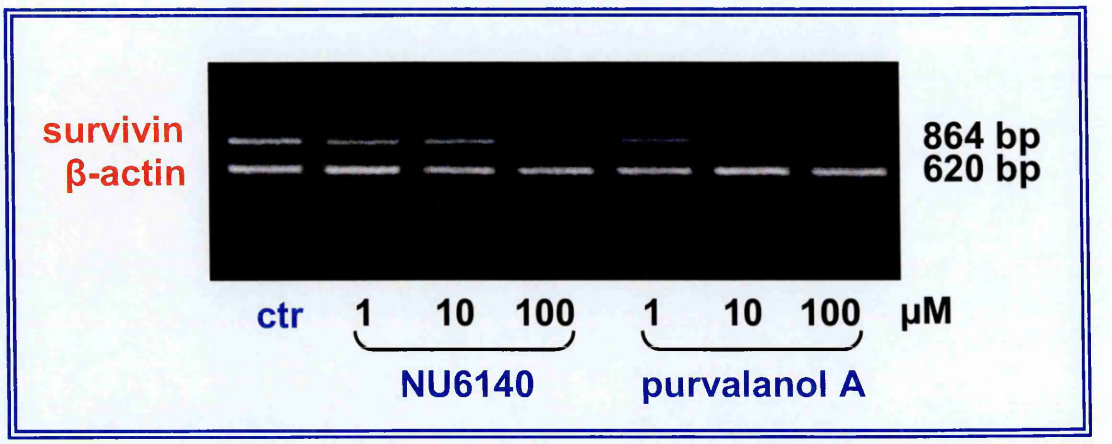

Figure 63. Down-regulation of survivin mRNA by cdk inhibitor treatment.
Tumour cells were exposed to 1% (v/v) DMSO (control cells) or treated with 1, 10, 100 μM of NU6140 and purvalanol A for 24 hours. Survivin mRNA expression was assessed by RT-PCR. β-actin was used as a control for amplification.

The possibility that NU6140 and purvalanol A inhibit survivin activation by interfering with cdk1, a kinase which is known to activate survivin through phosphorylation of its Thr^{34} residue [O'Connor *et al*, 2002] was also studied. Results from immunoblotting experiments using a phospho-specific antibody indicated that the levels of the active, Thr^{34}-phosphorylated form of survivin were reduced in a concentration-dependent fashion following treatment of HeLa cells with NU6140 and purvalanol A (Figure 64).

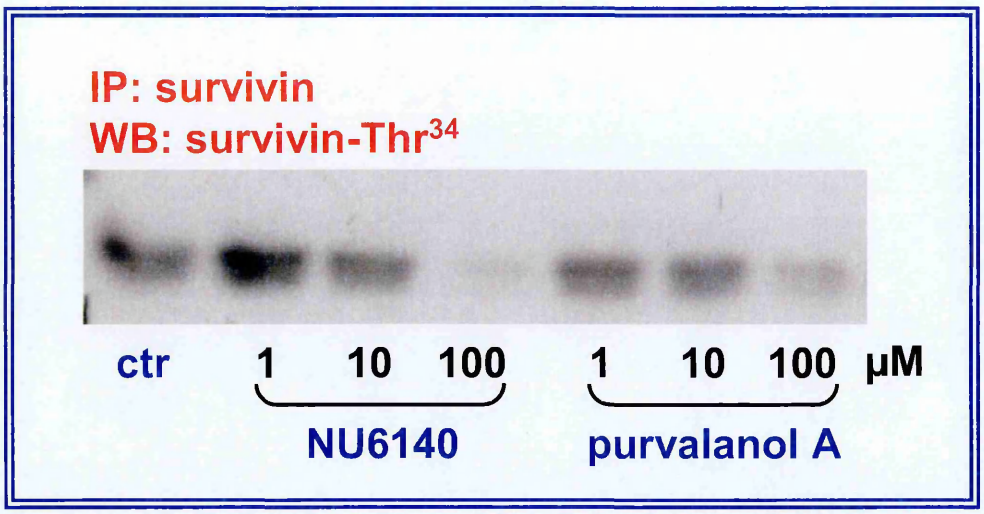

Figure 64. Effect of cdk inhibitor treatment on survivin phosphorylation. Survivin phosphorylation on Thr^{34} as evaluated by Western blot. Survivin was immunoprecipitated using the anti-human survivin antibody and analysed with the antibody to phosphorylated Thr^{34}.

4.4. Effects of Combined Treatment with Paclitaxel and Cdk Inhibitors on Cell Cycle Phase Distribution and Apoptosis

Next, we examined cell cycle perturbations induced by paclitaxel alone or paclitaxel followed by the cdk inhibitors (Figure 65). HeLa cells treated with paclitaxel alone for 24 hours accumulated in the G_2/M phase, and a fraction of sub-G_1 apoptotic cells, corresponding to 19 ± 1.2% of the overall cell population, was observed. When cells were treated sequentially with paclitaxel and NU6140, a reduction in G_2/M arrested was observed, and 86 ± 11% of cells underwent apoptosis. Such an apoptosis rate was significantly (p<0.01) higher than that observed after sequential treatment of cells with paclitaxel and purvalanol A (37 ± 8%) (Figure 65). However, it must be stressed that results of cell cycle analysis of cells undergoing apoptosis

have to be considered with some caution, since partial loss of DNA during the apoptotic process can make it difficult to distinguish between S-phase and G_2/M-phase cells.

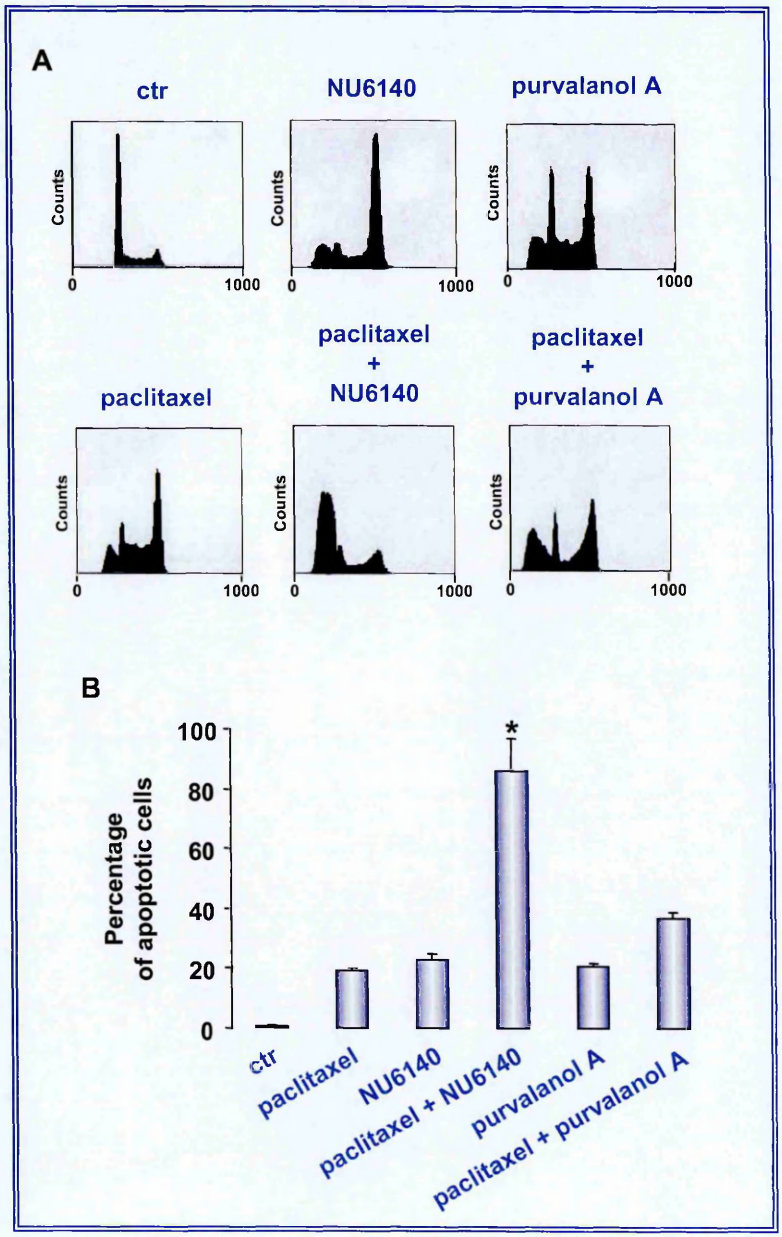

Figure 65. Effect of combined treatment with paclitaxel followed by cdk inhibitors on cell cycle progression and apoptosis.

(**A**) HeLa cells were incubated with paclitaxel (50 nM), NU6140 (10 μM) or purvalanol A (10 μM) alone for 24 hours, or with paclitaxel (50 nM) for 24 hours followed by a 24 hours-exposure to cdk inhibitors (10 μM). Following treatment cells were analysed by flow cytometry. (**B**) Quantification of sub-G_1 apoptotic cells. Data represent mean values ± sd of three independent experiments. *p<0.01, Student's t test.

We then assessed whether the increases apoptotic response induced by combined treatments was sustained by caspase activation in HeLa cells. Immunoblotting results indicated that treatment with paclitaxel and purvalanol A, singly administered or in combination, did not induce any proteolytic processing of the enzymes. Caspase-9 cleavage was detected only after the sequential treatment of cells with paclitaxel and NU6140 (Figure 66). Moreover, in response to NU6140, the 32 kDa pro-caspase-3 was partially cleaved to a 20 kDa intermediated form, whereas a complete activation of caspase-3 was observed after sequential treatment with paclitaxel followed by NU6140, as indicated by the presence of both the 20 and 17 kDa active cleaved products (Figure 66).

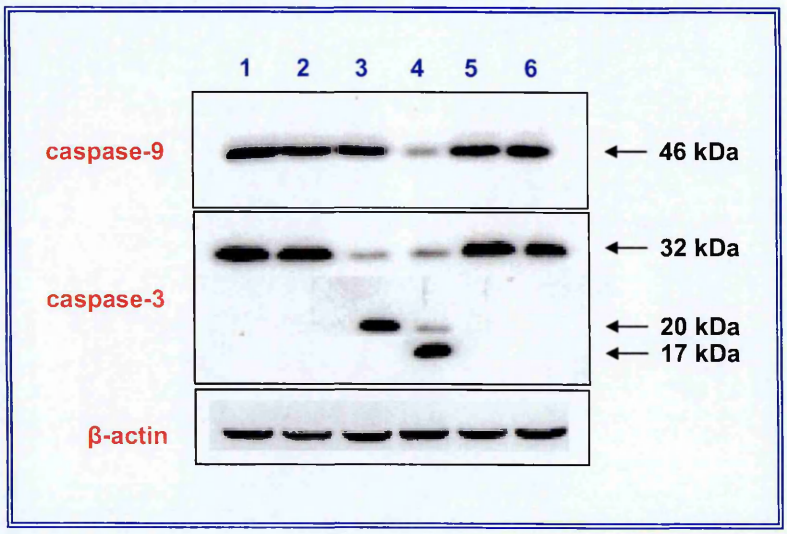

Figure 66. Proteolytic processing of caspase-9 and caspase-3 by combined treatment of tumour cells with paclitaxel followed by cdk inhibitors.

Cells were incubated with paclitaxel (50 nM), NU6140 (10 μM) or purvalanol A (10 μM) alone for 24 hours, or with paclitaxel (50 nM) for 24 hours followed by a 24 hours-exposure to cdk inhibitors (10 μM). The proteolytic processing of caspase-9 and caspase-3 was assessed by Western blot.
Lane 1, ctr; lane 2, paclitaxel; lane 3, NU6140; lane 4 paclitaxel + NU6140; lane 5, purvalanol A; lane 6, paclitaxel + purvalanol A.

The proteolytic processing of caspase-9 and caspase-3 coincided with an increased catalytic activity of both enzymes. Specifically, caspase-9 and caspase-3 activity, was about 3-fold (p<0.001) and 4-fold (p<0.01) higher, respectively, in HeLa cells treated with paclitaxel followed by NU6140 than in cells exposed to single agents or paclitaxel-purvalanol A combination (Figure 67).

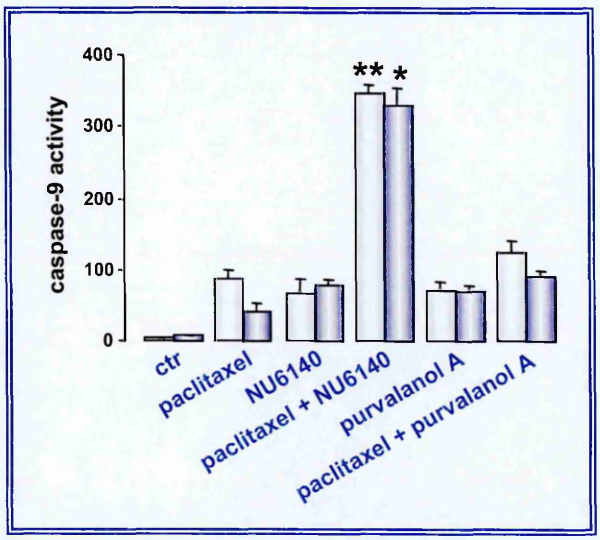

Figure 67. Activation of caspases by combined treatment of HeLa cells with paclitaxel followed by cdk inhibitors.

Cells were incubated with paclitaxel (50 nM), NU6140 (10 μM) or purvalanol A (10 μM) alone for 24 hours, or with paclitaxel (50 nM) for 24 hours followed by a 24 hours-exposure to cdk inhibitors (10 μM). Caspase-9 (empty column) and caspase-3 (blue column) catalytic activity as determined by hydrolysis of the fluorogenic substrate LEHD-AFC and Ac-DEVD-AMC AMC, respectively. Data are expressed as relative fluorescence units (r.f.u.) and represent mean values ± sd of three independent experiments. *p<0.01, **p<0.001, Student's t test.

Similarly, a 3-fold increase (p<0.001) in caspase-9 and caspase-3 catalytic activity was observed in OAW42/e cells exposed to paclitaxel followed by NU6140 compared to cells treated with individual agents (Figure 68). Conversely, a modest and non statistically significant increase in caspase

catalytic activities was found in OAW42/Surv cells treated with paclitaxel-NU6140 combination (Figure 68).

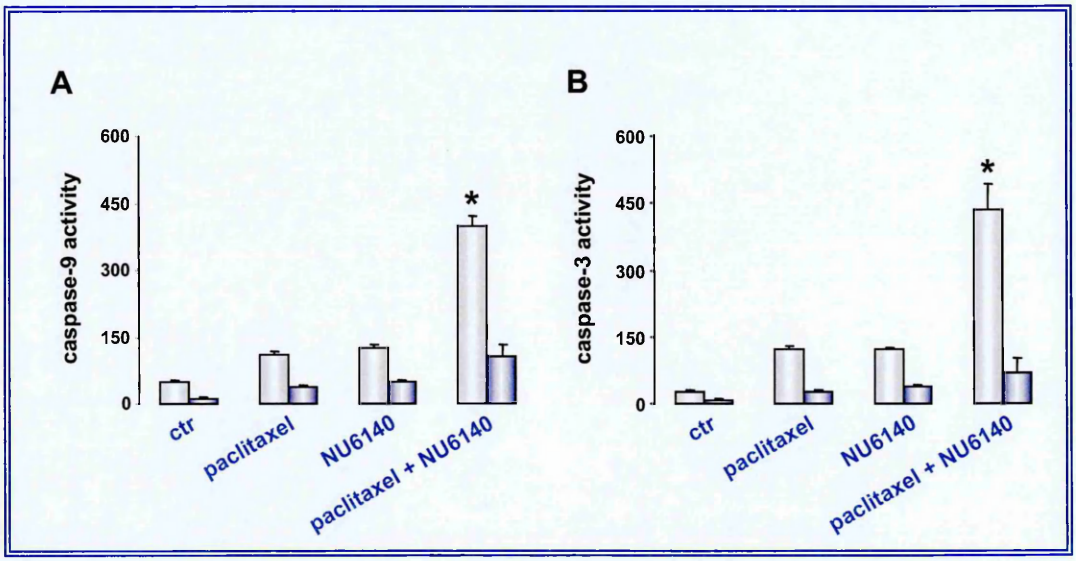

Figure 68. Activation of caspases by combined treatment of OAW42/e and OAW42/Surv cells with paclitaxel followed by cdk inhibitors.

Cells were incubated with paclitaxel (50 nM), NU6140 (10 μM) or purvalanol A (10 μM) alone for 24 hours, or with paclitaxel (50 nM) for 24 hours followed by a 24 hours-exposure to cdk inhibitors (10 μM). Caspase-9 (**A**) and caspase-3 (**B**) catalytic activity as determined by hydrolysis of the fluorogenic substrate LEHD-AFC and Ac-DEVD-AMC AMC, respectively, in OAW42/e (empty column) and OAW42/Surv (blue column) cells. Data are expressed as relative fluorescence units (r.f.u.) and represent mean values ± sd of three independent experiments. *p<0.001, Student's t test.

4.5. Effects of Combined Treatment with Paclitaxel and Cdk Inhibitors on Survivin Activation

Finally, the effects of paclitaxel, alone or in combination with NU6140 and purvalanol A, on survivin activation, as indicated by the level of the Thr^{34}-phosphorylated form of the protein, was assayed by immunoblotting. As expected, treatment with paclitaxel alone increased the level of phospho-survivin, whereas combined treatment with paclitaxel and cdk inhibitors

appreciably inhibited survivin phosphorylation, which was almost completely abrogated in cells exposed to the paclitaxel-NU6140 combination (Figure 69).

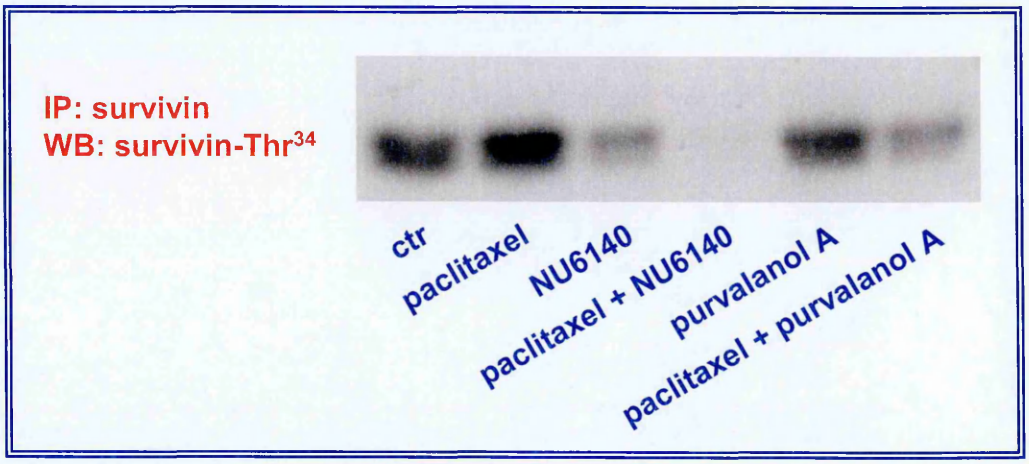

Figure 69. Effect of combined treatment of HeLa cells with paclitaxel followed by cdk inhibitors on survivin phosphorylation.

The phosphorylation of survivin on Thr^{34} residue was evaluated on HeLa cells treated with paclitaxel (50 nM), NU6140 (10 μM) or purvalanol A (10 μM) alone for 24 hours, or with paclitaxel (50 nM) for 24 hours followed by a 24 hours-exposure to cdk inhibitors (10 μM). Survivin was immunoprecipitated using the anti-human survivin antibody and analysed by Western blot with the antibody to phosphorylated Thr^{34}.

Chapter 5

DISCUSSION

Apoptosis is an attractive and well controlled cell suicide program that is evolutionary conserved among all animals [Steller, 1995; Nagata, 1997; Hengartner, 2000]. Deregulation of the apoptotic pathway is implicated in the pathogenesis of a variety of human diseases, including cancer [Reed, 1999; Yuan *et al*, 2003]. Many cancer cells circumvent normal apoptotic mechanisms to prevent their self-destruction, which may be of fundamental significance in the development of malignancy [Kerr, 1994; Hale *et al*, 1996]. In addition to the Bcl-2 family, a second anti-apoptotic gene family IAP has been identified [Deveraux & Reed, 1999; Hay, 2000; Salvesen & Duckett, 2002]. Among the IAPs, survivin plays an important role in inhibiting apoptosis and regulating mitotic progression [Altieri & Marchisio,1999]. Considering that apoptotic cell death is the major mode by which chemical and physical anticancer agents kill tumour cells, it appears reasonable that the inability to undergo programmed cell death is a major mechanism of the chemoresistance of tumour cells. As a consequence, the genes that control apoptosis provide interesting new targets for the rational development of strategies aimed at increasing the susceptibility of tumour cells to chemical and radiation treatment. In this context, the marked expression of survivin in cancer versus normal tissues [Altieri, 2003a] and its association with unfavourable disease outcome [Altieri, 2003a] have made survivin a promising therapeutic target for novel anticancer therapies [Altieri, 2003b].

To validate survivin as a potential therapeutic target in cancer cells, we evaluated the effects of the inhibition of survivin expression/activity on the proliferative potential, ability to undergo spontaneous apoptosis, and sensitivity to drug- and radiation-treatment of different tumour cell lines.

We first chose an approach based on the use of a hammerhead ribozyme since, due to its specific endoribonuclease activity, this small RNA molecule is able not only to specifically recognize its target RNA through complementary base pairing but also to cleave the substrate leading to its degradation and permanent inactivation [Sun *et al*, 2000]. These catalytic RNA motifs have received much attention in view of their potential usefulness for gene therapy due to their inherent simplicity, small size and ability to be incorporated into a variety of flanking sequence motifs without changing site-specific cleavage capacities. Moreover, the typical catalytic cycle of a ribozyme offers a considerable advantage with respect to the action mechanism of conventional antisense oligonucleotides [Sun *et al*, 2000]. Specifically, one molecule of hammerhead ribozyme can cleave several RNA target molecules, which implies that, theoretically, very low concentrations are required to obtain a significant biological effect. In fact, the efficacy of the ribozyme-mediated approach in inhibiting the expression of several cancer-related genes has been clearly demonstrated in a number of studies carried out on experimental human tumour models [Lewin & Hauswirth, 2001].

In the first part of the study we demonstrated the possibility to markedly attenuate the expression of the anti-apoptotic factor survivin in the JR8 human melanoma cell line, which inherently over-expresses the anti-apoptotic protein, by the use of a hammerhead ribozyme targeting a consensus sequence in exon 1 within survivin mRNA. This inhibitory effect was lost after inactivation of the catalytic core of the ribozyme (in JR8/mutRz cells), which strongly suggests specific cleavage activity of the anti-survivin ribozyme not only in the cell-free-system but also in intact cells. Active-

ribozyme transfectant cells showed enhanced sensitivity to topotecan and cisplatin with respect to cells transfected with the mutant ribozyme, as demonstrated by a reduced clonogenic cell survival and a lower IC_{50} value. Such an increased susceptibility to drug treatment as a consequence of survivin down-regulation was not observed for all DNA-interacting agents tested. Although the molecular basis for this putative selectivity is presently unknown, it is plausible that different signals are activated in response to DNA damage, depending on the type of genotoxic lesion, with a variable impact on the survivin pathway.

Ribozyme-transfectant melanoma cells also showed increased sensitivity to γ-irradiation with respect to parental cells and cells transfected with the mutant ribozyme, as demonstrated by a significantly reduced clonogenic cell survival. Specifically, cells expressing the active ribozyme were characterized by a survival curve with a reduced shoulder. Such a finding would suggest that, in the clinical setting, survivin inhibition could improve tumour sensitivity to fractionated therapy with multiple low radiation doses. Our results are in accord with previous evidence obtained in pancreatic carcinoma cell lines showing a direct relationship between the extent of survivin expression and the degree of in vitro radioresistance [Asanuma *et al*, 2000]. The same authors also showed that transduction of a dominant-negative mutant survivin gene into the radioresistant PANC-1 pancreatic cancer cells increased their radiation response [Asanuma *et al*, 2002]. Taken together these results support the hypothesis that survivin is a molecular determinant of radiation resistance.

In vitro sensitisation to drugs and radiation was paralleled by restoration of the susceptibility of JR8 cells expressing the active ribozyme to programmed cell death induced by the treatment. Such an enhanced apoptotic response was mediated by an increased activation of caspase-9 and caspase-3, which is consistent with the recognized function of survivin to counteract mitochondrial-death pathway [Altieri, 2003c; Beltrami *et al*, 2004]. However, it is still unclear whether survivin inhibits caspases through direct binding or indirectly, thereby requiring intermediate proteins [Reed, 2001]. Specifically, a possible direct interaction of survivin with caspase-9 has been reported by O'Connor *et al* [2000], whereas, more recently, Song *et al* [2003] suggested an alternative model for indirect inhibition of caspases by survivin based on its ability to physically interact with SMAC/Diablo. This mitochondrial factor, which is released into the cytosol in response to apoptotic stimuli, is known to bind to some IAPs (including XIAP, $cIAP_1$,$CIAP_2$ and livin), thus preventing them to inhibit caspases [Du *et al*, 2000; Vucic *et al*, 2002]. Accordingly to Song's model, the capability of survivin to sequester SMAC would allow other IAPs to block caspases without being antagonized. However, the possibility that survivin down-regulation also results in caspase-independent apoptosis was suggested by Liu *et al* [1998]. Specifically, they found the earliest pro-apoptotic event in melanoma cells transfected with a survivin dominant-negative mutant was nuclear translocation of mitochondrial apoptosis-inducing factor (AIF), known to trigger both apoptotic mitochondrial events and caspase-9 independent DNA fragmentation.

When tested in a human melanoma xenograft, ribozyme-mediated inhibition of survivin expression resulted in increased antitumorigenic activity

of topotecan, as demonstrated by the significantly delayed tumour establishment. Based on our *in vitro* findings indicating an enhanced susceptibility to topotecan-induced apoptosis of JR8 cells expressing the active ribozyme, it is conceivable to hypothesize that such an increased apoptotic response also occurred *in vivo*. The delayed growth in nude mice of tumour cells containing the active ribozyme after topotecan treatment reflected the survival of a limited number of cells that escaped drug-induced apoptosis, presumably as a consequence of a heterogeneous expression of survivin. Our findings corroborate and extend previous results indicating the possibility to target survivin pathway to obtain an improved response to apoptosis-inducing anticancer drugs in *in vivo* tumour models [Olie *et al*, 2000; O'Connor *et al*, 2002; Wall *et al*, 2003]. In this context, Yamamoto *et al* [2002] showed that down-regulation of survivin by forced expression of its natural antisense, the effector cell protease receptor-1 [Altieri, 1995], resulted in enhanced sensitivity to cisplatin and 5-fluorouracil of the HT29 colon adenocarcinoma cell line transplanted into nude mice. O'Connor *et al* [2002] observed that sequential inhibition of $p34^{cdc2}$ by purvalanol A (that blocks $p34^{cdc2}$ phosphorylation on Thr^{34}, which seems to be essential for the cytoprotective function of survivin [Altieri, 2003d]) enhanced the antitumour activity of taxol in an MCF-7 breast cancer xenograft.

In contrast to that reported in the aforementioned and other studies [Olie *et al*, 2000; Grossman *et al*, 2001; Mesri *et al*, 2001; Yamamoto *et al*, 2002], we did not observe any effect of survivin inhibition on proliferative potential, induction of spontaneous apoptosis and tumorigenicity of melanoma cells in the absence of other stimuli. It could be hypothesized that the concomitant

overexpression of other anti-apoptotic factors, such as Bcl-2 and Bcl-x_L, and cell survival factors in JR8 cells might produce a cytoprotective effect and contribute to prevent programmed cell death in this tumour model. When JR8 cells previously exposed for 48 hours to 3 μM of the Bcl-2 antisense oligonucleotide G3139 (which reduced by 50% the endogenous expression of the Bcl-2 protein) were γ-irradiated, however, no significant variation in their radio-sensitivity profile was observed. Such a finding would indicate that this anti-apoptotic factor does not play a major role in determining radiation response of these cells [Folini M, unpublished data].

However, it should be stressed that in JR8/Rz cells, survivin expression was attenuated but not completely abrogated. Possibly inhibition below a certain threshold is insufficient to abrogate the anti-apoptotic effect as well as to efficiently interfere with the major survivin function of preserving the mitotic apparatus and allowing normal cell cycle progression, as indicated by the lack of spontaneous apoptosis observed in JR8/Rz, which were also characterized by an *in vitro* proliferative potential similar to that of parental cells. Interestingly, and in keeping with this hypothesis, when we transduced two human androgen-independent prostate cancer cell lines with a Moloney-based retroviral vector carrying the catalytic sequence of the ribozyme Rz, we were able to select polyclonal cell populations characterized by a significant reduction of survivin expression compared to control cultures expressing the catalytically inactive ribozyme.

To obtain a high level of expression of the ribozyme within tumour cells and to target it to the same cellular compartment as its target mRNA substrate, we embedded the ribozyme sequence in the context of the

adenoviral VA1 gene and delivered it to cells through a retroviral vector. The gene is actively transcribed by RNA polymerase III in a variety of cell types, and the resulting transcript is characterized by a cytoplasmic localization [Prislei *et al*, 1997]. Moreover, it has been demonstrated that embedding a ribozyme in the context of this exogenous RNA molecule provides appropriate conformation for catalytic activity and stability [Cagnon & Rossi, 2000].

As expected, ribozyme-mediated down-regulation of survivin expression in polyclonal cell populations obtained from both DU145 and PC-3 cell lines resulted in a significant increase in the rate of spontaneous apoptosis, which was accompanied by the proteolytic activation of caspase-9 and caspase-3 and a significant increase in their *in vitro* catalytic activity. Inhibition of survivin expression also caused an increased apoptotic response of DU145/Rz cells to the anticancer drug cisplatin. Consistent with a major role of survivin in preserving the mitotic apparatus and allowing normal mitotic progression [Giodini *et al*, 2002], we found the appearance of a polyploid cell subpopulation in the DU145/Rz cell line as a possible consequence of the almost complete inhibition of survivin expression. The lack of evidence of polyploid cells in the PC-3/Rz cell line, in which a larger fraction of residual survivin protein was still present, further supports the hypothesis that inhibition below a certain threshold might be insufficient to abrogate survivin function in the control of mitotic progression. Moreover, a significant reduction of the *in vitro* proliferative potential, as indicated by a markedly increased doubling time, was only appreciable in DU145/Rz cells.

As regards the effect of survivin inhibition on the tumorigenic potential of prostate cancer cells, we found that DU145 cells were unable to grow when xenografted in athymic mice. Based on the results obtained in DU145/Rz cells as well as on previous evidence derived from *in vivo* studies (in which down-regulation of survivin through the use of survivin Thr^{34}-Ala mutant suppressed *de novo* tumour formation and inhibited the growth of established tumours in immunodeficient mice) [Grossman *et al*, 2001; Mesri *et al*, 2001], it could be assumed that the decreased tumorigenic potential of DU145/Rz was due an enhanced spontaneous apoptosis and reduced proliferative potential as a consequence of survivin inhibition.

The discovery that synthetic 21-23 nucleotide RNA duplexes (siRNAs) can trigger an RNAi response in mammalian cells and induce strong inhibition of specific gene expression [Elbashir *et al*, 2001] has opened the door to the therapeutic use of siRNAs. Specifically, several studies on experimental human tumour models have demonstrated the feasibility of this approach for the inhibition of a variety of cancer-related genes [Izquierdo, 2005]. Therefore, we used this interference approach to markedly reduce the expression of the cytoprotective factor survivin in human androgen-independent prostate cancer cells. Since it appears that target specificity can be attained depending on the position and sequence of a given siRNA [Ryther *et al*, 2005] in this study we used four 21-mer double-stranded siRNAs targeting different regions within survivin mRNA. A marked, though variable, extent of survivin inhibition in terms of mRNA and protein expression was observed with the different siRNAs, indicating the specificity of the inhibitory approach, which was also confirmed by the lack of an effect

on the expression of other anti-apoptotic proteins. However, the evidence of a modest but definite degree of survivin inhibition, mainly appreciable at the protein level, following transfection of cells with a control, unrelated siRNA suggests the occurrence of minor off-target effects induced by siRNAs. In this context microarray experiments aimed at evaluating whether global gene expression patterns change in the presence or absence of siRNAs already suggested that a small number of nontarget transcripts may also be affected [Semizarov *et al*, 2003].

As expected by our previous results indicating that interference with survivin function by the use of the hammerhead ribozyme led to increased apoptotic cell death in human androgen-independent prostate cancer cells, siRNA-mediated down-regulation of survivin expression in DU145 cells resulted in a significant decline of cell proliferation and an increase in the rate of spontaneous apoptosis, with a significant enhancement of *in vitro* caspase-9 catalytic activity in DU145 cells transfected with survivin-specific siRNAs. The possibility to restore the susceptibility to programmed cell death as a consequence of survivin gene silencing appears particularly relevant in human androgen-independent prostate cancer cells. In fact, one of the main events associated with the conversion to an androgen-independent phenotype and the concomitant loss of susceptibility not only to hormonal manipulation but also to chemotherapy and radiotherapy is an increased resistance to apoptosis due to dysregulation of the apoptotic pathways [Howell, 2000]. Specifically, a role for survivin in mediating resistance of prostate cancer cells to anti-androgen therapy with flutamide has been recently reported [Zhang *et al*, 2005].

Several *in vitro* and *in vivo* studies indicated that survivin down-regulation was able to sensitise human tumour cells of different histological origin to conventional chemotherapeutic drugs including taxol, doxorubicin, etoposide and cisplatin [Olie *et al*, 2000; Hayashi *et al*, 2005; Zhang *et al*, 2005] as well as to ionizing radiation [Lu *et al*, 2004; Kami *et al*, 2005]. However, thus far, no data are available concerning the effect of survivin down-regulation on the activity of ansamycin antibiotics, such as geldanamycin and 17-AAG, which inhibit Hsp90's chaperone function by targeting its ATPase activity [Schulte & Neckers, 1998]. Hsp90 inhibition results in proteasomal degradation of client proteins, leading to potent antitumour activity in experimental models [Kelland *et al*, 1999; Hostein *et al*, 2001]. In fact, although Hsp90 is highly expressed in most cells, Hsp90 inhibitors selectively kill cancer cells compared to normal cells. The molecular mechanism of such tumour selectivity is the result of an activated, high-affinity conformation of Hsp90 in tumour cells [Kamal *et al*, 2003]. Hsp90 inhibitors have been used as probes to definine the biological function of the chaperone at the molecular level and to validate it as a novel target for cancer therapy. One of these inhibitors, 17-AAG, has entered clinical trials, which served as proof of principle that Hsp90 function can be modulated pharmacologically without undue toxicity in humans [Workman, 2003]. The search for second-generation analogues with potential preferential pharmacological features is actively pursued. However, the best way to use Hsp90 inhibitors as anticancer agents remains to be defined, also because of the limited knowledge of the determinants of cellular sensitivity to these compounds.

We showed that the level of survivin expression influences the *in vitro* response of DU145 human prostate cancer cells to 17-AAG as suggested by the supra-additive cytotoxic effect observed after sequential treatment with a survivin-specific siRNA and the Hsp90 inhibitor, which was accompanied by a significantly increased caspase-9-dependent apoptotic response. This chemosensitising effect seems to be independent of the inherent susceptibility to 17-AAG of the tumour cell system, since it was also observed in PC-3 cell, which are considerably more resistant to the Hsp90 inhibitor than DU145 cells. Moreover, since 17-AAG itself induces an inhibition in survivin expression only when used at high concentrations (500 and 1000 ng/ml), it is unlikely that the supra-additive cytotoxic effects we observed with the survivin siRNA2-17-AAG sequential treatment at lower drug concentrations were due to a cooperative effect of the two agents in inducing survivin depletion. Our findings indicate that 17-AAG is more effective in cancer cells expressing reduced levels of survivin and suggest the opportunity to design combined treatments including survivin inhibitors and 17-AAG and test their antitumour potential against androgen-independent prostate cancer.

It has been previously reported that 17-AAG treatment reduced the expression of the androgen receptor (AR) in human prostate cancer xenografts and inhibited their growth in the animal [Solit *et al*, 2002]. Specifically, 17-AAG induced degradation of both wild-type and mutant AR, thus suggesting that this drug may be particularly effective in the treatment of androgen-independent prostate cancer. In fact, in a subset of patients treated with AR agonists, clinical progression is associated with AR gene

amplification or mutation [Cabrespine *et al*, 2004], which may result in sufficient AR pathway activation to allow tumour growth at low levels of testosterone or following constitutive ligand-independent activation of the receptor.

The specific inhibition of survivin levels combined with the collapse of Hsp90 function by ansamycin antibiotics would be expected to exert a strong antitumour effect by disabling multiple signalling networks required for prostate cancer cell maintenance. Moreover, we recently demonstrated that a peptidomimetic antagonist of the survivin-Hsp90 complex structurally different from 17-AAG, shepherdin, inhibited the chaperone activity and exhibited potent and selective anticancer activity in preclinical models [Plescia *et al*, 2005].

There is a widely diffused opinion that RNAi provides a powerful tool for targeted inhibition of gene expression, with respect to conventional antisense strategies (i.e. ribozymes), presumably because it relies on a natural process. Despite the unique assumed potential of RNAi, limitations in the use of this approach, such as the possibility that some mammalian cells may not be susceptible to RNAi, have been described. Cellular uptake and co localization to the specific target site within cells represent the main hurdles that have to be overcome for an efficient inhibition of gene expression. Although there are still no means to improve co-localization to the target site and to increase the efficacy of siRNAs in the presence of hardly accessible target RNA, a number of specific strategies have been demonstrated to be effective in inducing a sequence-directed colocalization of ribozymes and to improve their efficacy at the target site [Lee *et al*, 1999].

Ribozymes as well as siRNAs can lead to nonsequence specific effects (off-target effects) that are strongly dependent on the concentration of oligomers. However, it should be stressed that the double-stranded siRNAs may result in two single stranded oligomers which yield more pronounced off-target effects than those obtained with an equal molar amount of ribozymes [Scherer & Rossi, 2003]. However, lack of a study aimed to comparatively evaluate the efficacy of ribozymes and siRNAs in inhibiting the expression of the same gene on the same experimental systems makes it difficult to predict which is the better approach to be exploited for therapeutic purposes.

Whether selective inhibition of survivin can be used as a therapeutic modality aimed to inhibit the growth and enhance the sensitivity to specific anticancer drugs of melanoma and androgen-independent prostate cancer is an interesting issue that deserves further investigation. However, since multiple molecular pathways seem to play a role in mediating treatment resistance in these malignancies [Howell *et al*, 2000; Satyamoorthy *et al*, 2001], inhibition of a single target could be insufficient to adequately control tumour growth. In this context, exploration of additive or synergistic effects of combinations of selective inhibitors targeting different cellular pathways in preclinical models of melanoma and androgen-independent prostate cancer could provide the rational basis for the design of new multi-target clinical therapies.

Finally, since most human malignancies show aberrations in cell cycle control, the pharmacological modulation of cdks may be an important approach for the therapy of cancer. In this context, we evaluated the cellular effects of the purine derivative NU6140, a novel cdk inhibitor, in comparison

to purvalanol A, in HeLa cervical carcinoma, and OAW42/e and OAW42/Surv ovarian cancer cell lines. Both cdk inhibitors induced an impairment of cell cycle progression with a concentration-dependent accumulation of cells in the G_1 compartment, which was accompanied by a decline of cell growth and the induction of an apoptotic response. Treatment with NU6140 and purvalanol A also inhibited the expression of survivin by negatively interfering with the transcription of the gene. Moreover, NU6140- and purvalanol A-treated cells exhibited a lower abundance of the Thr^{34}-phosphorylated form of survivin, possibly as a consequence of drug-induced inhibition of cdk1 catalytic activity. It has been shown that during mitosis survivin physically associates with cdk1, and that phosphorylation on its Thr^{34} residue by cdk1 is a requirement for survivin-mediated cytoprotection [O'Connor *et al*, 2000]. Moreover, one of the mechanisms by which cdk1-mediated phosphorylation regulates survivin seems to be by increasing its stability at mitosis [O'Connor *et al*, 2002]. No appreciable interference with the expression of other anti-apoptotic proteins, such as Bcl-2 and Bcl-x_L, was observed after exposure of tumour cells to NU6140.

Taking into account the ability of NU6140 and purvalanol A to downregulate survivin, we tested the ability of the inhibitors to increase paclitaxel cytotoxicity. Results from preclinical studies as well as clinical data suggest a direct link between survivin expression and tumour cell susceptibility to paclitaxel. Initial reports showed that the forced expression of survivin was able to counteract apoptosis induced by paclitaxel in NIH3T3 fibroblasts [Liu *et al*, 2004]. We previously demonstrated that stable transfection of human ovarian carcinoma cells with survivin cDNA caused a

four- to six-fold increase in resistance to paclitaxel with a concomitant reduction in the apoptotic response of the cells to the drug [Zaffaroni *et al*, 2002]. The increased resistance of ovarian cancer cells ectopically expressing survivin to paclitaxel was also confirmed in the present study. These findings were indirectly supported by similar observations obtained analysing clinical tumour material where high levels of survivin protein expression, as detected by immunohistochemistry in advanced ovarian carcinomas, were significantly associated with clinical resistance to a paclitaxel/platinum-based regimen. Specifically, in these patients survivin overexpression correlated with a lower clinical or pathologic complete remission rate than absent/low protein expression [Zaffaroni *et al*, 2002].

The current results demonstrates that combination treatment of HeLa cells with paclitaxel and cdk inhibitors produced a sequence-dependent synergistic effect. Specifically, exposure of paclitaxel treated cells to NU6140 or purvalanol A strongly decreased clonogenic cell survival and increased caspase-9-mediated apoptotic response. However, such an enhancement was significantly greater for NU6140 than for purvalanol A. A synergistic effect of the paclitaxel-NU6140 combination, which was accompanied by a significantly enhanced caspase-9 and caspase-3 mediated apoptotic response was also observed in OAW42/e ovarian cancer cells. Conversely, a subadditive effect of the paclitaxel-NU6140 combined treatment and a lack of significant caspase activation was found in OAW42/Surv cells, which ectopically expressed survivin and showed a considerably higher level of survivin protein expression compared to OAW42 parental cells. Sequential treatment of HeLa cells with cdk inhibitors greatly reduced (or almost

completely abrogated, in the case of NU6140) the expression of the Thr^{34}-phosphorylated form of survivin, which, conversely, was significantly increased after treatment with paclitaxel alone. These data are consistent with a recently proposed model according to which microtubule stabilization by poisons such as paclitaxel engages a survival pathway that depends on elevated activity of cdk1 kinase activity and increased phosphorylation and expression of survivin [O'Connor *et al*, 2002]. These authors demonstrated that sequence-specific inhibition of cdk1 kinase with purvalanol A after paclitaxel treatment in HeLa cells removed this survival checkpoint and promoted strong antitumour activity *in vitro* an *in vivo*. As shown in the studies described here, NU6140 induces greater potentiation of paclitaxel cytotoxicity than purvalanol A, despite the generally lower potency of NU6140 as an inhibitor of cdks in purified enzyme inhibition assays. Studies with NU6140 in the SKUT1B uterine tumour cell line have shown that following exposure to an extracellular concentration of 10 μM NU6140 for 4 hours, cellular levels can exceed 200 pmole/10^6 cells, i.e. approximately 200 μM [Thomas H & Newell DR, unpublished results]. Hence the greater potentiation of paclitaxel cytotoxicity induced by NU6140 could in part be due to the preferential cellular accumulation of the compound by, as yet, undefined mechanisms. Moreover, although it has not been formally investigated in this study, the possibility that NU6140 inhibits the phosphorylation of the carboxyl-terminal domain of RNA polymerase II and interferes with DNA transcription and RNA processing, as already demonstrated for the cdk inhibitor flavopiridol [Li *et al*, 1998], cannot be excluded.

Results from our study indicate that NU6140 can potentiate the apoptotic effect of paclitaxel in cancer cells, and supports the hypothesis that inhibition of survivin phosphorylation, with the consequent disruption of the cdk1-mediated survival checkpoint, is a major mechanism. This may provide a rational approach to enhance the therapeutic efficacy of paclitaxel in the clinical setting. In fact, based on the evidence derived from preclinical studies, which demonstrate the concept of cell cycle-mediated drug resistance, the combination of cdk inhibitors with standard cytotoxic agents is now emerging as a promising approach to cancer therapy.

Overall, our results obtained from different studies aimed at targeting survivin expression/activity by means of different approaches demonstrated that inhibition of this cytoprotective factor was able to promote spontaneous apoptosis in tumour cells and to enhance the efficacy of several types of conventional treatments including chemotherapy and radiotherapy. Understanding how chemotherapeutic agents induces apoptosis is critical to design better anticancer treatments. To this purpose, results from our studies could have pharmacological implications for the improvement of antitumour therapy and are expected to provide a rational basis for the design of new therapeutic interventions based on the integration of different approaches.

Chapter 6

FUTURE PERSPECTIVES

As previously assessed, the genes that control apoptosis provide interesting new targets for the rational development of strategies aimed at increasing the susceptibility of tumour cells to chemical treatment. Considering the multitude of events involved in the response to drug-induced damage, it is reasonable to presume that approaches based on the simultaneous targeting of different genes would have a greater impact on the final outcome of the drug exposure in tumour cells than the modulation of a single factor. In this context, in order to enhance the susceptibility of cancer cells to apoptosis-inducing chemotherapeutic agents, we propose to develop strategies for the simultaneous inhibition of different anti-apoptotic factors in tumour cells.

Specifically, we propose to assess the effects of the down-regulation of survivin with the contemporary inhibition of the:

- ✓ expression of Apollon/BRUCE, through the use of chemically synthesised siRNAs;
- ✓ activity of XIAP, through the use of synthetic peptides.

Development of siRNAs targeting Apollon/BRUCE

Apollon/BRUCE is a recently identified member of the IAP family with unusual properties [Hauser *et al*, 1998]. It is a very large membrane-associated protein that contains the BIR and the ubiquitin-conjugating enzyme domains at amino- and carboxy-terminals, respectively [Hauser *et al*, 1998; Chen *et al*, 1999]. This protein is overexpressed in some drug-resistant cancer cells [Chen *et al*, 1999; Hao *et al*, 2004]. Unlike other mammalian

IAPs Apollon/BRUCE is essential for viability of various cell lines [Qiu *et al*, 2004] and the knockout of Apollon/BRUCE in mice causes embryonic or neonatal lethality [Hao *et al*, 2004]. It has been shown that Apollon/BRUCE is essential to inhibit apoptosis by promoting ubiquitination and proteasomal degradation of precursor and mature forms of Smac/DIABLO and caspase-9, but not the effector caspase-3 [Hao *et al*, 2004; Qiu & Goldberg, 2005]. Because it is important in inhibiting apoptosis under normal conditions, degradation of Apollon/BRUCE must be a important step in the initiation of the apoptotic process. We propose to use chemically synthesised siRNAs directed against Apollon/BRUCE, alone or in association with siRNA targeting survivin, to improve the chemosensitivity profiles of human tumour cells overexpressing this factor.

Development of Smac peptides able to interact with XIAP

It has been demonstrated that during the process of apoptosis, the inhibitory function of XIAP (a ubiquitous IAP-family member) can be antagonized by Smac/DIABLO, which is also released from mitochondria as cytochrome c [Thomadaki & Scorilas, 2006]. Smac/DIABLO is a dimeric protein and is post-translationally processed in mitochondria [Du *et al*, 2000; Verhagen *et al*, 2000]. The amino terminus of processed Smac/DIABLO, starting with the residues AVPI, has been shown to be necessary and sufficient for removal of inhibition of caspase-9 by XIAP [Chai *et al*, 2000]. Structural studies demonstrated that the four hydrophobic amino acids, Ala-Val-Pro-Ile (AVPI) residues at the amino terminus of mature Smac/DIABLO

interact specifically and tightly with a conserved groove within the XIAP BIR3 domain, and neutralise XIAP inhibition of caspase-9 by competing for the same specific binding site of XIAP with caspase-9 [Chai *et al*, 2000; Wu *et al*, 2000]. We propose to use peptides derived from the amino terminus of Smac/DIABLO to inhibit the anti-apoptotic function of XIAP in human cancer cell lines. To favour cellular uptake, Smac/DIABLO peptides will be conjugated with internalization peptides such as Antennapedia or HIV-Tat. The chemosensitivity effect of these peptides, single administered or in combination with siRNA targeting survivin, will be evaluated in different human tumour cell lines.

Chapter 7

BIBLIOGRAPHY

Adams JM & Cory S. The Bcl-2 apoptotic switch in cancer development and therapy. Oncogene 2007; 26:1324-1337.

Adida C, Crotty PL, McGrath J, Berrebi D, Diebold J & Altieri DC. Developmentally regulated expression of the novel cancer anti-apoptosis gene survivin in human and mouse differentiation. Am J Pathol 1998; 152:43-49.

Adida C, Haioun C, Gaulard P, Lepage E, Morel P, Briere J, Dombret H, Reyes F, Diebold J, Gisselbrecht C, Salles G, Altieri DC & Molina TJ. Prognostic significance of survivin expression in diffuse large B-cell lymphomaas. Blood 2000; 96:1921-1925.

Adida C, Recher C, Raffoux E, Daniel MT, Taksin AL, Rousselot P, Sigaux F, Degos L, Altieri DC & Dombret H. Expression and prognostic significance of survivin in de novo acute leukemia. Br J Haematol 2000; 111:196-203.

Ai Z, Yin L, Zhou X, Zhu Y, Zhu D, Yu Y & Feng Y. Inhibition of survivin reduces cell proliferation and induces apoptosis in human endometrial cancer. Cancer 2006; 107:746-756.

Ali M, Lemoine NR & Ring CJA. The use of DNA viruses as vectors for gene therapy. Gene Ther 1994; 4, 736-743.

Altieri DC. Xa receptor EPR-1. FASEB 1995; 9:860-865.

Altieri DC & Marchisio PC. Survivin apoptosis: an interloper between cell death and cell proliferation in cancer. Lab Invest 1999; 79:1327-1333.

Altieri DC. The molecular basis and potential role of survivin in cancer diagnosis and therapy. Trends Mol Med 2001; 7:542-547.

Altieri DC. Survivin, versatile modulation of cell division and apoptosis in cancer. Oncogene 2003a; 22:8581-8589.

Altieri DC. Validating survivin as a cancer therapeutic target. Nat Rev Cancer 2003b; 3:46-54.

Altieri DC. Blocking survivin to kill cancer cells. Methods Mol Biol 2003c; 223:533-542.

Altieri DC. Survivin and apoptosis control. Adv Cancer Res 2003d; 88:31-52.

Altieri DC. The case for survivin as a regulator of microtubule dynamics and cell-death decisions. Current Opinion in Cell Biology 2006; 18:1-7.

Altznauer F, Martinelli S, Yousefi S, Thurig C, Schmid I, Conway EM, Schoni MH, Vogt P, Mueller C, Fey MF, Zangemeister-Wittke U & Simon HU. Inflammation associated cell cycle-independent block of apoptosis by survivin in terminally differentiated neutrophils. J Exp Med 2004; 199:1343-1354.

Ambrosini G, Adida C & Altieri DC. A novel anti-apoptosis gene, survivin, expressed in cancer and lymphoma. Nat Med 1997; 3:917-921.

Ambrosini G, Adida C, Sirugo A & Altieri DC. Induction of apoptosis and inhibition of cell proliferation by survivin gene targeting. J Biol Chem 1998; 273:11177-11182.

Ansell SM, Arendt BK, Grote DM, Jelinek DF, Novak AJ, Wellik LE, Remstein ED, Bennett CF & Fielding A. Inhibition of survivin expression suppresses the growth of aggressive non-Hodgkin's lymphoma. Leukemia 2004; 18:616-623.

Asanuma K, Moriai R, Yajima T, Yagihashi A, Yamada M & Watanabe N. Survivin as a radioresistance factor in pancreatic cancer. Jpn J Cancer Res 2000; 91:1204-1209.

Asanuma K, Kobayashi D, Furuya D, Tsuji N, Yagihashi A & Watanabe N. A role for survivin in radioresistance of pancreatic cancer cells. Jpn J Cancer Res 2002; 93:1057-1062.

Ashkenazi A. Targeting death and decoy receptors of the tumour-necrosis factor superfamily. Nature Rev Cancer 2002; 2:420-430.

Au JL-S, Panchal N, Li D & Gan Y. Apoptosis: a new pharmacodynamic endpoint Pharmaceut Res 1997; 14:1659-1671.

Auchon D, Jiang X, Morgan DG, Heuser JE, Wang X, Akey CW. Three-dimensional structure of the apoptosome: implications for assembly, procaspase-9 binding, and activation. Mol Cell 2002; 9:423-32.

Azzam T & Domb AJ. Current developments in gene transfection agents. Curr Drug Deliv 2004; 1:165-193.

Badie C, Itzhaki JE, Sullivan MJ, Carpenter AJ & Porter AC. Repression of CDK1 and other genes with CDE and CHR promoter elements during DNA damage-induced G(2)/M arrest in human cells. Mol Cell Biol 2000; 20:2358-2366.

Badran A, Yoshida A, Wano Y, Mutoh M, Imamura S, Yamashita T, Tsutani H, Inuzuka M & Ueda T. Expression of the anti-apoptotic gene survivin in myelodysplastic syndrome. Int J Oncol 2003; 22:59-64.

Badran A, Yoshida A, Ishikawa K, Goi T, Yamaguchi A, Ueda T & Inuzuka M. Identification of a novel splice variant of the human anti-apoptopsis gene survivin. Biochem Biophys Res Commun 2004; 314:902-907.

Baidya N & Uhlenbeck OC. A kinetic and thermodynamic analysis of cleavage site mutations in the hammerhead ribozyme Biochemistry 1997; 36:1108-1114.

Baidya N, Ammons GE, Matulic-Adamic J, Karpeisky AM, Beigelman L & Uhlenbeck OC. Functional groups on the cleavage site pyrimidine nucleotide are required for stabilization of the hammerhead transition state. RNA 1997; 3:1135-1142.

Barquinero J, Eixarch H, Perez-Melgosa M. Retroviral vectors: new applications for an old tool. Gene Ther 2004; 11 Suppl 1:S3-S9.

Basu S & Kolesnick R. Stress signals for apoptosis: ceramide and c-Jun kinase. Oncogene 1998; 17:3277-3285.

Becker JC, Kampgen E & Brocker E. Classical chemotherapy for metastatic melanoma. Clin Exp Dermatol 2000; 25:503-508.

Beltrami E, Plescia J, Wilkinson JC, Duckett CS & Altieri DC. Acute ablation of survivin uncovers p53-dependent mitotic checkpoint functions and control of mitochondrial apoptosis. J Biol Chem 2004; 279:2077-2084.

Berenbaum MC. What is synergy? Pharmacol Rev 1989; 41:93-141.

Bernstein C, Bernstein H, Payne CM & Garewal H. DNA repair/pro-apoptotic dual-role proteins in five major DNA repair pathways: fail-safe protection against carcinogenesis. Mutat Res 2002; 511:145-178.

Bertrand E, Castanotto D, Zhou C, Carbonnelle C, Lee NS, Good P, Chalterjee S, Grange T, Pictet R, Kohn D, Engelke D & Rossi JJ. The expression cassette determines the functional activity of ribozymes in mammalian cells by controlling their intracellular localization. RNA 1997; 3:75-88.

Bilim V, Kasahara T, Hara N, Takahashi K & Tomita Y. Role of XIAP in the malignant phenotype of transitional cell cancer (TCC) and therapeutic

activity of XIAP antisense oligonucleotides against multidrug-resistant TCC in vitro. Int J Cancer 2003; 103:29-37.

Birnbaum MJ, Clem RJ & Miller LK. An apoptosis-inhibiting gene from a nuclear polyhedrosis virus encoding a polypeptide with Cys/His sequence motifs. J Virol 1994; 68:2521-2528.

Blanc-Brude OP, Yu J, Simosa H, Conte MS, Sessa WC & Altieri DC. Inhibitor of apoptosis protein survivin regulates vascular injury.Nature Med 2002; 8:987-994.

Blount KF & Uhlenbeck OC. The structure-function dilemma of the hammerhead ribozyme. Annu Rev Biophys Biomol Struct 2005; 34:415-40.

Boehm I. Apoptosis in physiological and pathological skin: implications for therapy. Curr Mol Med 2006; 6:375-394.

Bondensgaard K, Petersen M, Singh SK, Rajwanshi VK, Kumar R, Wengel J & Jacobsen JP. Structural studie of LNA:RNA duplexe by NMR:Conformation and implications for RNase H activity. Che Eur J 2000; 6:2687-2695.

Bonetti A, Zaninelli M, Leone R, Cetto GL, Pelosi G, Biolo S, Menghi A, Manfrin E, Bonetti F & Piubello Q. bcl-2 but not p53 expression is associated with resistance to chemotherapy in advanced breast cancer. Clin Cancer Res 1998; 4: 2331-2336.

Bottini A, Berruti A, Bersiga A, Brizzi MP, Brunelli A, Gorzegno G, DiMarco B, Aguggini S, Bolsi G, Cirillo F, Filippini L, Betri E, Bertoli G, Alquati P & Dogliotti L. p53 but not bcl-2 immunostaining is predictive of poor clinical complete response to primary chemotherapy in breast cancer patients. Clin Cancer Res 2000; 6:2751-2758.

Boulaiz H, Marchal JA, Prados J, Melguizo C & Aranega A. Non-viral and viral vectors for gene therapy. Cell Mol Biol 2005; 51:3-22.

Braasch DA & Corey DR. Locked nucleic acid (LNA): fine-tuning the recognition of DNA and RNA. Chem Biol 2001; 8:1-7.

Bradford MM. A rapid and sensitive method for the quantitation of microgram quantities of protein utilizing the principle of protein-dye binding. Anal Biochem 1976; 72:248-254.

Bratton DL, Fadok VA, Richter DA, Kailey JM, Guthrie LA & Henson PM. Appearance of phosphatidylserine on apoptotic cells requires calcium-mediated nonspecific flip-flop and is enhanced by loss of the aminophospholipid translocase. J Biol Chem 1997; 272:26159-26165.

Brown DA, Kang S-H, Gryaznov SM, DeDionisio L, Heidenreich O, Sullivan S, Xu X & Neerenberg MI. Effect of phosphorothioate modification of oligodeoxynucleotides on specific protein binding. J Biol Chem 1994; 43:26801-26805.

Brummelkamp TR, Bernards R, Agami R. A system for stable expression of short interfering RNAs in mammalian cells. Science 2002; 296:550-553.

Burke JM. Hairpin and hammerhead ribozymes: how different are they? Biochem Soc Trans 2002; 30:1115-1118.

Cabrespine A, Guy L, Chollet P, Debition E & Bay JO. Molecular mechanisms involved in hormone resistance of prostate cancer. Bull Cancer 2004; 91:747-757.

Cagnon L & Rossi JJ. Retroviral delivery and anti-HIV testing of hammerhead ribozymes. Methods Mol Biol 1997; 74:451-457.

Caldas H, Honsey LE & Altura RA. Survivin 2alpha: a novel Survivin splice variant expressed in human malignancies. Mol Cancer 2005; 4:11.

Caldas H, Jiang Y, Holloway MP, Fangusaro J, Mahotka C, Conway EM & Altura RA. Survivin splice variants regulate the balance between proliferation and cell death. Oncogene 2005; 24:1994-2007.

Campos L, Rouault JP, Sabido O, Oriol P, Roubi N, Vasselon C, Archimbaud E, Magaud JP & Guyotat D. High expression of bcl-2 protein in acute myeloid leukemia cells is associated with poor response to chemotherapy. Blood 1993; 81:3091-3096.

Cao C, Mu Y, Hallahan DE & Lu B. XIAP and survivin as therapeutic targets for radiation sensitization in preclinical models of lung cancer. Oncogene 2004; 23:7047-7052.

Carvalho A, Carmena M, Sambade C, Earnshaw WC & Wheatley SP. Survivin is required for stable checkpoint activation in taxol-treated HeLa cells. J Cell Sci 2003; 116:2987-2998.

Casey W, Colin W & Duckett S. Reawakening the cellular death program in neoplasia through the therapeutic blockade of IAP function. J Clin Invest 2005; 115:2673-2678.

Catz SD & Johnson JL. BCL-2 in prostate cancer: a minireview. Apoptosis 2003; 8:29-37.

Cecconi F & Gouss P. Apaf1 in developmental apoptosis and cancer: how many ways to die? Cell Mol Life Sci 2001; 58:1688-1697.

Cech TR. Structural biology.The ribosome is a ribozyme. Science 2000; 289:878-879.

Chai J, Du C, Wu JW, Kyin S, Wang X & Shi Y. Structural and biochemical basis of apoptotic activation by Smac/DIABLO. Nature 2000; 406:855-862.

Chakravarti A, Noll E, Black PM, Finkelstein DF, Finkelstein DM, Dyson NJ & Loeffler JS. Quantitatively determined survivin expression levels are of prognostic value in human gliomas. J Clin Oncol 2002; 20:1063-1068.

Chang CC, Heller JD, Kuo J & Huang RC. Tetra-O-methyl nordihydroguaiaretic acid induces growth arrest and cellular apoptosis by inhibiting Cdc2 and survivin expression. Proc Natl Acad Sci USA 2004; 101:13239-13244.

Chantalat L, Skoufias DA, Kleman JP, Jung B, Dideberg O & Margolis RL. Crystal structure of human survivin reveals a bow tie-shaped dimer with two unusual alpha-helical extensions. Mol Cell 2000; 6:183-189.

Chao SH, Fujinaga K, Marion JE, Taube R, Sausville EA, Senderowicz AM, Peterlin BM & Price DH. Flavopiridol inhibits P-TEFb and blocks HIV-1 replication. J Biol Chem 2000; 275:28345-48.

Chaudary KS, Abel PD, Stamp GW & Lalani E. Differential expression of cell death regulators in response to thapsigargin and adriamycin in Bcl-2 transfected DU145 prostatic cancer cells. J Pathol 2001; 193: 522-529.

Chen J, Wu W, Tahir SK, Kroeger PE, Rosenberg SH, Cowsert LM, Bennett F, Krajewski S, Krajewska M, Welsh K, Reed JC & Ng SC. Down-regulation of survivin by antisense oligonucleotides increases apoptosis, inhibits cytokinesis and anchorage-dependent growth. Neoplasia 2000; 2:235-241.

Chen Y, Li X & Gegenheimer P. Ribonuclease P catalysis requires Mg^{2+} coordinated to the pro-RP oxygen of the scissile bond. Biochemistry 1997; 36:2425-2438.

Chen JS, Liu JC, Shen L, Rau KM, Kuo HP, Li YM, Shi D, Lee YC, Chang KJ & Hung MC. Cancer-specific acrivation of the survivin promoter and its potential use in gene therapy. Cancer Gene Ther 2004; 11:740-747.

Chen Z, Naito M, Hori S, Mashima T, Yamori T & Tsuruo T. A human IAP-family gene, apollon, expressed in human brain cancer cells. Biochem Biophys Res Commun 1999; 264:847-854.

Chiodino C, Cesinaro AM, Ottani D, Fantini F, Riannetti A, Trentini GP & Pincelli C. Communication: expression of the novel inhibitor of apoptosis survivin in normal and neoplastic skin. J Invest Dermatol 1999; 113:415-418.

Chiou SK, Moon WS, Jones MK & Tarnawski AS. Survivin expression in the stomach: implications for mucosal integrity and protection. Biochem Biophys Res Commun 2003; 305:374-379.

Choi KS, Lee TH & Jung MH. Ribozyme-mediated cleavage of the human survivin mRNA and inhibition of antiapoptotica function of survivin in MCF-7 cells. Cancer Gene Ther 2003; 10:87-95.

Chou TC & Talalay P. Quantitative analysis of dose-effect relationships: the combined effects of multiple drugs or enzyme inhibitors. Adv Enzyme Regul 1984; 22:27-55.

Clem RJ & Miller LK. Control of programmed cell death by the baculovirus genes p35 and IAP. Mol Cell Biol 1994; 14:5212-5222.

Clem RJ, Cheng EH, Karp CL, Kirsch DG, Ueno K, Takahashi A, Kastan MB, Griffin DE, Earnshaw WC, Veliuona MA & Hardwick JM. Modulation of cell death by Bcl-XL through caspase interaction. Proc Natl Acad Sci USA 1998; 95:554-559.

Cohen JJ. Apoptosis. Immunol Today 1993; 14 ,126-130.

Colleoni M, Orvieto E, Nole F, Orlando L, Minchella I, Viale G, Peruzzotti G, Robertson C, Noberasco C, Galimberti V, Sacchini V, Veronesi P, Zurrida S, Orecchia R &Goldhirsch A. Prediction of response to primary chemotherapy for operable breast cancer. Eur J Cancer 1999; 35:574-579.

Collins CA & Guthrie C. The question remains: Is the spliceosome a ribozyme? Nat Struct Biol 2000; 10:850-854.

Colnaghi R, Connell CM, Barrett RMA & Wheatley SP. Separating the anti-apoptotic and mitotic roles of survivin. J Biol Chem 2006; 281:33450-33456.

Coma S, Noe V, Lavarino C, Adan J, Rivas M, Lopez-Matas M, Pagan R, Mitjans F, Vilaro S, Piulats J & Ciudad CJ. Use of siRNAs and antisense oligonucleotides against survivin RNA to inhibit steps leading to tumor angiogenesis. Oligonucleotides 2004; 14:100-113.

Conway EM, Pollefeyt S, Steiner-Mosonyi M, Luo W, Devriese A, Lupu F, Bono F, Leducq N, Dol F, Schaeffer P, Collen D & Herbert JM. Deficiency of survivin in transgenic mice exacerbates Fas-induced apoptosis via mitochondrial pathways. Gastroenterology 2002; 123:619-631.

Cory S & Adams JM. The Bcl2 family: Regulators of the cellular life-or-death switch. Nat Rev Cancer 2002; 2:647-656.

Crook ST & Bennett CF. Progress in antisense oligonucleotide therapeutics. Annu Rev Pharmacol Toxicol 1996; 36:107-129.

Crooke ST. Molecular mechanisms of action of antisense drugs. Biochim Biophys Acta 1999; 1489: 31-44.

Cryns V & Yuan Y. Proteases to die for. Genes Develop 1999; 12:1551-1570.

Cummings J, Ward TH, Ranson M & Dive C. Apoptosis pathway-targeted drugs - from the bench to the clinic. Biochim Biophys Acta 2004; 1705:53-66.

Dahm SC & Uhlenbeck OC. Role of divalent metal ions in the hammerhead RNA cleavage reaction. Biochemistry 1991; 30:9464-9469.

Dai Y & Steven Grant. Cyclin-dependent kinase inhibitors. Current Opinion in Pharmacology 2003; 3:362-370

Dallaporta B, Marchetti P, de Pablo MA, Maisse C, Duc HT, Metivier D, Zamzami N, Geuskens M & Kroemer G. Plasma membrane potential in thymocyte apoptosis. Immunol 1999; 162:6534-6542.

Danial NN & Korsmeyer SJ. Cell death: critical control points. Cell 2004; 116:205-219.

Dart DA, Adams KE, Akerman I & Lakin ND. Recruitment of the cell cycle checkpoint kinase ATR to chromatin during S-phase. J Biol Chem 2004; 279:16433-16440.

Darzynkiewicz Z, Juan G, Li X, Gorczyca W, Murakami T & Traganos F. Cytometry in cell necrobiology: Analysis of apoptosis and accidental cell death (necrosis). Cytometry 1997; 27: 1-20.

Daskivich TJ & Oh WK. Recent progress in hormonal therapy for advanced prostate cancer. Curr Opin Urol 2006; 16:173-178.

Davies TG, Bentley J, Arris CE, Boyle FT, Curtin NJ, Endicott JA, Gibson AE, Golding BT, Griffin RJ, Hardcastle IR, Jewsbury P, Johnson LN, Mesguiche V, Newell DR, Noble ME, Tucker JA, Wang L & Whitfield HJ. Structure-based design of a potent purine-based cyclin-dependent kinase inhibitor. Nat Struct Biol 2002; 9:745-49.

Davies TG, Pratt DJ, Endicott JA, Johnson LN & Noble MEM. Structure-based design of cyclin-dependent kinase inhibitors. Pharmacology & Therapeutics 2002; 93:125-133.

Dean NM & Bennett CF. Antisense oligonucleotide-based therapeutics for cancer. Oncogene 2003; 22:9087-9096.

Deguchi M, Shiraki K, Inoue H, Okano H, Ito T, Yamanaka T, Sugimoto K, Sakai T, Ohmori S, Murata K, Furusaka A, Hisatomi H & Nakano T. Expression of survivin during liver regeneration. Biochem Biophys Res Commun 2002; 297:59-64.

Deng GM, Nilsson IM, Verdrengh M, Collins LV & Tarkowski A. Intra-articularly localized bacterial DNA containing CpG motifs induces arthritis. Nat Med 1999; 5:702-705.

Denmeade SR, Lin XS & Isaacs JT. Role of programmed (apoptotic) cell death during the progression and therapy for prostate cancer. Prostate 1996; 28:251-65.

Dennis LK & Resnick MI. Analysis of recent trends in prostate cancer incidence and mortality. Prostate 2000; 42:247-52.

Deveraux QL, Takahashi R, Salvesen GS & Reed JC. X-linked IAP is a direct inhibitor of cell death prote-ases. Nature 1997; 388:300-304.

Deveraux Q & Reed J. IAP family proteins:suppressors of apoptosis. Genes Dev 1999; 13:239-252.

Dohi T, Beltrami E, Wall NR, Plescia J & Altieri DC. Mitochondrial survivin inhibits apoptosis and promotes tumorigenesis, J Clin Invest 2004; 114:1117-1127.

Dohi T, Okada K, Xia F, Wilford CE, Samuel T, Welsh K, Marusawa H, Zou H, Armstrong R, Matsuzawa S, Salvesen GS, Reed JC & Altieri DC. An IAP-IAP complex inhibits apoptosis. J Biol Chem 2004; 279:34087-34090.

Du C, Fang M, Li Y, Li L & Wang X. Smac, a mitochondrial protein that promotes cytochrome c-dependent caspase activation by eliminating IAP inhibition. Cell 2000; 102:33-42.

Du ZX, Zhang HY, Gaoda X, Wang HQ, Li YJ & Liu GL. Antisurvivin oligonucleotides inhibit growth and induce apoptosis in human medullary thyroid carcinoma cells. Exp Mol Med 2006; 38:230-240.

Duckett CS, Nava VE, Gedrich RW, Clem RJ, Van Dongen JL, Gilfillan MC, Sheils H, Hardwick JM & Thompson CB. A conserved family of cellular genes related to the baculovirus iap gene and encoding apoptosis inhibitors. EMBO J 1996;15:2685-2694.

Durocher D & Jackson SP. DNA-PK, ATMand ATR as sensors of DNA damage: Variations on a theme? Curr Opin Cell Biol 2001; 13:225-231.

Dykxhoorn DM, Novina CD & Sharp PA. Killing the messenger: short RNAs that silence gene expression. Nat Rev Mol Cell Biol 2003; 4:457-467.

Earnshaw DJ & Gait MJ. Hairpin Ribozyme cleavage catalyzed by aminoglycoside antibiotics and the polyamine spermine in the absence of metal ions.Nucleic Acid Res 1998; 26:5551-5561.

Earnshaw WC. Apoptosis. A cellular poison cupboard. Nature 1999; 397:387-389.

Edinger AL & Thompson CB. Death by design: apoptosis, necrosis and autophagy. Curr Opin Cell Biol 2004; 16: 663-669.

Egholm M, Buchardt O, Christensen L, Behrens C, Freier SM, Driver DA, Berg RH, Kim SK, Norden B & Nielsen PE. PNA hybridizes to complementary oligonucleotides obeying the Watson-Crick hydrogen-bonding rules. Nature 1993; 365: 566-568.

Elbashir S, Lendeckel W & Tuschl T. RNA interference is mediated by 21- and 22-nucleotide RNAs. Genes Dev 2001; 15:188-200.

Elbashir SM, Harborth J, Lendeckel W, Yalcin A, Weber K & Tuschl T. Duplexes of 21-nucleotide RNAs mediate RNA interference in cultured mammalian cells. Nature 2001; 411:494-98.

Elbashir SM, Harborth J, Lendeckel W, Yalcin A, Weber K & Tuschl T. Duplexe of 21-nucleotide RNAs mediate RNA interference in cultured mammalian cells. Nature 2001; 411:494-498.

Elbashir SM, Harborth J, Weber K & Tuschl T. Analysis of gene function in somatic mammalian cells using small interfering RNAs. Methods 2002; 26:199-213.

Emami KH, Nguyen C, Ma H, Kim DH, Jeong KW, Eguchi M, Moon RT, Teo JL, Kim HY, Moon SH, Ha JR & Kahn M. A small molecule inhibitor of β-catenin/cyclic AMP response element-binding protein transcription. Proc Natl Acad Sci USA 2004; 101:12682-12687.

Fadok VA, Bratton DL, Frasch SC Warner ML & Henson PM. Cell Death Differ 1998; 5:551-562.

Fan QL, Zou WY, Song LH, Wei W. Synergistic antitumor activity of TRAIL combined with chemotherapeutic agents in A549 cell lines in vitro and in vivo. Cancer Chemother Pharmacol 2004; 55: 189-196.

Fengzhi L, Yang J, Ramnath N, Javle MM & Tan D. Nuclear or cytoplasmic expression of survivin: what is the significance? Int J Cancer 2005; 114:509-512.

Ferri KF & Kroemer G. Organelle-specific initiation of cell death pathways. Nature Cell Biol 2001; 3:E255-263.

Fesik SW. Promoting apoptosis as a strategy for cancer drug discovery Nat Rev Cancer 2005; 5:876-885.

Flinterman M, Guelen L, Ezzati-Nik S, Killick R, Melino G, Tominaga K, Mymryk JS, Gäken J, Tavassoli M. E1A activates transcription of p73 and Noxa to induce apoptosis. J Biol Chem 2005; 280:5945-5959.

Flores ER, Tsai KY, Crowley D, Sengupta S, Yang A, McKeon F & Jacks T. p63 and p73 are required for p53-dependent apoptosis in response to DNA damage. Nature 2002; 416:560-564.

Fontanini G, Vignati S, Bigini D, Mussi A, Lucchi M, Angeletti CA, et al. Bcl-2 protein: a prognostic factor inversely correlated to p53 in non-small-cell lung cancer. Br J Cancer 1995; 71: 1003-1007.

Fortugno P, Wall NR, Giodini A, O'Connor DS, Plescia J, Padgett KM, Tognin S, Marchisio PC & Altieri DC. Survivin exists in immunochemically distinct subcellular pools and is involved in spindle microtubule function. J Cell Sci2002; 115:575-585.

Fortugno P, Beltrami E, Plescia J, Fontana J, Pradhan D, Marchisio PC, Sessa WC, Altieri DC. Regulation of survivin function by Hsp90. Proc Natl Acad Sci 2003; 100:13791-13796.

Foster AC & Sympson RH. Self cleavage of virusoid RNA is performed by the proposed 55-nucleotide active site. Cell 1987; 50:9-16.

Franz S, Gaipl US, Munoz LE, Sheriff A, Beer A, Kalden JR & Herrmann M. Apoptosis and autoimmunity: when apoptotic cells break their silence. Curr Rheumatol Rep 2006; 8:245-247.

Fuessel S, Kueppers B, Ning S, Kotzsch M, Kraemer K, Schmidt U, Meye A & Wirth MP. Systematic in vitro evaluation of survivin directed antisense oligodeoxynucleotides in bladder cancer cells. J Urol 2004; 171:2471-2476.

Fujita N, NagahashiA, Nagashima K, Rokudai S & TsuruoT. Acceleration of apoptotic cell death after the cleavage of Bcl-XL protein by caspase-3-like proteases Oncogene 1998; 17:1295-1304.

Fukuda S, Foster RG, Porter SB & Pelus LM. The antiapoptosis protein survivin is associated with cell cycle entry of normal cord blood CD34(+) cells and modulates cell cycle and proliferation of mouse hematopoietic progenitor cells. Blood 2002; 100:2463-2471.

Fukuda S & Pelus LM. Regulation of the inhibitor-of-apoptosis family member survivin in normal cord blood and bone marrow CD34(+) cells by hematopoietic growth factors: implication of survivin expression in normal hematopoiesis. Blood 2001; 98:2091-2100.

Fukuda S & Pelus LM. Activated H-Ras regulates hematopoietic cell survival by modulating Survivin. Biochem Biophys Res Commun 2004; 323:636-644.

Fukuda S & Pelus LM. Survivin, a cancer target with an emerging role in normal adult tissues. Mol Cancer Ther 2006; 5:1087-1098.

Fumarola C & Guidotti GG. Stress-induced apoptosis: toward a symmetry with receptor-mediated cell death. Apoptosis 2004; 9:77-82.

Galligan L, Longley DB, McEwan M, Wilson TR, McLaughlin K & Johnston PG. Chemotherapy and TRAIL-mediated colon cancer cell death: the roles of p53, TRAIL receptors, and c-FLIP. Mol Cancer Ther 2005; 4:2026-2036.

Galluzzi L, Larochette N, Zamzami N, Kroemer G. Mitochondria as therapeutic targets for cancer chemotherapy. Oncogene. 2006; 25:4812-4830.

Gambari R. Peptide-nucleic acids (PNAs): a tool for the development of gene expression modifiers. Curr Pharm Des 2001; 7:1839-1862.

Garcia JF, Camacho FI, Morente M, Fraga M, Montalban C, Alvaro T, Bellas C, Castano A, Diez A, Flores T, Martin C, Martinez MA, Mazorra F, Menarguez J, Mestre MJ, Mollejo M, Saez AI, Sanchez L & Piris MA. Hodgkin and Reed-Sternberg cells harbor alterations in the major tumor suppressor pathways and cell-cycle checkpoints: analyses using tissue microarrays. Blood 2003; 101:681-689.

Garcia-Barros M, Paris F, Cordon-cardo C, Lyden D, Rafii S, Haimovitz A, Fuks Z & Kolesnick R. Tumor response to radiotherapy regulated by endothelial cell apoptosis. Science2003; 300:1155-1159.

Garcia-Bermejo L, Perez C, Vilaboa NE, de Blas E & Aller P. cAMP increasing agents attenuate the generation of apoptosis by etoposide in promonocytic leukemia cells. J Cell Sci1998; 111:637-644.

Ghosh SS, Gopinath P & Ramesh A. Adenoviral vectors: a promising tool for gene therapy. Appl Biochem Biotechnol 2006; 133:9-29.

Gianani R, Jarboe E, Orlicky D, Frost M, Bobak J, Lehner R, Shroyer KR. Expression of survivin in normal, hyperplastic, and neoplastic colonic mucosa.Human Path 2001; 32:119-125.

Giodini A, Kallio MJ, Wall NR, Gorbsky GJ, Tognin S, Marchisio PC, Symons M & Altieri DC. Regulation of microtubule stability and mitotic progression by survivin. Cancer Res 2002; 62:2462-2467.

Gleave ME & Monia BP. Antisense therapy for cancer. Nature Rev Cancer 2005; 5:468-479.

Goldstein JC, Waterhouse NJ, Juen P, Evan GI, Green DR. The coordinate release of cytochrome c during apoptosis is rapid, complete and kinetically invariant. Nat Cell Biol 2000; 2:156-62.

Goping IS, Gross A, Lavoie JN, Nguyen M, Jemmerson R, Roth K, Korsmeyer SJ & Shore GC. Regulated targeting of BAX to mitochondria. J Cell Biol 1998; 143:207-215.

Grabowski P, Kuhnel T, Muhr-Wilkenshoff F, et al. Prognostic value of nuclear survivin expression in oesophageal squamous cell carcinoma. Br J Cancer 2003;88:115-119.

Gratas C, Tohma Y, Barnas C, Taniere P, Hainaut P, Ohgaki H. Up-regulation of Fas (APO-1/CD95) ligand and down-regulation of Fas expression in human esophageal cancer. Cancer Res 1998; 58:2057-2062.

Green DR. Apoptic pathways: paper wraps stone blunts scis-sors. Cell 2000; 102:1-4.

Gritsko T, Williams A, Turkson J, Kaneko S, Bowman T, Huang M, Nam S, Eweis I, Diaz N, Sullivan D, Yoder S, Enkemann S, Eschrich S, Lee JH, Beam CA, Cheng J, Minton S, Muro-Cacho CA & Jove R. Persistent activation of stat3 signaling induces survivin gene expression and confers resistance to apoptosis in human breast cancer cells. Clin Cancer Res 2006; 12:11-19.

Gross A, Jockel J, Wei MC & Korsmeyer SJ. Enforced dimerization of BAX results in its translocation, mitochondrial dysfunction and apoptosis. EMBO J 1998; 17:3878-3885.

Gross A, Yin X-M, Wang K, Wei MC, Jockel J, Milliman C, Erdjument-Bromage H, Tempst P & Korsmeyer SJ. Caspase cleaved BID targets mitochondria and is required for cytochrome c release, while BCL-XL prevents this release but not tumor necrosis factor-R1/Fas death. J Biol Chem 1999; 274:1156-1163.

Grossman D, MaNiff JM, Li F & Altieri DC. Expression of the apoptosis inhibitor,survivin,in nonmelanoma skin cancer and gene targeting in a keratinocyte cell line. Lab Invest 1998; 79:1121-1126.

Grossman D, McNiff JM, Li F & Altieri DC. Expression and targeting of the apoptosis inhibitor, survivin in human melanoma. J Invest Dermatol 1999; 113:1076-1081.

Grossman D & Altieri DC. Drug resistance in melanoma: mechanisms, apoptosis, and new potential therapeutic targets. Cancer Metastasis Rev 2001; 20:3-11.

Grossman D, Kim PJ, Schechner JS & Altieri DC. Inhibition of melanoma tumor growth in vivo by survivin targeting. Proc Natl Acad Sci USA 2001a; 98:635-640.

Grossman D, Kim PJ, Blanc-Brude OP, Brash DE, Tognin S, Marchisio PC & Altieri DC. J Clin Invest 2001b; 108:991-999.

Guo F, Nimmanapalli R, Paranawithana S Wittman S, Griffin D, Bali P, O'Bryan E, Fumero C, Wang HG & Bhalla K. Ectopic overexpression of second mitochondria-derived activator of caspases (smac/DIABLO)or cotreatment with N-terminus of Smac/DIABLO peptide potentiates epothilone B derivative-(BSM 247550) and Apo-2L/TRAIL-induced apoptosis. Blood 2002; 99:3419-3426.

Gupta S. Molecular mechanisms of apoptosis in the cells of the immune system in human aging. Immunol Rev 2005; 205:114-129.

Gurbuxani S, Xu Y, Keerthivasan G, Wickrema A & Crispino JD. Differential requirements for survivin in hematopoietic cell development. Proc Natl Acad Sci USA 2005; 102:11480-11485.

Gyurkocza B, Plescia J, Raskett CM, Garlick DS, Lowry PA, Carter BZ, Andreedd M, Meli M, Colombo G & Altieri DC. Antileukemic activity of shepherdin and molecular diversity of Hsp90 inhibitors. J Natl Cancer Inst 2006; 98:1068-1077.

Hale AJ, Smith CA, Sutherland LC, Stoneman VE, Longthorne VL, Culhane AC & Williams GT. Apoptosis: molecular regulation of cell death. Eur J Biochem 1996; 236:1-26.

Hammann C & Lilley DM. Folding and activity of the hammerhead ribozyme. Chembiochem 2002; 3:690-700.

Hampton MB, Vanags DM, Porn-Ares MI & Orrenius S. Involvement of extracellular calcium in phosphatidylserine exposure during apoptosis. FEBS Lett 1996; 399:277-282.

Hao Y, Sekine K, Kawabata A, Nakamura H, Ishioka T, Ohata H, Katayama R, Hashimoto C, Zhang X, Noda T, Tsuruo T & Naito M. Apollon ubiquitinates SMAC and caspase-9, and has an essential cytoprotection function. Nat Cell Biol 2004; 6:849-860.

Harvey AJ, Soliman H, Kaiser W & Miller LK. Anti- and pro-apoptotic activities of baculovirus and Drosophila IAPs in an insect cell line. Cell Death Differ 1997; 4: 733-744.

Hattori M, Sakamoto H, Satoh K & Yamamoto T. DNA demethylase is expressed in ovarian cancers and the expression correlates with demethylation of CpG sites in the promoter region of c-erbB-2 and survivin genes. Cancer Lett 2001; 169:155-164.

Hauser HP, Bardroff M, Pyrowolakis G & Jentsch S: A giant ubiquitin-conjugating enzyme related to iap apoptosis inhibitors. J Cell Biol 1998, 141:1415-1422.

Hay BA. Understanding IAP function and regulation: a view from Drosophila. Cell Death Differ 2000; 7:1045-1056.

Hayashi K, Asano K, Suzuki H, Yamamoto T, Tanigawa N, Egawa S & Manome Y. Adenoviral infection of survivin antisense sensitizes prostate cancer to etoposide in vivo. Prostate 2005; 65:10-19.

Hayward RL, Macpherson JS, Cummings J, Monia BP, Smyth JF & Jodrell DI. Enhanced oxaliplatin-induced apoptosis following antisense Bcl-xl down-regulation is p53 and Bax dependent: genetic evidence for specificity of the antisense effect. Mol Cancer Ther 2004; 3:169-178.

Heere-Ress E, Thallinger C, Lucas T, Schlagbauer-Wadl H, Wacheck V, Monia BP, Wolff K, Pehamberger H & Jansen B. Bcl-X(L) is a chemoresistance factor in human melanoma cells that can be inhibited by antisense therapy. Int J Cancer 2002; 99:29-34.

Heidenreich O, Benseler F, Fahrenholz A & Eckstein F. High activity and stability of hammerhead ribozymes containing 29-modified pyrimidine nucleotides and phosphorothioates. J Biol Chem 1994; 269:2131–2138.

Hengartner MO. The biochemistry of apoptosis. Nature 2000; 407:770-776.

Hermine O, Haioun C, Lepage E, d'Agay MF, Briere J, Lavi-gnac C, et al. Prognostic significance of bcl-2 protein expression in aggressive non-Hodgkin's lymphoma. Groupe d'Etude des Lymphomes de l'Adulte (GELA). Blood 1996; 87:265–272.

Hertel KJ, Herschlag D & Uhlenbeck OC. A kinetic and thermodynamic framework for the hammerhead ribozyme reaction. Biochemistry 1994; 33:3374-3385.

Hockenbery D, Nunez G, Milliman C, Schreiber RD & SKorsmeyer J. Bcl-2 is an inner mitochondrial membrane pro-tein that blocks programmed cell death. Nature 1990; 348:334-336

Hoffman WH, Biade S, Zilfou JT, Chen J & Murphy M. Transcriptional repression of the anti-apoptotic survivin gene by wild type p53. J Biol Chem 2002; 277:3247-3257.

Hostein I, Robertson D, Distefano F, Workman P & Clarke PA. Inhibition of signal transduction by the hsp90 inhibitor 17-allylamino-17-demethoxygeldanamycin results in cytostasis and apoptosis. Cancer Res 2001; 61:4003-4009.

Howell SB. Resistance to apoptosis in prostate cancer cells. Mol Urol 2002; 4:225-29.

Hu S, Vincenz C, Ni J, Gentz R & Dixit VM. I-FLICE, a novel inhibitor of tumor necrosis factor receptor-1- and CD-95-induced apoptosis. J Biol Chem 1997; 272:255-257.

Huang DC & Strasser A. BH3-only proteins: Essential initiators of apoptotic cell death. Cell 2000; 103:839-842.

Huang RC, Chang CC & Mold D. Survivin-dependent and –independent pathways and the induction of cancer cell death by tetra-O-methyl nordihydroguaiaretic acid. Semin Oncol 2006; 33:479-485.

Hughes MD, Hussain M, Nawaz Q, Sayyed P & Akhtar S. The cellular delivery of antisense oligonucleotides and ribozymes. Drug Discovery Today 2001; 6:303-315.

Ikeguchi M, Ueda T, Sakatani T, Hirooka Y & Kaibara N. Expression of survivin messenger RNA correlates with poor prognosis in patients with hepatocellular car-cinoma. Diagn Mol Pathol 2002;11:33-40.

Ikeguchi M, Ueta T, Yamane Y, Hirooka Y & Kaibara N. Inducible nitric oxide synthase and survivin messenger RNA expression in hepatocellular carcinoma. Clin Cancer Res 2002; 8:3131-3136.

Ionov Y, Yamamoto H, Krajewski S, Reed JC & Perucho M. Mutational inactivation of the proapoptotic gene BAX confers selective advantage during tumor clonal evolution. Proc Natl Acad Sci USA 2000; 97:10872–10877.

Isaacs JS, Xu W & Neckers L. Heat shock protein 90 as a molecular target for cancer therapeutics. Cancer Cell 2003; 3:213-17.

Islam A, Kageyama H, Hashizume K, Kaneko Y & Nakagawara A. Role of survivin, whose gene is mapped to 17q25, in human Neuroblastoma and identification of a novel dominant-negative isoform, survivin-beta/2B. Med Pediatr Oncol 2000; 35: 550-553.

Ismail IH, Nyström S, Nygren J & Hammarsten O. Activation of ataxia telangiectasia mutated by DNA strand break-inducing agents correlates closely with the number of DNA double strand breaks. J Biol Chem 2005; 280:4649-4655.

Ito T, Deng X, Carr B & May WS. Bcl-2 phosphorylation required for anti-apoptosis function. J Biol Chem 1997; 272:11671-11673.

Izquierdo M. Short interfering RNAs as a tool for cancer gene therapy. Cancer Gene Therapy 2005; 12:217-27.

Jacobson MD, Burne JF, King MP, Miyashita T, Reed JC & Raff MC. Bcl-2 blocks apoptosis in cells lacking mitochondrial DNA. Nature 1993; 361:365-369.

Jansen B, Schlagbauer-Wadl H, Brown BD, Bryan RN, van Elsas A, Muller M, Wolff K, Eichler HG & Pehamberger H. Bcl-1 antisense therapy chemosensitizes human melanoma in SCID mice. Nat Med 1998; 4:232-34.

Jansen B, Wacheck V, Heere-Ress E, Schlagbauer-Wadl H, Hoeller C, Lucas T, Hoermann M, Hollenstein U, Wolff K & Pehamberger H.

Chemosensitisation of malignant melanoma by BCL2 antisense therapy. Lancet 2000; 356:1728-33.

Jiang G, Li J, Zeng Z & Xian L. Lentivirus-mediated gene therapy by suppressing survivin in BALB/c nude mice bearing oral squamous cell carcinoma. Cancer Biol Ther 2006; 5:435-440.

Jiang Y, Saavedra HI, Holloway MP, Leone G & Altura RA. Aberrant regulation of survivin by the RB/E2F family of proteins. J Biol Chem 2004; 279:40511-40520.

Jung C, Motwani M, Kortmansky J, Sirotnak FM, She Y, Gonen M, Haimovitz-Friedman A & Schwartz GK. The cyclin-dependent kinase inhibitor flavopiridol potentiates gamma-irradiation-induced apoptosis in colon and gastric cancer cells. Clin Cancer Res 2003; 9:6052-6061.

Kajiwara Y, Yamasaki F, Hama S, Yahara K, Yoshioka H, Sugiyama K, Arita K & Kurisu K. Expression of survivin in astrocytic tumors: correlation with malignant grade and prognosis. Cancer (Phila) 2003; 97:1077-1083.

Kallio MJ, Nieminen M & Eriksson JE. Human inhibitor of apoptosis protein (IAP) survivin participates in regulation of chromosome segregation and mitotic exit. FASEB 2001; 15:2721-2723.

Kamal A, Thao L, Sensintaffar J, Zhang L, Boehm MF, Fritz LC & Burrows FJ. A high-affinity conformation of Hsp90 confers tumour selection on Hsp90 inhibitors. Nature 2003; 425:407-410.

Kamb A. Cell-cycle regulators and cancer. Trends Genet 1995; 11:136-140.

Kami K, Doi R, Koizumi M, Toyoda E, Mori T, Ito D, Kawaguchi Y, Fujimoto K, Wada M, Miyatake S, Imamura M. Downregulation of survivin by siRNA diminishes radioresistance of pancreatic cancer cells. Surgery 2005; 138:299-305.

Kamihira S, Yamada Y, Hirakata Y, Tomonaga M, Sugahara K, Hayashi T, Dateki N, Harasawa H & Nakayama K. Aberrant expression of caspase cascade regulatory genes in adult T-cell leukaemia: survivin is an important determinant for prognosis. Br J Haematol 2001; 114:63-69.

Kanwar JR,Shen WP,Kanwar RK,Berg RW & Krissansen GW. Effects of survivin antagonists on growth of established tumors and B7-1 immunogene therapy. J Nat Cancer Inst 2001; 93:1541-1552.

Kappler M, Taubert H, Bartel F, Blumke K, Panian M, Schmidt H, Dunst J & Bache M. Radiosensitization after a combined treatment of survivin siRNA and irradiation, is correlated with the activation of caspases 3 and 7 in a wt-p53 sarcoma cell line, but not in a mt-p53 sarcoma cell line. Oncol Rep 2005; 13:167-172.

Karkare S & Bhatnagar D. Promising nucleic acid analogs and mimics: characteristic features and applications of PNA, LNA, and morpholino. Appl Microbiol Biotechnol 2006; 71:575-586.

Kasof GM & Gomes BC. Livin, a novel inhibitor of apoptosis protein family member. J Biol Chem 2001; 276:3238-3246.

Kato J, Kuwabara Y, Mitani M, Shinoda N, Sato A, Toyama T, Mitsui A, Nishiwaki T, Moriyama S, Kudo J & Fujii Y. Expression of survivin in esophageal cancer: correlation with the prognosis and response to chemotherapy. Int J Cancer 2001; 95:92-95.

Kaufmann SH & Vaux DL. Alterations in the apoptotic machinery and their potential role in anticancer drug resistance. Oncogene 2003;22:7414-7430.

Kawasaki H, Altieri DC, Lu CD, Toyoda M, Tenjo T & Tanigawa N. Inhibition of apoptosis by survivin predicts shorter survival rates in colorectal cancer. Cancer Res 1998; 58:5071505074.

Kelland LR, Sharp SY, Rogers PM, Myers TG & Workman P. DT-diaphorase expression and tumor cell sensitivity to 17-allylamino, 17-demethoxygeldanamycin, an inhibitor of heat shock protein 90. J Natl Cancer Inst 1999; 91:1940-1949.

Kerr JF, Winterford CM & Harmon BV. Apoptosis. Its significance in cancer and cancer therapy. Cancer 1994; 73:2013-2026.

Kerr JF, Wyllie AH & Currie AR. Apoptosis: a basic biological phenomenon with wide-ranging implications in tissue kinetics. Br J Cancer 1972; 26:239-257.

Khaled AR, Kim K, Hofmeister R, Muegge K & Durum SK. Proc Natl Acad Sci USA 1999; 96:14476-14481.

Khan AU & Lal SK. Ribozymes: A Modern Tool in Medicine. J Biomed Sci 2003; 10:457-467.

Khan AU, Ahmad M & Lal SK. Restoration of mRNA splicing by a second-site intragenic supressor in the T4 ribonucleotide reductase (small subunit)self-splicing intron.Biochem Biophys Res Comm 200; 268:359-364.

Kiechle L & Zhang X. Apoptosis: biochemical aspects and clinical implications. Clin Chim Acta 2002; 326:27-45.

Kim PJ, Plescia J, Clevers H, Fearon ER & Altieri DC. Survivin and molecular pathogenesis of colorectal cancer. Lancet 2003; 362:205-209.

Kim R, Tanabe K, Emi M, Inoue H & Toge T. Current status of the molecular mechanisms of anticancer drug-induced apoptosis. The contribution of molecular-level analysis to cancer chemotherapy. Cancer Chemother Pharmacol 2002; 50:343-352.

Kirsebom LA. RNase P RNA-mediated catalysis. Biochem Soc Trans 2001; 30:1153-1158.

Knauert MP & Glazer PM. Triplex forming oligonucleotides: sequence-specific tools for gene targeting. Human Mol Genet 2001; 10:2243-2251.

Kobayashi K, Hatano M, Otaki M, Ogasawara T & Tokuhisa T. Expression of a murine homologue of the inhibitor of apoptosis protein is related to cell proliferation. Proc Natl Acad Sci USA 1999; 96:1457-1462.

Koch CA, Vortmeyer AO, Diallo R, Poremba C, Giordano TJ, Sanders D, Bornstein SR, Chrousos GP & Pacak K. Survivin: a novel neuroendocrine marker for pheochromocytoma. Eur J Endocrinol 2002; 146:381-388.

Koonin EV & Aravind L. The NACHT family - a new group of predicted NTPases implicated in apoptosis and MHC transcription activation. Trends Biochem Sci 2000; 25:223-224.

Kore AR, Vaish NK, Kutzke U & Eckstein F. Sequence specificity of the hammerhead ribozyme revisited; the NHH rule. Nucleic Acid Research 1998; 26:4116-4120

Korsmeyer SJ. BCL-2 gene family and the regulation of programmed cell death. Cancer Res 1999; 59:1693s-1700s.

Krajewska M, Fenoglio-Preiser CM, Krajewski S, Song K, Macdonald JS, Stemmerman G & Reed JC. Immunohistochemical analysis of Bcl-2 family proteins in adenocarcinomas of the stomach. Am J Pathol 1996; 148:1567-1576.

Krajewski S, Blomqvist C, Franssila K, Krajewska M, Wase-nius VM, Niskanen E, Nordling S & Reed JC. Reduced expression of proapoptotic gene BAX is associated with poor response rates to combina-tion chemotherapy and shorter survival in women with metastatic breast adenocarcinoma. Cancer Res 1995; 55: 4471-4478.

Krammer PH. CD95(APO-1/Fas)-mediated apoptosis: live and let die. Adv Immunol 1999; 71:163-210.

Krieg A, Mahotka C, Krieg T, Grabsch H, Muller W, Takeno S, Suschek CV, Heydthausen M, Gabbert HE & Gerharz CD. Expression of different survivin variants in gastric carcinomas: first clues to a role of survivin-2B in tumour progression. Br J Cancer 2002; 86:737-743

Kroemer G, Galluzzi L & Brenner C. Mitochondrial membrane permeabilization in cell death. Physiol Rev 2007; 87:99-163.

Kroemer G, Zamzami N & Susin SA. Mitochondrial control of apoptosis. Immunol Today 1997; 18:44-51.

Krueger A, Baumann S, Krammer PH & Kirchhoff S. FLICE-inhibitory proteins: regulators of death receptor-mediated apop-tosis. Mol Cell Biol 2001; 21:8247-8254.

Kumar S. Caspase function in programmed cell death. Cell Death and Differentiation 2007; 14:32-43.

Kurreck J. Antisense technologies. Improvement through novel chemical modifications. Eur J Biochem 2003; 270:1628-1644.

Kuttler F, Valnet-Rabier MB, Angonin R, Ferrand C, Deconinck E, Mougin C, Cahn JY & Fest T. Relationship between expression of genes involved in cell cycle control and apoptosis in diffuse large B cell lymphoma: a preferential survivin–cyclin B link. Leukemia 2002; 16:726-735.

Kymionis GD, Dimitrakakis CE, Konstadoulakis MM, Arzi-manoglou I, Leandros E, Chalkiadakis G, et al. Can expression of apoptosis genes, bcl-2 and bax, predict survival and responsive-ness to chemotherapy in node-negative breast cancer patients? J Surg Res 2001; 99:161-168.

LaCasse EC, Baird S, Korneluk RG & MacKenzie AE. The inhibitors of apoptosis (IAPs) and their emerging role in cancer. Oncogene 1998; 17: 3247-3259.

Laemmli UK. Cleavage of structural proteins during the assembly of the head of bacteriophage T4. Nature 1970; 227:680-685.

Lagace M, Xuan JY, Young SS, McRoberts C, Maier J, Rajcan-Separovic E & Korneluk RG. Genomic organization of the X-linked inhibitor of apoptosis and identification of a novel testis-specific transcript. Genomics 2001; 77:181-188.

Lal SK & Hall DH. Functional and sequence analysis of splicing defective nrdB mutants of bacteriophage T4 reveal new bases and a new sub-domain required for group I intron self-splicing. Biochim Biophys Acta 1997; 1350:89-97.

Lavin MF, Birrell G, Chen P, Kozlov S, Scott S & Gueven N. ATM signaling and genomic stability in response to DNA damage. Mutat Res 2005; 569:123-132.

Lee HR, Chang TH, Tebalt MJ 3rd, Senderowicz AM & Szabo E. Induction of differentiation accompanies inhibition of Cdk2 in a non-small cell lung cancer cell line. Int J Oncol 1999; 15:161-166.

Lee NS, Bertrand E & Rossi J. mRNA localization signals can enhance the intracellular effectiveness of hammerhead ribozymes. RNA 1999; 5:1200-1209.

Lee SW, Ko YG, Bang S, Kim KS & Kim S. Death effector domain of a mammalian apoptosis mediator, FADD, induces bacterial cell death. Mol Microbiol 2000; 35: 1540-1549.

Lens SM, Wolthuis RM, Klompmaker R, Kauw J, Agami R, Brummelkamp T, Kops G & Medema RH. Survivin is required for a sustained spindle checkpoint arrest in response to lack of tension. EMBO J 2003; 22:2934-2947.

Levin AA. A review of issues in the pharmacokinetic and toxicology of phosphorothioate antisense oligonucleotides. Biochim Biophys Acta 1999; 1489:69-84.

Levine JS & Koh JS. The role of apoptosis in autoimmunity: immunogen, antigen, and accelerant. Semin Nephrol 1999; 19:34-47.

Lewin AS & Hauswirth WW. Ribozyme gene therapy: applications for molecular medicine. Trends Mol Med 2001; 7:221-228.

Li F & Altieri DC. Transcriptional analysis of human survivin gene expression. Biochem J 1999; 344:305-311.

Li F, Ambrosini G, Chu EY, Plescia J, Tognin S, Marchisio PC & Altieri DC. Control of apoptosis and mitotic spindle checkpoint by survivin. Nature 1998; 396:580-584.

Li F, Ackermann EJ, Bennett CF, Rothermel AL, Plescia J, Tognin S, Villa A, Marchisio PC & Altieri DC. Pleiotropic cell-division defects and apoptosis induced by interference with survivin function. Nat Cell Biol 1999; 1:461-466.

Li H, Zhu H, Xu CJ & Yuan. Cleavage of BID by caspase 8 mediates the mitochondrial damage in the Fas pathway of apoptosis. Cell 1998; 94:491-501.

Li QX, Zhao J, Liu JY, Jia LT, Huang HY, Xu YM, Zhang Y, Zhang R, Wang CJ, Yao LB, Chen SY & Yang AG. Survivin stable knockdown by siRNA inhibits tumor cell growth and angiogenesis in breast and cervical cancers. Cancer Biol Ther 2006; 5:860-866.

Liang L, Liu D-P & Liang C-C. Optimizing the delivery ystems of chimeric RNA/DNA oligonucleotides: Beyond general oligonucleotide transfer. Eur J Bioche 2002; 269:5753-5758.

Lilly M, Sandholm J, Cooper JJ, Koskinen PJ & Kraft A. The PIM-1 serine kinase prolongs survival and inhibits apoptosis-related mitochondrial dysfunction in part through a bcl-2-dependent pathway. Oncogene 1999; 18:4022-4031.

Lin JH, Deng G, Huang Q & Morser. KIAP, a novel member of the inhibitor of apoptosis protein family. Biochem Biophys Res Commun 2000; 279:820-831.

Ling X, Bernacki RJ, Brattain MG & Li F. Induction of survivin expression by taxol (paclitaxel) is an early event, which is independent of taxol-mediated G_2/M arrest. J Biol Chem 2004; 279:15196-15203.

Liston P, Roy N, Tamai K, Lefebvre C, Baird S, Cherton-Horvat G, Farahani R, McLean M, Ikeda J-E, MacKenzie A & Kornluk RG. Suppression of apoptosis in mammalian cells by NAIP and a related family of IAP genes. Nature 1996; 379:349-353.

Liu Z, Sun C, Olejniczak ET, Meadows RP, Betz SF, Oost T, Herrmann J, Wu JC & Fesik SW. Structural basis for binding of Smac/DIABLO to the XIAP BIR3 domain. Nature 2000; 408:1004-1008.

Liu T, Brouha B & Grossman D. Rapid induction of mitochondrial events and caspase-independent apoptosis in Survivin-targeted melanoma cells. Oncogene 2004; 23:39-48.

Lo HW, Day CP & Hung MC. Cancer-specific gene therapy. Adv Genet 2005; 54:235-255.

Loisel S, LeGall C, Doucet L, Feree C & Floch V. Contribution of plasmid DNA to hepatotoxicity after systemic administration of lipoplexes. Hum Gene Ther 2001; 12:685-692.

Longley DB, Allen WL, McDermott U, Wilson TR, Latif T, Boyer J, Linch M & Johnston PG. The roles of thymidylate synthase and p53 in regu-lating Fas-mediated apoptosis in response to antimetabolites. Clin Cancer Res 2004; 10:3562-3571.

Los M, Mozoluk M, Ferrari D, Stepczynska A, Stroh C, Renz A, Herceg Z, Wang ZQ & Schulze-Osthoff K. Activation and caspase-mediated inhibition of PARP: a molecular switch between fibroblast necrosis and apoptosis in death receptor signaling. Mol Biol Cell 2002;13:978-988.

Lu B, Mu Y, Cao C, Zeng F, Schneider S, Tan J, Price J, Chen J, Freeman M & Hallahan DE. Survivin As a Therapeutic Target for Radiation Sensitization in Lung Cancer. Cancer Res 2004; 64:2840-2845.

Lu CD, Altieri DC & Tanigawa N. Expression of a novel antiapoptosis gene, survivin, correlated with tumor cell apoptosis and p53 accumulation in gastric carcinomas.Cancer Res 1998; 58:1808-1812.

Luo,X.;Budihardjo,I.;Zou,H.;Slaughter,C.;Wang,X. Bid, a Bcl2 interacting protein, mediates cytochrome c release from mitochondria in response to activation of cell surface death receptors. Cell 1998; 94:481490.

Mahotka C, Wenzel M, Springer E, Gabbert HE & Gerharz CD. Survivin-deltaEx3 and survivin-2B: two novel splice variants of the apoptosis inhibitor survivin with different antiapoptotic properties. Cancer Res 1999; 59:6097-6102.

Mahotka C, Krieg T, Krieg A, Wenzel M, Suschek CV, Heydthausen M, Gabbert HE & Gerharz CD. Distinct in vivo expression patterns of survivin splice variants in renal cell carcinomas. Int J Cancer 2002a; 100:30-36.

Mahotka C, Liebmann J, Wenzel M, Suschek CV, Schmitt M, Gabbert HE & Gerharz CD. Differential subcellular localization of functionally divergent survivin splice variants. Cell Death Differ 2002b; 9:1334-1342.

Maier JK, Lahoua Z, Gendron NH, Fetni R, Johnston A, Davoodi J, Rasper D, Roy S, Slack RS, Nicholson DW & MacKenzie AE. The neuronal apoptosis inhibitory protein is a direct inhibitor of caspases 3 and 7. J Neurosci 2002; 22:2035-2043.

Martinez A, Bellosillo B, Bosch F, Ferrer A, Marce S, Villamor N, Ott G, Montserrat E, Campo E & Colomer D. Nuclear survivin expression in mantle cell lymphoma is associated with cell proliferation and survival. Am J Pathol 2004; 164:501-510.

Marusawa H, Matsuzawa S, Welsh K, Zou H, Armstrong R, Tamm I & Reed JC. HBXIP functions as a cofactor of survivin in apoptosis suppression. EMBO J 2003; 22:2729-2740.

Maundrell K, Antonsson B, Magnenat E, Camps M, Muda M, Chabert C, Gillieron C, Boschert U, Vial Knecht E, Martinou J-C & Arkinstall A. Bcl-2 undergoes phosphorylation by c-Jun N-terminal kinase/stress-activated protein kinases in the presence of the constitutively active GTP-binding protein Rac1. J Biol Chem 1997; 272:25238-25242.

McEleny KR, Watson RWG, Coffey RNT, O'Neill AJ & Fitzpatrick JM. Inhibitors of apoptosis proteins in prostate cancer cell lines. Prostate 2002; 51:133-40.

McManus DC, Lefebvre CA, Cherton-Horvat G, St-Jean M, Kandimalla ER, Agrawal S, Morris SJ, Durkin JP & Lacasse EC. Loss of XIAP protein expression by RNAi and antisense approaches sensitizes cancer cells to functionally diverse chemotherapeutics. Oncogene 2004; 23:8105-8117.

Meijer L, Borgne A, Mulner O, Chong JP, Blow JJ, Inagaki N, Inagaki M, Delcros JG & Moulinoux JP. Biochemical and cellular effects of roscovitine, a potent and selective inhibitor of the cyclin-dependent kinases cdc2, cdk2 and cdk5. Eur J Biochem 1997; 243:527-536.

Meiler J & Schuler M. Therapeutic targeting of apoptotic pathways in cancer. Curr Drug Targets 2006; 7:1361-1369.

Meli M, Pennati M, Curto M, Daidone MG, Plescia J, Toba S, Altieri DC, Zaffaroni N & Colombo G. Small-molecule targeting of heat shock protein 90 chaperone function: rational identification of a new anticancer lead. J Med Chem 2006; 49:7721-7730.

Melillo G, Sausville EA, Cloud K, Lahusen T, Varesio L & Senderowicz AM. Flavopiridol, a protein kinase inhibitor, down-regulates hypoxic induction of vascular endothelial growth factor expression in human monocytes. Cancer Res 1999; 59:5433-5437.

Melino G, Bernassola F, Ranalli M, Yee K, Zong WX, Corazzari M, Knight RA, Green DR, Thompson C, Vousden KH. p73 Induces apoptosis via PUMA transactivation and Bax mitochondrial translocation. J Biol Chem 2004; 279:8076-8083.

Mendoza-Maldonado R, Zentilin L, Fanin R & Giacca M. Purging of chronic myelogenous leukemia cells by retrovirally expressed anti-bcr-abl ribozymes with specific cellular compartmentalization. Cancer Gene Ther 2002; 9:71-86.

Meng H, Lu CD, Sun YL, Dai DJ, Lee SW & Tanigawa N. Expression level of wild-type survivin in gastric cancer is an independent predictor of survival. World J Gastroenterol 2004; 10:3245-3250.

Mercatanti A, Rainaldi G, Mariani L & Citti L. A method for prediction of accessible sites on a mRNA sequence for target selection of hammerhead ribozymes. J Computational Biol 2002; 9:641-653.

Mesri M, Wall NR, Li J, Kim RW & Altieri DC. Cancer gene therapy using a surviving mutant adenovirus. J Clin Invest 2001; 108:981-990.

Mesri M, Morales-Ruiz M, Ackermann EJ, Bennett CF, Pober JS, Sessa WC & Altieri DC. Suppression of vascular endothelial growth factor-mediated endothelial cell protection by survivin targeting. Am J Pathol 2001; 158:1757-1765.

Mild G, Bachmann F, Boulay JL, Glatz K, Laffer U, Lowy A, Metzger U, Reuter J, Terracciano L, Herrmann R & Rochlitz C. DCR3 locus is a

predictive marker for 5-fluorouracil-based adjuvant chemotherapy in colorectal cancer. Int J Cancer 2002; 102:254-257.

Miller L. An exegesis of IAPs: salvation and surprises from BIR motifs. Trends Cell Biol 1999; 9:323-328.

Milligan JF, Matteucci MD & Martin JC. Current concepts in antisense drug design. J Med Chem 1993; 36:1923-1937.

Minn AJ, Swain RE, Ma A & Thompson CB. Recent progress on the regulation of apoptosis by Bcl-2 family members. Adv Immunol 1998; 70:245-279.

Mirza A, McGuirk M, Hockenberry TN, Wu Q, Ashar H, Black S, Wen SF, Wang L, Kirschmeier P, Bishop WR, Nielsen LL, Pickett CB & Liu S. Human survivin is negatively regulated by wild-type p53 and participates in p53-dependent apoptotic pathway. Oncogene 2002; 21:2613-2622.

Mita MM, Mita AC & Tolcher AW. Apoptosis: mechanism and implications for cancer therapeutics. Targ Oncol 2006; 1:197-214.

Mitsiades CS, Mitsiades N, Poulaki V, Schlossman R, Akiyama M, Chauhan D, Hideshima T, Treon SP, Munshi NC, Richardson PG & Anderson KC. Activation of NF-kB and upregulation of intracellular anti-apoptotic proteins via the IGF-1/Akt signaling in human multiple myeloma cells: therapeutic implications. Oncogene 2002; 21:5673-5683.

Miyachi K, Sasaki K, Onodera S, Taguchi T, Nagamachi M, Kaneko H & Sunagawa M. Correlation between survivin mRNA expression and lymph node metastasis in gastric cancer. Gastric Cancer 2003; 6:217-224.

Monzo M,Rosell R,Felip E,Astudillo J,Sanchez JJ,Maestre J,Martin C,Font A,Barnadas A & Abad A. A novel anti-apoptosis gene: Re-expression of survivin messenger RNA as a prognosis marker in non-small-cell lung cancers. J Clin Oncol 1999; 17:2100-2104.

Mooney EE, Ruis Peris JM, O'Neill A & Sweeney EC. Apoptotic and mitotic indices in malignant melanoma and basal cell carcinoma. J Clin Pathol 1995; 48:242-244.

Morgan DO. Cyclin-dependent kinases: engines, clocks, and microprocessors. Annu Rev Cell Dev Biol. 1997; 13:261-291.

Mottolese M, Buglioni S, Bracalenti C, Cardarelli MA, Ciabocco L, Giannarelli D, Botti C, Natali PG, Concetti A & Venanzi FM. Prognostic relevance of altered Fas (CD95)-system in human breast cancer. Int J Cancer 2000; 89:127-132.

Motwani M, Delohery TM & Schwartz GK. Sequential dependent enhancement of caspase activation and apoptosis by flavopiridol on paclitaxel-treated human gastric and breast cancer cells. Clin Cancer Res 1999; 5:1876-1883.

Muchmore SW, Chen J, Jakob C, Zakula D, Matayoshi ED, Wu W, Zhang H, Li F, Ng SC & Altieri DC. Crystal structure and mutagenic analysis of the inhibitor-of-apoptosis protein survivin. Mol Cell 2000; 6:173-182.

Murray JB, Seyhan AA, Walter NG, Burke JM & Scott WG. The hammerhead,hairpin and VS ribozyme are catalytically proficient in monovalent cations alone. Chem Biol 1998; 5:587-595.

Nagata S. Apoptosis by death factor. Cell 1997; 88:355-365.

Nakagawa T, Zhu H, Morishima N, Li E, Xu J, Yankner BA & Yuan J. Caspase-12 mediates endoplasmic-reticulum-specific apoptosis and cytotoxicity by amyloid-beta. Nature 2000; 403:98-103.

Nakagawa Y, Yamaguchi S, Hasegawa M, Nemoto T, Inoue M, Suzuki K, Hirokawa K & Kitagawa M. Differential expression of survivin in bone marrow cells from patients with acute lymphocytic leukemia and chronic lymphocytic leukemia. Leuk Res 2004; 28:487-494.

Nakao K, Hamasaki K, Ichikawa T, Arima K, Eguchi K & Ishii N. Survivin downregulation by siRNA sensitizes human hepatoma cells to TRAIL-induced apoptosis. Oncol Rep 2006; 16:389-392.

Niehans GA, Brunner T, Frizelle SP, Liston JC, Salerno CT, Knapp DJ, Green DR & Kratzke RA. Human lung carcinomas express Fas ligand. Cancer Res 1997; 57:1007-1012.

Nomura T, Yamasaki M, Nomura Y & Mimata H. Expression of the inhibitors of apoptosis proteins in cisplatin-resistant prostate cancer cells. Oncol Rep 2005; 14:993-997.

Noton EA, Colnaghi R, Tate S, Starck C, Carvalho A, Ko Ferrigno P & Wheatley SP. Molecular analysis of survivin isoforms: evidence that

alternatively spliced variants do not play a role in mitosis. J Biol Chem 2006; 281:1286-1295.

Nunez G & Del Peso L. Linking extracellular survival signals and the apoptotic machinery. Curr Opin Neurobiol 1998; 8:613-618.

Nyberg KA, Michelson RJ, Putnam CW & Weinert TA. Toward maintaining the genome: DNA damage and replication checkpoints. Annu Rev Genet 2002; 36:617-656.

Oancea M, Mani A, Hussein MA, Almasan A. Apoptosis of multiple myeloma. Int J Hematol 2004; 80:224-231.

O'Connor DS, Grossman D, Plescia J, Li F, Zhang H, Villa A, Tognin S, Marchisio PC & Altieri DC. Regulation of apoptosis at cell division by p34cdc2 phosphorylation of survivin. Proc Natl Acad Sci USA 2000; 97:13103-07.

O'Connor DS, Wall NR, Porter AC & Altieri DC. A p34(cdc2) survival checkpoint in cancer. Cancer Cell 2002; 2:43-54.

Oehlke J, Birth P, Klauschenz E, Wiesner B, Beyermann M, Oksche A & Bienert M. Cellular uptake of antisense oligonucleotides after complexing or conjugation with cell-penetrating model peptides. Eur J Bioche 2002; 269:4015-4032.

Olie RA, Simoes-Wust AP, Baumann B, Leech SH, Fabbro D, Stahel RA & Zangemeister-Wittke U. A novel antisense oligonucleotide targeting survivin expression induces apoptosis and sensitizes lung cancer cells to chemotherapy. Cancer Res 2000; 60:2805-2809.

Opferman JT, Korsmeyer SJ. Apoptosis in the development and maintenance of the immune system. Nat. Immunol 2003; 4:410-415.

Ørum H & Wengel J. Locked nucleic acids:a promising molecular family for gene-function analy is and antisense drug development. Curr Opinion Mol Ther 2001; 3:239-243.

Paik S, Shak S, Tang G, Kim C, Baker J, Cronin M, Baehner FL, Walker MG, Watson D, Park T, Hiller W, Fisher ER, Wickerham DL, Bryant J & Wolmark N. A multigene assay to predict recurrence of tamoxifen-treated, node-negative breast cancer. N Engl J Med 2004; 351:2817-2826.

Pan WH & Clawson GA. Identifying accessible sites in RNA: the first step in designing antisense reagents. Curr Med Chem 2006; 13:3083-3103.

Papapetropoulos A, Fulton D, Mahboubi K, Kalb RG, O 'Connor DS, Li F, Altieri DC & Sessa WC. Angiopoietin-1 inhibits endothelial cell apoptosis via the Akt/survivin pathway. J Biol Chem 2000; 275:9102-9105.

Paradiso A, Simone G, Lena MD, Leone B, Vallejo C, Lacava J, Della pasqua S, Daidome MG, Costa A. Expression of apoptosis-related markers and clinical out-come in patients with advanced colorectal cancer. Br J Cancer 2001; 84:651-658.

Park R, Chang CC, Liang YC, Chung Y, Henry RA, Lin E, Mold DE & Huang RC. Systemic treatment with tetra-O-methyl nordihydroguaiaretic acid suppresses the growth of human xenograft tumors. Clin Cancer Res 2005; 11:4601-4609.

Parker AL, Newman C, Briggs S, Seymour L & Sheridan PJ. Nonviral gene delivery: techniques and implications for molecular medicine. Expert Rev Mol Med 2003; 2003:1-15.

Passalaris TM, Benanti JA, Gewin L, Kiyono T & Galloway DA. The G2 checkpoint is maintained by redundant pathways. Mol Cell Biol 1999; 19:5872-5881.

Pavletich NP. Mechanisms of cyclin-dependent kinase regulation: structures of Cdks, their cyclin activators, and Cip and INK4 inhibitors. J Mol Biol 1999; 287:821-28.

Perreault JP, Wu TF, Cousineau B, Ogilvie KK & Cedergren R. Mixed deoxyribo- and ribo-oligonucleotides with catalytic activity. Nature 1990; 344:565–567.

Petak I, Tillman DM & Houghton JA. p53 dependence of Fas induction and acute apoptosis in response to 5-fluorouracil-leucovorin in human colon carcinoma cell lines. Clin Cancer Res 2000; 6:4432-4441.

Peter ME. The flip side of FLIP. Biochem J 2004; 382:e1-3.

Piret B, Schoonbroodt S Piette J. The ATM protein is required for sustained activation of NF-kappa B fol-lowing DNA damage. Oncogene 1999; 18:2261-2271.

Pirollo KF, Rait A, Sleer LS & Hang EH. Antisense therapeutics: from theory to clinical practice. Pharm Ther 2003; 99: 55-77.

Plantaz D, Mohapatra G, Matthay KK, Pellarin M, Seeger RC & Feuerstein BG. Gain of chromosome 17 is the most frequent abnormality detected in neuroblastoma by comparative genomic hybridization. Am J Pathol 1997; 150:81-89.

Plescia J, Salz W, Xia F, Pennati M, Zaffaroni N, Daidone MG, Meli M, Dohi T, Fortugno P, Nefedova Y, Gabrilovich DI, Colombo G & Altieri DC. Rational design of Shepherdin, a novel anticancer agent. Cancer Cell 2005; 7:457-467.

Pooga M, Land T, Bartfai T, Langel U. PNA oligomers as tools for specific modulation of gene expression. Biomol Eng 2001; 17:183-192.

Pouton CW & Seymour LW. Key issues in non-viral gene delivery. Adv. Drug Deliv Rev 1998; 34:3-12.

Prislei S, Buonomo SB, Michienzi A & Bozzoni I. Use of adenoviral VAI small RNA as a carrier for cytoplasmic delivery of ribozymes. RNA 1997; 3:677-687.

Proskuryakov SY, Konoplyannikov AG, Gabai VL. Necrosis: a specific form of programmed cell death? Exp Cell Res 2003; 283:1-16.

Puerta-Fernandez E, Romero-Lopez C, Barroso-delJesus A, Berzal-Herranz A. Ribozymes: recent advances in the development of RNA tools. FEMS Microbiology Reviews 2003; 27:75-97.

Puthalakath H & Strasser A. Keeping killers on a tightleash: transcriptional and post-translational control of the pro-apoptotic activity of BH3-only proteins. Cell Death Differ 2002; 9:505-508.

Qiu XB, Markant SL, Yuan J & Goldberg AL. Nrdp1-mediated degradation of the gigantic IAP, BRUCE, is a novel pathway for triggering apoptosis. EMBO J 2004; 23:800-810.

Qiu XB & Goldberg AL. The membrane-associated inhibitor of apoptosis protein, BRUCE/Apollon, antagonizes both the precursor and mature forms of Smac and caspase-9. J Biol Chem 2005; 280:174-182.

Rampino N, Yamamoto H,Ionov Y,Li Y,Sawai H,Reed JC & Perucho M. Somatic frameshift mutations in the BAX gene in colon cancers of the microsatellite mutator phenotype. Science 1997; 275:967-969.

Ranger AM, Malynn BA & Korsmeyer SJ. Mouse models of cell death. Nat Genet 2001; 28:113-118.

Reed JC. Dysregulation of apoptosis in cancer. J Clin Oncol 1999; 17:2941-2953.

Reed JC. Mechanisms of apoptosis. Am J Pathol 2000; 157:1415-1430.

Reed JC. The Survivin saga goes in vivo. J Clin Invest 2001; 108:965-969.

Reed JC & Pellecchia M. Apoptosis-based therapies for hematologic malignancies. Blood 2005; 106:408-418.

Rehemtulla A, Hamilton CA, Chinnaiyan AM & Dixit VM. Ultraviolet radiation-induced apoptosis is mediated by activation of CD-95 (Fas/APO-1). J Biol Chem 1997; 272:25783-25786.

Relph KL, Harrington KJ & Pandha H. Adenoviral strategies for the gene therapy of cancer. Semin Oncol 2005; 32:573-582.

Richter BW, Mir SS, Eiben LJ, Lewis J, Reffey SB, Frattini A, Tian L, Frank S, Youle RJ, Nelson DL, Notarangelo LD, Vezzoni P, Fearnhead HO & Duckett CS. Molecular cloning of ILP-2, a novel member of the inhibitor of apoptosis protein family. Mol Cell Biol 2001; 21:4292-4301.

Richter K & Buchner J. Hsp90: chaperoning signal transduction. J Cell Physiol 2001;188:281-290.

Rickert P, Seghezzi W, Shanahan F, Cho H & Lees E. Cyclin C/CDK8 is a novel CTD kinase associated with RNA polymerase II. Oncogene 1996; 12:2631-40.

Rockwell P, O'Connor W, King K, Goldstein NI, Zhang LM & Stein CA. Cell-surface pertubations of the epidermal growth factor and vascular endothelial growth factor receptors by phosphorothioate oligodeoxynucleotides. Proc Natl Acad Sci USA 1998; 94:6523-6528.

Rodel C, Haas J, Groth A, Grabenbauer GG, Sauer R & Rodel F. Spontaneous and radiation-induced apoptosis in colorectal carcinoma cells with different intrinsic radiosensitivities: survivin as a radioresistance factor. Int J Radiat Oncolo Biol Phys 2003; 55:1341-1347.

Rodel F, Hoffmann J, Distel L, Herrmann M, Noistenig T, Papadopoulos T, Sauer R & Rodel C. Survivin as a radioresistance factor, and prognostic and therapeutic target for radiotherapy in rectal cancer. Cancer Res 2005; 65:4881-4887.

Rodrigues T, Carrondo MJ, Alves PM & Cruz PE. Purification of retroviral vectors for clinical application: biological implications and technological challenges. J Biotechnol 2007; 127:520-541.

Romano G, Pacilio C, Giordano A. Gene Transfer Technology in Therapy: Current Applications and Future Goals. Stem cells 1999; 17:191-202.

Roos WP & Kaina B. DNA damage-induced cell death by apoptosis. TRENDS Mol Med 2006; 12:440-450.

Rossi JJ. Ribozymes, genomics and therapeutics. Chem Biol 1999; 6:R33-37.

Rothe M, Pan M-G, Henzel WJ,Ayres TM & Goeddel DV. The TNFR2-TRAF signaling complex contains two novel proteins related to baculoviral inhibitor of apoptosis proteins. Cell 1995; 83:1243-1252.

Roy N, Deveraux QL, Takahashi R, Salvesen GS & Reed JC. The c-IAP-1 and c-IAP-2 proteins are direct inhibitors of specific caspases. EMBO J 1997; 16:6914-6925.

Roy N, Mahadevan MS, McLean M, Shutler G, Yaraghi Z, Farahani R, Baird S, Besner-Johnston A, Lefebvre C, Kang X, Salih M, Aubry H, Tamai K, Guan X, Ioannou P, Crawford TO, de Jong PJ, Surh L, Ikeda J-E, Korneluk RG & MacKenzie A. The gene for neuronal apoptosis inhibitory protein is partially deleted in individuals with spinal muscular atrophy. Cell 1995; 80:167-178.

Ruffolo SC, Breckenridge DG, Nguyen M, Goping IS, Gross A, Korsmeyer SJ, Li H, Yuan J & Shore GC. BID-dependent and BID-independent pathways for BAX insertion into mitochondria. Cell Death Differ 2000; 7:1101-1108.

Ryther RCC, Flynt AS, Phillips JA III & Patton JG. siRNA therapeutics: big potential from small RNAs. Gene Therapy 2005; 12:5-11.

Sah NK, Munshi A, Hobbs M, Carter BZ, Andreeff M & Meyn RE. Effect of downregulation of survivin expression on radiosensitivity of human epidermoid carcinoma cells. Int J Radiat Oncol Biol Phys 2006; 66:852-859.

Saitoh Y, Yaginuma Y & Ishikawa M. Analysis of Bcl-2, Bax and Survivin genes in uterine cancer. Int J Oncol 1999; 15:137-141.

Sakakura C, Sweeney EA, Shirahama T, Igarashi Y, Hakomori S, Tsujimoto H, et al. Overexpression of bax sensitizes breast cancer MCF-7 cells to cisplatin and etoposide. Surg Today 1997; 27:676-679.

Salvesen GS & Duckett CS. IAP proteins: blocking the road to death's door. Nat Rev Mol Cell Biol 2002; 3:401-410.

Sancar A, Lindsey-Boltz LA, Unsal-Kacmaz K & Linn S. Molecular mechanisms of mammalian DNA repair and the DNA damage checkpoints. Annu Rev Biochem 2004; 73:39-85.

Sarela AI, Macadam RC, Farmery SM, Markham AF, Guillou PJ. Expression of the antiapoptosis gene, survivin, predicts death from recurrent colorectal carcinoma. Gut 2000; 46:645-650.

Sarin A, Wu ML & Henkart PA. Different interleukin-1 beta converting enzyme (ICE) family protease requirements for the apoptotic death of T lymphocytes triggered by diverse stimuli. J Exp Med 1996; 184:2445-2450.

Sasaki H, Sheng Y, Kotsuji F & Tsang BK. Down-regulation of X-linked inhibitor of apoptosis protein induces apoptosis in chemoresistant human ovarian cancer cells. Cancer Res 2000; 60:5659–5666.

Satoh K, Kaneko K, Hirota M, Masamune A, Satoh A & Shimosegawa T. Expression of survivin is correlated with cancer cell apoptosis and is involved in the development of human pancreatic duct cell tumors. Cancer 2001; 92:271-278.

Satyamoorthy K, Bogenrieder T & Herlyn M. No longer a molecular black box-new clues to apoptosis and drug resistance in melanoma. Trends Mol Med 2001; 7:191-194.

Scheffler IE. Mitochondria make a come back. Adv Drug Deliv Rev 2001; 49:3-26.

Scherer LJ & Rossi JJ. Approaches for the sequence-specific knock-down of mRNA. Nat Biotechnol 2003; 21:1457-1465.

Schlegel RA, Callahan M, Krahling S, Pradham D & Williamson P. Mechanisms for recognition and phagocytosis of apoptotic lymphocytes by macrophages. Adv Exp Biol Med 1996; 406:21-28.

Schmitt CA, Rosenthal CT & Lowe SW. Genetic analysis of chemoresistance in primary murine lymphomas. Nature Med 2000; 6:1029-1035.

Schmitt E, Paquet C, Beauchemin M & Bertrand R. DNA-damage response network at the crossroads of cell-cycle checkpoints, cellular senescence and apoptosis. J Zhejiang Univ Sci B 2007; 8:377-397.

Schulte TW & Neckers LM. The benzoquinone ansamycin 17-allylamino-17-demethoxygeldanamycin binds to hsp90 and shares important biologic activities with geldanamycin. Cancer Chem Pharmacol 1998; 42:273-279.

Schultz IJ, Kiemeney LA, Witjes JA, Schalken JA, Willems JL, Swinkels DW & de Kok JB. Survivin mRNA expression is elevated in malignant urothelial cell carcinomas and predicts time to recurrence. Anticancer Res 2003;23:3327–31.

Schwartz GK, Farsi K, Maslak P, Kelsen DP & Spriggs D. Potentiation of apoptosis by flavopiridol in mitomycin-C-treated gastric and breast cancer cells. Clin Cancer Res 1997; 3:1467-72.

Schwartz GK, Ilson D, Saltz L, O'Reilly E, Tong W, Maslak P, Werner J, Perkins P, Stoltz M & Kelsen D. Phase II study of the cyclin-dependent kinase inhibitor flavopiridol administered to patients with advanced gastric carcinoma. J Clin Oncol 2001; 19:1985-92.

Scott AM & Saleh M. The inflammatory caspases: guardians against infections and sepsis. Cell Death Differ 2007; 14:23-31.

Semizarov D, Frost L, Sarthy A, Kroeger P, Halbert DN & Fesik SW. Specificity of short interfering RNA determined through gene expression signatures. Proc Natl Acad Sci USA 2003; 100:6347-6352.

Senderowicz AM. Small-molecule cyclin-dependent kinase modulators. Oncogene 2003; 22:6609-6620.

Senderowicz A & Sausville E. Preclinical and clinical development of cyclin-dependent kinase modulators. J. Natl. Cancer Inst 2000; 92:376-385.

Shah MA & Schwartz GK. The relevance of drug sequence in combination chemotherapy. Drug Resist Updat 2000; 3:335-356.

Shankar SL, Mani S, O'Guin KN, Kandimalla ER, Agrawal S & Shat-Zagardo B. Survivin inhibition induces human neural tumor cell death through caspase-independent and -dependent pathways. J Neurochem 2001; 79:426-436.

Shapiro GI, Supko JG, Patterson A, Lynch C, Lucca J, Zacarola PF, Muzikansky A, Wright JJ, Lynch TJ Jr & Rollins BJ. A phase II trial of the cyclin-dependent kinase inhibitor flavopiridol in patients with previously untreated stage IV non-small cell lung cancer. Clin Cancer Res 2001; 7:1590-1599.

Sharma H, Sen S, LoMuzio L, Mariggio A & Singh N. Antisense-mediated downregulation of anti-apoptotic proteins induces apoptosis and sensitizes head and neck squamous cell carcinoma cells to chemotherapy. Cancer Biol Ther 2005; 4:720-727.

Sherr CJ. Cancer cell cycles. Science 1996; 274:1672-1677.

Shi N, Boado RJ & Pardridge WM. Antisense imaging of gene expression in the brain in vivo. Proc Natl Acad Sci USA 2000; 97:14709-14714.

Shi Y. Survivin structure: crystal unclear. Nat Struct Biol 2000; 7:620-623

Shi Y. A conserved tetrapeptide motif: potentiating apoptosis through IAP-binding. Cell Death Differ 2002; 9:93-95

Shi Y. Mechanisms of caspase inhibition and activation during apoptosis. Mol Cell 2003; 9:459–470.

Shimizu A, Masuda Y, Kitamura H, Ishizaki M, Ohashi R, Sugisaki Y & Yamanaka N. Complement-mediated killing of mesangial cells in experimental glomerulonephritis: cell death by a combination of apoptosis and necrosis. Nephron 2000; 86:152–160

Shimizu S, Matsuoka Y, Shinohara Y, Yoneda Y & Tsujimoto Y. Essential role of voltage-dependent anion channel in various forms of apoptosis in mammalian cells. J Cell Biol 2001; 152:237-250.

Shimizu S, Eguchi Y, Kamiike W, Waguri S, Uchiyama Y, Matsuda H & Tsujimoto Y. Bcl-2 blocks loss of mitochondrial membrane potential while ICE inhibitors act at a different step during inhibition of death induced by respiratory chain inhibitors. Oncogene 1996; 13:21-29.

Shimizu S & Tsujimoto Y. Proapoptotic BH3-only Bcl-2 family members induce cytochrome c release, but not mitochondrial membrane potential loss, and do not directly modulate voltage-dependent anion channel activity. Proc Natl Acad Sci USA 2000; 97:577-582.

Shin S, Sung BJ, Cho YS, Kim HJ, Ha NC, Hwang JI, Chung CW, Jung YK & Oh BH. An anti-apoptotic protein human survivin is a direct inhibitor of caspase-3 and -7. Biochemistry 2001; 40:1117-1123.

Shiozaki A, Kataoka K, Fujimura M, Yuki H, Sakai M & Saito S. Survivin inhibits apoptosis in cytotrophoblasts. Placenta 2003; 24:65-76.

Shiozaki EN, Chai J, Rigotti DJ, Riedl SJ, Li P, Srinivasula SM, Alnemri ES, Fairman R & Shi Y. Mechanism of XIAP-mediated inhibition of caspase-9. Mol Cell 2003; 11:519-527.

Silvestrini R, Gornati D, Zaffaroni N, Bearzatto A & De Marco C. Modulation by Ionidamine on the combined activity of cisplatin and epidoxorubicin in human breast cancer cells. Breast Cancer Res Treat 1997; 42:103-112.

Simorre JP, Legault P, Baidya N, Uhlenbeck OC, Maloney L, Wincott F, Usman N, Beigelman L & Pardi A. Structural variation induced by different nucleotides at the cleavage site of the hammerhead ribozyme. Biochemistry 1998; 37:4034-4044.

Sjostrom J, Blomqvist C, von Boguslawski K, Bengtsson NO, Mjaaland I, Malmstrom P, Ostenstadt B, Wist E, Valvere V, Takayama S, Reed JC & Saksela E. The predictive value of bcl-2, bax, bcl-xL, bag-1, fas, and fasL for chemotherapy response in advanced breast cancer. Clin Cancer Res 2002; 8:811-816.

Skoufias DA, Mollinari C, Lacroix FB & Margolis RL. Human survivin is a kinetochore-associated passenger protein.J Cell Biol, 2000;151:1575-1581.

Slee EA, Adrain C & Martin SJ. Serial killers: ordering caspase activation events in apoptosis. Cell Death Differ 1999; 6:1067-1074.

Smets LA, Van den Berg J, Acton D, Top B, Van Rooij H & Verwijs-Janssen M. BCL-2 expression and mitochondrial activity in leukemic cells with different sensitivity to glucocorticoid-induced apoptosis. Blood 1994; 84:1613-1619.

Smulevitch SV, Simmons CG, Norton JC, Wise TW & Corey DR. Enhancement of strand invasion by oligonucleotides through manipulation of backbone charge. Nat Biotechnol 1996; 14:1700-1704.

Soengas MS & Lowe SW. Apoptosis and melanoma chemoresistance. Oncogene 2003; 22:3138-3151.

Soengas MS, Capodieci P, Polsky D, Mora J, Esteller M, Opitz-Araya X, McCombie R, Herman JG, Gerald WL, Lazebnik YA, Cordon-Cardo C & Lowe SW. Inactivation of the apoptosis effector Apaf-1 in malignant melanoma. Nature 2001; 409:207-211.

Solit DB, Zheng FF, Drobnjak M, Munster PN, Higgins B, Verbel D, Heller G, Tong W, Cordon-Cardo C, Agus DB, Scher HI & Rosen N. 17-allylamino-17-demethoxygeldanamycin induces the degradation of androgen receptor and HER-2/neu and inhibitor growth of prostate cancer xenografts. Clin Cancer Res 2002; 8:986-993.

Somia NV, Miyoshi H, Schmitt MJ & Verma IM. Retroviral vector targeting to human immunodeficiency virus type 1-infected cells by receptor pseudotyping. J Virol 2000; 74:4420-4424.

Sommer KW, Schamberger CJ, Schmidt GE, Sasgary S & Cerni C. Inhibitor of apoptosis protein (IAP) survivin is up-regulated by oncogenic c-H-Ras. Oncogene 2003; 22:4266-4280.

Song J, So T, Cheng M, Tang X & Croft M. Sustained survivin expression from OX40 costimulatory signals drives T cell clonal expansion. Immunity 2005; 22:621-631.

Song Z, Yao X & Wu M. Direct interaction between survivin and Smac/DIABLO is essential for the anti-apoptotic activity of survivin during taxol-induced apoptosis. J Biol Chem 2003; 278:23130-23140.

Sowery RD, So AI & Gleave ME. Therapeutic options in advanced prostate cancer: present and future. Curr Urol Rep 2007; 8:53-59.

Srinivasula SM, Ahmad M, Ottilie S, Bullrich F, Banks S, Wang Y, Fernandes-Alnemri T, Croce CM, Litwack G, Tomaselli KJ, Armstrong RC & Alnemri ES. FLAME-1, a novel FADD-like anti-apoptotic molecule that regulates Fas/TNFR1-induced apoptosis. J Biol Chem 1997; 272:18542-18545.

Srinivasula SM, Datta P, Fan XK, Fernandes-Alnemri T, Huang Z & Alnemri ES. Molecular determinants of the caspase-promoting activity of Smac/DIABLO and its role in the death receptor pathway. J Biol Chem 2000; 275:36152-36157.

Stage-Zimmermann TK & Uhlenbeck OC. Hammerhead ribozyme kinetics. RNA 1998; 4:875-889.

Steller H. Mechanisms and genes of cellular suicide. Science 1995; 267:1445-1449.

Strasser A, Harris AW, Bath ML & Cory S. Novel primitive lymphoid tumours induced in transgenic mice by cooperation between myc and bcl-2. Nature 1990; 348:331-333.

Strasser A, O'Connor L & Dixit VM. Apoptosis signaling. Annu Rev Biochem 2000; 69:217-245.

Strasser A, Whittingham S, Vaux DL Bath ML, Adams JM, Cory S & Harris AW. Enforced BCL2 expression in B-lymphoid cells prolongs antibody responses and elicits auto-immune disease. Proc Natl Acad Sci USA 1991; 88:8661-8665.

Sui G, Soohoo C, Affar el B, Gay F, Shi Y, Forrester WC & Shi Y. A DNA vector-based RNAi technology to suppress gene expression in mammalian cells. Proc Natl Acad Sci USA 2002; 99:5515-5520.

Sun C, Cai M, Meadows RP, Xu N, Gunasekera AH, Herrmann J, Wu JC, Fesik SW. NMR structure and mutagenesis of the inhibitor-of-apoptosis protein XIAP. Nature 1999; 401:818-821

Sun LQ, Cairns MJ, Saravolac EG, Baker A & Gerlach WL. Catalytic nucleic acids: from lab to applications. Pharmacol Reviews 2000; 52:325-347.

Sun LQ, Warrilow D, Wang L & Symonds. Ribozyme-mediated suppres-sion of moloney murine leukemia virus and human immunodeficiency virus type 1 replication in permissive cell lines. Proc Natl Acad Sci USA 1994; 91:9715-9719.

Suyama E, Kawasaki H, Nakajima M & Taira K. Identification of genes involved in cell invasion by using a library of randomized ribozymes. Proc Natl Acad Sci USA 2003; 100:5616-5621

Suzuki A, Hayashida M, Ito T, Kawano H, Nakano T, Miura M, Akahane K & Shiraki K. Survivin initiates cell cycle entry by the competitive interaction with Cdk4/p16 (INK4a) and Cdk2/cyclin E complex activation. Oncogene 2000; 19:3225-3234.

Suzuki A, Ito T, Kawano H, Hayashida M, Hayasaki Y, Tsutomi Y, Akahane K, Nakano T, Miura M & Shiraki K. Survivin initiates procaspase 3/p21 complex formation as a result of interaction with Cdk4 to resist Fas-mediated cell death. Oncogene 2000; 19:1346 -1353.

Swanson GP. Management of locally advanced prostate cancer: past, present, future. J Urol 2006; 176:S34-41.

Tachibana R, Harashima H, Shinohara Y & Kiwada H. Quantitative studies on the nuclear transport of plasmid DNA and gene expression employing nonviral vectors. Adv Drug Deliv Rev 2001; 52:219-221.

Takahashi R, Deveraux Q, Tamm I, Welsh K, Assa-Munt N, Salvesen GS & Reed JC. A single BIR domain of XIAP sufficient for inhibiting caspases. J Biol Chem 1998; 273:7787-7790.

Takeuchi Y, Cosset FL, Lackmann PJ Okada H, Weiss RA, Collins MK. Type C retro-virus inactivation by human complement is determined by both the viral genome and the producer cell. J Virol 1994; 68:8001-8007.

Tamm I, Wang Y, Sausville E, Scudiero DA, Vigna N, Oltersdorf T & Reed JC. IAP-family protein survivin inhibits caspase activity and apoptosis induced by Fas (CD95), Bax, caspases, and anticancer drugs. Cancer Res 1998; 58:5315-5320.

Tan PH, Tan PL, George AJ & Chan CL. Gene therapy for transplantation with viral vectors--how much of the promise has been realised? Expert Opin Biol Ther 2006; 6:759-772.

Tanaka K,Iwamoto S,Gon G,Nohara T,Iwamoto M & Tanigawa N. Expression of survivin and its relationship to loss of apoptosis in breast carcinomas. Clin Cancer Res 2000; 6:127-134.

Tang L, Tron VA, Reed JC, Mah KJ, Krajewska M, Li G, Zhou X, Ho VC & Trotter MJ. Expression of apoptosis regulators in cutaneous malignant melanoma. Clin Cancer Res 1998; 4:1865-1871.

Teixeira C, Reed JC & Pratt MA. Estrogen promotes chemotherapeutic drug resistance by a mechanism involving Bcl-2 proto-oncogene expression in human breast cancer cells. Cancer Res 1995; 55:3902-3907.

Thallinger C, Wolschek MF, Wacheck V, Maierhofer H, Gunsberg P, Polterauer P, Pehamberger H, Monia BP, Selzer E, Wolff K & Jansen B. Mcll-1 antisense therapy chemosensitizes human melanoma in a SCID mouse xenotransplantation model. J Invest Dermatol 2003; 120:1081-1086.

Thomadaki H & Scorilas A. BCL2 family of apoptosis-related genes: functions and clinical implications in cancer. Crit Rev Clin Lab Sci 2006; 43:1-67.

Thomas WD & Hersey P. TNF-related apoptosis-inducing ligand (TRAIL) induces apoptosis in Fas ligand-resistant melanoma cells and mediated CD4 T cell killing of target cells. J Immunol 1998; 161:2195-200.

Thornberry NA & Lazebnik Y. Caspases: enemies within. Science 1998; 281:1312–1316.

Tiera MJ, Winnik FO & Fernandes JC. Synthetic and natural polycations for gene therapy: state of the art and new perspectives. Curr Gene Ther 2006; 6:59-71.

Timmer T, de Vries EG & de Jong S. Fas receptor-mediated apoptosis: a clinical application? J Pathol 2002; 196:125-134.

Tirro E, Consoli ML, Massimino M, Manzella L, Frasca F, Sciacca L, Vicari L, Stassi G, Messina L, Messina A & Vigneti P. Altered expression of c-IAP1, survivin, and Smac contributes to chemotherapy resistance in thyroid cancer cells. Cancer Res 2006; 66:4263-4272.

Tran J, Master Z, Yu JL, Rak J, Dumont DJ & Kerbel RS. A role for survivin in chemoresistance of endothelial cells mediated by VEGF. Proc Natl Acad Sci USA 2002; 99:4349-4354.

Trauth BC, Klas C, Peters AM, et al. Monoclonal antibody-mediated tumor regression by induction of apoptosis. Science 1989; 245: 301–305.

Tsujimoto Y, Cossman J, Jaffe E & Croce CM. Involvement of the bcl-2 gene in human follicular lymphoma. Science 1985; 228:1440-1452.

Tu SP, Cui JT, Liston P, Huajiang X, Xu R, Lin MC, Zhu YB, Zou B, Ng SS, Jiang SH, Xia HH, Wong WM, Chan AO, Yuen MF, Lam SK, Kung HF & Wong BC. Gene therapy for colon cancer by adeno-associated viral vector-

mediated transfer of survivin Cys84Ala mutant. Gastroenterology 2005; 128:361-375.

Turkson,J. STAT proteins as novel targets for cancer drug discovery. Expert Opin Ther Targets 2004; 8:409-422.

Uren AG, Wong L, Pakusch M, Fowler KJ, Burrows FJ, Vaux DL & Choo KH. Survivin and the inner centromere protein INCENP show similar cell-cycle localization and gene knockout phenotype. Curr Biol 2000; 10:1319-1328.

Uren AG, Pakusch M, Hawkins CJ, Puls KL & Vaux DL. Cloning and expression of apoptosis inhibitory protein homologs that function to inhibit apoptosis and/or bind tumor necrosis factor receptor-associated factors. Proc Natl Acad Sci USA 1996; 93:4974-4978.

Urist M, Tanaka T, Poyurovsky MV & Prives C. p73 induction after DNA damage is regulated by checkpoint kinases Chk1 and Chk2. Genes Dev 2004; 18:3041-3054.

Vagnarelli P & Earnshaw WC. Chromosomal passengers: the four-dimensional regulation of mitotic events. Chromosoma 2004; 113:211-222.

Vaira V, Lee CW, Goel HL, Bosari S, Languino LR & Altieri DC. Regulation of survivin expression by IGF-1/mTOR signalling. Oncogene 2006; 1-7.

Van Geelen CM, de Vries EG & de Jong S. Lessons from TRAIL-resistance mechanisms in colorectal cancer cells: paving the road to patient-tailored therapy. Drug Resist. Updat 2004; 7:345-358.

Van Houdt WJ, Haviv YS, Lu B, Wang M, Rivera AA, Ulasov IV, Lamfers ML, Rein D, Lesniak MS, Siegal GP, Dirven CM, Curiel T & Zhu ZB. The human survivin promoter: a novel transcriptional targeting strategy for treatment of glioma. J Neurosurg 2006; 104:583-592.

Vaux DL, Cory S & Adams JM. Bcl-2 gene promotes haemopoietic cell survival and cooperates with c-myc to immortalize pre-B cells. Nature 1988; 335: 440-442.

Vaux DL & Silke J. Mammalian mitochondrial IAP binding proteins. Biochem Biophys Res Commun 2003;304:499-504.

Velculescu VE, Madden SL, Zhang L, Lash AE, Yu J, Rago C, Lal A, Wang CJ, Beaudry GA, Ciriello KM, Cook BP, Dufault MR, Ferguson AT, Gao Y, He TC, Hermeking H, Hiraldo SK, Hwang PM, Lopez MA, Luderer HF,

Mathews B, Petroziello JM, Polyak K, Zawel L & Kinzler KW. Analysis of human transcriptomes. Nat Gen 1999; 23:387-388.

Verdecia MA, Huang H, Dutil E, Kaiser DA, Hunter T & Noel JP. Structure of the human anti-apoptotic protein survivin reveals a dimeric arrangement. 2000; 7:602-608.

Verhagen AM, Ekert PG, Pakusch M, Silke J, Connolly LM, Reid GE, Moritz RL, Simpson RJ & Vaux DL. Identification of DIABLO, a mammalian protein that promotes apoptosis by binding to and antagonizing IAP PROTEINS. Cell 2000; 102:43-53.

Verhagen AM, Coulson EJ & Vaux DL. Inhibitor of apoptosis proteins and their relatives: IAPs and other BIRPs. Genome Biol 2001; 2:1-10.

Vester B & Wengel J. LNA (locked nucleic acid): high-affinity targeting of complementary RNA and DNA. Biochemistry 2004; 43:13233-13241.

Vetter CS, Muller-Blech K, Schrama D, Brocker EB & Becker JC. Cytoplasmic and nuclear expression of survivin in melanocytic skin lesions. Arch Dermatol Res 2005; 297:26-30.

Vogelstein,B. & Kinzler,K.W. Cancer genes and the pathways they control. Nat Med 2004; 10:789-799.

Vogt PK & Reed SI. Cyclin dependent kinase (CDK) inhibitors. Current Topics in Microbiology and Immunology. New York: Springer-Verlag 1998; Vol 227.

von Reyher U, Strater J, Kittstein W, Gschwendt M, Kram-mer PH & Moller P. Colon carcinoma cells use different mecha-nisms to escape CD95-mediated apoptosis. Cancer Res 1998; 58:526-534.

Vucic D, Stennicke HR, Pisabarro MT, Salvesen GS & Dixit VM. ML-IAP, a novel inhibitor of apoptosis that is preferentially expressed in human melanomas. Curr Biol 2000; 10:1359-1366.

Wadhwa R, Sunil C, Miyagishi KM & Taira K. Know-how of RNA interference and its applications in research and therapy. Mutation Research 2004; 567: 71-84.

Wall NR, O'Connor DS, Plescia J, Pommier Y & Altieri DC. Suppression of survivin phosphorylation on Thr34 by flavopiridol enhances tumor cell apoptosis. Cancer Res 2003; 63:230-235.

Walsh K, Smith RC & Kim HS. Vascular cell apoptosis in remodeling, restenosis, and plaque rupture. Circ Res 2000; 87:184-188.

Wang HW, Sharp TV, Koumi A, Koentges G & Boshoff C. Characterization of an anti-apoptotic glycoprotein encoded by Kaposi's sarcoma-associated herpesvirus which resembles a spliced variant of human survivin. EMBO J 2002; 21:2602-2615.

Wang X. The expanding role of mitochondria in apoptosis. Genes Dev 2001; 15:2922-2933.

Wang Y, Suominen JS, Hakovirta H, Parvinen M, Martinand-Mari C, Toppari J & Robbins I. Survivin expression in rat testis is up-regulated by stem-cell factor. Mol Cell Endocrinol 2004; 218:165-174.

Warny M, Keates AC, Keates S, Castagliuolo I, Zacks JK, Aboudola S, Qamar A, Pothoulakis C, LaMont JT & Kelly CP. p38 MAP kinase activation by Clostridium difficile toxin A mediates monocyte necrosis, IL-8 production, and enteritis. J Clin Invest 2000; 105:1147-1156.

Warrington KH Jr & Herzog RW. Treatment of human disease by adeno-associated viral gene transfer. Hum Genet 2006; 119:571-603.

Weber CH & Vincenz C. A docking model of key components of the DISC complex: death domain superfamily interactions redefined. FEBS Lett 2001; 492:171-176.

Welch PJ, Barber JR & Wong-Staal F. Expression of ribozymes in gene transfer systems to modulate target RNA levels. Curr Opin Biotechnol 1998; 9:486-496.

Williams NS, Gaynor RB, Scoggin S, Verma U, Gokaslan T, Simmang C, Fleming J, Tavana D, Frenkel E & Becerra C. Identification and validation of genes involved in the pathogenesis of colorectal cancer using cDNA microarrays and RNA interference. Clin Cancer Res 2003; 9:931-946.

Willis S, Day CL, Hinds MG & Huang DC. The Bcl-2-regulated apoptotic pathway. J Cell Sci 2003; 116:4053-4056.

Wilson KP, Black JA, Thomson JA, Kim EE, Griffith JP, Navia MA, Murcko MA, Chambers SP, Aldape RA, Raybuck SA & Livingston DJ. Structure and mechanism of interleukin-1 beta converting enzyme. Nature 1994; 370:270-275.

Wolf BB & Green DR. Suicidal tendencies: apoptotic cell death by caspase family proteinases. J Biol Chem 1999; 274:20049-20052.

Wolter KG, Hsu YT, Smith CL, Nechushtan A, Xi XG & Youle RJ. Movement of Bax from the cytosol to mitochondria during apoptosis. J Cell Biol 1997; 139:1281-1293.

Woodson SA. Folding mechanisms of group I ribozymes: role of stability and contact order. Biochem Soc Trans 2002; 30:1166-1169.

Workman P, Twentyman P, Balkwill F, Balmain A, Chaplin D, Double J, Embleton J, Newell D, Raymond R, Stables J, Stephen T & Wallace J. United Kingdom Co-ordinating Committee on Cancer Res. (UKCCCR) guidelines for the welfare of animals in experimental neoplasia (ed.2). Br J Cancer 1998; 77:1-10.

Workman P. Overview: translating Hsp90 biology into Hsp90 drugs. Curr Cancer Drug Targets 2003; 3:297-300.

Wu G, Chai J, Suber TL, Wu JW, Du C, Wang X & Shi Y. Structural basis of IAP recognition by Smac/DIABLO. Nature 2000; 408:1008-1012.

Wu XX, Ogawa O, Kakehi Y. TRAIL and chemotherapeutic drugs in cancer therapy. Vitam Horm 2004; 67:365-383.

Wurl P, Kappler M, Meye A, Bartel F, Kohler T, Lautens-chlager C, Bache M, Schmidt H & Taubert H. Co-expression of survivin and TERT and risk of tumour-related death in patients with soft-tissue sarcoma. Lancet 2002; 359:943-945.

Xia C, Xu Z, Yuan X, Uematsu K, You L, Li K, Li L, McCormick F & Jablons DM. Induction of apoptosis in mesothelioma cells by antisurvivin oligonucleotides. Mol Cancer Ther 2002; 1:687-694.

Xia F & Altieri DC. Mitosis-independent survivin gene expression in vivo and regulation by p53. Cancer Res 2006; 66:3392-3395.

Xia W, Bisi J, Strum J, Liu L, Carrick K, Graham KM, Treece AL, Hardwicke MA, Dush M, Liao Q, Westlund RE, Zhao S, Bacus S & Spector NL. Regulation of survivin by ErbB2 signaling: therapeutic implications for ErbB2-overexpressing breast cancers. Cancer Res 2006; 66:1640-1647.

Xing Z, Conway EM, Kang C & Winoto A. Essential role of survivin, an inhibitor of apoptosis protein, in T cell development, maturation, and homeostasis. J Exp Med 2004; 199:69-80.

Yamada Y, Kuroiwa T, Nakagawa T, Kajimoto Y, Dohi T, Azuma H, Tsuji M, Kami K & Miyatake S. Transcriptional expression of survivin and its splice variants in brain tumors in humans. J Neurosurg 2003; 99:738-745.

Yamamoto T, Manome Y, Nakamura M & Tanigawa N. Downregulation of survivin expression by induction of the effector cell protease receptor-1 reduces tumor growth potential and results in an increased sensitivity to anticancer agents in human colon cancer. Eur J Cancer 2002; 38:2316-2324.

Yan H, Thomas J, Liu T, Raj D, London N, Tandeski T, Leachman SA, Lee RM & Grossman D. Induction of melanoma cell apoptosis and inhibition of tumor growth using a cell-permeable Survivin antagonist. Oncogene 2006; 25:6968-6974.

Yang D, Welm A & Bishop JM. Cell division and cell survival in the absence of surviving. Proc Natl Acad Sci USA 2004; 101:15100-15105.

Yang E, Zha J, Jockel J, Boise LH, Thompson CB & Korsmeyer S. Bad, a heterodimeric partner for Bcl-XL and Bcl-2, displaces Bax and promotes cell death. J Cell 1995; 80:285-291.

Yonesaka K, Tamura K, Kurata T, Satoh T, Ikeda M, Fukuoka M & Nakagawa K. Small interfering RNA targeting survivin sensitizes lung cancer cell with mutant p53 to adriamycin. Int J Cancer 2006; 118:812-820.

Yoshida H, Ishiko O, Sumi T, Matsumoto Y & Ogita S. Survivin, bcl-2 and matrix metalloproteinase-2 enhance progression of clear cell- and serous-type ovarian carcinomas. Int J Oncol 2001; 19:537-542.

Young LS, Searle PF, Onion D & Mautner V. Viral gene therapy strategies: from basic science to clinical application. J Pathol 2006; 208:299-318.

Yuan J. Transducing signals of life and death. Curr Opin Cell Biol 1997; 9:247–251.

Yuan J, Lipinski M & Degterev A. Diversity in the mechanisms of neuronal cell death. Neuron 2003; 40:401-413.

Zaffaroni N, Pennati M, Colella G, Perego P, Supino R, Gatti L, Pilotti S, Zunino F & Daidone MG. Expression of the anti-apoptotic gene survivin correlates with taxol resistance in human ovarian cancer. Cell Mol Life Sci 2002; 59:1406-1412.

Zamzami N & Kroemer G. Condensed matter in cell death. Nature 1999; 401:127-128.

Zangemeister-Wittke U. Antisense to apoptosis inhibitors facilitates chemotherapy and TRAIL-induced death signaling. Ann N Y Acad Sci 2003; 1002:90-94.

Zha J, Harada H, Yang E, Jockel J & Korsmeyer S. Serine phosphorylation of death agonist BAD in response to survival factor results in binding to 14-3-3 not BCL-X(L). Cell 1996; 87:619-628.

Zhang L, Yu J, Park BH, Kinzler KW & Vogelstein B. Role of BAX in the apoptotic response to anticancer agents. Science 2000; 290: 989-992.

Zhang M, Latham DE, Delaney MA & Chakravarti A. Survivin mediates resistance to antiandrogen therapy in prostate cancer. Oncogene 2005; 24:2474-2482.

Zhang M, Mukherjee N, Bermudez RS, Latham DE, Delaney MA, Zietman AL, Shipley WU & Chakravarti A. Adenovirus-mediated inhibition of survivin expression sensitize human prostate cancer cells to paclitaxel in vitro an in vivo. Prostate 2005; 64:293-302.

Zhang T, Otevrel T, Gao Z, Ehrlich SM, Fields JZ & Boman BM. Evidence that APC regulates survivin expression: a possible mechanism contributing to the stem cell origin of colon cancer. Cancer Res 2001; 61:8664-8667.

Zhao J, Tenev T, Martins LM, Downward J & Lemoine NR. The ubiquitin-proteasome pathway regulates survivin degradation in a cell cycle-dependent manner. J Cell Sci 2000; 113:4363-4371.

Zhou BB & Elledge SJ. The DNA damage response: Putting checkpoints in perspective. Nature 2000; 408:433-439.

Zhou J, O'Brate A, Zelnak A & Giannakakou P. Survivin deregulation in beta-tubulin mutant ovarian cancer cells underlies their compromised mitotic response to taxol. Cancer Res 2004; 64:8708-8714.

Zhou M, Gu L, Li F, Zhu Y, Woods WG & Findley HW. DNA damage induces a novel p53-survivin signaling pathway regulating cell cycle and apoptosis in acute lymphoblastic leukemia cells J Pharmacol Exp Ther 2002; 303:124-131.

Zimmerman KC, Bonzon C & Green DR. The machinery of programmed cell death. Pharmacol Ther 2002; 92:57-70.

Zinkel S, Gross A & Yang E. BCL2 family in DNA damage and cell cycle control. Cell Death Differ 2006; 13:1351-1359.

Zundel W & Giaccia A. Inhibition of the anti-apoptotic PI(3)K/Akt/Bad pathway by stress. Genes Devel 1998; 12:1941-1946.

Appendix

ABBREVIATIONS

This appendix contains a key of the most common acronyms and abbreviations used in this thesis.

17-AAG = 17-allylamino-17-demethoxy-geldanamycin

Ac-DEVD-AMC = N-acetyl-Asp-Glu-Val-Asp-aldehyde-7-amino-4-methylcoumarin

Apaf-1 = Apoptotic protease activating factor-1

APS = Ammonium persulfate

ATCC = American Type Culture Collection

BIR = Baculoviral IAP Repeat

BSA = Bovine Serum Albumin

CARD = Caspase Recruitment Domain

cdk = Cyclin-Dependent Kinase

DD = Death Domain

DED = Death Effector Domain

DEPC = Diethylpirocarbonate

DISC = Death-Inducing Signalling Complex

DMSO = Dimethyl Sulfoxide

DOTAP = N-(1-(2,3 dioleoyloxy) propyl)-N,N,N-trimethylammoniummethyl sulphate

EDTA = Ethylenediaminetetraacetic Acid

FADD = Fas-Associated protein with Death Domain

Fas = Fibroblast-Associated protein

FBS = Fetal Bovine Serum

Flip = FADD-like interleukin-1-converting enzyme-inhibitory protein

Hsp90 = Heat Shock Protein 90

IAP = Inhibitor of Apoptosis Proteins

LB = Loading Buffer

LB medium = Luria-Bertani medium

LEHD-AFC = leu-glu-his-asp-7-amino-4-trifluoromethylcoumarin

PBS = Phosphate-Buffered Saline

RIP = Receptor-Interacting Protein

SDS = Sodium Dodecyl Sulfate

TAE = TRIS-Acetate-EDTA

TBE = Tris-Borate-EDTA

TGS buffer = Tris-Glycine-SDS buffer

TNF = Tumour Necrosis Factor

TNF-R = Tumour Necrosis Factor Receptor

TRADD = TNF Receptor-Associated protein with Death Domain

TRAIL-R = TNF-Related Apoptosis-Inducing Ligand Receptor

TRAP = Telomere Repeat Amplification Protocol

TUNEL = Terminal dUTP Nick-End Labeling